



Simulation et optimisation énergétique de procédés agroalimentaires dans un logiciel de génie chimique. Modélisation du séchage convectif d'aliments solides et application à une sucrerie de betteraves

Charlène Lambert

► To cite this version:

Charlène Lambert. Simulation et optimisation énergétique de procédés agroalimentaires dans un logiciel de génie chimique. Modélisation du séchage convectif d'aliments solides et application à une sucrerie de betteraves. Génie des procédés. Université Paris Saclay (COmUE), 2015. Français. NNT : 2015SACLAD004 . tel-02923626

HAL Id: tel-02923626

<https://pastel.hal.science/tel-02923626>

Submitted on 27 Aug 2020

HAL is a multi-disciplinary open access archive for the deposit and dissemination of scientific research documents, whether they are published or not. The documents may come from teaching and research institutions in France or abroad, or from public or private research centers.

L'archive ouverte pluridisciplinaire **HAL**, est destinée au dépôt et à la diffusion de documents scientifiques de niveau recherche, publiés ou non, émanant des établissements d'enseignement et de recherche français ou étrangers, des laboratoires publics ou privés.

NNT : 2015SACLA004

THÈSE DE DOCTORAT
DE
L'UNIVERSITÉ PARIS-SACLAY
PRÉPARÉE À
AGROPARISTECH

ÉCOLE DOCTORALE N°581

Agriculture, alimentation, biologie, environnement et santé

Spécialité de doctorat : Génie des procédés

Par

Charlène LAMBERT

Simulation et optimisation énergétique de procédés agroalimentaires dans un logiciel de génie chimique. Modélisation du séchage convectif d'aliments solides et application à une sucrerie de betteraves.

Thèse présentée et soutenue à Massy, le 20 novembre 2015 :

Composition du jury :

Pr. Patrick PERRÉ, LGPM, École Centrale-Supélec
Pr. Lionel BOILLEREAUX, GEPEA-ONIRIS
Pr. Xavier JOULIA, LGC-INPT-ENSIACET
Pr. Francis COURTOIS, UMR 1145, AgroParisTech
Dr. Hédi ROMDHANA, UMR 1145, AgroParisTech
Dr. Franck GELIX, Veolia Recherche et Innovation

Examinateur
Rapporteur
Rapporteur
Directeur
Co-directeur
Invité

Remerciements

Au terme de ce travail, c'est avec beaucoup d'émotion que je remercie toutes celles et tous ceux qui, de près ou de loin, m'ont aidée dans ce travail.

En premier lieu, je tiens à remercier mes deux directeurs de thèse, Francis Courtois et Hédi Romdhana. Ces trois années de collaboration ont été un vrai bonheur. J'espère que nos chemins professionnels se recroiseront.

Francis, ton soutien permanent, ta compréhension et ta disponibilité ont grandement participé à la réussite de ce travail. Merci pour tes grandes qualités humaines et scientifiques.

Hédi, merci pour ton soutien, tes conseils et tes remarques constructives.

Je remercie également les membres du jury : Lionel Boillereaux, Xavier Joulia, Patrick Perré et Franck Gélix, d'avoir accepté d'examiner mon travail ainsi que pour les riches discussions scientifiques qui l'ont suivi.

Je remercie les membres de mon comité de thèse, Philippe Baudet, Olivier Baudouin, Catherine Bonazzi, Martine Esteban-Decloux et Xuan Meyer pour l'intérêt porté au projet et leurs remarques constructives. Elles ont grandement contribué à la réalisation de ce travail.

Martine, je te remercie de m'avoir fait bénéficier de ton expertise dans le domaine de l'industrie sucrière et pour tes qualités humaines.

Ce travail n'aurait jamais pu aboutir sans la contribution et l'investissement personnel de plusieurs personnes, et en particulier :

- Julien Cartailler, Monica Pinto, Benoît Hareng, Abir Hosni et Giana Perré pour l'acquisition de données expérimentales. Giana, merci pour ton aide à l'interprétation des isothermes d'adsorption/désorption.
- Quentin Duval pour ton aide sans relâche concernant le développement du module de séchage. Merci à Louis Campagnolo, Philippe Guittard, Silvère Massebeuf et Fabrice Bonnet pour le support technique concernant l'utilisation du logiciel ProSimPlus. Grâce à vous, j'ai beaucoup appris dans le domaine de la thermodynamique et de la simulation de procédés !
- Benjamin Laulan, avec qui j'ai beaucoup collaboré pour réaliser la simulation et l'optimisation énergétique de la sucrerie. Merci pour ta disponibilité, ta bonne humeur et tes aptitudes pédagogiques. Grâce à toi, j'ai pu me former à l'utilisation de ProSimPlus. Merci à Alexandre Lima et Clément Rebillard pour leur réactivité et la bonne conduite de ce projet.
- Raphaele Hetreux, Pascal Floquet et Stéphane Gourmelon, également membres du projet, merci pour votre réactivité et vos qualités humaines.
- L'ANR pour le financement de mon doctorat.

Je tiens à remercier l'ensemble de l'équipe Calipro pour son accueil et son soutien, et en particulier Marie-Elisabeth Cuvelier, Nicolas Descharles, Daniel Goujot, Bertrand Heyd,

Séverine Keller, Even Le Roux, Marie-Noëlle Maillard, Paola Soto, Richard Rocca, Stéphanie Roux et Colette Wong. Je garderai en mémoire la bonne ambiance régnant dans votre équipe, nos discussions souvent surprenantes en salle de pause et vos qualités humaines. Certains d'entre vous sont devenus de vrais amis. Colette, merci pour ta gentillesse, ta disponibilité et ton aide concernant les démarches administratives. Daniel, merci pour ton aide précieuse lors de mes déboires avec TexMaker... Stéphanie, merci pour tes conseils, toujours judicieux.

Je remercie aussi l'ensemble de l'équipe SP2 pour son accueil pendant quelques semaines et en particulier Brigitte Deau, Anne-Marie Gibon, Delphine Huc, Véronique Bosc, Camille Michon, Gabrielle Moulin, Artémio Plana-Fattori, Fabrice Ducept, Cindy Villemeyeane et Gérard Cuvelier. Je n'oublierai pas votre bonne humeur ni les éclats de rire lors des pauses café.

Christophe Doursat, Denis Flick et Christian Tréléa, j'ai beaucoup apprécié l'enseignement de l'ASD à vos côtés.

Je remercie d'une manière générale l'ensemble du personnel de l'UMR avec qui j'ai pris beaucoup de plaisir à collaborer lors d'activités collectives.

Aux doctorants, qui sont passés ou passeront par les mêmes étapes que moi, Sarah Abidh, Pierre Awad, Christiane Azagoh, Josselin Bousquieres, Yacine Chryat, Marine Dewaest, Adrien Douady, Christian Felipe-Puentes, Marion Gaff, Farnaz Hanaei, Lucie Huault, Gaëlle Le Goff, Cassandre Leverrier, Damien Mat, Anne-Flore Monnet, Marine Moussier, Aurélia Pernin, Etienne Pluyette, Eugénie Séguineau de Préval : je n'oublierai pas votre bonne humeur, votre soutien et bien évidemment ces pauses café et soirées dans la salle Chevreul ou dans les bars... Vous avez contribué à rendre ces trois dernières années exceptionnelles et bon nombre d'entre vous sont devenus des amis proches. Aurélia, Adrien, Anne-Flore et Damien, cela a été un vrai bonheur de partager votre bureau même pour une courte durée !

Je voudrais également remercier mes amis de l'Agro : Apolline, Clémence, Alice, Nicolas, Marie, Clément et Louisette, de Grenoble, Pierre et Axel, du CEA, Jelle, Tiphaïne, et de Caen, Anaïs, Joffrey, David, Adeline, Boris et Camille. Merci pour votre soutien et les soirées et week ends de décompression !

Merci également à ma mère, à Colette, et à Sylvie pour la relecture d'une partie du manuscrit.

Enfin, je dédie ce travail aux deux hommes qui m'accompagnent au quotidien, Maxime et Valentin. Maxime, merci pour ta patience, ton soutien immuable et tes nombreux conseils. Tu as toujours su trouver les mots pour m'aider à persévirer dans cette aventure qu'est la thèse et à atteindre les objectifs comme je le souhaitais. Le bonheur tiré de cette aventure s'en est vu considérablement amélioré grâce à toi.

Merci également à toi, Valentin, qui a énormément participé au bon déroulement des derniers mois de la thèse. Chaque moment passé avec toi, regard échangé, quelle que soit l'heure du jour ou de la nuit, me permettaient de décompresser et de me motiver encore plus chaque jour pour aller au bout de cette belle aventure.

Clés de lecture

Cette thèse sur publications est articulée en 7 chapitres distincts. Le premier chapitre contient une synthèse de ce travail de doctorat en français. Les chapitres suivants contiennent les articles en anglais déjà publiés, en cours de révision ou à soumettre. Chaque article est précédé d'un résumé en français. Enfin, les versions d'articles présentes dans ce manuscrit sont les versions envoyées aux éditeurs avant corrections.

Publications scientifiques issues de ce doctorat

Articles scientifiques dans des périodiques internationaux

- A1 **C. Lambert**, H. Romdhana, and F. Courtois, "Reverse methodology to identify moisture diffusivity during air-drying of foodstuffs," Drying Technology 33(9), pp. 1076-1085, 2015.
- A2 **C. Lambert**, D. Goujot, H. Romdhana, and F. Courtois, "Toward a generic approach to build-up air drying models," Drying Technology 34(3), pp. 346-359, 2016.
- A3 H. Romdhana, **C. Lambert**, D. Goujot, and F. Courtois, "Model reduction technique for faster simulation of drying of spherical solid foods," Journal of Food Engineering 170, pp. 125-135, 2016.
- A4 **C. Lambert** J. Cartailler, S. Rouchouse, G. Almeida, and F. Courtois, "Characterization and modeling of cooling and drying of pellets for animal feed," Submitted to Drying Technology (under revision) 2016.

Communications orales dans des congrès internationaux ou français

- C1 S. Gourmelon, E. Letournel, P. Baudet, C. Rebillard, R. Hetreux, L. Campagnolo, **C. Lambert**. "Optimizing food and beverage plants thanks to exergy, pinch and by-product valorization. E biofuel production plant case study". 10th European congress of chemical engineering, 3rd European congress of applied biotechnology, 5th European process intensification conference, 15th SFGP congress, 27th September-1st October 2015, Nice (France).
- C2 **C. Lambert**, J. Cartailler, S. Rouchouse, G. Almeida, F. Courtois. "Characterization of pellet cooling by modelling hot air drying". 5th European drying conference EURODRYING, 21-23th October 2015, Budapest (Hungary).
- C3 **C. Lambert**, H. Romdhana, O. Baudouin, P. Baudet, F. Courtois. "A first step in drying simulation with a commercial chemical engineering software". 19th international drying symposium IDS, 24-27th August 2014, Lyon (France).
- C4 **C. Lambert**, F. Courtois, H. Fibrianto, L. Boillereaux, S. Rouchouse, F. Putier. "Hybrid modelling of cooling-drying process in animal feed-pellets industries". FOODSIM, 23-25th June 2014, Brest(France).
- C5 **C. Lambert**, H. Romdhana, F. Courtois, "Toward a generic simulator for food processes : bridging the gap between chemical engineering and food engineering". 14ème congrès de la SFGP, 8-10th October 2013, Lyon (France).
- C6 **C. Lambert**, H. Romdhana, F. Courtois. Reversing classical methodology for hot air drying of foodstuffs. 4th European drying conference EURODRYING, 2-4th October 2013, Paris (France).

Communications par poster dans des congrès internationaux

- P1 H. Romdhana, **C. Lambert**, D. Goujot, F. Courtois. "Comparing simulations from compartmental and classic PDE approaches to model drying of food solids". 19th international drying symposium IDS, 24-27th August 2014, Lyon (France).
- P2 **C. Lambert**, H. Romdhana, F. Courtois. "Toward another method to determine effective diffusion coefficients in foodstuffs". 19th international drying symposium IDS, 24-27th August 2014, Lyon (France).

P3 **C. Lambert**, A. Zemmouri, A. Hosni, H. Romdhana, F. Courtois. "Toward a generic approach to build up air drying models". 4th European drying conference EURO-DRYING, 2-4th October 2013, Paris (France).

Table des matières

1 Synthèse du travail de doctorat	13
1.1 Introduction générale	13
1.2 Estimation de propriétés thermophysiques des aliments requises à la simulation du séchage convectif	16
1.3 Développement d'un modèle générique de séchage convectif de produits alimentaires solides par air chaud	22
1.4 Simulation et optimisation énergétique d'une usine agroalimentaire : cas d'une sucrerie de betteraves	28
1.5 Conclusions générales et perspectives	32
Références	34
2 Toward a generic approach to build-up air drying models	41
2.1 Introduction	41
2.2 Available commercial simulators for drying processes	42
2.2.1 Overview	42
2.2.2 SD2P®, a specific example for spray drying simulation	43
2.2.3 Dryer3000®, a specific example for grain drying	43
2.3 Discussion on available modelling approaches	44
2.3.1 Approaches used to model food drying processes	44
2.3.2 Compatibility requirements for commercial simulation	45
2.3.3 Selecting the ‘best’ modelling approach	46
2.4 Estimation of food thermo-hydro-physical properties	50
2.4.1 Effective heat capacity	50
2.4.2 Effective Thermal conductivity	50
2.4.3 Isotherm or isobar of water desorption	51
2.4.4 Effective water diffusion coefficients	51
2.4.5 Optimized experimental strategies to identify parameters of effective moisture diffusion model	51
2.5 Discussion	54
2.6 Conclusions	58
2.7 Acknowledgments	58
2.8 References	60
3 Reversing classical methodology to identify effective moisture diffusivity during air-drying of foodstuffs	63
3.1 Introduction	63
3.2 Theory: deep bed and thin layer drying model	65
3.2.1 Heat and mass balance on the particles	66

3.2.2 Heat and mass balance on the air	66
3.3 Materials and methods	67
3.3.1 Materials	67
3.3.2 Geometry and density measurements	67
3.3.3 Moisture content measurement	67
3.3.4 Sorption isotherm measurement	67
3.3.5 Identification of effective moisture diffusivity	68
3.3.6 Drying kinetics measurement	68
3.3.7 Simulation and optimization	70
3.4 Results and discussion	70
3.4.1 Identification of effective moisture diffusivity on a deep bed kinetic	70
3.4.2 Validation of effective moisture diffusivity correlations on thin layer kinetics	73
3.5 Conclusion	75
3.6 Acknowledgments	76
3.7 References	76
4 Characterization and modeling of cooling and drying of pellets for animal feed	79
4.1 Introduction	79
4.2 Materials and methods	81
4.2.1 Origin of the pellets	81
4.2.2 Moisture content measurement	82
4.2.3 Geometry measurement	82
4.2.4 Sorption isotherm measurement	82
4.2.5 Drying experiment	83
4.2.6 Identification of D_{eff}	84
4.3 Modeling of the drying-cooling	86
4.3.1 Heat and mass balances	86
4.3.2 Simulation and optimization	88
4.4 Results and discussion	89
4.4.1 Sorption isotherms	89
4.4.2 Identification of D_{eff}	92
4.5 Conclusion	92
References	96
5 Model reduction technique for faster simulation of drying of spherical solid foods	99
5.1 Introduction	100
5.2 Nomenclature	101
5.3 Diffusion/convection models	104
5.3.1 Mass balance	104
5.3.2 Heat balance	104
5.3.3 Evaporation rate	105
5.3.4 Finite volume numerical solution	106
5.4 Three-compartment model (noted $[3X \bullet 3T \bullet \Delta a_w]$ and $[3X \bullet 1T \bullet \Delta a_w]$)	108
5.5 Exact solution of mass transfer uncoupled from heat transfer (noted $[\nabla X \bullet 0T \bullet \Delta X]$)	109
5.6 Results and discussion	110

5.6.1	Optimisation of compartment sizes	110
5.6.2	Validation of heat transfers	112
5.6.3	Validation with coupled heat and mass transfers and non-constant diffusivity	113
5.7	Conclusion	115
5.8	Acknowledgements	115
	References	115
6	Simulation and data reconciliation of a food process using a generic simulator (ProSimPlus®): case of a sugar beet factory	119
6.1	Introduction	119
6.2	Sugar beet process description	121
6.3	Sugar beet process modelling	123
6.3.1	Constituents and thermodynamic model	123
6.3.2	Modelling of the sugar beet process	125
6.4	Results and discussion	132
6.5	Conclusion and perspectives	133
6.6	Acknowledgments	134
	References	134
7	Combined Pinch and exergy analysis for energy optimization of a sugar beet factory using a generic simulator (ProSimPlus®)	137
7.1	Introduction	137
7.2	Sugar beet process description	139
7.3	Sugar beet process modelling	140
7.4	Energy optimization methods	142
7.4.1	Exergy analysis	142
7.4.2	Pinch analysis	143
7.5	Results and discussion	145
7.5.1	Energy analysis of the current factory	145
7.5.2	Energy analysis of the improved case studies	149
7.5.3	Discussion	151
7.6	Acknowledgments	153
	References	153

Chapitre 1

Synthèse du travail de doctorat

1.1 Introduction générale

À quelques jours de la conférence sur le climat à Paris, la lutte contre le réchauffement climatique est au cœur des préoccupations politiques mondiales. L'objectif de la COP21/CMP11¹ est d'aboutir à un accord international, applicable dans tous les pays, visant à maintenir le réchauffement climatique mondial en deçà de 2 °C [1]. Des solutions potentielles de limitation du réchauffement climatique sont la réduction des émissions de gaz à effet de serre, le développement d'énergies renouvelables (*e.g.* éolien, solaire) et l'amélioration de l'efficacité énergétique des procédés industriels [2]. L'efficacité énergétique peut être définie comme la quantité d'énergie nécessaire à la production d'une tonne de produit [3]. Les réglementations européennes récentes encadrent l'amélioration de cette efficacité. Elles imposent d'une part aux grandes entreprises (> 250 employés ou dont le CA/an ≥ 50 M€) d'effectuer tous les 4 ans un audit énergétique de leurs usines [4], et d'autre part, la mise en place d'actions concrètes afin de réduire de 40 % les émissions de gaz à effet de serre par rapport à 1990, d'améliorer de 20 % l'efficacité énergétique des industries et habitations et d'utiliser 27 % d'énergies renouvelables d'ici à 2030 [5]. Pour faire face à la réglementation européenne et aux coûts croissants des énergies fossiles, les industriels sont tenus d'améliorer continuellement leurs procédés. Afin de les aider à atteindre les objectifs fixés, le développement d'outils de simulation et d'analyse énergétique des sites industriels est nécessaire.

En génie chimique, des logiciels génériques permettent de simuler des usines complètes (*e.g.* ProSimPlus®, Aspen Plus®, Aspen HYSIS®, PRO/II®, gPROMS®). Ces simulateurs sont constitués d'une part d'un module de calcul des propriétés thermophysiques et d'équilibre et d'autre part d'une bibliothèque de modules d'opérations unitaires en régime permanent. Ces simulateurs sont dédiés à l'étude de mélanges de corps purs à l'état liquide et/ou vapeur. Les propriétés thermophysiques des mélanges peuvent être calculées à l'aide de modèles thermodynamiques fondés sur des équations d'état (modèle "prédictif" adapté aux composés non polaires) ou sur des coefficients d'activité (adaptés aux composés polaires ou apolaires). Les modèles utilisant les coefficients d'activités sont "empiriques" (*e.g.* NRTL, UNIQUAC) ou "prédictifs" (*e.g.* UNIFAC, basé sur des contributions de groupes moléculaires) [6]. Contrairement aux modèles "empiriques", les modèles "prédictifs" peuvent être utilisés directement sans identification de paramètres. Certains simulateurs sont également dotés d'outils d'analyses énergétiques telles que les analyses de pincement

1. Conférence des parties de la convention-cadre des Nations Unies sur les changements climatiques de 2015

ou d'exergie (*e.g.* ProSimPlus® [7], Aspen Plus® et PRO/II® [8]). L'analyse de pincement permet d'optimiser un réseau d'échangeurs de chaleur en maximisant la récupération de chaleur au sein de l'usine tout en minimisant le besoin en utilités chaudes et froides. L'analyse exergétique permet d'identifier le potentiel d'économie d'énergie en calculant l'efficacité de son utilisation au sein de chaque opération unitaire du procédé industriel (*i.e.* irréversibilité, pertes d'exergie physique et chimique, production d'entropie).

En génie alimentaire, l'amélioration de l'efficacité énergétique des opérations unitaires se fait essentiellement via l'amélioration des équipements (*e.g.* amélioration des rendements des moteurs, gestion des recyclages de l'air ou de la vapeur d'eau dans les séchoirs/fours). Contrairement au génie chimique, le génie alimentaire ne dispose pas d'outils de simulation et d'optimisation énergétique à l'échelle d'une usine complète. En effet, de nombreux produits alimentaires sont des mélanges de gaz, de liquides et de solides, et sont le siège de nombreuses réactions chimiques au cours des opérations unitaires, induisant de profondes modifications de la structure et de la composition de l'aliment. Les propriétés thermophysiques des aliments solides ne peuvent être prédites par des modèles thermodynamiques basés sur des équations d'état ou des coefficients d'activités. Les logiciels de simulation de procédés sont généralement spécifiques à la fois d'une sous-classe de procédés alimentaires (*e.g.* le séchage par atomisation à l'air chaud) et d'une sous-classe de produit (*e.g.* le lait). Ces logiciels sont le plus souvent développés au sein de laboratoires et simulent une opération unitaire en régime transitoire ou permanent. Dans le domaine du séchage, on peut citer quelques logiciels commerciaux tels que Symprosis® [9], DryPAK® [10], DrySel® [11], Dryer3000®, et SP2P® [12]. À ce jour, aucun logiciel commercial n'est capable de simuler à la fois un ensemble d'opérations unitaires alimentaires et de calculer les propriétés thermophysiques nécessaires des aliments. Trois verrous scientifiques majeurs en sont responsables :

1. prédire les propriétés thermophysiques des produits alimentaires,
2. inclure des modules spécifiques des opérations unitaires alimentaires dans un logiciel générique,
3. adapter les modules logiciels génériques existants aux opérations unitaires alimentaires.

Le projet *COOPERE-2 (COmbiner Optimisation des ProcédÉs, Récupération énergétique et analyse Exergétique pour une meilleure efficacité énergétique des sites industriels)* aspire à développer des outils de simulation et d'analyse énergétique des sites industriels, notamment alimentaires. L'optimisation énergétique porte sur une combinaison de l'intégration thermique (méthode de pincement) et de l'analyse exergétique élargie aux procédés chimiques et alimentaires ainsi que sur la valorisation des coproduits. Les principaux développements logiciels du projet ont été effectués dans ProSimPlus®, logiciel de simulation de procédés en régime permanent, et s'articulent autour de deux axes :

- le développement de modules d'opérations unitaires spécifiques aux procédés alimentaires et leur validation à l'aide de données à l'échelle pilote ou industrielle,
- le développement de modules de production d'utilités (moteur à gaz, chaudière), de l'intégration thermique (pompe à chaleur, cycle de Rankine, turbine à gaz) et de valorisation des coproduits (méthanisation et combustion), et leur validation à l'aide de données à l'échelle pilote ou industrielle,
- le développement d'un module d'estimation de l'exergie des courants d'un procédé et de l'évaluation de l'efficacité exergétique de chaque opération unitaire. La validation de ce module est réalisée à l'aide d'analyses énergétiques de sites industriels.

Ce projet, financé par l’A.N.R. (Agence Nationale de la Recherche), est coordonné par *V.E.R.I.* (Veolia Recherche et Innovation) et regroupe également trois partenaires académiques (Laboratoire de Génie Chimique à Toulouse et AgroParis-Tech - UMR 1145 Ingénierie, Procédés, Aliments à Massy) et industriel (ProSim S.A.). Ce doctorat, partie intégrante de ce projet, traite de l’adaptation de logiciels génériques issus du génie chimique à la simulation et à l’optimisation énergétique de procédés alimentaires.

Le séchage est l’une des opérations unitaires les plus répandues dans l’industrie agroalimentaire. Son principe est l’élimination par évaporation (ou par ébullition) de l’eau d’un corps humide (liquide ou solide), le produit final étant toujours à l’état solide. La consommation énergétique des séchoirs représente entre 10 et 15 % de la consommation énergétique industrielle totale de la France, des États-Unis, du Canada et du Royaume-Uni et entre 20 et 25 % de celle du Danemark et de l’Allemagne. De surcroît, 85 % des séchoirs industriels sont de type convectifs [13]. Pour ces raisons, le développement de modules logiciels de séchage convectif est prioritaire par rapport aux autres opérations unitaires spécifiques de l’alimentaire. Un des axes de ce doctorat porte sur le développement d’un module logiciel de séchage convectif. De nombreuses propriétés thermophysiques sont nécessaires à la simulation du séchage par convection (dimensions, porosité, densité, conductivité thermique apparente, capacité calorifique à pression constante apparente, diffusion apparente de l’eau, activité de l’eau, coefficients de transfert par convection). Étant donné que les utilisateurs du module seront majoritairement des industriels, le minimum d’essais expérimentaux devrait être requis pour estimer ces propriétés. Idéalement, toutes les propriétés devraient pouvoir être estimées à l’aide de corrélations disponibles dans la littérature. Un des axes de ce travail traite de l’étude des méthodes d’estimation des propriétés thermophysiques nécessaires à la simulation du séchage convectif.

Proposer une démarche d’analyse énergétique pour les procédés alimentaires dans un simulateur et démontrer la capacité des modèles à prendre en compte l’ensemble des aspects énergétiques représente un vrai challenge scientifique. Un des axes de ce travail porte sur le développement d’une méthode de modélisation d’une usine agroalimentaire dans ProSimPlus®, à l’aide de modules d’opérations unitaires génériques et basiques existants. Ce type de modèle permet à la fois de réconcilier des données industrielles et de pouvoir appliquer des méthodes d’optimisation énergétique, telles que la combinaison des analyses de pincement et d’exergie. Le cas d’étude porte sur une sucrerie de betteraves.

Trois volets scientifiques sont développés dans la suite de cette synthèse. Le premier traite des méthodes d’estimation des propriétés thermophysiques des aliments nécessaires à la simulation du séchage convectif. Le second porte sur la description du modèle de séchage convectif développé et de ses applications. Le troisième traite de la simulation et de l’analyse énergétique d’une sucrerie de betteraves. Enfin, les principales conclusions générales et perspectives de ce travail de doctorat sont développées dans la dernière section.

1.2 Estimation de propriétés thermophysiques des aliments requises à la simulation du séchage convectif

Cet état de l'art, sur l'estimation de quelques propriétés thermophysiques nécessaires à la simulation du séchage convectif, fait en partie l'objet d'un article publié dans *Drying Technology* [14] et du chapitre 2. L'estimation des propriétés suivantes a été étudiée : dimensions, masse volumique apparente, conductivité thermique apparente, capacité calorifique apparente à pression constante, diffusion apparente de l'eau, activité de l'eau, et coefficients de transfert par convection. Certaines propriétés sont facilement mesurables expérimentalement (coût d'appareils de mesures faible, peu d'essais expérimentaux et de données nécessaires). On peut par exemple citer les mesures de géométrie et de dimensions (*e.g.* avec un pied à coulisse ou un scanner et un logiciel d'analyse d'image). D'autres propriétés, dont la mesure requiert un travail expérimental plus important, peuvent être estimées à l'aide de corrélations disponibles dans la littérature. Ces corrélations, prédictives ou empiriques, dépendent généralement de variables d'état telles que la température et la composition. La composition de la plupart des aliments, et plus généralement des matériaux d'origine biologique, est disponible dans des bases de données (*e.g.* CIQUAL [15], USDA nutrient database [16]) ou des ouvrages [17]. Leur composition est exprimée sous la forme de fractions massiques en pseudo-constituants (eau, sucres totaux, protéines, lipides et minéraux). La fraction massive de quelques composés majoritaires de chaque pseudo-constituant est également fournie. Contrairement aux corrélations empiriques, les corrélations prédictives peuvent être utilisées directement sans identification de paramètres. Les corrélations (prédictives ou empiriques) sont génériques ou spécifiques (valables pour un nombre restreint de produits et/ou de conditions opératoires). Pour chacune des propriétés estimées par une corrélation, Gulati et Datta [18] indiquent que l'erreur commise est généralement inférieure à 10 % et qu'un compromis doit être fait entre :

- une validité sur l'ensemble des conditions opératoires,
- le moins possible de données expérimentales requises,
- le plus faible écart possible entre les valeurs expérimentales et estimées,
- une corrélation la moins complexe possible en terme d'implémentation informatique.

L'estimation des coefficients de transfert thermique par convection est largement discutée dans la littérature [19, 20]. Quelques éléments sont rappelés ici. Ils peuvent être estimés à l'aide de corrélations prédictives, fonctions de nombres adimensionnels (Reynolds et Prandtl). De nombreuses corrélations ont été développées pour le séchage en lit fixe et fluidisé et pour différentes géométries idéales (cylindre, sphère, plaque infinie, cube). Les plus citées sont les suivantes :

- Ranz-Marshall [21] valable pour une sphère isolée en lit fluidisé,
- Whitaker [22], valable pour des cylindres infinis en lit fluidisé ou fixe,
- Wakao et Kaguei [23], valable pour des sphères en lit fixe,
- Gupta et Todos [24], valable pour des sphères, cylindres et cubes en lit fluidisé et fixe.

Les coefficients de transfert massique par convection peuvent également être estimés à l'aide de corrélations prédictives dépendant notamment de nombres adimensionnels et de coefficients de transfert thermique par convection. Les plus citées dans la littérature sont les

analogies de Chilton-Colburn [25] et de Lewis [26].

La densité, la conductivité thermique apparente et la capacité calorique apparente à pression constante des aliments peuvent être estimées par des corrélations. De nombreuses corrélations prédictives sont disponibles pour la capacité calorifique apparente à pression constante des aliments, avec une erreur inférieure à 10 %. La corrélation générique de Choi et Okos [27], valable pour tout aliment, est l'une des plus citées dans la littérature. Elle dépend de la pseudo-composition des aliments (eau, sucres totaux, protéines, lipides minéraux et air) et de la température. De nombreuses corrélations prédictives et empiriques permettent d'estimer la densité apparente des aliments avec une erreur inférieure à 10 %. Parmi les corrélations prédictives, celle de Choi et Okos [27] est la plus utilisée. Des corrélations génératives et empiriques, comme celle de Khaloufi *et al.* [28] dépendent de la porosité, de la teneur en eau et du rétrécissement au cours du séchage. Des corrélations génératives telles que celles de Choi et Okos [27] sont communément conseillées par la communauté pour l'estimation de la masse volumique apparente et de la capacité calorifique apparente à pression constante dans le cadre de la simulation de procédés thermiques (*e.g.* cuisson, séchage).

Les corrélations disponibles dans la littérature pour l'estimation de la conductivité thermique apparente sont classées en fonction des types de produits (produits alimentaires poreux/non poreux et surgelés/non surgelés). Concernant les produits alimentaires non surgelés, des corrélations prédictives sont valables uniquement pour les produits poreux et non poreux, l'erreur de prédiction est alors de l'ordre de 15 %. Ces corrélations sont des fonctions polynomiales dépendant de la pseudo-composition des aliments et de la température (*e.g.* corrélation de Choi et Okos [27] pour tous les aliments, corrélation de Sweat [29] pour les fruits et légumes). Des corrélations empiriques sont valables pour des produits poreux et non poreux. Ces corrélations, sous la forme d'un quotient de polynômes, sont des fonctions de la température, de la pseudo-composition sous la forme d'un mélange binaire et d'un facteur structurel. Le facteur structurel doit être identifié pour chaque produit alimentaire à l'aide de données expérimentales. L'erreur de prédiction est généralement inférieure à 10 % [30]. Dans le cas des aliments non poreux, les modèles de Maxwell-Eucken [31], de Levy [30] et de Kopelman [30] sont les plus répandus dans la littérature. Pour les produits alimentaires poreux, on peut notamment citer les corrélations d'Hamilton [30], de Kriesher [31], de Chaudhary-Bandary [32], de Kirpatrick [32], et de Maxwell-modifiée par Carson [33]. D'autres auteurs ont également appliqué la méthode des réseaux de neurones seule ou couplée à la logique floue à l'estimation de la conductivité thermique apparente de produits issus de la boulangerie [34], et de fruits et légumes [35, 36]. Les erreurs de prédictions sont respectivement de l'ordre de 15 % dans le cas de l'application des réseaux de neurones seule et inférieur à 2 % dans le cas de couplage avec la logique floue. Dans les deux cas, le nombre de données expérimentales requises est supérieur à 500. Ainsi, bien que plus précise par rapport aux corrélations adaptées aux aliments poreux et non poreux, l'utilisation de réseaux de neurones couplés à la logique floue semble difficile pour un industriel. Pour les aliments poreux et non poreux, les corrélations empiriques, fonction d'un facteur structurel, sont conseillées par le groupe Cost90 (COSTHERM) [37]. Les corrélations prédictives, directement utilisables, peuvent cependant être utilisées en première approche d'une modélisation de procédés alimentaires incluant des produits non poreux.

L'estimation de l'activité de l'eau requiert un travail expérimental beaucoup plus important. Cette propriété est identifiée à partir des isothermes d'adsorption/désorption obtenues

par méthode gravimétrique ou manométrique. Par ailleurs, de nombreuses corrélations empiriques, disponibles dans la littérature, sont valables pour des aliments à l'état liquide et solide. Les cinq corrélations recommandées par l'ASAE² [38] sont les corrélations de BET (Brunauer, Emmet, Teller) [39], de GAB (Guggenheim, Anderson et Boer) [40, 41], de Ferro-Fontan [42, 43], de Chung-Pfost [44] et d'Henderson modifiée [45, 46]. Les erreurs de prédictions sont inférieures à 5 % [47, 48]. Des modèles thermodynamiques, fonctions de coefficients d'activité, sont également utilisés pour estimer l'activité de solutés dans l'eau en concentration à dilution infinie avec une erreur de prédition inférieure à 5 %. On peut notamment citer les corrélations de Flory-Huggins [49, 50], de Norrish [51], de Ross [52], de Tesch *et al.* [53] et de Caurie [54]. Certains auteurs [55, 56] ont appliqués ces modèles à des produits alimentaires réels (fruits, légumes et féculents). L'erreur de prédition obtenue est inférieure à 20 %. Des modèles thermodynamiques classiques issus du génie chimique, basés sur les coefficients d'activité ont également été appliqués à l'estimation des propriétés thermophysiques de mélanges de solutés dilués dans l'eau :

- modèles de type UNIFAC (UNIFAC, UNIFAC-Larsen) modifiés pour prendre en compte les interactions électrostatiques entre les ions [57, 58], les équilibres d'hydratation et de conformation des sucres [59, 60, 61, 62, 63, 64]. L'erreur de prédition est inférieure à 5 %.
- modèles de type UNIQUAC appliqués aux mélanges liquide-liquide et liquide-solides de sucres dans l'eau [65]. L'erreur de prédition est inférieure à 1 %.
- modèles de type ASOG appliqués aux solutions de carbohydrates diluées à concentrées [66]. L'erreur de prédition est inférieure à 5 %.
- modèles de type COSMO-RS-PDHS utilisé pour estimer les propriétés thermophysiques de solutés dans l'eau en concentration infinie (*i.e.* alcanes, alcools, phénols, aldéhydes et composés aromatiques) [67, 68]. L'erreur de prédition est inférieure à 5 %.

Les modèles thermodynamiques classiquement utilisés en génie chimique sont prometteurs. Néanmoins, ils ne sont pas applicables aux aliments solides. Ainsi, pour l'estimation de l'activité de l'eau des aliments solides, l'utilisation des corrélations recommandées par l'ASAE est préconisée. Cependant, l'identification des paramètres de ces corrélations est requise pour chaque formulation d'aliment.

L'estimation de la diffusion apparente de l'eau requiert également un travail expérimental important. Cette propriété est identifiée à partir de données acquises à l'équilibre par méthode gravimétrique ou acquises en régime stationnaire à partir de cinétiques de séchage ou d'isothermes d'adsorption/désorption [69]. Pour identifier la diffusion apparente de l'eau à partir de données à l'équilibre, un bilan global de matière est nécessaire. Le plus souvent la première loi de Fick est utilisée. Cette méthode, simple et peu coûteuse, est très utilisée pour la caractérisation de matériaux. Cependant, cette propriété identifiée en régime permanent ne peut être utilisée dans un modèle de séchage convectif en régime stationnaire [70]. Deux prérequis existent avant toute identification de la diffusion apparente de l'eau à partir de données acquises en régime stationnaire : d'une part, le développement d'un modèle de séchage par convection, consistant en un bilan microscopique de matière et d'énergie le plus souvent basé sur les secondes lois de Fick et de Fourier, et d'autre part, la mesure ou l'estimation à l'aide de corrélations de toutes les propriétés listées ci-dessus [70]. De nombreux auteurs [71, 72, 73, 74, 32, 75] relatent l'effet des conditions expérimentales des cinétiques de séchage ou des isothermes d'adsorption/désorption (température, humidité relative, vitesse

2. Association américaine des ingénieurs agricoles

d'air) ainsi que des propriétés des aliments (propriétés hygroscopiques, structure, composition) sur les valeurs identifiées. De nombreuses corrélations empiriques sont disponibles dans la littérature ; elles ont été compilées par Zogsas *et al.* [73]. La plupart des auteurs confirment que l'effet de la température est bien prédit par une loi de type Arrhenius. L'effet de la teneur en eau, moindre que celui de la température, est souvent représenté par une loi exponentielle ou polynomiale [73]. Pour les produits ayant un rétrécissement important au cours du séchage, la corrélation de la diffusivité apparente devrait également tenir compte de l'évolution de la porosité [74].

L'identification est généralement réalisée en trois étapes :

1. mesure ou estimation des propriétés nécessaires à la simulation du séchage (*e.g.* dimension, porosité, capacité calorifique à pression constante, conductivité thermique, activité de l'eau *etc.*), et acquisition des cinétiques de séchage en couche mince ou des isothermes d'adsorption/désorption (lot d'apprentissage) en conditions constantes,
2. identification des paramètres de la corrélation de la diffusion apparente de l'eau,
3. validation de la corrélation à l'aide de cinétiques de séchage en couche épaisse à l'échelle pilote ou industrielle.

La diffusion apparente de l'eau étant une propriété intrinsèque des matériaux, les valeurs identifiées à l'échelle d'une particule ou d'une couche fine de particules devraient être valables à l'échelle d'une couche épaisse. Cependant, un écart non négligeable est souvent observé entre les variables de l'air mesurées et simulées en sortie de séchoir (température, humidité relative). De plus, les valeurs identifiées sont généralement valables pour une gamme de conditions opératoires restreintes (plage de variations maximale de 20 à 30 °C sur la température d'entrée de l'air) [73]. Les données mesurables lors de cinétiques en couche mince ou d'isothermes d'adsorption/désorption sont les variables de l'air en entrée (température, humidité relative, vitesse) et l'évolution de la masse de produit. Contrairement aux données mesurées lors d'une cinétique en couche épaisse, celles mesurées lors de cinétique en couche mince sont uniquement représentatives du transfert de matière alors que les transferts de matière et d'énergie sont couplés au cours du séchage [76]. Le développement d'une méthode innovante d'estimation de la diffusion apparente de l'eau dans les produits alimentaires constitue un des résultats majeurs de ce travail. Cette méthode est présentée dans la sous-section suivante et détaillée dans le chapitre 3. Elle a été développée dans un article publié dans *Drying Technology* [77].

Développement d'une nouvelle méthode pour identifier la diffusivité apparente de l'eau dans les produits alimentaires

Par définition, une couche épaisse est un ensemble de couches minces, où chacune d'entre elle sèche dans des conditions d'air variables (température et humidité relative). On peut s'attendre à ce qu'une cinétique en couche épaisse apporte beaucoup plus d'informations qu'une cinétique en couche mince. La méthode proposée dans ce travail consiste en l'inverse de la méthode classique :

1. mesure ou estimation des propriétés nécessaires à la simulation du séchage (*e.g.* dimension, porosité, capacité calorifique à pression constante, conductivité thermique, activité de l'eau *etc.*),
2. identification des paramètres de la corrélation de la diffusion apparente de l'eau à partir d'une ou deux cinétiques en couche épaisse,

3. validation de la corrélation à l'aide de cinétiques de séchage en couche mince et épaisse à l'échelle pilote ou industrielle.

Les avantages attendus sont l'obtention de meilleures intervalles de confiance pour l'estimation des paramètres de la corrélation de la diffusion apparente de l'eau ainsi que la réduction du nombre d'essais expérimentaux à réaliser (une à deux couches épaisses versus de nombreuses couches minces).

Cette méthode a été appliquée au séchage de différentes formulations de même géométrie mais de composition différente de granulés pour animaux (granulés pour poulets et lapins). Ces résultats ont été valorisés sous la forme d'articles publiés [77] et récemment soumis [78].

Concernant l'aliment pour poulets, deux corrélations ont été testées (loi d'Arrhenius et la corrélation d'Abud *et al.* [79]). Les conditions opératoires de la cinétique d'apprentissage en couche épaisse sont les suivantes : une hauteur de couche de 18 cm et une température, humidité relative et vitesse d'air en entrée de séchoir respectivement de 90 °C, de 3,4 % HR et de 1 m.s⁻¹. Nous montrons qu'avec une identification à l'aide d'une seule cinétique en couche épaisse mesurée à haute température, quelle que soit la corrélation, les valeurs identifiées sont valables :

- pour toute cinétique de séchage en couche mince obtenue à des températures inférieures ou égales à 70 °C [77].
- pour une cinétique de séchage-refroidissement en couche épaisse dont les conditions opératoires sont les suivantes : température initiale des granulés de 60 °C, température, humidité relative et vitesse d'air en entrée de séchoir respectivement de 30 °C, de 27 % et de 1 m.s⁻¹ [78].

Concernant l'aliment pour lapins, deux cinétiques de séchage en couche épaisse (40 et 80 °C) ont été utilisées pour estimer les paramètres de la corrélation d'Abud *et al.* [79]. Les valeurs estimées sont valables pour toutes les cinétiques en couche mince dont les températures d'air d'entrée sont inférieures ou égales à 80 °C [78]. Quelle que soit la formulation, les erreurs moyennes d'estimation sont dans l'ordre de grandeur des incertitudes de mesures expérimentales (*i.e.* ± 0,018 *d.b.* pour la teneur en eau moyenne et ± 2,5 °C pour la température de l'air en sortie de séchoir).

Conclusions et perspectives

Les coefficients de transfert par convection, la densité apparente, la capacité calorifique apparente à pression constante peuvent être estimés à l'aide de corrélations prédictives. L'utilisation de corrélations empiriques est conseillée pour l'estimation de la conductivité thermique apparente des aliments. Des corrélations prédictives peuvent cependant être utilisées dans une première approche de simulation du séchage de produits alimentaires ayant un faible rétrécissement au cours de celui-ci. L'activité de l'eau des aliments peut être estimée à l'aide de corrélations empiriques ou de modèles thermodynamiques (empiriques et prédictifs) classiquement utilisés en génie chimique. L'utilisation des modèles thermodynamiques est prometteuse, néanmoins ces derniers ne sont pas applicables aux aliments solides. Ainsi, l'utilisation des corrélations empiriques est préconisée pour l'estimation de l'activité de l'eau des aliments solides. Cependant, l'identification des paramètres de ces corrélations est requise pour chaque formulation. Enfin, l'estimation de la diffusivité apparente de l'eau à partir de cinétiques de séchage en couche mince requiert également un travail expérimental important. Une méthode rapide et innovante d'estimation de cette propriété a été développée dans le cadre de ce doctorat. Cette méthode consiste à identifier les paramètres de la corrélation

à l'aide d'une à deux cinétiques en couche épaisse et à les valider à l'aide de cinétiques en couche mince et épaisse. Les valeurs identifiées sont valables pour de grandes et hautes plages de conditions opératoires (température de l'air en entrée de séchoir comprise entre 30 et 80 °C).

Selon notre analyse, ces résultats ouvrent sur de nombreuses perspectives. Concernant l'activité de l'eau, une piste de recherche pourrait être l'étude de l'impact de la formulation et du procédé sur les isothermes d'adsorption/désorption. A partir d'une compilation de données expérimentales disponibles dans la littérature, on pourrait ainsi regarder si une même corrélation (avec les mêmes valeurs de paramètres) ne pourrait pas être utilisée pour estimer l'activité de l'eau d'une classe d'aliments. Par ailleurs, une piste d'amélioration de la méthode d'identification de la diffusivité apparente de l'eau serait l'utilisation de la planification expérimentale non linéaire *NLMBSDOE* (Non Linear Model Based Sequential Design of Optimal Experiments) [80] pour estimer les conditions opératoires optimales de la cinétique d'apprentissage. Des conditions opératoires variables permettraient d'apporter davantage d'informations. On pourrait alors s'attendre à ce que l'erreur moyenne d'estimation soit plus faible. La diffusivité apparente de l'eau étant une propriété intrinsèque, une autre perspective serait de s'assurer que les valeurs de paramètres identifiés soient valables pour le séchage d'une seule particule. Un dispositif expérimental, constitué d'une chambre dans laquelle la température et l'humidité relative sont contrôlées à l'entrée et mesurées dans l'enceinte, et d'un plateau dans lequel reposeraient l'échantillon, relié à une balance gravimétrique précise, pourrait être utilisé.

1.3 Développement d'un modèle générique de séchage convectif de produits alimentaires solides par air chaud

Les éléments présentés dans cette section font l'objet d'un article publié dans *Drying Technology* [14] et sont détaillés dans le chapitre 2. Le cahier des charges attendu pour un modèle d'opération unitaire implémenté sous la forme d'un module dans un logiciel générique de simulation de procédés est le suivant :

- temps de simulation court : le temps de simulation du module ne devrait pas durer plus de "quelques secondes" à au maximum "une à deux minutes",
- travail expérimental réduit : idéalement toutes les propriétés thermophysiques requises devraient être estimables à l'aide de corrélations, ou du moins mesurées ou identifiées par méthode inverse avec le minimum de travail expérimental,
- validité sur une large gamme de conditions opératoires (*e.g.* 30 - 80 °C dans le cas du séchage convectif par air chaud),
- "généricité" du modèle : le module devrait être valable pour une classe ou une sous-classe de produits (*e.g.* céréales) et également pour plusieurs technologies d'une même catégorie d'opérations unitaires (*e.g.* séchoir tapis/multi-tapis, en lit fluidisé, tambour, par atomisation, pneumatique, tunnel),
- implémentation standardisée du modèle : afin de pouvoir simuler un ensemble de modules d'opérations unitaires, tous les modules doivent avoir la même structure générale (uniformité de toutes les entrées et sorties des modules). Idéalement, le module devrait être compatible avec un standard d'interopérabilité des logiciels (CAPE-OPEN [83]).

Dans le cadre de ce doctorat, nous nous sommes intéressés à la modélisation du séchage par convection d'aliments solides. Les différents modèles disponibles dans la littérature peuvent être classés en trois catégories : les modèles "boîte noire", "boîte blanche simplifiée" et "boîte blanche sophistiquée". Les caractéristiques ainsi que les avantages et inconvénients de ces catégories sont donnés dans le tableau 1.1. Ces catégories de modèles peuvent être comparées entre elles à travers différentes caractéristiques correspondant aux prérequis du cahier des charges d'un module logiciel. D'après notre analyse, un modèle "boîte blanche simplifiée" constitue le meilleur compromis entre ces trois catégories.

Un modèle de séchage par convection en couches minces et épaisses a été développé. La couche épaisse peut être assimilée à une série de couches minces dans lesquelles un transfert de matière et d'énergie se produit. Chaque couche mince peut également être assimilée à une (seule) particule moyenne. Un bilan de matière et d'énergie entre l'air et les particules est également réalisé après chaque couche mince afin de tenir compte de la diminution de la température et de l'enrichissement en eau de l'air au fur et à mesure de la traversée de la couche épaisse [76]. Les hypothèses suivantes sont considérées pour les particules :

- une géométrie idéale (cylindre infini ou sphère),
- un rétrécissement ou gonflement négligeable,
- un comportement isotrope (transferts en 1D dans la direction radiale),
- une conduction négligeable entre les particules.

Pour des produits alimentaires et conditions opératoires classiques, les valeurs des nombres de Biot thermique et massique sont respectivement comprises entre 0,1 et 100, et largement

TABLE 1.1 – Caractéristiques et avantages et inconvénients des différents types de modèles de séchage convectif de solides disponibles

	<i>Caractéristiques</i>	<i>Facilité de validation du modèle</i>	<i>Capacité d'extrapolation</i>	<i>Signification physique des paramètres</i>	<i>Géométrie complexe</i>	<i>Temps de simulation</i>	<i>Facilité de l'implémentation informatique</i>
<i>Modèles</i> "Boîte noire"	Modèle statique, Transfert en 0D - 1V (\bar{X}). ex : CDC, modèle de Page	++	-	-	-	++	++
<i>Modèles</i> "Boîte blanche simplifiée"	Modèle dynamique basé sur les secondes lois de Fick et Fourier, Transfert en 1D - 2V ou 3V (\bar{X}, T et parfois P), Estimation/mesure de propriétés physiques requises [18].	++	++	++	-	-	+
<i>Modèles</i> "Boîte blanche sophistiquée"	Modèle dynamique basé sur les secondes lois de Fick et Fourier, Transfert en 2D ou 3D - 3V (\bar{X}, T et parfois P), Estimation complexes de propriétés physiques requises [81]. ex : Transpore [82]	--	++	++	++	--	-(souvent réalisée à l'aide de codes commerciaux tels que COMSOL®, FLUENT®)

0D, 1D, 2D, 3D : transferts en zéro, une, deux ou trois dimensions
 1V, 2V, 3V : modèles décrit par une seule, deux ou trois variables d'état indépendantes
 \bar{X} : teneur en eau moyenne
 T : température
 P : pression
 ++ à - : du plus au moins performant pour le critère considéré

supérieures à 100. Ainsi, les phénomènes suivants sont considérés : conduction thermique et diffusion de l'eau au sein des particules et évaporation de l'eau en surface [84]. Dans les conditions opératoires classiques, les valeurs des nombres de Péclet thermique et massique étant largement supérieures à 1, l'écoulement de l'air est supposé unidirectionnel et la variation de pression au sein de la couche épaisse est négligée [84]. Il est cependant important de noter que ce modèle ne peut s'appliquer aux produits ayant une forte teneur en eau initiale, du fait de la non-prise en compte du rétrécissement au cours du séchage [74].

Dans ce modèle, les transferts sont décrits par deux variables (température et teneur en eau). La diffusion de l'eau liquide (équation 1.1) et la conduction thermique (équation 1.2) au sein des particules sont respectivement décrites par les secondes lois de Fick et de Fourier [84].

$$\frac{dX_t^{r,z}}{dt} = \frac{1}{r^n} \cdot \frac{\partial}{\partial r} \left(r^n \cdot D_{ap} \cdot \frac{\partial X_t^{r,z}}{\partial r} \right) \quad (1.1)$$

$$\frac{d(\rho_{ms} \cdot (Cp_{ms} + Cp_e \cdot X_t^{r,z}) \cdot Tp_t^{r,z})}{dt} = \frac{1}{(r)^n} \cdot \frac{\partial}{\partial r} \left(r^n \cdot \lambda_{ap} \cdot \frac{\partial Tp_t^{r,z}}{\partial r} \right) \quad (1.2)$$

Où X est la teneur en eau (b.s.), r la position radiale dans la particule (m), z la position de la particule dans la couche épaisse (m), t le temps (s), n le facteur de forme (1 ou 2 respectivement pour un cylindre infini ou une sphère), D_{ap} la diffusivité apparente de l'eau ($\text{m}^2.\text{s}^{-1}$), Tp la température de la particule (K), λ_{ap} la conductivité thermique apparente ($\text{W}.\text{m}^{-1}.\text{K}^{-1}$), ρ_{ms} la masse volumique de la matière sèche ($\text{kg}.\text{m}^{-3}$), Cp_{ms} et Cp_e la capacité calorifique à pression constante de la matière sèche et de l'eau ($\text{J}.\text{kg}^{-1}.\text{K}^{-1}$).

Les conditions aux limites sont données dans les équations 1.3 à 1.5.

$$\frac{\partial X_t^{0,z}}{\partial r} = 0 \text{ et } \frac{\partial Tp_t^{0,z}}{\partial r} = 0 \quad (1.3)$$

$$-\rho_{ms} \cdot \frac{\partial (D_{ap} \cdot X_t^{r_{max},z})}{\partial r} = k_m \cdot \frac{M_e}{R} \cdot \left(\frac{a_w \cdot Pv_{sat}(Tp_t^{r_{max},z})}{Tp_t^{r_{max},z}} - \frac{HR \cdot Pv_{sat}(Ta_t^z)}{Ta_t^z} \right) = \varphi_m \quad (1.4)$$

$$\lambda_{ap} \cdot \frac{\partial Tp_t^{r_{max},z}}{\partial r} = h_{glob} \cdot (Ta_t^z - Tp_t^{r_{max},z}) - \varphi_m \cdot \Delta H_v(Tp_t^{r_{max},z}) = \varphi_q \quad (1.5)$$

Où k_m est le coefficient de transfert par convection de matière ($\text{m}.\text{s}^{-1}$), M_e la masse molaire de l'eau ($\text{kg}.\text{mol}^{-1}$), R la constante des gaz parfaits ($\text{J}.\text{kg}^{-1}.\text{K}^{-1}$), a_w l'activité de l'eau (Pa/Pa), Pv_{sat} la pression de vapeur saturante (Pa), HR l'humidité relative (Pa/Pa), h_{glob} le coefficient de transfert global de chaleur par convection ($\text{W}.\text{m}^{-2}.\text{K}^{-1}$), Ta la température de l'air (K), ΔH_v l'enthalpie de vaporisation de l'eau pure ($\text{J}.\text{kg}^{-1}$), φ_m la densité de flux de matière ($\text{kg}_e.\text{s}^{-1}.\text{m}^{-2}$) et φ_q la densité de flux de chaleur ($\text{J}.\text{s}^{-1}.\text{m}^{-2}$).

Un bilan de matière et d'énergie est réalisé après chaque traversée de couche mince au sein de la couche épaisse (équations 1.6 et 1.7). La teneur en eau et la température de l'air en entrée de séchoir sont fixées et peuvent être variables au cours d'une cinétique de séchage.

$$\frac{d(\rho_{as} \cdot Y_t^z)}{dt} = -\frac{\partial (\rho_{as} \cdot v_a \cdot Y_t^z)}{\partial z} + \frac{\varphi_m \cdot a \cdot (1 - \varepsilon)}{\varepsilon} \quad (1.6)$$

$$\frac{d(\rho_{as} \cdot (Cp_{as} + Y_t^z \cdot Cp_v) \cdot Ta_t^z)}{dt} = -\frac{\partial (v_a \cdot \rho_{as} \cdot (Cp_{as} + Y_t^z \cdot Cp_{as}) \cdot Ta_t^z)}{\partial z} - \frac{a \cdot (1 - \varepsilon) \cdot \varphi_q}{\varepsilon} \quad (1.7)$$

Où ρ_{as} est la masse volumique de l'air sec ($\text{kg} \cdot \text{m}^{-3}$), a la surface spécifique (surface par volume de particule) (m^{-1}), ε la porosité du tas de particules (décimale), Y la teneur en eau (b.s.), Cp_{as} et Cp_v la capacité calorifique à pression constante de l'air sec et de la vapeur d'eau ($\text{J} \cdot \text{kg}^{-1} \cdot \text{K}^{-1}$).

Le système dynamique composé de 6 équations aux dérivées partielles (équations 1.1 à 1.5) sont discrétisées dans l'espace en équations différentielles ordinaires (EDO) par la méthode des volumes finis. Ces EDO sont intégrées dans le temps par la méthode de Runge-Kutta Cash-Karp (d'ordre 4 et 5) [85]. Par ailleurs, 13 paramètres, ayant tous une signification physique sont requis pour la simulation du modèle de séchage (dimensions des particules, porosité, masse volumique apparente, conductivité thermique apparente, capacité calorifique à pression constante apparente, diffusion apparente de l'eau, activité de l'eau, coefficients de transfert par convection, chaleur latente de vaporisation). Comme indiqué dans la section précédente, ces propriétés peuvent être mesurées directement, estimées à l'aide de corrélations ou identifiées par méthode inverse (cas de la diffusivité apparente et de l'activité de l'eau).

Ce modèle a été appliqué au séchage en couche mince et épaisse de divers produits céréaliers de formulations et de géométries différentes (de forme sphérique pour le maïs et les graines de soja, de forme cylindrique pour les granulés pour poulets et lapins). Il a également été appliqué à une autre technologie de séchage, le séchage-refroidissement de granulés pour poulets. Ces résultats ont été valorisés sous la forme d'articles publiés [77, 14] et récemment soumis [78]. Le modèle permet de simuler différentes technologies de séchage. Le modèle en couche épaisse permet de simuler un séchage en lit fixe, de type tapis ou un séchage-refroidissement. Le modèle en couche mince permet de simuler un séchage en lit fluidisé.

Ce modèle de séchage convectif a été développé dans 2 langages :

- un code en C++, notamment pour identifier les paramètres de la corrélation de la diffusion apparente et valider le modèle à l'aide de cinétiques de séchage obtenues à l'échelle pilote,
- un code propriétaire en Fortran : ce code constitue un module logiciel en cours d'implémentation dans la base de données de modules d'opérations unitaires du logiciel ProSimPlus®.

Le module de séchage peut être relié à tout autre module déjà existant dans ProSimPlus®, par exemple à des modules de production d'utilités. Il est également relié à la base de données d'estimation de propriétés thermophysiques Simulis Thermodynamics®. L'utilisateur doit fournir certaines entrées du module :

- communes à tous les modules : débit, température, pression et composition des flux entrants (air humide et produits solides humides)
- spécifiques au module de séchage :
 - géométrie et dimensions des particules,
 - porosité et hauteur du tas de particules,
 - temps de séjour ou fraction massique finale des particules,
 - choix entre diverses corrélations de diffusivité apparente et d'activité de l'eau et renseignement des valeurs des paramètres,
 - choix entre des coefficients de transfert par convection constants ou calculés à l'aide de corrélations.

Toutes les autres propriétés thermophysiques requises des aliments ainsi que celles de l'air (autres entrées du module) sont calculées dans Simuls Thermodynamics® (densité apparente, capacité calorifique apparente à pression constante et conductivité thermique apparente). Les sorties du module sont le débit, la température, la pression et la composition de l'air humides et des solides secs, l'énergie consommée, ainsi que quelques graphiques (évolution de la teneur en eau moyenne, de la température et de l'humidité relative de l'air). Un descriptif détaillé de l'utilisation du module de séchage a été publié dans *Drying Technology* [14].

Le modèle de séchage présenté dans ce travail correspond au cahier des charges d'un module d'opération unitaire classiquement implémenté dans les logiciels génériques de simulation issus du génie chimique. Cependant, le temps de calcul du module dans l'environnement de ProSimPlus® est de l'ordre de deux à trois minutes, ce qui est dix à quinze fois supérieur au temps de simulation moyen des autres opérations unitaires de ce logiciel. Pour cette raison, nous nous sommes intéressés à la réduction du modèle de séchage.

Ce travail s'inscrit dans la continuité de celui de Van der Sman [86] qui a développé un modèle simple de transfert d'énergie : chaque particule est divisée en deux compartiments (le corps et la surface). Le modèle de Van der Sman permet d'estimer la température moyenne et surfacique de particules de forme sphérique, cylindrique ou de plaque infinie au cours d'un refroidissement avec évaporation d'eau en surface aussi précisément qu'un modèle classique basé sur la seconde loi de Fourier. Le ratio des volumes des compartiments a été identifié pour chaque géométrie de particules. Le temps de simulation de son modèle est inférieur d'un facteur supérieur à 100 à celui d'un modèle classique, cependant son modèle ne peut être utilisé dans le cas de transferts couplés de matière et d'énergie. D'autres auteurs ont également développé des modèles compartimentaux pour différentes opérations unitaires (l'agglomération [87], le mélange [88], la séparation liquide-liquide [89], le séchage par convection de céréales [90, 76, 79]). Dans le cas particulier du séchage convectif de céréales, les particules sont divisées en 2 ou 3 compartiments dans lesquels le transfert de matière seul ou couplé au transfert de chaleur est considéré. La teneur en eau et la température sont considérées uniformes dans chaque compartiment. Tous les paramètres de ces modèles compartimentaux sont identifiés par méthode inverse à partir de cinétiques de séchage et n'ont aucune signification physique.

Dans un travail récemment soumis à *Journal of Food Engineering* (en cours de révision) [91], nous démontrons numériquement qu'un modèle compartimental composé de 2 ou 3 compartiments est équivalent à un modèle classique de transfert de matière et de chaleur, fondé sur les secondes lois de Fick et de Fourier. Les prédictions équivalentes des teneurs en eau et des températures moyennes des particules sphériques dans le cas d'un transfert de matière ou d'énergie seul, et de transferts couplés sont obtenus après optimisation de la taille des compartiments (fraction volumique de chaque compartiment). Les fractions volumiques des compartiments sont identifiées une fois pour toutes dans le cas d'un transfert de matière seul, en comparant les estimations du modèle compartimental à celles de la solution analytique de Crank [92]. De plus, les paramètres du modèle compartimental ont une signification physique et dépendent du rayon et des coefficients de transfert d'un modèle classique (diffusivité apparente de l'eau, conductivité thermique apparente et coefficients de transfert de matière et d'énergie par convection). Enfin, le temps de calcul du modèle compartimental est inférieur d'un facteur 100+ à celui d'un modèle classique, grâce au nombre réduit d'équations différentielles ordinaires à résoudre (6 équations au maximum pour le modèle compartimental versus généralement plus d'une centaine dans le cas d'un modèle classique).

Conclusions et perspectives

Le modèle de séchage convectif développé dans le cadre de ce travail semble répondre au cahier des charges d'un module d'opérations unitaires implémenté dans un logiciel générique de simulation de procédés issus du génie chimique. Il semble en effet pouvoir s'appliquer à différentes technologies de séchage de produits alimentaires de formulation et de géométrie différentes. Il est également valable pour une large gamme de conditions opératoires et le code de calcul a été développé de manière à être compatible avec les autres modules d'opérations unitaires du logiciel ProSimPlus®. Cependant, son temps de calcul dans l'environnement de ProSimPlus® est supérieur d'un facteur 15+ à celui des autres modules. Un travail sur la réduction de modèle a été réalisé pour pallier ce problème. Nous avons démontré que les prédictions d'un modèle compartimental, composé de 2 ou 3 compartiments, étaient équivalentes à un modèle classique comme celui développé dans ce travail, dans le cas d'un séchage en couche mince de particules sphériques. Le modèle compartimental est composé de paramètres ayant une signification physique et son temps de simulation est inférieur d'un facteur supérieur à 100 à celui d'un modèle classique.

Plusieurs perspectives émergent de ces résultats. D'une part, deux perspectives du travail sur la réduction de modèle pourraient être l'identification des ratio-volumiques des compartiments dans le cas du séchage de particules cylindriques et la vérification que les modèles classiques et compartimentaux sont bien équivalents dans le cas d'un séchage en couche épaisse. D'autre part, l'implémentation du module de séchage dans l'environnement ProSimPlus® est en cours. La finalisation du module constitue la priorité numéro 1 de la fin de ce doctorat. Par ailleurs, le modèle de séchage a jusqu'ici été validé à l'aide de données expérimentales obtenues à l'échelle pilote. Il serait intéressant de vérifier que les estimations de ce dernier sont également valables à l'échelle industrielle. Une autre perspective possible serait l'adaptation du modèle à d'autres technologies telles que les séchoirs multi-tapis ou verticaux à céréales/à grains. Dans ce cas, il serait nécessaire de prendre en compte le recyclage de l'air au sein du séchoir ainsi que le retournement du produit entre chaque tapis ou étage du séchoir. Le modèle en couche épaisse constituerait la brique élémentaire de la simulation de ce type de séchoir. Enfin, de nombreux projets de recherche portent actuellement sur le développement à l'échelle industrielle de séchoir en vapeur d'eau surchauffée dont la consommation énergétique est nettement inférieure à celle d'un séchage par entraînement. Cette technologie ne peut cependant être appliquée au séchage de produits thermosensibles. Le développement d'un module de séchage en vapeur d'eau surchauffée permettrait de pouvoir comparer différentes technologies de séchage d'un point de vue énergétique, tout en tenant compte des caractéristiques des produits alimentaires en sortie de séchoir.

1.4 Simulation et optimisation énergétique d'une usine agroalimentaire : cas d'une sucrerie de betteraves

Des méthodologies développées dans le domaine du génie chimique telles que la conception ou l'analyse énergétique assistées par ordinateur d'usines ou d'ateliers commencent à être appliquées au domaine du génie alimentaire. On peut notamment citer les travaux effectués dans le domaine de l'industrie laitière (atelier de concentration par évaporation du lait [93, 94]) ou de l'industrie sucrière (atelier de concentration par évaporation et de production d'éthanol essentiellement [95, 96, 97]). Ces ateliers sont uniquement constitués d'opérations unitaires communes avec le génie chimique et de produits à l'état liquide ou vapeur, pour lesquels les propriétés thermophysiques et d'équilibre peuvent être estimées par des modèles thermodynamiques classiques. Dans le domaine de l'industrie sucrière, certains logiciels commerciaux (Sugar® [98]) ou codes programmés au sein de laboratoires (à l'aide des langages EES® [99], QBasic® [100, 101], Matlab® [102]) permettent de simuler et parfois de calculer les productions d'irréversibilité de l'ensemble des opérations unitaires de ce procédé (spécifiques et non spécifiques). Un logiciel de simulation de procédé issu du génie chimique, Aspen Plus® a également été utilisé pour simuler l'ensemble des opérations unitaires d'une sucrerie de canne et de production d'éthanol ainsi que pour réaliser l'analyse exergétique du site [103]. À l'instar des modèles développés au sein de laboratoires, les opérations unitaires spécifiques sont simulées à l'aide de bilans globaux massiques, enthalpiques et exergétiques dans Aspen Plus®, sans modélisation des phénomènes physiques [103]. Cette méthode ne permet pas de représenter finement les productions d'irréversibilités des opérations unitaires non spécifiques ainsi que d'étudier l'effet des paramètres opératoires sur les variables de sortie et sur la production d'irréversibilités. Les contributions originales de ce travail concernant la simulation et l'optimisation énergétique d'usines agroalimentaires sont les suivantes :

- le développement d'une méthode de simulation d'une usine agroalimentaire dans un logiciel générique issu du génie chimique, incluant la modélisation des propriétés thermophysiques des flux et la modélisation de toutes les opérations unitaires (phénomènes physiques se produisant au cours des opérations unitaires spécifiques inclus),
- l'analyse énergétique d'une usine agroalimentaire, combinant l'analyse de pincement et exergétique. L'analyse de pincement comprend toutes les étapes de la minimisation des utilités à celle de la conception des réseaux d'échangeurs. Différentes améliorations techniques sont également proposées et simulées à la suite de l'analyse exergétique de l'usine actuelle.

Selon notre analyse, la modélisation d'une usine dans l'optique d'en réaliser une analyse de pincement et exergétique, dans un logiciel générique de simulation de procédé issu du génie chimique, se produit en trois étapes distinctes :

- 1. réaliser un schéma détaillé du réseau d'opérations unitaires de l'usine et collecter toutes les données disponibles** (paramètres opératoires, débit, température, pression et composition des flux),
- 2. lister les constituants à suivre tout au long du procédé ou dans certains ateliers et choisir un modèle thermodynamique adéquat pour estimer les propriétés thermophysiques et d'équilibre des flux.** Valider également les prédictions du modèle thermodynamique à l'aide de données disponibles dans la littérature ou expérimentales. Si les estimations du modèle thermodynamique ne sont pas validées,

les propriétés thermophysiques propres des constituants ou le modèle thermodynamique sont à modifier.

3. **modéliser le réseau d'opérations unitaires de l'usine et valider les prédictions du modèle à l'aide des données industrielles récoltées.** Des réconciliations de données industrielles sont requises si les prédictions du modèle ne sont pas validées. Les bilans de matière, d'énergie et d'exergie sont réalisés directement dans le logiciel. Le niveau de détail d'un modèle dépend des objectifs de son utilisation. Ainsi un modèle réalisé dans le but de boucler un bilan de matière ou d'énergie requiert un niveau de détail beaucoup plus faible que celui pour réaliser une analyse exergétique [7]. Dans ce dernier cas, toutes les productions d'irréversibilités potentielles (modification de la température, de la pression ou de la composition) de chaque opération unitaire doivent être modélisées séparément. Ainsi, une même opération unitaire peut être simulée par une combinaison de modules d'opérations unitaires telles que des turbines, des compresseurs, des vannes de détente, des échangeurs ou des séparateurs liquide-vapeur.

Les étapes 2 et 3 constituent les verrous scientifiques de la méthodologie présentée. D'une part, comme indiqué précédemment, l'estimation des propriétés thermophysiques des aliments est complexe de par leur structure (mélange solide, liquide et vapeur) et de par la mesure difficile de leur composition précise. Cette composition peut être exprimée sous la forme d'une pseudo-composition. Les propriétés des pseudo-constituants peuvent être estimées à l'aide de corrélations ou alors, les pseudo-constituants peuvent être assimilés à l'une de leurs molécules majoritaires dont le comportement est bien connu et déjà implémenté dans les bases de données de propriétés thermodynamiques [94]. D'autre part, les modules d'opérations unitaires spécifiques au génie alimentaire n'existent pas dans ces logiciels. Pour pallier ce problème, une combinaison de modules simples et génériques (mélangeurs et diviseurs de courants, séparateurs de constituants, séparateurs liquide-vapeur, vannes ou turbines) et de boucles de régulation peut être agencée. Les boucles de régulation permettent d'imposer les variables de sortie d'un module (température, pression, débit ou composition) en ajustant les paramètres opératoires des autres. Cette manière de représenter les opérations unitaires spécifiques présente néanmoins certaines limites. Si la plupart des sorties des modules sont imposées par des boucles de régulation, le modèle développé de l'usine risque de ne pas être "prédictif", empêchant la prédiction de l'effet d'un changement de composition de la matière première ou de la cadence de l'usine sur les variables de sortie. Le modèle développé permet cependant de réaliser une analyse exergétique et de pincement de l'usine, ce qui est l'objectif principal de cette étude.

Avec ces limites, cette méthodologie a été appliquée à la simulation et à l'optimisation énergétique d'une sucrerie de betteraves dans ProSimPlus®. Ce logiciel est doté de nombreux modules d'opérations unitaires ainsi que de modules permettant de réaliser une analyse exergétique (estimation de l'exergie des courants, évaluation de l'efficacité exergétique de chaque opération unitaire) et de pincement. Le procédé sucrier consiste à produire du sucre blanc et divers coproduits (pulpes pressées, écumes et sirop basse pureté) à partir de betteraves. Il est divisé en 4 principaux ateliers : extraction du sucre, clarification, concentration par évaporation et cristallisation. Par ailleurs, ce travail a été réalisé en collaboration avec V.E.R.I. et un industriel français. Pour des raisons de confidentialité, le nom de l'industriel et les caractéristiques de l'usine ne sont pas détaillés dans cette synthèse.

Les résultats concernant la modélisation de la sucrerie font l'objet du chapitre 6 et d'un article à soumettre dans *Computer and Chemical engineering Journal* courant septembre

2015 [104]. Le modèle UNIFAC-LARSEN permet d'estimer les propriétés thermophysiques. Les constituants nécessaires à la représentation des courants du procédé sont le saccharose, les "non-sucres", l'eau (communs à tous les ateliers), les résidus cellulaires (uniquement dans l'atelier d'extraction du sucre) ainsi que le dioxygène, le diazote, le dioxyde de carbone, l'oxyde de calcium et le carbonate de calcium (uniquement dans l'atelier de clarification). Les "non-sucres" et les résidus cellulaires sont constitués de nombreuses molécules. Leur composition précise n'étant généralement pas mesurée, ces derniers ont respectivement été assimilés à du saccharose (une molécule ayant un comportement très proche) et à la cellulose (un de ses constituants majoritaires). Tous les autres constituants sont déjà présents dans la base de données de propriétés thermodynamiques Simulis Thermodynamics® liée à ProSimPlus®. Les prédictions de propriétés thermophysiques des courants (capacité calorifique à pression constante et retard à l'ébullition) ont été comparées à celles des corrélations de références de Bubnik *et al.* [105]. Les écarts de prédiction sont compris dans l'ordre des incertitudes sur les mesures expérimentales.

Toutes les opérations unitaires présentes dans ce procédé ont été modélisées à l'aide de modules préexistants dans ProSimPlus®. Les opérations spécifiques (diffuseurs, presses, filtration et centrifugation) ont été modélisées à l'aide de combinaisons de modules basiques et génériques ainsi que de boucle de régulation. Par exemple, les presses ont été représentées par une combinaison d'un séparateur de constituants et de boucles de régulation. Les boucles de régulation permettent d'imposer la composition des pulpes pressées en ajustant les ratios de séparation des différents constituants.

Le modèle de la sucrerie développé a été validé par comparaison des données simulées avec celles fournies par l'industriel. Une réconciliation de données a été nécessaire dans certains ateliers (atelier de clarification, de concentration par évaporation et de cristallisation). Dans l'atelier de clarification, les données industrielles étaient parcimonieuses et fournies avec des incertitudes de mesure importantes dues à deux facteurs. Premièrement, certains flux de cet atelier sont constitués de composés solides baignant dans un liquide (jus chaulé et boues de carbonatation) rendant difficile la mesure de leur composition et débit. Deuxièmement, une fluctuation légère des variables du jus entrant (débit et composition) entraîne des variations importantes des variables des autres courants de l'atelier. Des écarts entre les données simulées et fournies de l'ordre de 25 % sur les débits et de 60 % sur les compositions ont été obtenus avant réconciliation des données. Un bilan de matière global a permis d'identifier et de recalculer les variables "non fiables" des courants. Les données considérées comme "fiables" sont celles dont les mesures sont faites en routine dans l'usine et portent sur des flux à l'état liquide uniquement. Les paramètres opératoires de certaines opérations unitaires de cet atelier ont également été recalculés (*e.g.* efficacité des filtres³). Toutes les données recalculées sont de l'ordre de grandeur de celles des autres sucreries. Au global, quel que soit l'atelier, l'écart entre les valeurs simulées et réconciliées est généralement inférieur à 1 %, attestant d'une bonne représentation du site actuel.

Les résultats concernant l'optimisation énergétique de la sucrerie sont en cours de valorisation sous la forme d'un article à soumettre dans *Energy Journal* [106] dans le courant du mois de septembre et sont détaillés dans le chapitre 7. L'analyse exergétique a montré que les irréversibilités de l'usine sont essentiellement produites dans les ateliers d'extraction du sucre (préchauffage des *cosslettes*⁴) et de concentration par évaporation (production de la vapeur

3. Efficacité des filtres : ratio des débits massiques de boues et de jus filtré

4. Cosslettes : fines lamelles de betteraves, obtenues mécaniquement, et utilisées pour l'extraction du sucre

alimentant cet atelier). Des améliorations techniques de ces parties du procédé ont été testées par simulation. Les résultats obtenus permettent une diminution de 12 % de l'irréversibilité totale de la sucrerie et une diminution nette du débit de vapeur alimentant l'atelier de concentration par évaporation, conduisant à une réduction annuelle de la facture énergétique de l'usine de l'ordre de 1 M€. L'analyse de pincement a confirmé que le réseau d'échangeurs actuel est déjà bien optimisé. Les besoins en utilités froides et chaudes ne peuvent être diminués. Le nombre d'échangeurs et la surface totale d'échange peuvent néanmoins être réduits de 25 % induisant une réduction des coûts annuels de maintenance d'environ 100 k€. L'étude démontre également que les réseaux d'échangeurs des sites "améliorés" sont déjà optimisés : les besoins en utilités froides et chaudes ainsi que la surface d'échange totale ne peuvent être diminués. Enfin, L'énergie thermique étant déjà bien intégrée dans cette sucrerie, l'optimisation du réseau d'échangeur n'a que peu d'effet sur la production totale d'irréversibilités (réduction de 1,6 %).

Conclusions et perspectives

Le modèle développé permet de représenter fidèlement les données de l'usine, et c) d'extraire directement des modules les données nécessaires à l'analyse de pincement et exergétique. Cependant, la méthodologie développée présente certaines limites, en raison de l'utilisation des boucles de régulation. Le modèle proposé ne peut prédire l'effet d'un changement de composition de la matière première ou de la cadence de l'usine sur les variables de sortie. Les analyses exergétiques et de pincement ont conduit à plusieurs résultats intéressants. Plusieurs améliorations techniques ont été proposées, conduisant à une réduction conséquente de l'irréversibilité totale et de la facture énergétique de l'usine. L'analyse des pincements a confirmé que le réseau actuel était déjà optimisé.

Plusieurs perspectives sont possibles pour le rendre plus "prédictif". Une première méthode (rapide) serait de remplacer les valeurs de variables fixées par des ratios de variables d'entrée et de sortie. Une deuxième méthode serait de développer les modules d'opérations unitaires spécifiques soit de manière simplifiée au sein de modules "script" dans ProSimPlus® (environ 7 jours de travail par module), soit de manière plus complexe conduisant au développement d'un module logiciel à part entière par opération unitaire spécifique (environ trois mois de travail par module). Contrairement au développement d'un module à part entière, chaque utilisateur différent du logiciel devra développer son propre module "script".

1.5 Conclusions générales et perspectives

Pour faire face aux réglementations européennes et au coût croissant des énergies fossiles, l'industrie alimentaire a un besoin crucial d'outils informatiques pour simuler l'ensemble de ses usines en vue d'améliorer l'efficacité énergétique de ses procédés. Il s'avère que dans le domaine du génie chimique, des logiciels commerciaux, permettant la simulation et l'optimisation énergétique de toute une usine, existent. Ces logiciels sont dédiés à des mélanges de gaz et de liquide dont les propriétés thermophysiques peuvent être correctement prédites par des modèles thermodynamiques. L'industrie alimentaire est dépourvue de ce type de logiciels en raison de la structure complexe des aliments (mélanges de solide-liquide-vapeur). Les propriétés thermophysiques des aliments solides, nécessaires à la simulation des opérations unitaires spécifiques de ce domaine, ne peuvent être prédites par des modèles thermodynamiques.

Ce travail de doctorat, effectué au sein d'AgroParisTech-UMR1145, dans le cadre du projet *COOPERE-2* porte sur l'adaptation des logiciels issus du génie chimique à la simulation et à l'optimisation énergétique de procédés alimentaires. Les contributions de ce travail sont les suivantes :

- **développement d'une méthode innovante et rapide d'estimation de la diffusivité apparente de l'eau dans les aliments solides [77]⁵** : une seule cinétique en couche épaisse est nécessaire pour identifier les paramètres de la corrélation de cette propriété. Les paramètres identifiés sont valables pour des cinétiques mesurées en couche mince et épaisse et pour l'ensemble des conditions opératoires classiques de séchage.
- **développement d'un modèle "générique" de séchage convectif par air chaud d'aliments solides [14]⁶** : Le modèle développé semble être applicable à des produits de compositions et de géométries (sphère et cylindre infini) différentes et ayant un faible rétrécissement au cours du séchage. Il est également valable pour de larges gammes de condition opératoires et pour différentes technologies de séchage (lit fixe, tapis et lit fluidisé). Enfin, le code de calcul est compatible avec les modules d'opérations unitaires existants dans ProSimPlus[®].
- **développement d'une méthodologie générique de réduction de modèle dynamique de séchage [91]⁷** : nous démontrons numériquement qu'un modèle compartimental (constitué de 2 ou 3 compartiments) est équivalent à un modèle déterministe classique, tel que celui développé dans ce travail, dans le cas de transferts couplés de matière et d'énergie. Cette méthodologie est appliquée au séchage en couche mince de particules sphériques. Les paramètres du modèle compartimental ont tous une signification physique et son temps de simulation est inférieur d'un facteur supérieur à 100 par rapport à un modèle classique.
- **développement d'une méthodologie générique de modélisation d'une usine agroalimentaire dans un logiciel générique issu du génie chimique [104]** : cette méthodologie comprend l'estimation des propriétés thermophysiques et d'équilibre des

5. Ces résultats font également l'objet d'une communication orale aux congrès IDS (2014, Lyon, France) et SFGP (2013, Lyon, France) et par poster au congrès EuroDrying (2013, Paris, France)

6. Ces résultats ont également fait l'objet de communications orales aux congrès IDS (2014, Lyon, France) et SFGP (2013, Lyon, France)

7. Ces résultats ont également fait l'objet d'une communication par poster au congrès IDS (2014, Lyon, France)

aliments, la modélisation du réseau d'opérations unitaires du procédé à l'aide de modules préexistants et la validation des prédictions du modèle (réconciliation des données industrielles). Elle a été appliquée à une sucrerie de betteraves. L'analyse énergétique de cette usine, combinant l'analyse de pincement et exergétique, a également été réalisée [106].

Les perspectives de ce travail ont été présentées en détail dans chacune des sections de cette synthèse. Nous proposons ici de les hiérarchiser en fonction de leur ordre de priorité. Selon notre analyse, les perspectives à réaliser se présentent ainsi :

1. terminer la commercialisation du module de séchage,
2. valider les prédictions du modèle de séchage développé à l'échelle industrielle,
3. étudier l'impact de la composition et du procédé sur les isothermes d'adsorption/désorption et ainsi sur les paramètres des corrélations de l'activité de l'eau valables pour des aliments liquides et solides,
4. adapter le module de séchage développé à d'autres technologies (séchage multi-tapis, à céréales/à grains),
5. vérifier que les paramètres de la corrélation de la diffusivité apparente identifiés en couche épaisse sont bien valables à l'échelle d'une seule particule,
6. utiliser les techniques de la planification expérimentale non linéaire(NLMBSDOE) pour identifier les conditions opératoires optimales de la cinétique d'apprentissage (de séchage en couche épaisse) pour l'identification de la diffusivité apparente de l'eau,
7. développer d'autres modules d'opérations unitaires spécifiques au génie agroalimentaire.

Bibliographie

- [1] Gouvernement Francais , “Enjeux de la COP21.” <http://www.cop21.gouv.fr/fr/cop21-cmp11/enjeux-de-la-cop21>, 2015.
- [2] R. K. Pachauri and L. A. Meyer, Climate Change 2014, ch. Climate Change 2014 : Synthesis Report, p. 1535. Cambridge university press, Swizeland, Genova, 2014.
- [3] M. G. Patterson, “What is energy efficiency ? : Concepts, indicators and methodological issues,” Energy Policy **24**(5), pp. 377–390, 1996.
- [4] European Commission, Energy Efficiency Directive. Article 8 : Energy audits and energy management systems, 2013.
- [5] European Council, “The 2030 framework for climate and energy policy,” (Belgium, Brussels), 24 October 2014.
- [6] J. Vidal, Thermodynamique, application au génie chimique et à l'industrie pétrolière. Editions Technip, 1997.
- [7] S. Gourmelon, R. Thery-Hetreux, P. Floquet, O. Baudouin, P. Baudet, and L. Campagnolo, “Exergy analysis in prosimplus simulation software : A focus on exergy efficiency evaluation,” Computers & Chemical Engineering **79**, pp. 91–112, 2015.
- [8] CCS Energie Advies , “ What is ExerCom ? .” http://www.cocos.nl/en/548/ccs/Wat_is_ExerCom.html, 2014.
- [9] S. Devahastin, “Software for drying/evaporation simulations : Simprosys,” Drying Technology **24**(11), pp. 1533–1534, 2006.
- [10] Z. Pakowski, “Simulation of the process of convective drying : Identification of generic computation routines and their implementation in a computer code drypak,” Computers and Chemical Engineering **23**, Supplement(0), pp. S719–S722, 1999. European Symposium on Computer Aided Process Engineering Proceedings of the European Symposium.
- [11] I. C. Kemp, “Progress in dryer selection techniques,” Drying Technology **17**(7-8), pp. 1667–1680, 1999.
- [12] P. Schuck, A. Dolivet, S. Méjean, P. Zhu, E. Blanchard, and R. Jeantet, “Drying by desorption : A tool to determine spray drying parameters,” Journal of Food Engineering **94**(2), pp. 199–204, 2009. Food Powder Technology.
- [13] A. S. Mujumdar, Handbook of Industrial Drying, ch. Principles, Classification and Selection of Dryers, pp. 4–32. third edition, CRC, 2006.
- [14] C. Lambert, D. Goujot, H. Romdhana, and F. Courtois, “Toward a generic approach to build-up air drying models,” Drying Technology **34**(3), pp. 346–359, 2016.
- [15] Agence Nationale de la Sécurité Sanitaire (A.N.S.E.S.), “CIQUAL Food composition database.” <https://pro.anses.fr/tableciqual/index.htm>, 2013.
- [16] Food and Nutrition Information Center (F.N.I.C), “USDA Food composition database.” <http://ndb.nal.usda.gov/>, 2014.
- [17] S. W. Souci, W. Fachmann, H. Kraut, H. Scherz, and F. Senser, Food composition and nutrition tables, p. 1364. Sixth and completed edition, CRC Press, Boca Raton, 2014.
- [18] T. Gulati and A. K. Datta, “Enabling computer-aided food process engineering : Property estimation equations for transport phenomena-based models,” Journal of Food Engineering **116**(2), pp. 483–504, 2013.

- [19] M. K. Krokida, N. P. Zogzas, and Z. B. Maroulis, "Heat transfer coefficient in food processing : compilation of literature data," *International Journal of Food Properties* **5**(2), pp. 435–450, 2002.
- [20] N. P. Zogzas, M. K. Krokida, P. A. Michailidis, and Z. B. Maroulis, "Literature data of heat transfer coefficients in food processing," *International Journal of Food Properties* **5**(2), pp. 391–417, 2002.
- [21] J. Bimbenet, A. Duquenoy, and G. Trystram, *Génie des procédés alimentaires, des bases aux applications*, ch. 3, Bilans et échanges de chaleur, échangeurs, évaporateurs, p. 107. Dunod, 2007.
- [22] S. Whitaker, "Forced convection heat transfer correlations for flow in pipes, past flat plates, single cylinders, single spheres, and for flow in packed beds and tube bundles," *AIChE Journal* **18**(2), pp. 361–371, 1972.
- [23] N. Wakao and S. Kaguei, *Heat and Mass transfer in packed beds*, ch. 8, Particle to fluid transfer coefficients, pp. 292–296. Gordon and Breach Science, 1982.
- [24] R. H. Perry and D. W. Green, *Perry chemical engineers handbook*, ch. 5, Heat and mass transfer, p. 72. Donelly and Sons Company, 1999.
- [25] T. H. Chilton and A. P. Colburn, "Mass transfer (absorption) coefficients prediction from data on heat transfer and fluid friction," *Industrial and Engineering Chemistry* **26**, pp. 1183–1187, 1934.
- [26] M. Loncin and R. Merson, *Food Engineering*. Academic Press, 1979.
- [27] Y. Choi and M. Okos, "Effects of temperature and composition on the thermal properties of foods," *Journal of Food Process and Applications* **1**(1), pp. 93–101, 1986.
- [28] S. Khaloufi, C. Almeida-Rivera, and P. Bongers, "A fundamental approach and its experimental validation to simulate density as a function of moisture content during drying processes," *Journal of Food Engineering* **97**(2), pp. 177–187, 2010.
- [29] V. E. Sweat, "Experimental values of thermal conductivity of selected fruits and vegetables," *Journal of Food Science* **39**, pp. 1080–1083, 1974.
- [30] J. K. Carson, "Review of effective thermal conductivity models for foods," *International journal of Refrigeration* **29**, pp. 958–967, 2006.
- [31] M. A. Rao, S. S. H. Rizvi, and A. K. Datta, *Engineering properties of foods*, ch. 4, Thermal properties of unfrozen foods, p. 738. 3thd edition, Taylor and Francis, 2005.
- [32] G. D. Saravacos and Z. B. Maroulis, *Transport properties of foods*, p. 415. Food Science and Technology, 2001.
- [33] J. K. Carson, S. J. Lovatt, D. J. Tanner, and A. C. Cleland, "Predicting the effective thermal conductivity of unfrozen, porous foods," *Journal of Food Engineering* **75**(3), pp. 297–307, 2006.
- [34] S. S. Sablani, O. Baik, and M. Marcotte, "Neural networks for predicting thermal conductivity of bakery products," *Journal of Food Engineering* **52**, pp. 299–304, 2002.
- [35] S. S. Sablani and M. S. Rahman, "Using neural networks to predict thermal conductivity of food as a function of moisture content, temperature and apparent porosity," *Food Research International* **36**, pp. 617–623, 2003.
- [36] M. S. Rahman, M. M. Rashid, and M. A. Hussain, "Thermal conductivity prediction of foods by neural network and fuzzy (anfis) modeling techniques," *Food and Bioproduct Processing* **90**, pp. 333–340, 2012.

- [37] W. E. L. Spiess and W. R. Wolf, Physical properties of foods, ch. Results of the COST 90 on water activity. Sixth and completed edition, Applied Science, London, 1983.
- [38] Standards ASAE, “D245-6 Moisture relationships of plant based agricultural products,” ASAE , 2007.
- [39] S. Brunauer, P. H. Emmett, and E. Teller, “Modifications of the brunauer, emmett and teller equation1,” Journal of the American Chemical Society **60**, 1938.
- [40] J. De Boer, The Dynamical Character of Adsorption. Clarendon Press, 1961.
- [41] E. A. Guggenheim, Applications of Statistical Mechanics. Clarendon Press, 1966.
- [42] C. Ferro Fontan, J. Chirife, E. Sancho, and H. A. Iglesias, “Analysis of a model for water sorption phenomena in foods,” Journal of Food Science and Technology **47**(5), pp. 1590–1594, 1982.
- [43] J. Chirife, R. Boquet, C. Ferro Fontan, and H. Iglesias, “A new model for describing the water sorption isotherm of foods,” Journal of Food Science **48**(4), pp. 1382–1383, 1983.
- [44] D. S. Chung and H. B. Pfost, “Adsorption and desorption of water vapor by cereal grains and their products. part i : Heat and free energy changes of adsorption and desorption,” Transactions of the ASAE **10**(4), pp. 549–555, 1967.
- [45] S. M. Henderson, “A basic concept of equilibrium moisture,” Agricultural Engineering **33**, pp. 29–32, 1952.
- [46] T. L. Thompson, R. M. Peart, and G. H. Foster, “Mathematical simulation of corn drying : A new model,” Transactions of the American Society of Agricultural Engineers **24**, pp. 582–586, 1968.
- [47] H. Iglesias and J. Chirife, “An alternative to the guggenheim, anderson and de boer model for the mathematical description of moisture sorption isotherms of foods,” Food Research International **28**(3), pp. 317–321, 1995.
- [48] R. P. Singh and D. R. Heldman, Introduction to food engineering, p. 659. 3thd Edition, Academic Press, 2001.
- [49] P. J. Flory, “Thermodynamics of high polymer solutions,” The Journal of Chemical Physics **10**(1), pp. 51–61, 1942.
- [50] M. L. Huggins, “Thermodynamic properties of solutions of long-chain compounds,” Annals of the New York Academy of Sciences **43**(1), pp. 1–32, 1942.
- [51] R. S. Norrish, “An equation for the activity coefficients and equilibrium relative humidities of water in confectionery syrups,” International Journal of Food Science and Technology **1**(1), pp. 25–39, 1966.
- [52] K. D. Ross, “Estimation of water activity in intermediate moisture foods,” Food Technology **3**, pp. 26–34, 1975.
- [53] R. Tesch, O. Ramon, I. Ladyzhinski, Y. Cohen, and S. Mizrahi, “Water sorption isotherm of solution containing hydrogels at high water activity,” International Journal of Food Science and Technology **34**(3), pp. 235–243, 1999.
- [54] M. Caurie, “Water activity of multicomponent mixture of solutes and non-solutes,” International Journal of Food Science and Technology **40**(3), pp. 295–303, 2005.
- [55] A. D. Roman, E. Herman-Lara, M. A. Salgado-Cervantes, and M. A. Garcia-Alvarado, “Food sorption prediction using the ross equation,” Drying Technology **22**(8), pp. 1829–1843, 2004.

- [56] R. Moreira, F. Chenlo, and M. D. Torres, "Simplified algorithm for the prediction of water sorption isotherms of fruits, vegetables and leumes based upon chemical composition," *Journal of Food Eng.* **94**, pp. 334–343, 2009.
- [57] C. Achard, C. G. Dussap, and J. B. Gros, "Prediction of ph in complex aqueous mixtures using a group contribution method," *AICHE Journal* **40**, pp. 1210–1222, 1994.
- [58] L. Ben Gaida, J. B. Gros, and C. G. Dussap, "Activity coefficients of concentrated strong and weak electrolytes by a hydratation equilibrium and group contribution model," *Fluid Phase Equilibria* **289**, pp. 40–48, 2010.
- [59] M. Catte, C. G. Dussap, and J. B. Gros, "A physical chemical unifac model for aqueous solutions of sugars," *Fluid Phase Equilibria* **105**, pp. 1–25, 1995.
- [60] A. Perres and E. A. Macedo, "A modified unifac model for the calculation of thermodynamic properties of aqueous and non aqueous solutions containing sugars," *Fluid Phase Equilibria* **139**, pp. 47–74, 1997.
- [61] A. Perres and E. A. Macedo, "Prediction of thermodynamic properties using a modified unifac model : application to sugar industrial systems," *Fluid Phase Equilibria* **158-160**, pp. 391–399, 1999.
- [62] O. Ferreira, E. A. Brignole, and E. A. Marcedo, "Phase equilibria in sugar solutions using the a-unifac model," *Industrial and Engineering Chemistry Research* **42**, pp. 6212–6222, 2003.
- [63] J. B. Gros and C. G. Dussap, "Estimation of equilibrium properties in formulation or processing of liquid foods," *Food Chemistry* **82**, pp. 41–49, 2003.
- [64] L. Ben Gaida, C. G. Dussap, and J. B. Gros, "Variable hysdration of small carbohydrates for predicting equilibrium properties in diluted and concentrated solutions," *Food Chemistry* **96**, pp. 387–401, 2006.
- [65] A. Perres and E. A. Macedo, "Phase equilibria of d-glucose and sucrose inmixed solvent mixtures : Comparison of uniuac based models," *Carbohydrate Research* **303**, pp. 135–151, 1997.
- [66] A. Correa, J. F. Comesana, J. M. Correa, and A. M. Sereno, "Measurement and prediction of water activity in electrolyte solutions by a modified asog group contribution method," *Fluid Phase Equilibria* **129**, pp. 267–283, 1997.
- [67] O. Toure, F. Audonnet, A. Lebert, and C.-G. Dussap, "Development of a thermodynamic model of aqueous solution suited for foods and biological media. part a : Prediction of activity coefficients in aqueous mixtures containing electrolytes," *The Canadian Journal of Chemical Engineering* **93**(2), pp. 443–450, 2015.
- [68] O. Toure, F. Audonnet, A. Lebert, and C.-G. Dussap, "Development of a thermodynamic model of aqueous solution suited for foods and biological media. part b : Prediction of standard formation properties," *The Canadian Journal of Chemical Engineering* **93**(2), pp. 465–470, 2015.
- [69] N. P. Zogzas, Z. B. Maroulis, and D. Marinos-Kouris, "Moisture diffusivity methods of experimental determination : a review," *Drying Technology* **12**(3), pp. 483–515, 1994.
- [70] P. Perré, F. Pierre, J. Casalinho, and M. Ayouz, "Determination of the mass diffusion coefficient based on the relative humidity measured at the back face of the sample during unsteady regimes," *Drying Technology* **33**(9), pp. 1068–1075, 2015.

- [71] G. D. Saravacos, "Effect of the drying method on the water sorption of dehydrated apple and potato," *Journal of Food Science* **32**(1), pp. 81–84, 1967.
- [72] V. T. Karathanos, G. K. Vagenas, and G. D. Saravacos, "Water diffusivity in starches at high temperatures and pressures," *Biotechnology Progress* **7**(2), pp. 178–184, 1991.
- [73] N. P. Zogzas and Z. B. Maroulis, "Effective moisture diffusivity estimation from drying data. a comparison between various methods of analysis," *Drying Technology* **14**(7-8), pp. 1543–1573, 1996.
- [74] P. Perré and B. K. May, "A numerical drying model that accounts for the coupling between transfers and solid mechanics. case of highly deformable products," *Drying Technology* **19**(8), pp. 1629–1643, 2001.
- [75] L. Hassini, S. Azzouz, R. Peczalski, and A. Belghith, "Estimation of potato moisture diffusivity from convective drying kinetics with correction for shrinkage," *Journal of Food Engineering* **79**(1), pp. 47–56, 2007.
- [76] F. Courtois, *Dynamic Modelling of Drying to Improve Processing Quality of Corn*. PhD thesis, ENSIA, Massy, France, 1991.
- [77] C. Lambert, H. Romdhana, and F. Courtois, "Reverse methodology to identify moisture diffusivity during air-drying of foodstuffs," *Drying Technology* **33**(9), pp. 1076–1085, 2015.
- [78] C. Lambert, J. Cartailler, S. Rouchouse, G. Almeida, and F. Courtois, "Characterization and modeling of cooling and drying of pellets for animal feed," *Submitted to Drying Technology (under revision)*, 2016.
- [79] M. Abud-Archila, F. Courtois, C. Bonazzi, and J. Bimbenet, "A compartmental model of thin-layer drying kinetics of rough rice," *Drying Technology* **18**(7), pp. 1389–1414, 2000.
- [80] D. Goujot, X. M. Meyer, and F. Courtois, "Exoptim : design d'expériences optimales planifiées variables en temps et identification pour la modélisation," *Agence pour la Protection des Programmes IDDN.FR.001.370015.000.R.P.2013.000.20700* (Inter Deposit Digital Number), pp. Logibox numéro 77010, 1 CDrom, 2013.
- [81] P. Perré, "A review of modern computational and experimental tools relevant to the field of drying," *Drying Technology* **29**(13), pp. 1529–1541, 2011.
- [82] P. Perré and I. W. Turner, "A 3-d version of transpore : a comprehensive heat and mass transfer computational model for simulating the drying of porous media," *International Journal of Heat and Mass Transfer* **42**(24), pp. 4501–4521, 1999.
- [83] The CAPE-OPEN Laboratories Network, "General informations." www.colan.org, 2014.
- [84] R. B. Bird, W. E. Stewart, and E. N. Lightfoot, *Transport phenomena*. Wiley and Sons, 2002.
- [85] M. Galassi, J. Theiler, and J. Davies, *Gnu Scientific Library Reference Manual*. 3rd edition, Network Theory Ltd, 2009.
- [86] R. G. M. Van der Sman, "Simple model for estimating heat and mass transfer in regular-shaped foods," *Journal of Food Engineering* **60**(4), pp. 383–390, 2003.
- [87] M. Hussain, J. Kumar, M. Peglow, and E. Tsotsas, "On two-compartment population balance modeling of spray fluidized bed agglomeration," *Computers and Chemical Engineering* **61**, pp. 185–202, 2014.

- [88] A. Delafosse, M.-L. Collignon, S. Calvo, F. Delvigne, M. Crine, P. Thonart, and D. Toye, “Cfd-based compartment model for description of mixing in bioreactors,” *Chemical Engineering Science* **106**, pp. 76–85, 2014.
- [89] X. Peng, Z. Liu, J. Tan, and W. Bu, “Compartmental modeling and solving of large-scale distillation columns under variable operating conditions,” *Separation and Purification Technology* **98**, pp. 280–289, 2012.
- [90] K. Toyoda, “Study on intermittent drying of rough rice in a recirculation dryer,” in *Sixth International Drying Symposium IDS'88*, **2**, pp. 171–178, September 1988.
- [91] H. Romdhana, C. Lambert, D. Goujot, and F. Courtois, “Model reduction technique for faster simulation of drying of spherical solid foods,” *Journal of Food Engineering* **170**, pp. 125–135, 2016.
- [92] J. Crank, *The mathematics of diffusion*, Oxford University Press, US, 1975.
- [93] J. Bon, G. Clemente, H. Vaquiro, and A. Mulet, “Simulation and optimization of milk pasteurization processes using a general process simulator (prosimplus),” *Computers & Chemical Engineering* **34**(3), pp. 414–420, 2010.
- [94] M. Madoumier, C. Azzaro-Pantel, G. Tanguy, and G. Gésan-Guiziou, “Modelling the properties of liquid foods for use of process flowsheeting simulators : Application to milk concentration,” *Journal of Food Engineering* **164**, pp. 70–89, 2015.
- [95] A. V. Ensinas, S. A. Nebra, M. A. Lozano, and L. M. Serra, “Analysis of process steam demand reduction and electricity generation in sugar and ethanol production from sugarcane,” *Energy Conversion and Management* **48**(11), pp. 2978–2987, 2007. 19th International Conference on Efficiency, Cost, Optimization, Simulation and Environmental Impact of Energy Systems.
- [96] R. Palacios-Bereche, K. J. Mosqueira-Salazar, M. Modesto, A. V. Ensinas, S. A. Nebra, L. M. Serra, and M.-A. Lozano, “Exergetic analysis of the integrated first- and second-generation ethanol production from sugarcane,” *Energy* **62**, pp. 46–61, 2013.
- [97] P. S. Ortiz and S. de Oliveira Jr., “Exergy analysis of pretreatment processes of bioethanol production based on sugarcane bagasse,” *Energy* **76**, pp. 130–138, 2014.
- [98] L. W. Weiss, “Sugar factory process optimization using the sugars computer program,” tech. rep., American society of sugar beet technologists, Englewood, Colorado 80110 USA, March 1989.
- [99] A. Ensinas, M. Modesto, S. Nebra, and L. Serra, “Reduction of irreversibility generation in sugar and ethanol production from sugarcane,” *Energy* **34**(5), pp. 680–688, 2009. 4th Dubrovnik Conference, 4th Dubrovnik conference on Sustainable Development of energy, Water and Environment.
- [100] T. Tekin and M. Bayramoglu, “Exergy analysis of the sugar production process from sugar beets,” *International Journal of Energy Research* **22**(7), pp. 591–601, 1998.
- [101] T. Tekin and M. Bayramoglu, “Exergy and structural analysis of raw juice production and steam-power units of a sugar production plant,” *Energy* **26**(3), pp. 287–297, 2001.
- [102] S. D. Peacock, “The use of simulink for process modelling in the sugar industry,” in *Proceedings of South African Sugar Technologists' Association*, pp. 444–455, 2002.
- [103] J. Q. Albarelli, A. V. Ensinas, and M. A. Silva, “Product diversification to enhance economic viability of second generation ethanol production in brazil : The case of the sugar and ethanol joint production,” *Chemical Engineering Research and Design* **92**(8), pp. 1470–1481, 2014. Green Processes and Eco-technologies-Focus on Biofuels.

- [104] C. Lambert, B. Laulan, M. Decloux, H. Romdhana, and F. Courtois, “Simulation and data reconciliation of a food process using a generic simulator (ProSimPlus) : case of a sugar beet factory ,” To submit to Computer and Chemical Engineering Journal , p. 23, 2015.
- [105] Z. Bubnik, P. Kadlec, D. Urban, and M. Bruhns, Sugar technologists manual, Chemical and physical data for sugar manufacturers and users. Bartens, 1995.
- [106] C. Lambert, B. Laulan, M. Decloux, and H. Romdhana, “Combined Pinch and exergy analysis for energy optimization of a sugar beet factory using a generic simulator (ProSimPlus) ,” To submit to Energy Journal , p. 24, 2015.

Chapitre 2

Toward a generic approach to build-up air drying models

Résumé

Peu logiciels polyvalents, permettant la simulation précise du séchage au sein d'un réseau d'opérations unitaires, sont disponibles. Ce travail a été réalisé au cours de la création d'un simulateur de séchage convectif générique d'aliments solides dans ProSimPlus®, un logiciel de simulation générique de procédés pétrochimiques. Les approches de modélisation disponibles dans la littérature sont discutées dans cette étude. Parmi elles, un compromis doit être fait entre un temps de simulation court, un travail expérimental réduit et une capacité de prédiction sur une large gamme de conditions opératoires, de produits et de technologies de séchage. Un état de l'art sur les modèles d'estimations de certaines propriétés des produits alimentaires nécessaires à la simulation du séchage est également présenté. Dans cette étude, deux boîtes à outils ont été créés : une pour estimer les propriétés physiques des aliments et une autre pour simuler les transferts de matière et d'énergie dans l'air et le produit. Cette approche est validée sur 4 produits alimentaires (avec diverses formulations et formes).

Mots-clés : Séchage d'aliments, modèle mathématique, propriétés physiques, simulation.

Cet article a été publié dans *Drying Technology*¹.

2.1 Introduction

On the one hand, few drying simulators are available in food industry to help design, setup and control dryers. On the other hand, many publications in the Drying Technology journal deal with drying models. These models are usually validated on experimental data, and can be designed in either a bottom-up or a top-down approach. The bottom-up models contain empirical equations, but have no extrapolation or generic capabilities. The top-down models contain equations of physical phenomena (also known as first principle models) and are potentially compatible with various kinds of products and drying conditions. The caveats are their greater complexity and their requirements for product properties.

1. C. Lambert, D. Goujot, H. Romdhana, and F. Courtois, "Toward a generic approach to build-up air drying models," *Drying Technology* 34(3), pp. 346-359, 2016.

For the Top-down simulation of chemical processes, several commercial software are available (*e.g.* AspenPlus[®], ProSimPlus[®]). The latter allow simulation of whole chemical plants. In contrast, food industry can barely use such powerful tools to simulate their specific processes. As a matter of fact, simulators dedicated to chemical processes are limited to gas or liquid mixtures of pure components for which properties can be correctly predicted by thermodynamic theories. In contrary, many solid food products are mixtures of gas, liquids and solid components for which almost no commercially-available equations can predict their properties. Hence, to implement food processes in a commercial simulation software, two problems are faced: i) implement food compatible modules for unit operations, ii) predict complex food properties, including transfer coefficients^[1]. The implementation proposed in the present work was done in the course of the creation of the first drying module for solid food products in the ProSimPlus[®] commercial software. Such type of software is a convenient and useful tool for food industry and food engineer's education. On the one hand, recent European rules impose a decrease of energy consumption of 20 % by 2030^[2]. Hence, food industry needs the development of software which can simulate their whole plant and in which energy optimization methods (*e.g.* Pinch and/or exergy analysis) can be applied. On the other hand, in the context of budget restrictions in higher education, software simulators tend to be a low cost replacement for expensive hands-on sessions. In addition, putting professional software commonly used in industry in the practice of students is a nice way of preparing them for their upcoming career. Finally, while many simulators are available in laboratories, none of them is suited for the global simulation of an entire workshop, or a whole plant. Hence, we intend, throughout this first step, to demonstrate the potential of this type of software tools for food industry.

In this study, classical modelling approaches of convective drying process are discussed, then a close-to generic method is proposed to model the air drying of food products with a special emphasis on the prediction of all needed food product properties. Some of the most common equations of structural, thermodynamic and transport properties are described. Most of them are functions of food composition and temperature. Strategies to identify effective moisture diffusion coefficients are also proposed. In this work, we discuss how to obtain an efficient trade-off between, a reduced lab effort and accuracy of predictions of kinetics on a wide range of drying conditions, with low simulation time. This approach is validated on 4 different products including soybean and corn and two formulations of pellets for animal feed.

2.2 Available commercial simulators for drying processes

2.2.1 Overview

Commercially available simulators provide programs designed for specific unit operations and for specific products. The latter are generally developed in laboratories. Among the available simulators, some of them allow dryer design including heat and mass balance calculations as well as the estimation of gas handling power requirements (*e.g.* Simprosys[®], dryPAK[®]). Others contain a database to help process engineers to select the right design (*e.g.* DrySel[®]). More precisely, Simprosys[®]^[3] essentially contains dryers for solids and liquids, production of utilities (including burners, heaters and steam jets), mixers, and separators. dryPAK[®]^[4] is a computer code that combines calculation routines and a database. The

routines include drying rate and flux calculations. The database includes all the necessary property data used in drying simulation: specific heat, diffusivity, isotherm of desorption, drying kinetic equations, shrinkage equation etc. DrySel® (Dryer Selection), marketed by Aspen Technology, is a useful software tool that can simulate 50 different types of dryers. It was initially developed by Kemp and Snowball^[5] and consists of a rules-based expert system using fuzzy logic providing numerical scores for each dryer technology. Moreover, it is worth to notice that several laboratories designed their own software (not listed above). They are usually programmed by only one person in a specific development environment, and are no longer maintained over time. This obsolescence would be limited if such programming work had been done in the frame of a “universal” simulation software. Dryer3000® and SD2P®, two examples of a specific drying simulator available for specific food products family (respectively grains and dairy products), are presented below. Their potentialities and limitations are discussed.

2.2.2 SD2P®, a specific example for spray drying simulation

SD2P® (Spray Drying Parameters Simulation and Determination), developed within the joint research unit UMR1253 STLO (Rennes, France), is a commercial software dedicated to spray drying simulation. It can predict drying parameters such as inlet air temperature after heating, outlet air temperature and absolute humidity, air and powder flow-rate and energy consumption^[6]. To predict them, one has to enter some information:

- drying kinetics data, determined from desorption curves according to methods described in^[7] or^[8];
- ambient inlet temperature and relative humidity;
- evaporation capacity and heat loss through the dryer walls;
- flow rate, temperature, total solid content and heat capacity of the concentrate;
- total solid content of the powder.

It is easy to validate the method on others formulations knowing all the required information. SD2P® was already validated on more than 100 dairy and non-dairy products, so it can be applied on a wide range of food products.

2.2.3 Dryer3000®, a specific example for grain drying

Dryer3000® is a commercial software dedicated to grain mixed-flow dryers (like its ancestor Dryer2000®). It allows simulating new designs or new settings for both corn and rice grains. Its two main advantages are that 1) it is able to predict the final product quality and 2) its prediction errors are lower than 5 - 10 %. This software was originally developed in 1991 during the PhD of F. Courtois^[9] specifically for corn mixed-flow dryers. It was programmed in Pascal language for Macintosh® OS. Unfortunately, in the late 90's, these initial choices happened to be inappropriate with a growing market share of PCs running Windows® and the leadership of the C/C++ languages. Furthermore, having a simulator specific to only one grain product (corn) was too restrictive. Hence, it was rewritten in an object-oriented language (C++), and the results from another PhD work concerning rice were added at the same time^[10, 11]. In that perspective, it was expected 1) to allow for easy addition of any number of granular products and 2) to be available on all Windows®, MacOS® and Linux® flavors and 3) to be based on open source software for better sustainability. The core simulator is hence designed as an object-oriented library while the graphical interface

is based on the free wxWidgets[®] library which is natively available on most common OS (Windows[®], MacOS[®] and Linux[®]).

For example, if one wants to add a soybean drying module to predict water loss kinetics (excluding quality prediction), the Dryer3000[®] requires only a few properties (heat capacity, water activity, density, etc.) and transfer coefficients (heat and mass). Indeed, if a publication with a compartmental drying model for soybeans was found, it would only takes a few minutes to implement that model in Dryer3000[®] without requiring to write any transfer equation thanks to the object oriented nature of the core simulator.

2.3 Discussion on available modelling approaches

2.3.1 Approaches used to model food drying processes

Many approaches can be used to build-up a simulator of food drying processes. Still, this diversity can be summarized in a few categories:

Black-box models

Most of black-box models are static (*i.e.* focused on the final measurements rather than on the evolution in time) and based on fitting experimental data with curves. The well-known Characteristic Drying Curve (CDC) (also known as Universal Drying Curve), the Page model, etc. are typical examples. Transfers are assumed to be zero dimensional and only described by one independent variable (moisture content). Such models require many drying experiments to insure a sufficiently wide range of validity due to their limited capability of extrapolation. On the one hand, this kind of models does not require i) high mathematical and programming skills and, ii) costly laboratory measurements of density, porosity, etc. On the other hand, they can hardly simulate complex dynamic drying processes during which important variations of both air temperature and relative humidity occur^[12].

It should be noted that even if a dryer is in steady state, the product, locally, is usually in unsteady state. This statement justifies the need for white box -dynamic- models^[12].

Simplified white-box models

All white-box models are constituted with ordinary or partial differential equations, making them suitable to simulate dynamic processes. They are usually called first-principle models since they are often based on Fick and Fourier laws, describing heat and mass transfers within the product and between products and surrounding drying media (air or super-heated steam, usually). Depending on their equation set, they may be called gray-box models. In any case, one may consider them as ‘simplified’ because the geometry is assumed to be simple (infinite slab, sphere or infinite cylinder), and/or the shrinkage is neglected. Transfers inside the particles are assumed to be one dimensional and generally described by two or three independent variables (moisture content, temperature and sometimes pressure variations). They require the determination, at the laboratory, of many thermo-hydro-physical properties (density, sorption isotherms, isobars, etc.). Some of these properties and the required transfer coefficients can be either found in literature or identified on the basis of a set of experimental kinetics or lab determinations. All parameters have physical meaning and they can be compared and discussed. Moreover, these models are assumed to have good extrapolation capabilities.

Sophisticated white-box models

One can consider this category as an extension of the previous one for 3D (possibly 2D) representations of complex geometries and/or combined heat and mass transfers with shrinkage and/or air/steam heterogeneous flows. They require heavy computation usually based on commercial codes like FLUENT®, COMSOL®, etc. Hence, they can hardly simulate an industrial dryer as a whole. Their purpose is rather for research and optimization of the design of some parts of a dryer. However, a sophisticated white-box model is not always better than a simplified one because:

- 1) some of the additional required properties (for the sophisticated white box model) cannot be accessed by direct measurements (numerical identification is needed);
- 2) the prediction error accumulates the errors coming from both measurements and estimations of these additionally required properties. It can be higher than the prediction error from a simplified white-box model as shown by^[13];
- 3) accessible experimental measurements from a drying kinetic do not give enough information to discriminate between sophisticated and simplified white box models.

2.3.2 Compatibility requirements for commercial simulation

All drying models are not compatible with an implementation in a commercial software for daily use in the industry. A non-exhaustive list of requirements can be:

- Low computation requirements (accessible, parsimonious, user friendly):

The simulation of the whole industrial dryer should not last longer than a few minutes. With actual performance of current computers, 3D simulation of coupled heat and mass transfers, with particle and gas flows, cannot be expected. If the simulator is integrated in an optimization scheme then each run should not exceed a few seconds of duration.

- Wide range of validity (usability):

When looking carefully at publications describing drying models, it occurs in most cases that the range of validity is either not disclosed or too narrow to be usable for industry. It is of commercial importance to ensure that drying models are valid over a wide range of air temperature for instance.

- Multi-product compatibility (versatile, modular):

As opposed to what is classically done in research laboratories, it is necessary to separate the product specific properties (equations and constants) from heat and mass transfer equations. In other terms, the drying simulator should be at least composed of two modules: one providing product properties and, another one solving (with respect to time and space) heat and mass transfer equations related to the process itself. Moreover, this structure allows multi-product compatibility, which permits the late addition of new products without changing anything in the process simulator module.

- Multi-technology compatibility (versatile, modular):

While there is a wide variety of drying technologies available, depending on product typology and expected end-use, a short classification is possible. For instance, we may consider the following categories: moving deep bed drying (hot air or steam; *e.g.* conveyor-belt dryers, mixed-flow dryers), flowing particle dryers (hot air or steam; *e.g.* rotary dryers, fluidized bed dryers), dryers for viscous liquids (*e.g.* drum dryers), dryers for liquids (*e.g.* spray dryers), etc. Ideally, there should be as many drying modules as above mentioned categories. For

a given category, hence for a given simulation module, the simulator should be compatible with most variants.

- Reduction of the required volume of experiment work (parsimonious):

Unlike what is found in chemical engineering, currently there is no commercially-available database that can predict the needed food product properties (including heat and mass transfer coefficients). As a consequence, some laboratory work is required to determine both product thermo-physical constants and equations, and transfer coefficients throughout identification based on drying kinetics. For a commercial food simulator, such a database should exist.

- Standardized computer implementation (sustainable, modular):

Most scientists designing drying models are not programming experts. The computer implementation of their models is usually done *a minima* in a commercial coding framework (*e.g.* MATLAB[®], SCILAB[®], gPROMS[®], COMSOL[®]). Their code is not compliant with any interoperability standards (*e.g.* CAPEOPEN[®] which is promoted by <http://www.colan.org>). A commercial simulator should allow coding a simulation model using a unified framework in agreement with interoperability standards.

2.3.3 Selecting the ‘best’ modelling approach

In order to develop a versatile food drying simulator, a compromise has clearly to be found. It is important to note that our work is in the continuation of the long experience of our drying laboratory, but is also part of a global research project (COOPERE-2 in France, funded by Agence Nationale de la Recherche and leaded by company) aiming at implementing food processes (for a whole industry plant) and optimize their energy consumption and exergy in a commercial software (ProSimPlus[®]) specific to chemical industry. Hence, the aim of COOPERE-2 is double: 1) implement the simulation routine, in FORTRAN language, as a new module at the core of ProSimPlus[®] software, 2) extend the concept of DRYER3000[®] in terms of multiplicity of products types and drying technologies. It should be emphasized that the software perspectives of these two aims of COOPERE-2 are slightly different. On the one hand, precision of the simulation results is important but it is of the utmost importance that each module can be connected with each other and run smoothly to produce a satisfactory estimation of the plant production for further water, energy and exergy minimizations. It is the case in the ProSimPlus[®] commercial software, which can simulate an entire plant where many other unit operations are combined all together. On the other hand, the approach of DRYER3000[®] is different. It focuses on the ability to transform all data available in our drying laboratory into a usable versatile drying simulator. It can be seen as an object-oriented database (*i.e.* combining constants, equations and functions).

A convective drying model was build up both for deep bed and thin layer and was developed in two languages:

1. a C++ version of the simulator which can identify diffusion coefficients on a learning set and validate the simulator on a validation set of drying kinetics. The latter can aggregate all existing and upcoming drying data available in our laboratory as an object-oriented library of data and functions dedicated to the simulation of food drying processes;
2. a proprietary FORTRAN version of the simulator for conveyor-belt and fluidized bed classes of dryers. This version is expected to be inserted as a compiled module, among

many others, inside ProSimPlus[®], capable of communicating with other modules (unit operations or utility production) and with the Simulis Thermodynamics[®] property database;

It should be noted that object-oriented language C++ is very interesting for several reasons:

- open-source availability ensuring OS-independent and long term sustainability of the code (DRYER3000[®], coded in C++, has run on all Windows[®], MacOS[®], and Linux[®] flavors, since 2003);
- inheritance property allowing the creation of classes of products and/or technology variants with minimal work (*e.g.* a subclass ‘fatty product’ can inherit most functions and properties from its parent class ‘food product’).

In this model, the following assumptions were considered for the particles:

- ideal geometry (infinite cylinder or spherical shape) and negligible shrinkage or swelling are assumed;
- an isotropic behavior within the product is assumed (heat and mass transfers are in the radial direction);
- the conduction heat transfer between particles is negligible;
- the thermal expansion coefficient is negligible;
- heat conduction and liquid water diffusion occur within the particles (see below);
- evaporation, heat and mass convection occur only at the surface.

The model is developed for thin layer and deep bed drying. One usually assimilates the deep bed as a series of thin layers for which the only transfer occurs between air and grain, and a thin layer as an equivalent average (single) particle. Moreover, deep bed drying involves energy and mass transfer in air, after each thin layer crossing^[9]. Furthermore, the thermal Biot (Bi_{th}) and mass Biot (Bi_m) number values are respectively between 0.1 and 100 and much higher than 100. Therefore, both external and internal heat and mass transfers are considered^[14]. The thermal Peclet (Pe_{th}) and mass Peclet (Pe_m) number values are much higher than 1, therefore a plug-type airflow and negligible pressure variation are assumed.

Heat and mass balance on the particles

Liquid water diffusion and thermal conduction phenomena are based on Fourier and Fick law. Mass and energy balances lead to:

$$\left(\frac{\partial X_t^{r,z}}{\partial t} \right) = \frac{1}{r^n} \bullet \frac{\partial}{\partial r} \left(r^n \bullet D_{eff} \bullet \frac{\partial X_t^{r,z}}{\partial r} \right) \quad (2.1)$$

$$\left(\frac{\partial Tp_t^{r,z}}{\partial t} \right) = \frac{1}{\rho_{dm} \bullet (Cp_{dm} + X_t^{r,z} \bullet Cp_w) \bullet r^n} \bullet \frac{\partial}{\partial r} \left(r^n \bullet \lambda_{eff} \bullet \frac{\partial Tp_t^{r,z}}{\partial r} \right) \quad (2.2)$$

Where X is the water content (dry basis), r the radial position in the particle (m), z the particle position in the height of the bed (m), t the elapsed time (s), n the shape factor (1 or 2, respectively for cylindrical and spherical symmetry), D_{eff} the effective water diffusion coefficient ($m^2.s^{-1}$), Tp the product temperature (K), λ_{eff} the effective thermal conductivity ($W.m^{-1}.K^{-1}$), ρ_{dm} the density of the dry matter ($kg.m^{-3}$) and Cp_{dm} the heat capacity at constant pressure of dry matter ($J.kg^{-1}.K^{-1}$), for the considered particle, Cp_w the heat capacity at constant pressure of the pure water ($J.kg^{-1}.K^{-1}$).

Initial conditions are the followings: temperature and water content within the particles are assumed to be uniform. Boundary conditions are shown in equations 2.3 to 2.6.

$$\left(\frac{\partial X_t^{0,z}}{\partial r} \right) = 0 \quad (2.3)$$

$$\left(\frac{\partial T p_t^{0,z}}{\partial r} \right) = 0 \quad (2.4)$$

$$-\rho_{dm} \bullet \left(\frac{\partial X_t^{r_{max},z}}{\partial r} \right) = \varphi_m = k_m \bullet \frac{M_w}{R} \left(\frac{a_w \bullet P v_{sat}(T p_t^{r_{max},z})}{T p_t^{r_{max},z}} - \frac{RH \bullet P v_{sat}(Ta_t^z)}{Ta_t^z} \right) \quad (2.5)$$

$$-\lambda_{eff} \bullet \left(\frac{\partial T p_t^{r_{max},z}}{\partial r} \right) = h_{glob} \bullet (T p_t^{r_{max},z} - Ta_t^z) + \varphi_m \bullet \Delta H_v (T p_t^{r_{max},z}) \quad (2.6)$$

Where φ_m is the mass flux density ($kg.m^{-2}.s^{-1}$), k_m the convective mass transfer coefficient ($m.s^{-1}$), M_w the molar mass of water ($g.mol^{-1}$), R the gas constant ($J.mol^{-1}.K^{-1}$), a_w the water activity of the particle (Pa/Pa), $P v_{sat}$ the pressure of saturated vapor (Pa), RH the relative humidity (Pa/Pa), h_{glob} the external heat transfer coefficient by convection ($W.m^{-2}.K^{-1}$), Ta the air temperature (K) and ΔH_v the enthalpy of vaporization of pure water ($J.kg^{-1}$).

Heat and mass balance on the air

An infinitesimal balance is made on the air after each thin layer crossing (equations 2.7 and 2.8).

$$\frac{\partial (\rho_a \bullet Y_t^z)}{\partial t} = \frac{-\partial}{\partial z} \left(\frac{\varphi_a \bullet Y_t^z}{\varepsilon} \right) + \varphi_m \bullet a \bullet \frac{1 - \varepsilon}{\varepsilon} \quad (2.7)$$

with $a = \frac{S_p}{V_p}$ and $\varphi_a = \varepsilon \bullet \rho_a \bullet v_a$

$$\begin{aligned} & \frac{\partial (\rho_a \bullet (C p_{da} + Y_t^z \bullet C p_v) \bullet Ta_t^z + Y_t^z \bullet \Delta H_v (T p_t^{r_{max},z}))}{\partial t} \\ &= \frac{-\partial}{\partial z} \left(\frac{\varphi_a \bullet (C p_{da} + Y_t^z \bullet C p_v) \bullet Ta_t^z + Y_t^z \bullet \Delta H_v (T p_t^{r_{max},z})}{\varepsilon} \right) \\ &+ a \bullet (h_{glob} \bullet (T p_t^{r_{max},z} - Ta_t^z) + \varphi_m \bullet \Delta H_v (T p_t^{r_{max},z})) \bullet \frac{1 - \varepsilon}{\varepsilon} \end{aligned} \quad (2.8)$$

Where ρ_a is the density ($kg.m^{-3}$), a the particle specific surface area (surface area per particle volume) (m^{-1}), ε the bed porosity (decimal), Y the air absolute humidity (*dry basis*), φ_a the density of the mass flow, v_a the interstitial velocity ($m.s^{-1}$), and $C p_{da}$ and $C p_v$ the specific heat capacity at constant pressure of respectively dry air and water vapor ($J.kg^{-1}.K^{-1}$), for the considered air.

Inlet air water content and temperature are known. Their values may not be constant during a drying experiment.

Simulation and optimization

The dynamic system consists of a set of 8 Partial differential Equations (PDEs 2.1 to 2.8). These equations were discretized into a set of Ordinary Differential Equations (ODEs) using an explicit finite volume scheme in space. This set was numerically integrated with respect to both time and space by backward differentiation formulas^[15] (for stiff systems). The integration time step is automatically adjusted in the course of the simulation process to maintain both absolute and relative errors within given tolerances. Hence, the integration time step is not constant during the drying simulation.

To quantify the quality of the model prediction, Weighted-Root-Mean-Square values (*WRMS*) between experimental and simulation data were calculated according to equations 9 and 10 respectively for thin layer and deep bed drying kinetics, valid for any time *t*. The aim is to minimize the total relative error made on the measurable variables using the Nelder and Mead method (Downhill Simplex method)^[16]. To avoid numerical inconsistencies, the parameter set of the correlations between the effective moisture diffusivity, product moisture content and temperature was reparameterized using a log10 transform as suggested by Goujot *et al.*^[17].

$$WRMS_{TL}^2 = \frac{1}{N_{Data} - N_P} \sum_{i=1}^{N_{Data}} \left(\frac{\bar{X}_S - \bar{X}_E}{\bar{\bar{X}}_E} \right)_i^2 \quad (2.9)$$

$$WRMS_{DB}^2 = \frac{1}{N_{Data} - N_P} \sum_{i=1}^{N_{Data}} \left(\left(\frac{\bar{\bar{X}}_S - \bar{\bar{X}}_E}{\bar{\bar{X}}_E} \right)_i^2 + \left(\frac{Ta_S^{out} - Ta_E^{out}}{Ta_E^{out}} \right)_i^2 + \left(\frac{RH_S^{out} - RH_E^{out}}{RH_E^{out}} \right)_i^2 \right) \quad (2.10)$$

Where, $WRMS_{TL}$ and $WRMS_{DB}$ are the Weighted Root Mean Square values (over *t*) respectively for thin layer and deep bed kinetics, N_{Data} and N_p respectively the number of experimental data and the number of parameters to identify, \bar{X}_s and $\bar{\bar{X}}_s$ the simulated mean moisture content, \bar{X}_E and $\bar{\bar{X}}_E$ the experimental mean moisture content, Ta_S^{out} and Ta_E^{out} the simulated and experimental output air temperature, and RH_S^{out} and RH_E^{out} the simulated and experimental output air relative humidity.

Thirteen parameters are needed to use this model:

1. heat and mass transfer coefficients at the surface are estimated with well-known correlations^[18];
2. product dimensions, density, bulk porosity are obtained by lab measurements;
3. heat capacity and sorption isotherms are obtained either by lab measurements, extractions from literature or from predictive equations based on composition;
4. internal transfer coefficients (heat and water diffusion) have to be identified on the basis of experimental drying kinetics.

It appears clearly that the main difficulty does not come from the modelling of the drying operation itself, but rather from the prediction of the food properties and coefficients. While, in chemical engineering, ProSimPlus® takes the benefits of Simulis Thermodynamics® to estimate all such properties from the composition of the product (limited to gas/liquid mixtures of pure chemicals), in the food engineering field, no database can be compared to Simulis Thermodynamics®. The purpose of this work is hence to modestly place this database by a methodology and to validate it on several applications.

2.4 Estimation of food thermo-hydro-physical properties

Some properties can easily be measured in the laboratory: the geometric characteristics of size, volume, area, shape (using a caliper or a scanner with image analysis software), and the density of a particle and porosity of a stack (using a pycnometer). Most other properties require much more experimental work and/or may be extracted from literature. In the latter case, several models are available (most properties are depending on a state variable, such as temperature or composition. Food composition can be obtained from the USDA® (United States Department of Agriculture) and the CIQUAL® Nutrient Database for Standard Reference^[1].

A few property models are predictive, while most others are empirical. Predictive models are more suitable for extrapolation (to other operating conditions or drying processes) than empirical ones. Indeed, empirical models require experimental data to fit some parameters. The applicability of empirical models is often limited to specific products and operating conditions (*i.e.* temperature, pressure). Besides, one should know whether a property model (predictive or empirical) is generic (valid for many products) or specific (limited to few products).

2.4.1 Effective heat capacity

Both predictive and empirical models are available to predict effective heat capacity of solid food products. They depend on volume or mass fraction and heat capacity of pseudo-components (water, air, sugars, proteins, and ashes). For example, some of them are valid on a wide range of temperatures (from -40 °C to 150 °C) and their prediction errors are less than 5 %^[1, 19]. For a few food products, some specific models of heat capacity are also available. For instance, in the case of fruits and vegetables, the property model of Sahin and Sumnu^[19] relates heat capacity to water content. It should be noted that prediction errors and application fields are rarely given.

2.4.2 Effective Thermal conductivity

Both predictive and empirical models are available to predict effective thermal conductivity. On the one hand, the predictive models are usually generic and depend on food pseudo-composition and temperature. For example, some of them can be used within a wide range of temperature (from -40 °C to 150 °C), and both for porous or non-porous solid food materials. Estimation errors are not known^[1, 19]. On the other hand, many empirical models are also present in literature. Some of them are generic and depend on food pseudo-composition, pseudo-compounds thermal conductivity and a structural factor estimated by data fitting. Prediction error close to 10 % is reported^[1, 20] in this case. Likewise, a wide number of specific empirical models exist. They are valid for a narrow list of products and prediction errors are uneven. Percentage error can be higher than 15 %. Furthermore, statistical learning methods are used to predict thermal conductivity of food materials. Neural networks are also applied to estimate thermal conductivity of fruits and vegetables^[21] and bakery products^[22]. Prediction error between 10 and 15 % is reported. A combination of two statistical learning methods (neural network and fuzzy method) is also used to predict effective thermal conductivity of fruits and vegetables^[23]. Prediction error is less than 2 %. The latter method is really interesting but statistical learning methods have some serious

drawbacks: a lot of experimental datasets at different operating conditions are necessary. Indeed, around 500 parameter values have to be estimated. Moreover, this combination cannot be applied to other operating conditions, other processes or other products. In addition, statistical learning algorithms are much more complicated than an algebraic equation. Finally, prediction errors are in the same order of magnitude as what is obtained from any empirical model based on an algebraic equation. To conclude, models based on algebraic equations represent the best trade-offs between minimal experimental work requirement and minimal prediction error.

2.4.3 Isotherm or isobar of water desorption

Isotherms or isobars of water desorption data are required to model the drying process. They relate the moisture content in drying product to its water activity, which is essential to solve mass transfer at the product surface. Again, empirical and predictive models exist. On the one hand, empirical models exist for solid and liquid food materials such as BET^[24], GAB^[25, 26], Ferro-Fontan^[27] and Henderson^[28, 29] models. Most of empirical models are specific to a single product, because parameter values are estimated by fitting experimental dataset. Their prediction errors are generally less than 10 %^[30]. Otherwise, neural network method is used to estimate water activity of fruits^[31]. Prediction error is less than 10 %. Furthermore, UNIQUAC model, which is an empirical thermodynamic model, is also applied for water activity estimation of simple liquid mixtures^[32]. Prediction error is less than 1.5 % which makes this model accurate. On the other hand, the research team of chemical and biochemical engineering laboratory of the University of Clermont-Ferrand developed several predictive thermodynamic models^[33-35]. These models are derived from the UNIFAC-Larsen model. They predict water activity of a mixture composed of electrolytes and sugars in water. Prediction errors are always less than 5 %. However, no article has yet dealt with the applicability of these models to predict water activity of solid food materials.

2.4.4 Effective water diffusion coefficients

Effective water diffusion follows Fick law. Currently, there is no method to predict *a priori* diffusion coefficient values, for solid foods, without any experimental work (and use of inverse methods). Empirical equations, developed from individual experimental datasets, are an important source for the prediction *a posteriori* of this physical property. Various empirical parametric equations of effective moisture diffusivity can be found in literature. Compilations of such equations have been published^[36]. Most authors confirm that the temperature effect can be satisfactorily described by an Arrhenius-type relation^[1, 37-39]. Moisture content has a minor effect and is often correlated by simple exponential or linear functions^[36]. For strongly shrinking materials, the mathematical model should account for bulk porosity^[40].

In this work, two different -experimental- strategies have been tested to reduce the amount of experimental work needed to identify parameters of effective water diffusion equation (see section below).

2.4.5 Optimized experimental strategies to identify parameters of effective moisture diffusion model

The classical strategy, used in food drying, to identify effective moisture diffusivity is the following:

1. measure, at the lab scale, the accessible product properties (water activity, heat capacity, dimension and porosity);
2. collect experimental measurements of thin layer drying kinetics under constant air drying conditions over a wide range of air temperatures;
3. identify the effective moisture diffusivity coefficient by fitting predictions on these thin layer drying kinetics (using variations of recorded product moisture content);
4. validate the model over some thin layer (on product moisture content) or deep bed drying kinetics (on product moisture content and possibly output air moisture and temperature).

Two different strategies, both variant of the classical strategy, have been developed. The first tested strategy has a major difference: drying kinetics of the learning set are composed of thin layer kinetics obtained under *variable drying conditions* in an optimal sequence. This is also known as Non Linear Model Based Sequential Design of Optimal Experiments (NLMBSDOE). Since our models are strongly non-linear both in their variables and parameters, usual linear DOE (Design of Experiments) software tools are not applicable. Hence a new toolbox for MATLAB[®], EXOPTIM[®][17, 41, 42] was developed in our laboratory and applied for the identification of mass transfer coefficient (effective moisture diffusivity and heat transfer coefficient by convection) of steamed rice drying. A compartmental model is used in these simulations (with two compartments) and heat and mass transfer are assumed to be one dimensional and are described by two independent variables (moisture content and temperature of the particles). Contrary to moisture content, temperature is supposed to be uniform within the particles (but not constant during the drying kinetics). In this work, it was demonstrated that with only three successive drying experiments at variable drying temperatures, identified parameters were associated with confidence intervals that are comparable to those obtained with nine kinetics under constant air temperatures. While the advantages of such approach are obvious, it must be emphasized that it requires heavy time-consuming computations (a day; see figure 2.1) improved (expensive) instrumentation, and an approximate knowledge about the static and dynamic limitations (*e.g.* 50% on thermal inertia) of the pilot dryer. To lower calculation duration, it is possible to use multi-core PCs and/or clusters with parallel programming.

The second strategy is also a variant of the classical strategy, but reverses thin layer and deep bed layer experiments. Instead of the classical one, the product effective moisture diffusivity is identified at the deep bed level, and thin layer kinetics are used as a validation support^[43]. In this example, drying kinetics were obtained with pellets for chickens, and the heat and mass transfer model is described by equations (2.1 - 2.8), in section 3.3 “Selecting the ‘best’ modelling approach”. The underlying reason for the choice of this second strategy is the fact that using the classical strategy, some problems arise when comparing experimental and simulated output air moisture contents and temperatures for the thin layer drying case. The product mass variation is the only experimental data used to identify the effective moisture diffusivity. Indeed, input-output differences of air temperature and moisture content are not large enough to get reliable measurements (sensors are not accurate enough). These data alone are insufficient because their representativeness is limited only to the mass transfer, while in drying, this transfer is strongly coupled to the energy change. Hence, the obtained fit is not fed with precise information about the heat exchanges^[9]. In addition, while each thin layer kinetic is classically obtained at a given constant air temperature, all the contrary in a deep bed experiment, each layer of grain within the depth is drying at a different air temperature, all being significantly lower than inlet air temperature.

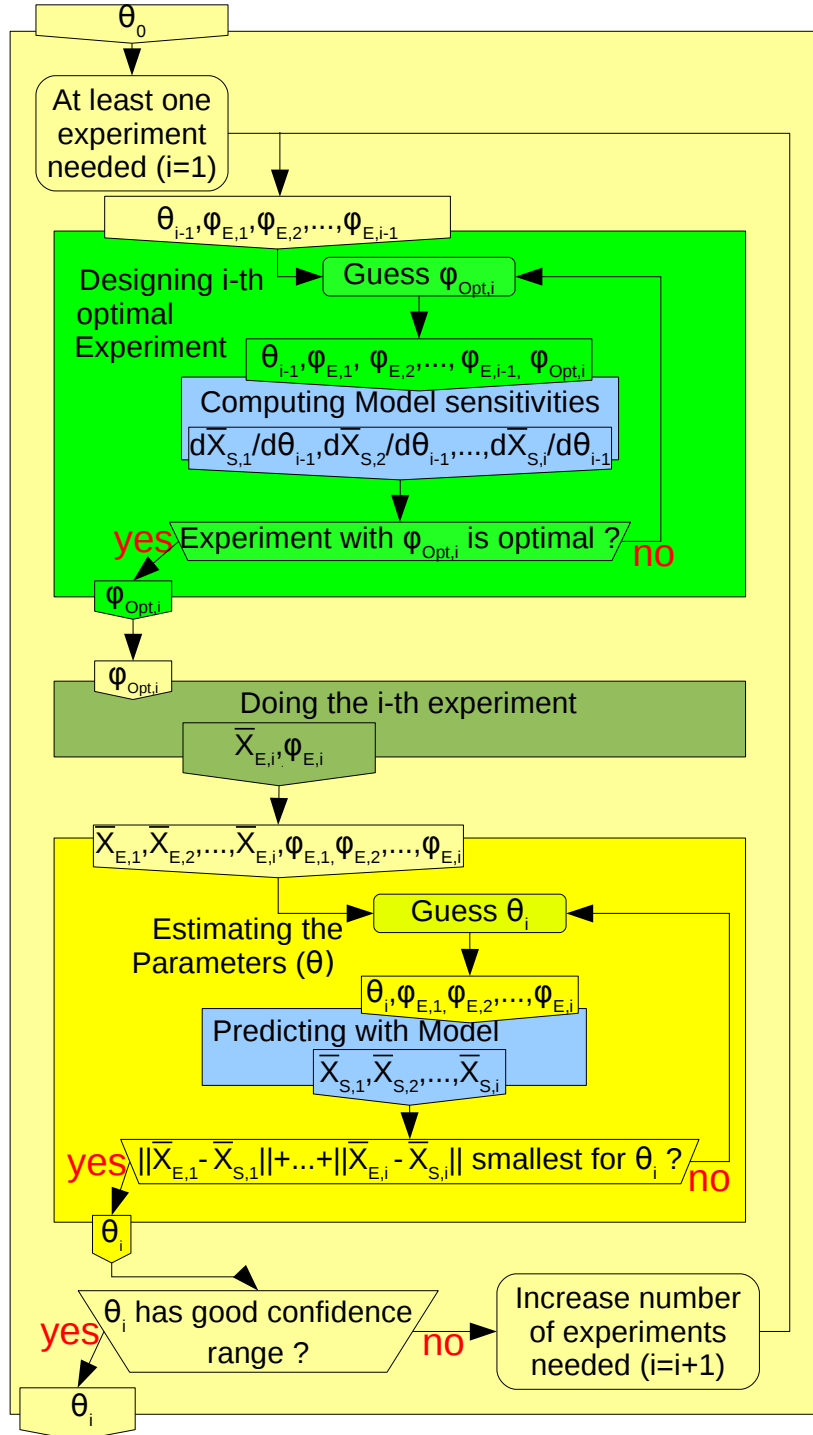


Figure 2.1 – Iterative procedure for the sequential non-linear model-based design of optimal experiments (adapted from^[17]) where φ is the protocol vector, θ the parameter vector, and \bar{X}_E and \bar{X}_S respectively the experimental and simulated values.

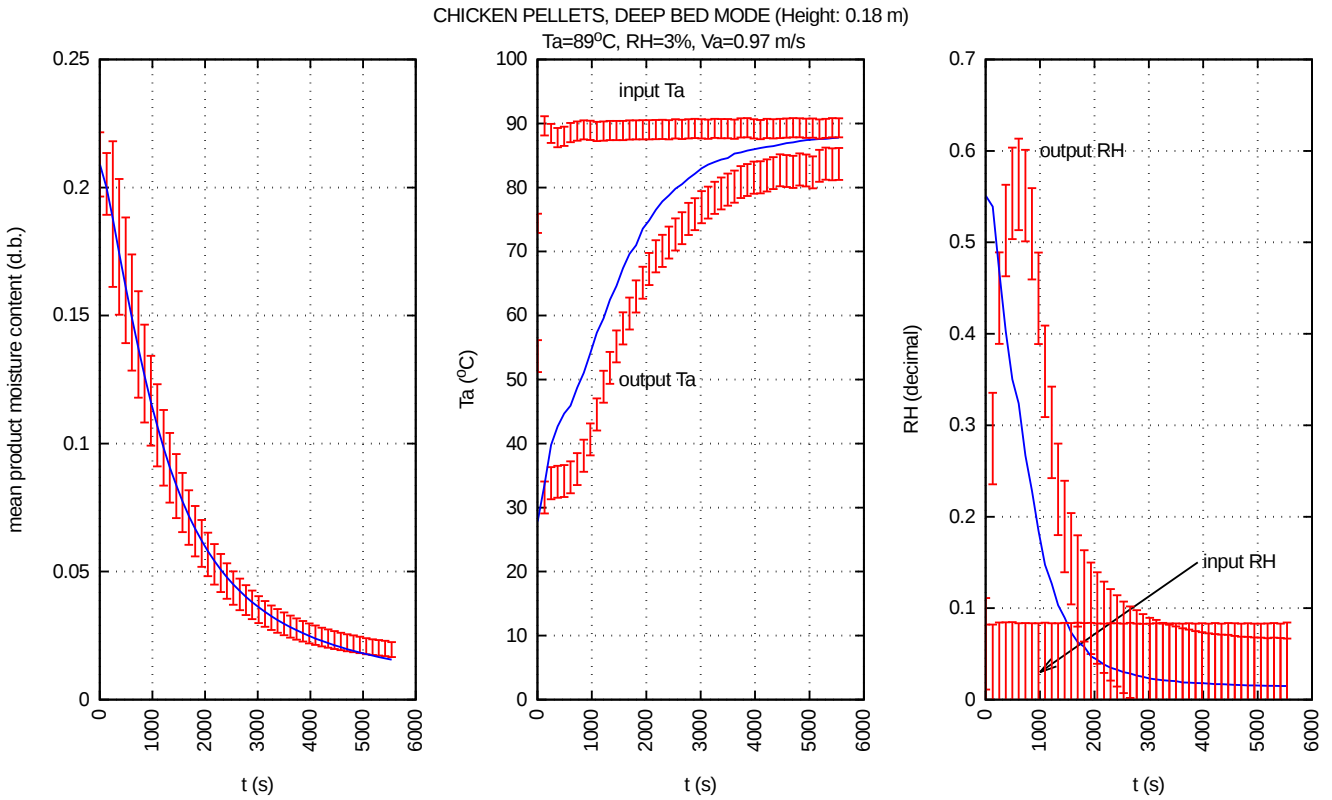


Figure 2.2 – Comparison of experimental (dots with error bars) and simulated (-) data of deep bed drying kinetics of pellets for chickens (learning set) (adapted from [43]).

Hence, one may expect a single deep bed drying kinetic to bring far more information to the identification procedure, as compared to several thin layer kinetics. Combining three recorded data vectors (product moisture content and output air temperature and moisture content), it is possible to identify an effective diffusion coefficient on a single deep bed kinetic at high constant temperature (see figure 2.2)^[43]. The identified coefficient is then used to predict correctly all thin layer kinetics at temperatures lower than the temperature set-point of the deep bed experiment (mean prediction error is less than 15 %; see figure 2.3).

2.5 Discussion

A hot air drying model was developed according to all specifications defined previously. This model is available both for thin layer and deep bed drying, the latter being assumed to be equivalent to thin layers in series. Each specification is illustrated and discussed below:

- Multi-product compatibility

The model was applied to the hot air drying of four different food products (the list is growing). Differences are mostly on composition and shape:

1. soybean and corn are supposed to be of spherical shape;
2. pellets for rabbits and chickens have different compositions and are assumed to be of near-infinite cylinder shape.

All experimental data -thin-layer and deep-bed kinetics- were obtained with the dryer located in AgroParisTech/INRA drying laboratory (see^[9, 10, 43] for the description of the pilot) under mostly constant operatory conditions (except for the DoE approach discussed above).

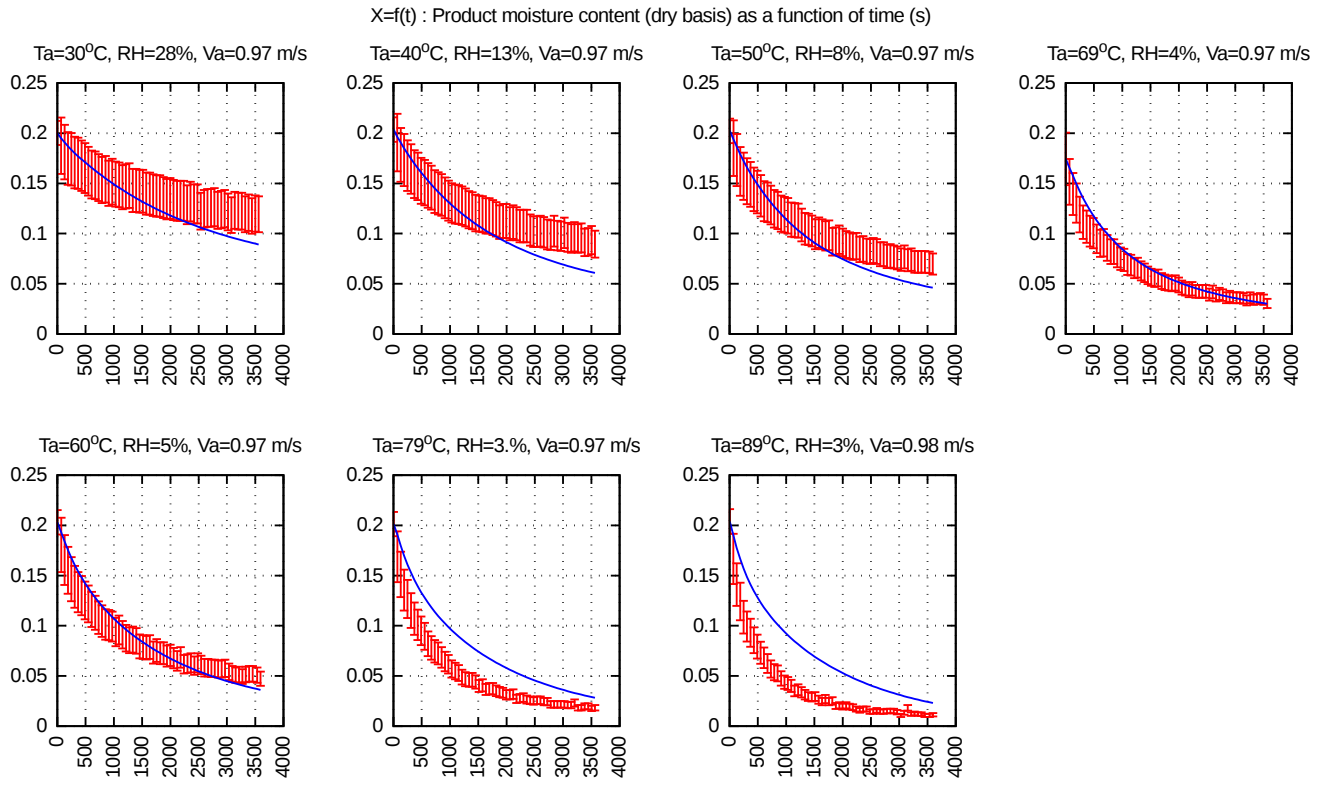


Figure 2.3 – Comparison of experimental (dots with error bars) and simulated (-) data of thin layer drying kinetics of pellets for chickens (validation set) (adapted from [43]).

The proposed modelling approach presents several advantages. Among them, it is noteworthy that parameter identification might be reduced to a single coefficient: effective moisture diffusivity within the solid food matrix. On the one hand, a constant effective moisture diffusivity is usually preferred as long as it fits well on the expected validity domain. On the other hand, an effective moisture diffusivity depending on moisture and temperature, more difficult to identify, will provide a better fit on a wider range of operating conditions. Hence, two variants were tested for effective moisture diffusivity: constant/uniform value and moisture and temperature (varying in space and/or time) dependent. Moreover, several validation methods were tested as summarized in Table 2.1. The limited, yet diverse, list of food products already tested has shown quite a good agreement between model and experimental data, over a wide range of drying conditions. Therefore, the methodology seems robust and promising enough to provide a reliable simulator for hot air thin layer and deep bed drying for most solid foods with different formulations and shapes.

► Wide range of validity

Optimization of drying (*e.g.* to lower its energy consumption) usually requires a broad exploration of operating domain. Hence, the larger the validity domain of a model, the more reliable the simulation. For instance, the thin layer model was systematically tested over a wide range of drying kinetics at different air temperatures. Indeed, corn was dried at temperature between 20 and 150 °C which can be considered to be a large domain. Figure 2.4 shows a good agreement between experimental and simulated data (mean prediction error $\approx 9\%$).

► Multi-technology compatibility

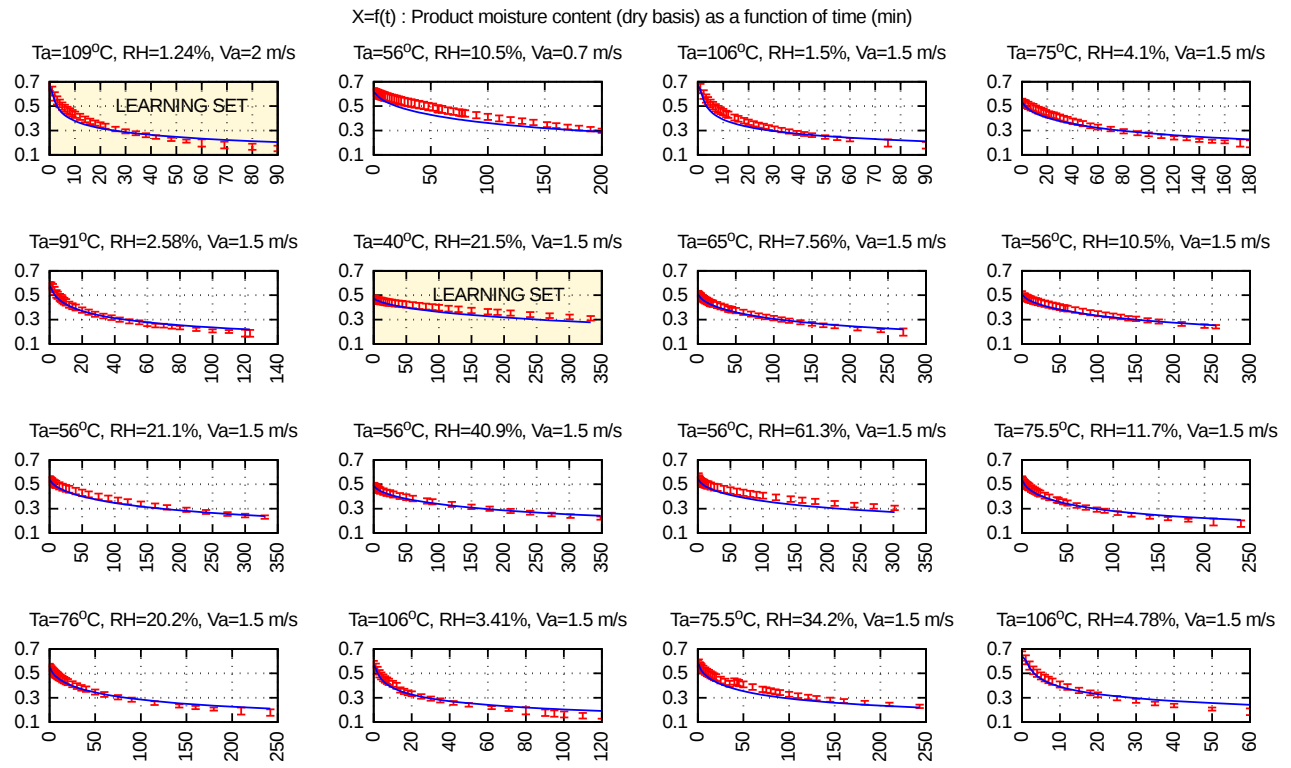


Figure 2.4 – Comparison of experimental (dots with error bars) and simulated (-) data of thin layer corn drying kinetics obtained at air temperature between 40 and 110 °C (kinetics of the learning set are colored and labelled).

The models can be easily adapted to different hot air drying technologies. Indeed, a thin layer model can simulate a fluidized bed drying, while a deep bed drying model can simulate fixed bed and conveyor belt dryers. Moreover, one can consider that the deep bed drying model, with modifications involving little programing effort, can simulate other drying technologies. Assuming that mixed flow dryers and ambient grain coolers can be considered as networks of deep beds, the deep bed drying model is the elementary brick to simulate these technologies. It is also possible to simulate multi-conveyor belt dryers with the addition of a function simulating the product mixing (between each conveyor).

► Standardized computer implementation

The deep bed and thin layer drying models are implemented, as stated before, in two computer languages: C++ and FORTRAN 90. The latter is currently developed as a compiled module of conveyor belt and fluidized bed dryers in ProSimPlus® (work still in progress). To perform a drying simulation, one has to:

- list all the compounds involved in the drying process (for air and solid product) and their thermophysical properties -if available- in Simulis Thermodynamics® (see figure 2.5);
- enter relative composition, temperature and flow rate of the streams (“dry air” and “wet solid products”) in ProSimPlus® (see figure 2.6);
- configure the dryer module in ProSimPlus® (see figures 2.6 and 2.7) defining:
 - solid products shape and its properties;
 - type of layer and its properties in the case of a deep bed;

Table 2.1 – 3 validation methods for the identification of effective moisture diffusivity (with both constant and varying D_{eff} being systematically tested)

	Case 1	Case 2	Case 3
Learning set	Thin layer kinetics	Thin layer kinetics	Deep bed kinetics
Validation set	Thin layer kinetics	Deep bed kinetics	Thin layer kinetics
Tested products	Soybeans, corn and pellets for chickens and rabbits	Corn and pellets for chickens and rabbits	Corn and pellets for chickens and rabbits

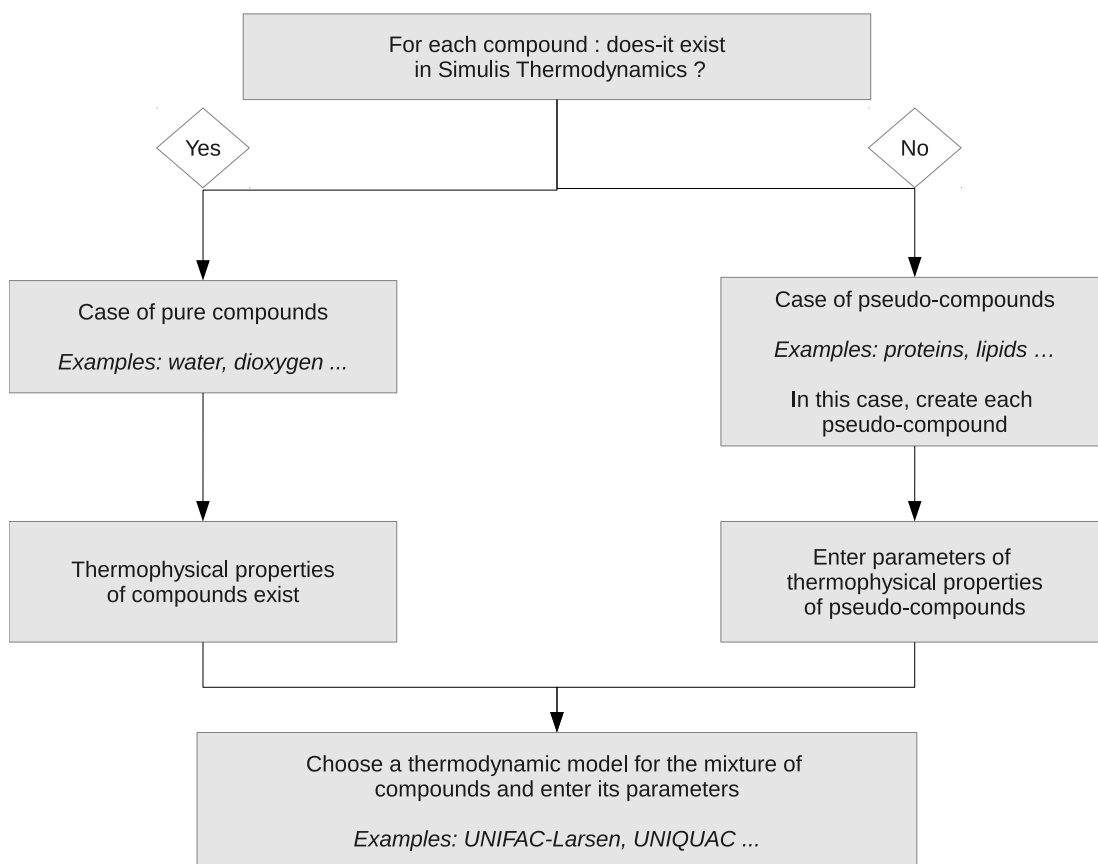


Figure 2.5 – Configuration steps of compounds mixture in Simulis Thermodynamics®.

- solid products and bed meshes;
- equilibrium properties (effective moisture diffusivity, water activity and heat and mass transfer coefficients) of the solid products.

More precisely, compounds are either existing ones in the database, or pseudo-compounds created by user. In the latter case, their physical properties can be estimated by fractional or polynomial functions already available in Simulis Thermodynamics®. For each pseudo-compound, one identifies or enters directly parameter values into the properties equations. Moreover, general equations are directly implemented in the drying models for the equilibrium properties of solid products (work in progress). One chooses an equation and enters their parameter values.

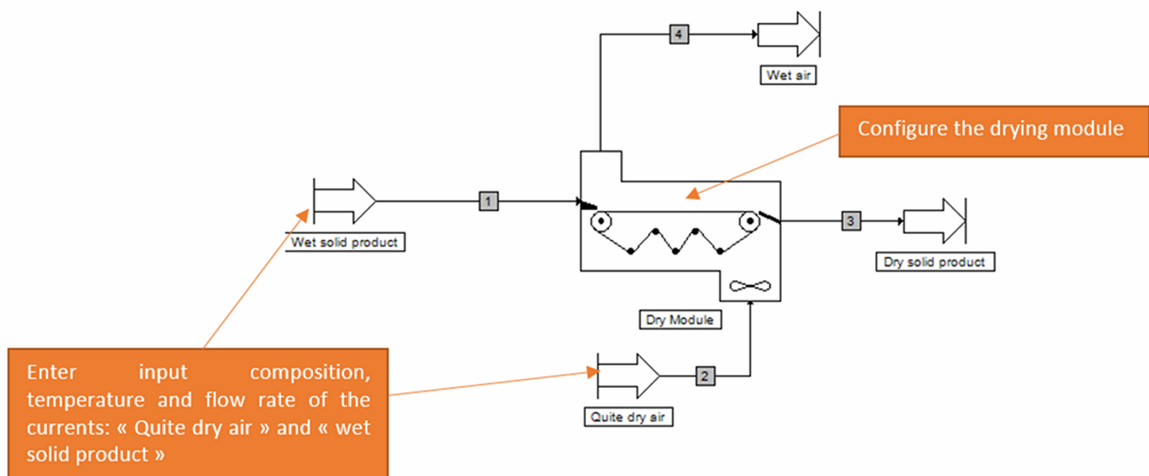


Figure 2.6 – Configuration step of the dryer module in ProSimPlus[®] (prototype, work in progress).

2.6 Conclusions

This study proposes a methodology to build up generic drying models in chemical engineering software such as ProSimPlus[®]. A hot air drying model for thin layer and deep bed was developed according to the following specifications: i) multi-product compatibility (application to different formulations and shapes), ii) wide range of validity (according to inlet air temperatures), and iii) multi-technology compatibility (available for fluidized bed, conveyor belt, mixed flow dryer and gains cooler). Further developments in air-drying modelling will lead to the creation of generic tools able to investigate the drying characteristics at various drying conditions. This work is a first yet significant step toward a generic hot air drying simulator.

Current work in progress is focused on 1) the optimal strategy to identify effective moisture diffusivity with best confidence interval and reduced experimental work, based on the C++ programs, 2) the model reduction to deal with the simulation time constraints in a commercial software, 3) applying the methodology to the other products of the kinetics database of our drying laboratory, 4) the development of a model variant dedicated to steam drying.

2.7 Acknowledgments

The authors wish to thank the French Agence Nationale de la Recherche (ANR) for their funding, and the partners of the project COOPERE-2 leaded by Veolia Research and Innovation, in collaboration with ProSim and ENSIACET. The authors wish also to thank the French Agency ADEME (Agence Nationale de l'environnement et de la maîtrise de l'énergie) and the technical center TECALIMAN for their funding of the experimental characterization and modelling of the drying of animal pellets.

In addition, the authors wish to thank several master and PhD students (Perrine Leclercq, Analia Aparecida Vanzo, Abir Hosni, Azziz Zemmouri, Monica Pinto, Benoit Hareng) and our colleagues Giana Perré and Julien Cartailler for their valuable help in acquiring experimental data supporting the modelling and simulation work.

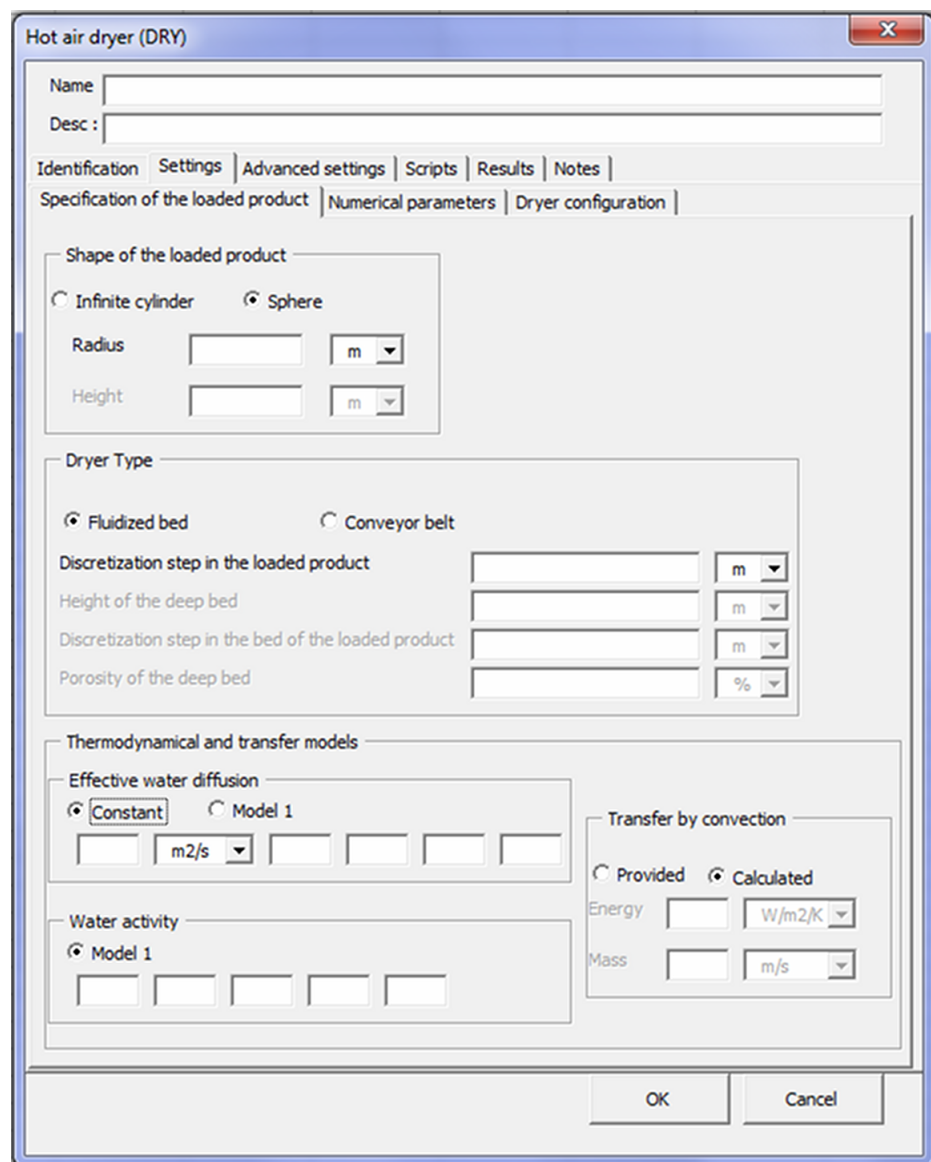


Figure 2.7 – Main configuration dialog of the drying module in ProSimPlus® (prototype, work in progress).

Finally, the authors would like to thank the anonymous reviewers for their valuable comments.

2.8 References

1. Gulati, T.; Datta, A.K. Enabling computer-aided food process engineering: Property estimation equations for transport phenomena-based models. *Journal of Food Engineering* 2013, 116(2), 483-504.
2. European Commission. Green paper, A 2030 framework for climate and energy policies, COM(2013) 169 final. <http://eur-lex.europa.eu/legal-content/EN/ALL/?uri=CELEX:52013DC0169> (accessed March 17, 2015); Report 2013.
3. Devahastin, S. Software for Drying/Evaporation Simulations: Simprosys. *Drying Technology* 2006, 24(11), 1533-1534.
4. Pakowski, Z. Simulation of the process of convective drying: Identification of generic computation routines and their implementation in a computer code dryPAK. *Computers and Chemical Engineering* 1999, 23(1), S719 - S722.
5. Kemp, I.C. Progress in dryer selection techniques. *Drying Technology* 1999, 17(7-8), 1667-1680.
6. Schuck, P.; Dolivet, A.; Méjean, S.; Zhu, P.; Blanchard, E.; Jeantet, R. Drying by desorption: A tool to determine spray drying parameters. *Journal of Food Engineering* 2009, 94(2), 199-204.
7. Schuck, P.; Roignant, M.; Brule, G.; Davenel, A.; Famelart, M.H.; Maubois, J.L. Simulation of water transfer in spray drying. *Drying Technology* 1998, 16(7), 1371-1393.
8. Zhu, P.; Méjean, S.; Blanchard, E.; Jeantet, R.; Schuck, P. Prediction of drying of dairy products using a modified balance-based desorption method. *Dairy Science and Technology* 2013, 93(4-5), 347-355.
9. Courtois, F. Dynamic Modelling of Drying to Improve Processing Quality of Corn. Ph.D. thesis, ENSIA, Massy, France; 1991. <https://tel.archives-ouvertes.fr/tel-00308506/en/>
10. Abud Archila, M. Modélisation simultanée des transferts et de l'évolution de la qualité technologique du riz paddy en vue d'optimiser les conditions de séchage. Ph.D. thesis, ENSIA, Massy, France; 2000.
11. Courtois, F.; Archila, M.A.; Bonazzi, C.; Meot, J.M.; Trystram, G. Modeling and control of a mixed-flow rice dryer with emphasis on breakage quality. *Journal of Food Engineering* 2001, 49(4), 303-309.
12. Fohr, J.P.; Arnaud, G.; Ali Mohamed, A.; Ben Moussa, H., Validity of drying kinetics, in *Drying 89*, Mujumdar, A., Roques, M., Editors. 1990, Hemisphere Publication: New York. p. 269-275.
13. Kemp, I.C. Drying Models, Myths, and Misconceptions. *Chemical Engineering and Technology* 2011, 34(7), 1057-1066.
14. Bird, R.B.; Stewart, W.E.; Lightfoot, E.N., *Transport phenomena*, 2002, Wiley and Sons: New-York.
15. Shampine, L.F.; Reichelt, M.W.; Kierzenka, J.A. Solving Index-1 DAEs in MATLAB and Simulink. *SIAM Review* 1999, 41, 538-552.
16. Nelder, J.; Mead, R. A simplex method for function minimization. *Computer Journal* 1965, 7(4), 308-313.
17. Goujot, D.; Meyer, X.; Courtois, F. Identification of a rice drying model with an improved sequential optimal design of experiments. *Journal of Process Control* 2012, 22(1),

95-107.

18. Krokida, M.K.; Zogzas, N.P.; Maroulis, Z.B. Heat transfer coefficient in food processing: compilation of literature data. *International Journal of Food Properties* 2002, 5(2), 435-450.
19. Sahin, S.; Sumnu, S.G.; Size, shape, volume and related physical attributes. In *Physical properties of foods*; Springer, Ed.; Food Science, 2006; 1-37.
20. Carson, J.K. Review of effective thermal conductivity models for foods. *International journal of Refrigeration* 2006, 29, 958-967.
21. Sablani, S.S.; Rahman, M.S. Using neural networks to predict thermal conductivity of food as a function of moisture content, temperature and apparent porosity. *Food Research International* 2003, 36, 617-623.
22. Sablani, S.S.; Baik, O.D.; Marcotte, M. Neural networks for predicting thermal conductivity of bakery products. *Journal of Food Engineering* 2002, 52, 299-304.
23. Rahman, M.S.; Rashid, M.M.; Hussain, M.A. Thermal conductivity prediction of foods by Neural Network and Fuzzy (ANFIS) modeling techniques. *Food and Bioproduct Processing* 2012, 90, 333-340.
24. Brunauer, S.; Emmett, P.H.; Teller, E. Modifications of the Brunauer, Emmett and Teller Equation1. *Journal of the American Chemical Society* 1938, 60.
25. De Boer, J.H., *The Dynamical Character of Adsorption*, 1953, Oxford, Clarendon Press. p. 239.
26. Guggenheim, E.A., *Applications of Statistical Mechanics*, 1966, Oxford University Press. p. 220.
27. Ferro Fontan, C.; Chirife, J.; Sancho, E.; Iglesias, H.A. Analysis of a model for water sorption phenomena in foods. *Journal of Food Science and Technology* 1982, 47(5), 1590–1594.
28. Henderson, S.M. A basic concept of equilibrium moisture. *Agricultural Engineering* 1952, 33, 29–32.
29. Thompson, T.L.; Peart, R.M.; Foster, G.H. Mathematical simulation of corn drying: A new model. *Transactions of the American Society of Agricultural Engineers* 1968, 24, 582–586.
30. Singh, R.P.; Heldman, D.R., *Introduction to food engineering*, 2014, Elsevier: USA.
31. Myhara, R.M.; Sablani, S. Unification of fruit water sorption isotherms using artificial neural network. *Drying Technology* 2001, 19(8), 1543-1554.
32. Perres, A.M.; Macedo, E.A. Phase equilibria of D-Glucose and sucrose in mixed solvent mixtures: Comparison of UNIQUAC based models. *Carbohydrate Research* 1997, 303, 135-151.
33. Achard, C.; Dussap, C.G.; Gros, J.B. Prediction of pH in complex aqueous mixtures using a group contribution method. *AIChE J.* 1994, 40, 1210-1222.
34. Catte, M.; Dussap, C.G.; Gros, J.B. A physical chemical UNIFAC model for aqueous solutions of sugars. *Fluid Phase Equilibria* 1995, 105, 1-25.
35. Gros, J.B.; Dussap, C.G. Estimation of equilibrium properties in formulation or processing of liquid foods. *Food Chemistry* 2003, 82, 41-49.
36. Zogzas, N.P.; Maroulis, Z.B.; Marinos-Kouris, D. Moisture Diffusivity Data Compilation in Foodstuffs. *Drying Technology* 1996, 14(10), 2225-2253.
37. Chen, D.; Zheng, Y.; Zhu, X. Determination of effective moisture diffusivity and drying kinetics for poplar sawdust by thermogravimetric analysis under isothermal condition. *Bioresource Technology* 2012, 107(0), 451 - 455.
38. Guillard, V.; Broyart, B.; Bonazzi, C.; Guilbert, S.; Gontard, N. Moisture Diffusivity

in Sponge Cake as Related to Porous Structure Evaluation and Moisture Content. *Journal of Food Science* 2003, 68(2), 555-562.

39. Roca, E.; Broyart, B.; Guillard, V.; Guilbert, S.; Gontard, N. Predicting moisture transfer and shelf-life of multidomain food products. *Journal of Food Engineering* 2008, 86(1), 74 - 83.

40. Kudra, T.; Mujumdar, A.S., *Advanced Drying Technologies*, 2009, Taylor & Francis Group.

41. Goujot, D.; Courtois, F., Improved experimental strategy for best parameter identification of a drying model, in *Proceedings of the EuroDrying congress*, October 2013: Paris, France.

42. Goujot, D.; Meyer, X.M.; Courtois, F., EXOPTIM: dEsign d'eXpériences Optimales Planifiées variables en Temps et Identification pour la Modélisation, 2013, Agence pour la Protection des Programmes: Logibox numéro 77010, 1 CDrom, IDDN.FR.001.370015.000. R.P.2013.000.20700.

43. Lambert, C.; Romdhana, H.; Courtois, F. Reverse methodology to identify moisture diffusivity during air-drying of foodstuffs. *Drying Technology* 2015, 33(9), 1076 - 1085.

Chapitre 3

Reversing classical methodology to identify effective moisture diffusivity during air-drying of foodstuffs

Résumé

La diffusivité apparente de l'eau est un paramètre clés pour la simulation du procédé de séchage de produits alimentaires. La méthode classique comprend une étape d'identification effectuée à l'aide de cinétiques de séchage en couche mince, suivie d'une étape de validation à l'aide de cinétiques en couche épaisse. Plusieurs cinétiques à des températures d'air différentes sont requises pour la phase d'identification. Malheureusement, un écart non négligeable est souvent observé entre les variables de l'air simulées et expérimentales en sortie de séchoir, lors de la validation en couche épaisse. Seules des données concernant le transfert de matière sont utilisées lors de l'étape d'identification, alors que les transferts de matière et d'énergie sont couplés au cours du séchage. Pour cette raison, une approche inverse a été développée. Les résultats ont montré que l'identification sur une seule cinétique en couche épaisse est valable pour des cinétiques en couche mince sur une large gamme de températures. En outre, deux corrélations de diffusivité apparente de l'eau ont été testées.

Mots-clés : Propriétés physiques, séchage d'aliments, diffusivité de l'eau, identification.

Cet article a été publié dans *Drying Technology*¹.

3.1 Introduction

In drying process, correlations based on similarity invariants allow estimating external heat and mass transfer coefficients of food products. Unfortunately, these approaches are not suitable to predict internal heat and mass diffusivities without further experimental work. For most food products, the moisture diffusion is far slower than the heat diffusion as well as the vaporization flux, it justifies why it is commonly admitted that drying of food is limited by water diffusion. Hence, the experimental determination of moisture diffusion within the solid food matrix is at the core of this work.

1. C. Lambert, H. Romdhana, and F. Courtois, “Reverse methodology to identify moisture diffusivity during air-drying of foodstuffs,” *Drying Technology* 33(9), pp. 1076-1085, 2015.

The moisture diffusivity in food is of special interest for the modelling of the air-drying kinetics. Literature data of effective diffusivity is not readily available because of its variability upon several parameters, such as temperature, hygroscopic state (water content, water activity) and structure (porosity, tortuosity). However, there is no standard method that allows for the estimation of diffusivity. The methods published in the literature are based essentially on drying^[1,2], sorption, desorption^[3,4], permeation^[5] or penetrant distribution experiments^[6]. Measurements usually require some data processing. Kinetic results are then processed according to analytical, numerical or graphical methods. A critical presentation of the moisture diffusivity estimation methods was presented by Zogzas *et al.*^[7]. According to data processing results, the moisture diffusivity may be expressed in terms of one or more parameters and variables. Such variables can be both drying conditions and food product properties (hygroscopic state, physical structure and elementary composition). A large number of studies have shown that these parameters play an important role in the diffusion of water within the product during drying, rehydration or storage processes. Diffusivity in air-dried potato significantly increased with temperature and moderately with moisture content^[2]. Nonetheless, this assertion may be discussed when considering dry product (*i.e.* with water activity below 0.5). Saravacos^[8] illustrated the impact of the presence of fats by measuring the diffusivity in whole and defatted soybeans. The results showed a significant decrease of the diffusivity with decreasing of moisture within whole soybeans. Some operating parameters, in particular pressure, have an inverse effect on the diffusivity. Karathanos *et al.* ^[6] experimented the starch drying at high pressure. They showed that the pressure resulting from the product compression reduces the porosity and therefore the moisture diffusivity. Saravacos and Maroulis^[9] compiled several data of moisture diffusivity obtained from starch drying at low temperature. The result showed a clear difference in effective diffusivity for an extruded, gelatinized, granular or pressed granular materials. Higher and lower diffusivities were observed respectively in extruded and gelatinized materials. Granular product has a slightly higher diffusivity than a pressed one. Various empirical parametric equations of moisture diffusivity can be found in literature. Compilations of such equations have been published^[1]. Most authors confirmed that the temperature effect can be satisfactorily described by an Arrhenius-type relation. Moisture content has a minor effect and is often correlated by simple exponential or linear functions. For strongly shrinking materials the mathematical correlation should account for bulk porosity^[10]. Indeed, identifying the effective moisture diffusivity of such materials without considering the variation of the exchange surface may lead to huge errors on the identified parameters^[11]. However, parameters values of all of these correlations are often valid for a small range of operating conditions (maximum variation of inlet air temperature between 20 or 30 °C).

For each correlation, the common methodology used to estimate the effective moisture diffusivity of a food product is:

1. measure at the lab scale product properties (a_w , C_p , etc.) and drying kinetics under constant conditions over a wide range of air temperatures;
2. identify the effective moisture diffusivity coefficient by fitting on a set of several thin layer drying kinetics (using variations of recorded product moisture content);
3. validate the correlation over some deep bed drying kinetics on product moisture content and -possibly- output air moisture and temperature.

However, some problems arise when comparing experimental and simulated output air moisture contents and temperatures. Indeed, the product mass variation is the only experimental data used to identify the effective moisture diffusivity. These data alone are

insufficient because their representativeness is limited only to the mass transfer, while in drying, this transfer is strongly coupled to the energy change. Hence, the obtained fit is not fed with precise information relatively to the heat exchanges^[12]. In addition, while each thin layer kinetic is usually obtained at a given constant air temperature, all the contrary in a deep bed experiment, each layer of grain within the depth is drying at a different air temperature, all being significantly lower than inlet air temperature. Hence, one may expect a single deep bed drying kinetic to bring far more information to the identification procedure, as compared to several thin layer kinetics. Therefore, the aim of this work is to integrate additional data in term of heat transfer in order to improve the heat and mass transfer modeling during air-drying. This work provides a description of an inverse method and an application on a real case of drying food:

1. identify the effective moisture diffusivity coefficient by fitting on some deep bed drying kinetics (using variations of recorded product moisture content and air temperature and relative humidity);
2. validate the correlation over all thin layer drying kinetics using product moisture content.

The expected benefit of such approach is double: a) better confidence intervals on parameter estimation due to the triple dimension of the data vector used and, b) reduction of the experimental work strictly necessary to estimate unknown parameters (*i.e.* one deep bed experiment versus many thin layer experiments).

3.2 Theory: deep bed and thin layer drying model

A convective drying model was build up both for deep bed and thin layer. The following assumptions were considered for the particles:

- ideal geometry (infinite cylinder or spherical shape) and no shrinkage or swelling are assumed;
- an isotropic behavior within the product is assumed (heat and mass transfers are in the radial direction);
- the conduction heat transfer between particles is negligible;
- the thermal expansion coefficient is negligible;
- heat conduction and liquid water diffusion occur within the particles (see below);
- evaporation, heat and mass convection occur only at the surface.

The model is developed for thin layer and deep bed drying. One usually assimilates the deep bed as a serie of thin layers for which the only transfer occurs between air and grain, and a thin layer as an equivalent average (single) particle. Moreover, deep bed drying involves energy and mass transfer in air, after each thin layer crossing^[12]. Furthermore, the heat and mass Biot number values (Bi_{th} and Bi_m) are respectively between 0.1 and 100 and much higher than 100. Therefore, heat conduction and liquid water diffusion within the particles and water evaporation, heat and mass convection at their surface are considered^[13]. The heat and mass Peclet number values (Pe_{th} and Pe_m) are much higher than 1, therefore a plug-type airflow and no pressure variation are assumed^[13].

3.2.1 Heat and mass balance on the particles

Liquid water diffusion (equation 3.1) and thermal conduction (equation 3.2) phenomena are based on Fourier and Fick law respectively^[13].

$$\left(\frac{\partial X_t^{r,z}}{\partial t} \right) = \frac{1}{r^n} \cdot \frac{\partial}{\partial r} \left(r^n \cdot D_{eff} \cdot \frac{\partial X_t^{r,z}}{\partial r} \right) \quad (3.1)$$

$$\left(\frac{\partial Tp_t^{r,z}}{\partial t} \right) = \frac{1}{\rho_{d.m.} \cdot (Cp_{d.m.} + X_t^{r,z} \cdot Cp_w) \cdot r^n} \cdot \frac{\partial}{\partial r} \left(r^n \cdot \lambda_{eff} \cdot \frac{\partial Tp_t^{r,z}}{\partial r} \right) \quad (3.2)$$

Where X (d.b.) is the water content, r radial position in the particle (m), z particle position in the height of the bed (m), t the elapsed time (s), n the shape factor (1, or 2, respectively for cylindrical, or spherical symmetry), D_{eff} the effective water diffusion coefficient ($m^2.s^{-1}$), T_p the product temperature (K), λ_{eff} the effective thermal conductivity ($W.m^{-2}.K^{-1}$), $\rho_{d.m.}$ the density of the dry matter ($kg.m^{-3}$) and $Cp_{d.m.}$ and Cp_w the heat capacity at constant pressure of dry matter and water ($J.kg^{-1}.K^{-1}$), for the considered particle.

Initial conditions are the followings: temperature and water content within the particles are assumed to be uniform. Boundary conditions are shown in equations 3.3 to 3.6.

$$\left(\frac{\partial X_t^{0,z}}{\partial r} \right) = 0 \quad (3.3)$$

$$\left(\frac{\partial Tp_t^{0,z}}{\partial r} \right) = 0 \quad (3.4)$$

$$-\rho_{d.m.} \cdot \left(\frac{\partial D_{eff} \cdot X_t^{r_{max},z}}{\partial r} \right) = \phi_m = k_m \cdot \frac{M_w}{R} \cdot \left(\frac{a_w \cdot Pv_{sat}(Tp_t^{r_{max},z})}{Tp_t^{r_{max},z}} - \frac{RH \cdot Pv_{sat}(Ta_t^z)}{Ta_t^z} \right) \quad (3.5)$$

$$-\lambda_{eff} \cdot \left(\frac{\partial Tp_t^{r_{max},z}}{\partial r} \right) = h_{glob} \cdot (Tp_t^{r_{max},z} - Ta_t^z) + \phi_m \cdot \Delta H_v = \phi_q \quad (3.6)$$

Where k_m the convective mass transfer coefficient ($m.s^{-1}$), M_w the molar mass of water ($g.mol^{-1}$), R the gas constant ($J.kg^{-1}.K^{-1}$), a_w the water activity of the particle (Pa/Pa), Pv_{sat} the pressure of saturated vapor (Pa), RH the relative humidity (decimal), h_{glob} the external heat transfer coefficient including the heat transfer effectiveness by convection ($W.m^{-2}.K^{-1}$), Ta the air temperature (K), ΔH_v the enthalpy of vaporization of pure water ($J.kg^{-1}$), ϕ_m the mass flux density ($kg.m^{-2}.s^{-1}$) and ϕ_q the heat flux density ($J.m^{-2}.s^{-1}$).

3.2.2 Heat and mass balance on the air

A microscopic balance is made on the air after each thin layer crossing (equations 3.7 and 3.8).

$$\frac{\partial (\rho_{da} \cdot Y_t^z)}{\partial t} = -\frac{\partial}{\partial z} \left(\frac{\varphi_a}{\varepsilon} \cdot Y_t^z \right) + \phi_m \cdot a \cdot \left(\frac{1-\varepsilon}{\varepsilon} \right) \quad (3.7)$$

with $a = \frac{S_p}{V_p}$ and $\varphi_a = \varepsilon \cdot \rho_{da} \cdot v_a$

$$\frac{d(\rho_{da} \cdot (Cp_{as} + Y_t^z \cdot Cp_v) \cdot Ta_t^z)}{dt} = -\frac{\partial (\rho_{da} \cdot v_a \cdot (Cp_{as} + Y_t^z \cdot Cp_{as}) \cdot Ta_t^z)}{\partial z} - \frac{a \cdot (1-\varepsilon) \cdot \phi_q}{\varepsilon} \quad (3.8)$$

Table 3.1 – Composition of pellets for chickens

	% db
Proteins	20.9
Lipids	19.1
Total sugar	54.5
Ashes	5.5

Where ρ_{da} is the density of the dry air ($kg.m^{-3}$), a the particle specific surface area (surface area per particle volume) (m^{-1}), ε the porosity (decimal), Y the water content (d.b.), φ_a the density of the mass flow, T_a the temperature (K) and $Cp_{d.a.}$ and Cp_v the specific heat capacity at constant pressure of respectively dry air and water vapor ($J.kg^{-1}.K^{-1}$), for the considered air.

Air water content and temperature are fixed at the entry of the first thin layer. Their values may not be constant during a drying experiment.

3.3 Materials and methods

3.3.1 Materials

The model is applied to deep bed and thin layer drying of pellets for chickens, produced by Tecaliman® (technical center for french feed industry). The pellets are a mixture of corn, wheat, barley, soybean, sugar beet pulp and rape, and have a cylindrical shape. Dry mater composition of the pellets is given in table 3.1.

3.3.2 Geometry and density measurements

Density of the pellets is measured using Fontainebleau sand and the radius and characteristic length of the pellets using a caliper.

3.3.3 Moisture content measurement

Moisture content is measured according to the AFNOR French norm NF V 18-109^[14], before thin layer and deep bed drying and after thin layer drying.

3.3.4 Sorption isotherm measurement

Isotherm analyses were performed using a Dynamic Vapor Sorption (D.V.S.) intrinsic apparatus (Surface Measurement Systems, London, UK). This apparatus is equipped with an ultra-sensitive microbalance. Samples were milled using a IKA M20 Universal Mill apparatus. Approximately 10 mg of each sample was inserted in the pan. In this device, a constant flow of nitrogen gas, into which nitrogen containing a preset amount of water vapor is mixed, passes through the chamber to maintain the desired relative humidity level. The air relative humidity accuracy of this system is of about $\pm 0.5\%$. All sorption cycles applied in this work started from 0 % relative humidity (RH), the dry mass is determined at the end of this plateau. Isotherms were measured at two levels of temperature (25 °C and 40 °C). Adsorption/desorption cycles of relative humidity (RH) ranged from 0 % - 90 % at steps of 10 % of RH.

Equilibrium moisture content (X_{eq}) and relative humidity (RH) data were fitted using the modified Henderson Equation^[15, 16] (equation 3.9). This isotherm equation is one of the five equations recommended by ASAE Standard D245.6 for fitting sorption data of several agri-food materials^[17].

$$RH = 1 - \exp(A.(X_{eq})^B) \quad (3.9)$$

Where A and B are constants, X_{eq} is the equilibrium moisture content (% d.b.), RH the relative humidity (decimal).

3.3.5 Identification of effective moisture diffusivity

Effective moisture diffusivity is identified using one deep bed drying kinetic obtained under the following operating conditions: air velocity is fixed at 1 m.s^{-1} , inlet air temperature at $90\text{ }^\circ\text{C}$ and inlet air relative humidity at 3 %, initial moisture content and temperature of the pellets respectively at 0.204 d.b and $20\text{ }^\circ\text{C}$. The height of the deep bed is 18 cm (equivalent to 4.23 kg of pellets for chickens). Moreover, the validation set is composed of 7 thin layer kinetics obtained under the following operating conditions: inlet air temperature is between 30 to $90\text{ }^\circ\text{C}$, air velocity is fixed at 1 m.s^{-1} , and initial mass, temperature and moisture content of the pellets are respectively about 190 g, $20\text{ }^\circ\text{C}$, and 0.204 d.b.

Two correlations of effective moisture diffusivity were tested: an Arrhenius^[1] one (equation 3.10) and one proposed by Abud^[18] (equation 3.11).

$$D_{eff} = D_0 \cdot \exp\left(\frac{-E_a}{R \cdot T_p}\right) \quad (3.10)$$

$$D_{eff} = \exp(-d_1 + d_2 \cdot X \cdot T_p) \quad (3.11)$$

Where D_0 , d_1 and d_2 are constants, and E_a the energy of activation ($J.kg^1.K^1$).

3.3.6 Drying kinetics measurement

Experimental data -thin-layer and deep-bed kinetics- was obtained with the dryer located in AgroParisTech/INRA/CNAM drying laboratory (Massy, France) under constant and controlled operating conditions. Thin layer experiments were done in triplicates. Scheme of the pilot is given in figure 3.1. The following parameters are measured each minute on this pilot:

- inlet and outlet air temperature and relative humidity;
- inlet air velocity;
- mass of the product (with discontinuous weighing system with an air being bypassed)

According to relative humidity and temperature sensor precision and their position in the pilot, the following uncertainties on the measures are retained:

- inlet air temperature: $\pm 1.5\text{ }^\circ\text{C}$ ($\sigma = 0.5\text{ }^\circ\text{C}$)
- outlet air temperature: $\pm 2.5\text{ }^\circ\text{C}$ ($\sigma = 0.8\text{ }^\circ\text{C}$)
- inlet and outlet relative humidity: $\pm 5\text{ \%}$ ($\sigma = 1.7\text{ \%}$)

Precision on mean moisture content was calculated using repetitions of thin layer kinetic and the following uncertainties on the measures are retained:

- mean moisture content: $\pm 6\text{ \%}$ ($\sigma = 2\text{ \%}$) if $X > 0.2\text{ d.b.}$ and $\pm 15\text{ \%}$ ($\sigma = 5\text{ \%}$) if $X < 0.2\text{ d.b.}$ (for thin layer)

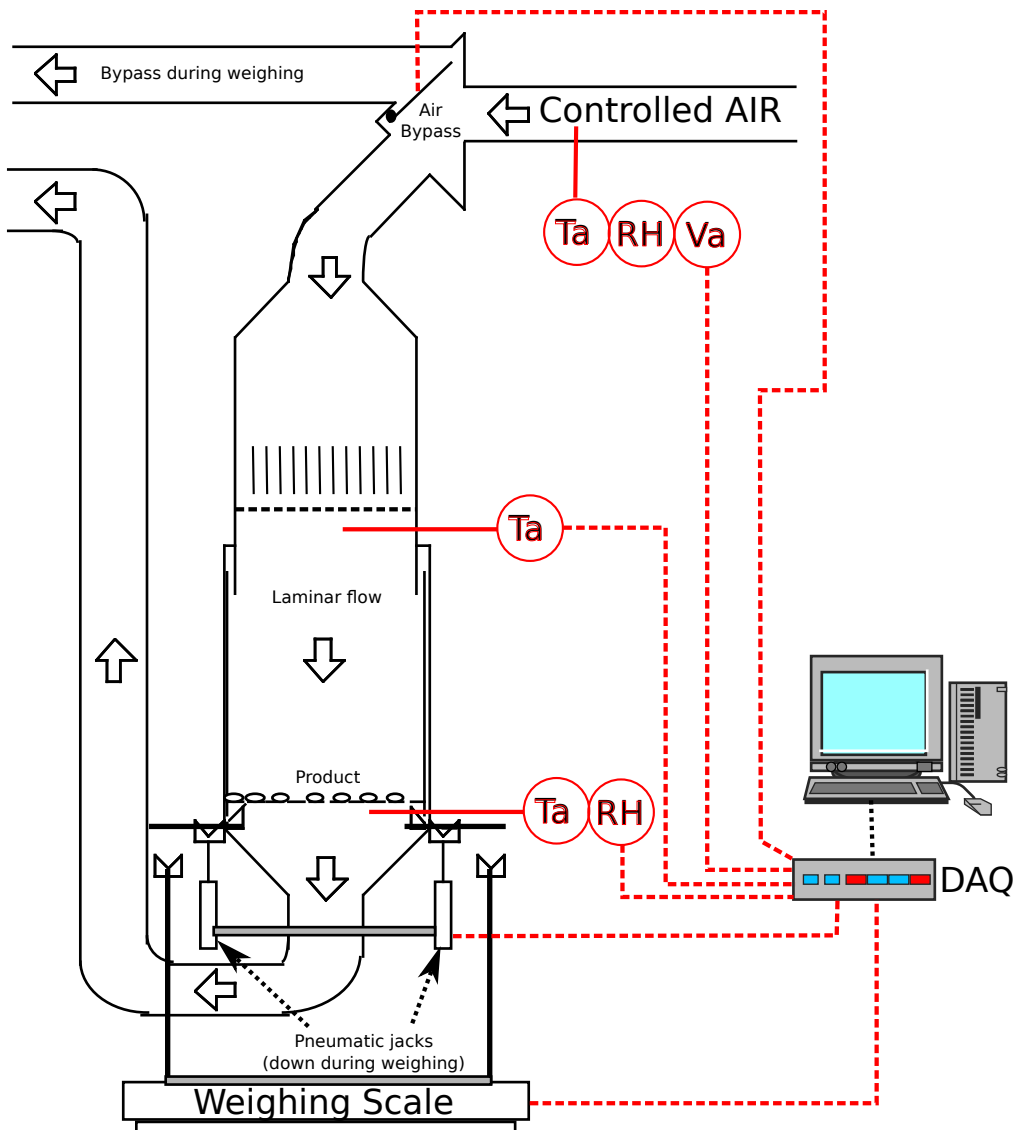


Figure 3.1 – Scheme of the drying pilot

However, measurements of outlet air temperature and relative humidity and the uncertainties retained can be discussed. On the one hand, regarding the experimental pilot, the outlet air temperature measurement is highly influenced by the thermocouple position with respect to the dryer walls and the sieve. First, due to the intermittent mass measurement, locally below the sieve, there are minor air leaks and a reduced thermal insulation. Second, if the thermocouple is too close to the sieve, the measure can be biased because of thermal radiation. Third, due to the deep bed crossing, the air flow after the sieve is less homogeneous. For these three reasons, the outlet air temperature can be considered as slightly underestimated. On the other hand, the response time of the relative humidity sensor (45 s) is not negligible compared to the sudden relative humidity variations in the first minutes of the drying process. As a consequence, comparing experimental and simulated data during this period should be done very carefully.

3.3.7 Simulation and optimization

The dynamic system consists in a set of 8 Partial differential Equations (PDEs 3.1 to 3.8). These equations were discretized into an Ordinary Differential Equations (ODEs) set using an explicit finite volume scheme in space to be numerically integrated with respect to both time and space by explicit embedded Runge-Kutta Cash-Karp (4, 5) method^[19] (for stiff systems). The integration time is automatically adjusted at each step of the simulation process to ensure the absolute and relative tolerances (cf. table 3.2). Hence, the integration time is not constant during the drying simulation. A general sequential method used to solve the deep bed drying system is illustrated in figure 3.2.

To quantify the quality of the model prediction, the maximum of a relative error between experimental and simulation data (MINMAX algorithm) were calculated according equations 3.12 and 3.13 respectively for thin layer and deep bed drying kinetics, valid for any time t . The aim is to minimize the maximum relative error made on the measurable variables using the Nelder and Mead method (Downhill Simplex method)^[20]. To avoid numerical inconsistencies, the parameter set (D_0 , E_a , d_1 and d_2 in equations 3.10 and 3.11) of the correlations between the effective moisture diffusivity, product moisture content and temperature was reparameterized using a \log_{10} transform as suggested by Goujot *et al.*^[21].

$$MRE_{TL} = \max \left(\left(\frac{\bar{X}_{sim,t} - \bar{X}_{exp,t}}{\bar{X}_{exp,t}} \right)^2 \right) \quad (3.12)$$

$$MRE_{DB} = \max \left(\left(\frac{\bar{X}_{sim,t} - \bar{X}_{exp,t}}{\bar{X}_{exp,t}} \right)^2, \left(\frac{T_{a,out,sim,t} - T_{a,out,exp,t}}{T_{a,out,exp,t}} \right)^2 \right) \quad (3.13)$$

Where, MRE_{TL} and MRE_{DB} are the maximum relative error (over t) respectively for thin layer and deep bed kinetics, $\bar{X}_{sim.}$ and $\bar{X}_{sim.}$ the simulated mean moisture content, $\bar{X}_{exp.}$ and $\bar{X}_{exp.}$ the experimental mean moisture content, and $T_{a,out,sim.}$ and $T_{a,out,exp.}$ the simulated and experimental output air temperatures.

Properties of the pellets and numerical parameters used in the simulations are summarized in table 3.2.

3.4 Results and discussion

3.4.1 Identification of effective moisture diffusivity on a deep bed kinetic

Firstly, the identified values of the effective moisture diffusivity are given for the Arrhenius correlation in equation 3.14.

$$D_{eff} = 6.54 \cdot 10^{-10} \cdot \exp \left(\frac{-597.3}{R \cdot T_p} \right) \quad (3.14)$$

Figure 3.3 shows the simulated and experimental data of the mean moisture content of the particle and the inlet and outlet air temperature and relative humidity obtained using the Arrhenius correlation. Maximum relative error is 41.5 %. More precisely, on the one hand, for the mean moisture content, the mean relative error is 23.9 % (with a maximum of 24.9 %), and the mean absolute error is 0.005 d.b. (with a maximum of 0.012 d.b). On the other hand, for the outlet air temperature, the mean relative error is 12.5 % (with a

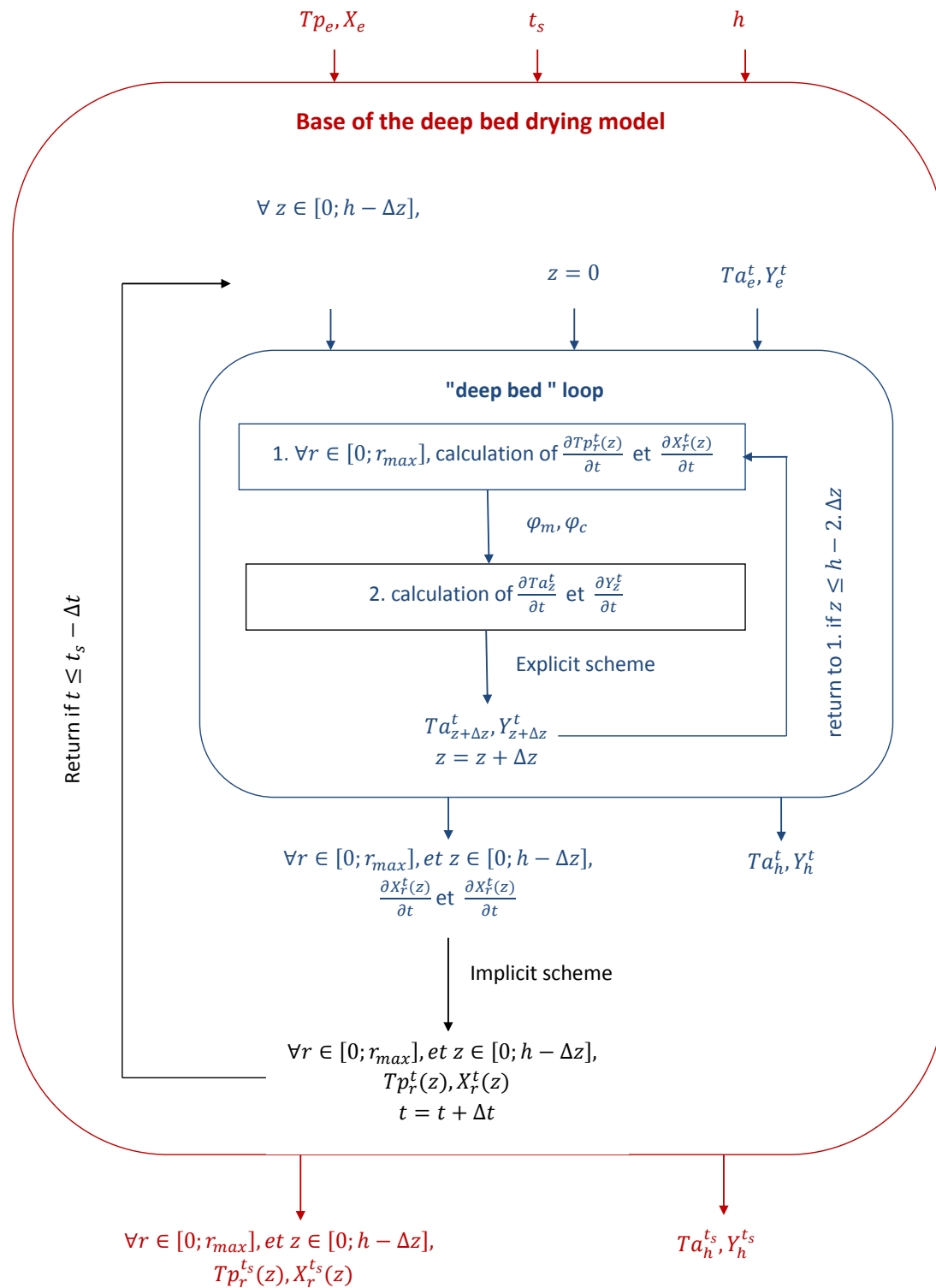


Figure 3.2 – Algorithm description, case of the simulation of deep bed drying

Table 3.2 – Physical properties of pellets for chickens and parameters used in drying simulation

Property	Equation or value
Radius	$2.14 \cdot 10^{-3} \text{ m}$
Characteristic length	$6.09 \cdot 10^{-3} \text{ m}$
Density	1325 kg.m^{-3}
Height of the deep bed	0.18 m
Porosity of the deep bed	0.3
Initial temperature	$20 \text{ }^{\circ}\text{C}$
Initial moisture content	0.204 d.b.
Heat Capacity	Choi and Okos correlation ^[22]
Thermal conductivity	Choi and Okos correlation ^[22]
Latent heat of vaporization	$2.357 \cdot 10^6 \text{ J.Kg}^{-1}$
Coefficient of heat transfer by convection	$20 \text{ W.m}^{-2}.K^{-1}$
Coefficient of mass transfer by convection	Lewis analogy
Water activity	Modified Henderson correlation ^[15, 16]
Effective moisture diffusivity	Arrhenius ^[1] or Abud ^[17] correlation
Number of thin layer within the particle	10
Number of thin layer within the deep bed	20
Absolute tolerance	10^{-6}
Relative tolerance	10^{-6}
Initial time variation	10^{-3}

maximum of 41.5 %) and the mean absolute error is $6.6 \text{ }^{\circ}\text{C}$ (with a maximum of $16.4 \text{ }^{\circ}\text{C}$). According to these errors, the outlet air temperature and the mean moisture content are well predicted. However, the identified activation energy is lower than values identified for similar products by a factor of 100^[1]. A low and/or uncertain activation energy (E_a) normally means a negligible influence of temperature which is probably due, in this case, to the limited information available to the optimization algorithm. In a deep bed experiment at $90 \text{ }^{\circ}\text{C}$ for instance, most of the time and in most places within the deep bed, air flows at temperatures far below the inlet value. Hence the temperature range is narrow and possibly not sensitive enough to identify correctly its related coefficients.

Secondly, the identified values of the effective moisture diffusivity are given for Abud correlation in equation 3.15.

$$D_{eff} = \exp(-22.153 + 0.207 \cdot X \cdot T_p) \quad (3.15)$$

Figure 3.4 shows the simulated and experimental data of the mean moisture content of the particle and the inlet and outlet of air temperature and relative humidity, obtained using the Abud correlation. The maximum relative error is 35.3 %. More precisely, on the one hand, for the mean moisture content, the mean relative error is 4.6 % (with a maximum of 20.0 %), and the mean absolute error is 0.001 d.b. (with a maximum of 0.004 d.b.). Indeed, simulated mean moisture content values are within or close to the confidence interval of experimental measurements. On the other hand, for the outlet air temperature, the mean relative error is 12.0 % (with a maximum of 35.3 %) and the mean absolute error is $6.7 \text{ }^{\circ}\text{C}$ (with a maximum of $13.4 \text{ }^{\circ}\text{C}$). Although, for both correlations, simulated and experimental outlet air temperatures follow the same trend, simulated ones are systematically greater. However, as explained in the drying kinetics measurement section (see materials and

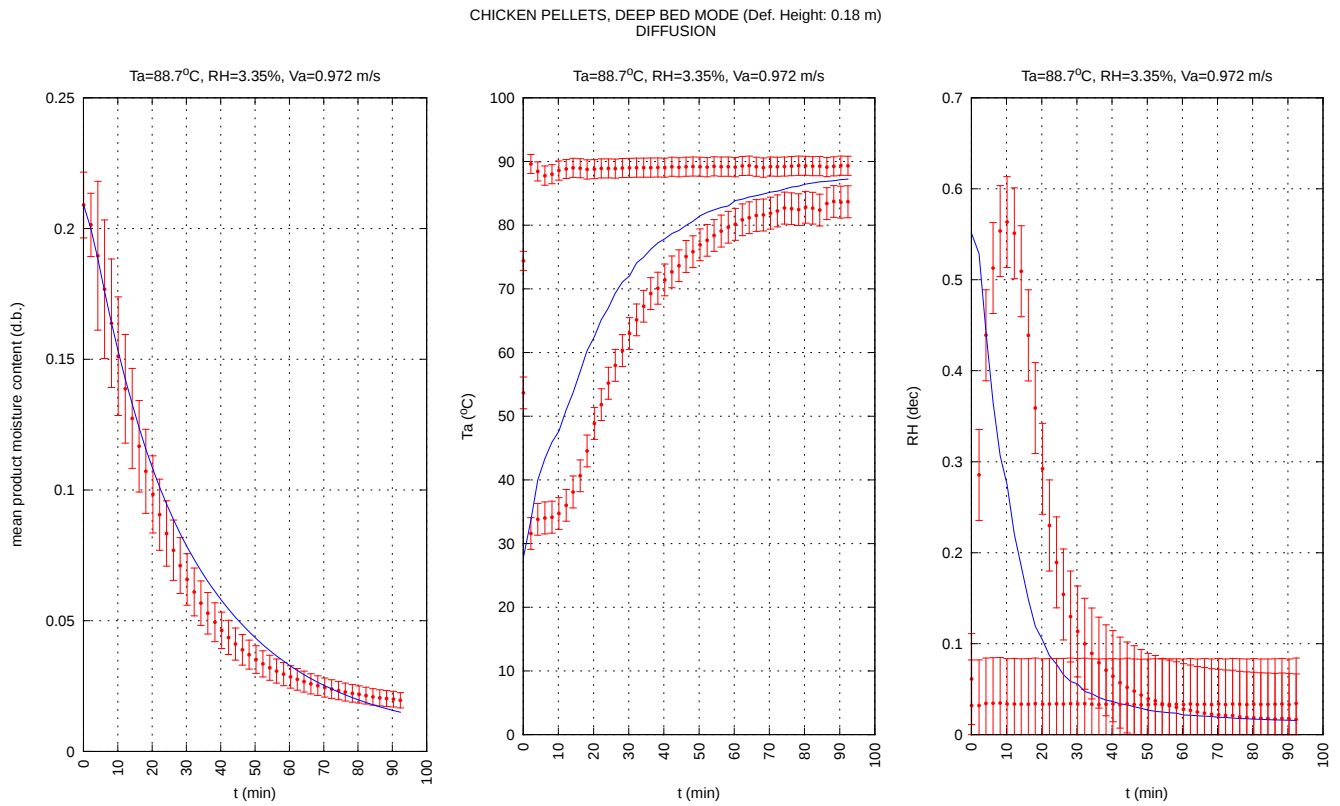


Figure 3.3 – Comparison of experimental (*) and simulated (-) data of **deep bed drying kinetics** of pellets for chickens (learning set) obtained using **Arrhenius correlation**.

methods), the experimental outlet air temperature is underestimated. This can explain the differences between experimental and simulated values. In addition, the slow response time of the relative humidity sensor may explain the observed differences between experimental and simulated relative humidity during the first minutes of the drying kinetic. Therefore one can conclude that the simulator using the Abud correlation can simulate correctly the drying kinetics, as well as the effective moisture diffusivity variation of pellets for chicken.

3.4.2 Validation of effective moisture diffusivity correlations on thin layer kinetics

Firstly, figure 3.5 shows the simulated and experimental data of the mean moisture content of the particle obtained with the simulator using Arrhenius correlation. One can note that mean moisture content is well predicted only for inlet air temperatures between 30 and 70 °C. Indeed, the mean relative error is less than 15.4 % (with a maximum of 35.1 %) and the mean absolute error is 0.016 d.b (with a maximum of 0.032 d.b). However the proposed methodology doesn't work if the inlet air temperature is higher. The latter is discussed below. However, using an Arrhenius law describing the dependency of diffusion coefficient over the temperature, implies the identification of two unknown parameters (*i.e.* D_0 and E_a). The latter one, the activation energy, should be comparable with values found in literature. In this work, the identification of these 2 parameters with deep bed drying kinetics led to low values for activation energy with large uncertainties.

Secondly, figure 3.6 shows the simulated and experimental data of the mean moisture content of the particle obtained with the simulator using the Abud correlation. One can

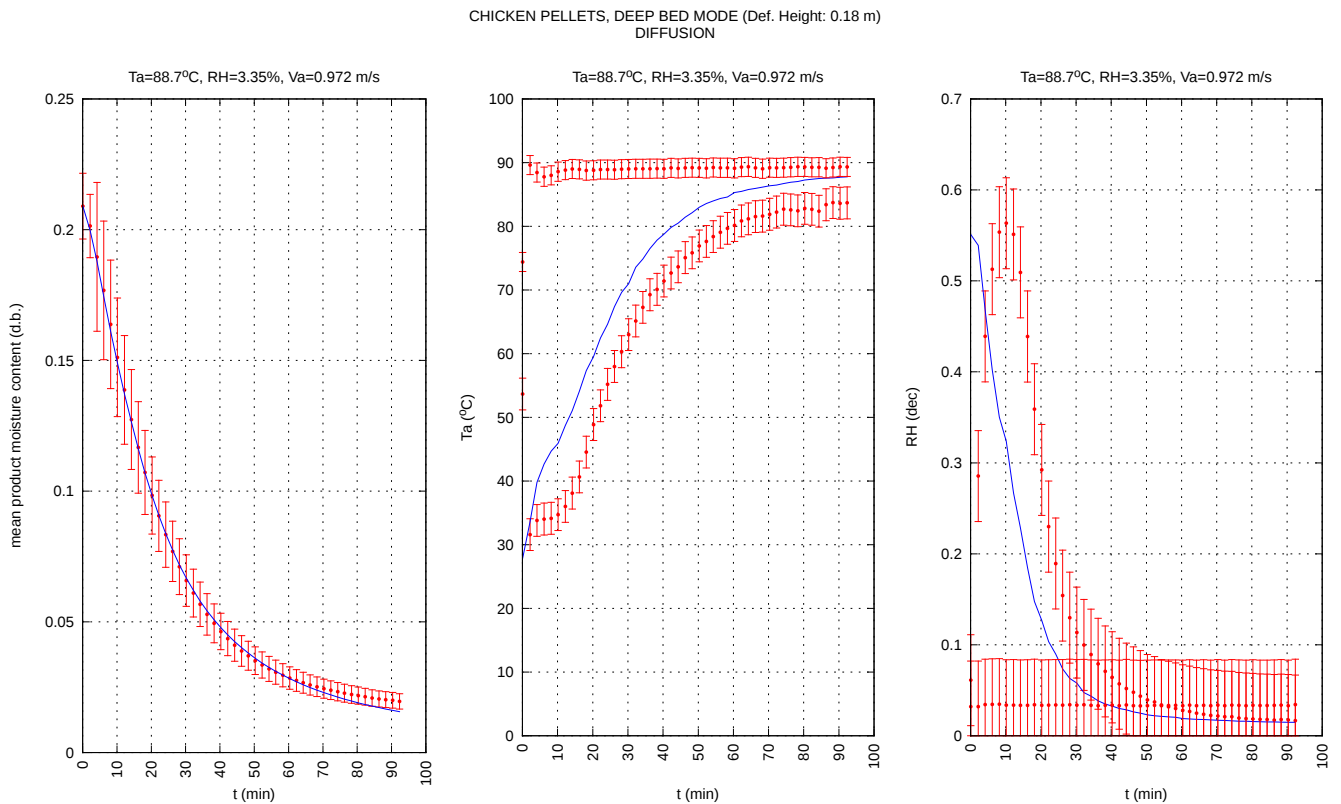


Figure 3.4 – Comparison of experimental (*) and simulated (-) data of **deep bed drying kinetics** of pellets for chickens (learning set) obtained using **Abud correlation**.

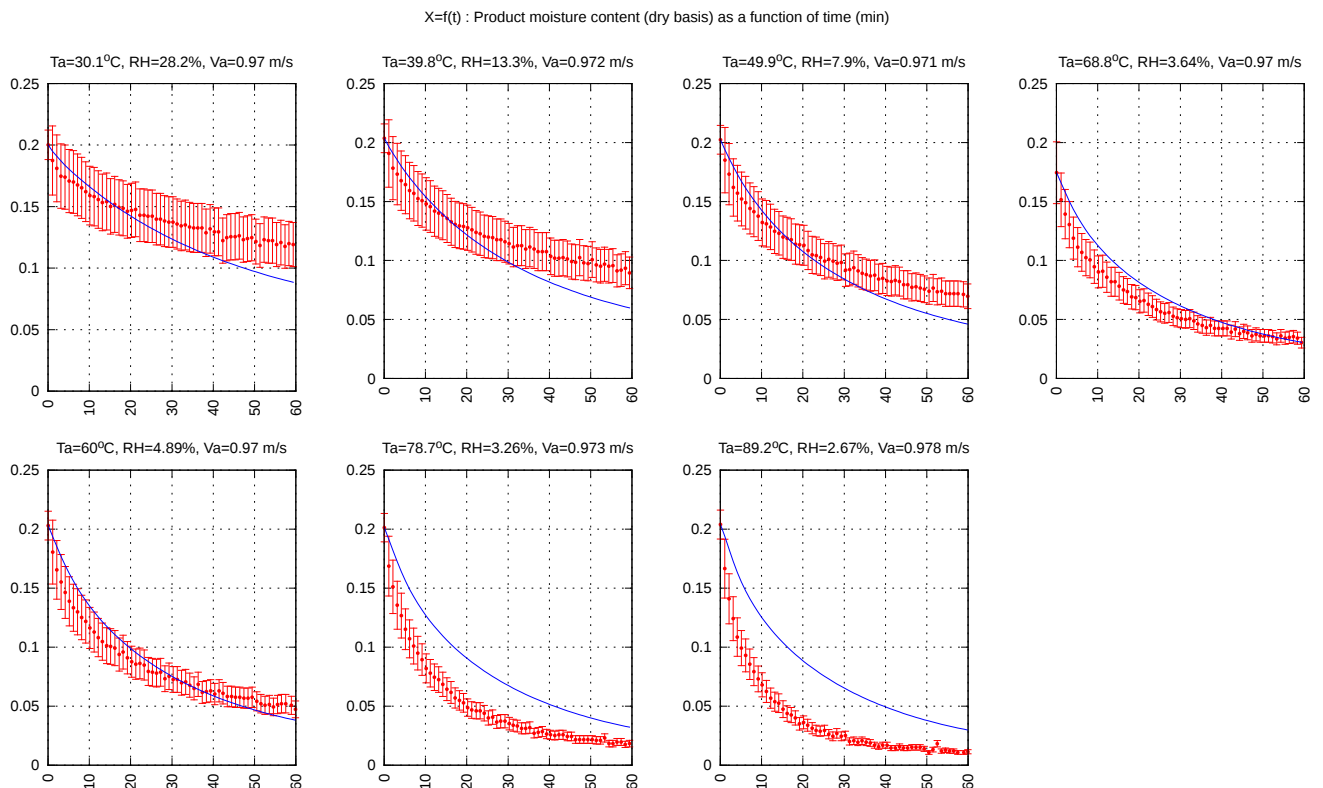


Figure 3.5 – Comparison of experimental (*) and simulated (-) data of **thin layer drying kinetics** of pellets for chickens (validation set) obtained using **Arrhenius correlation**.

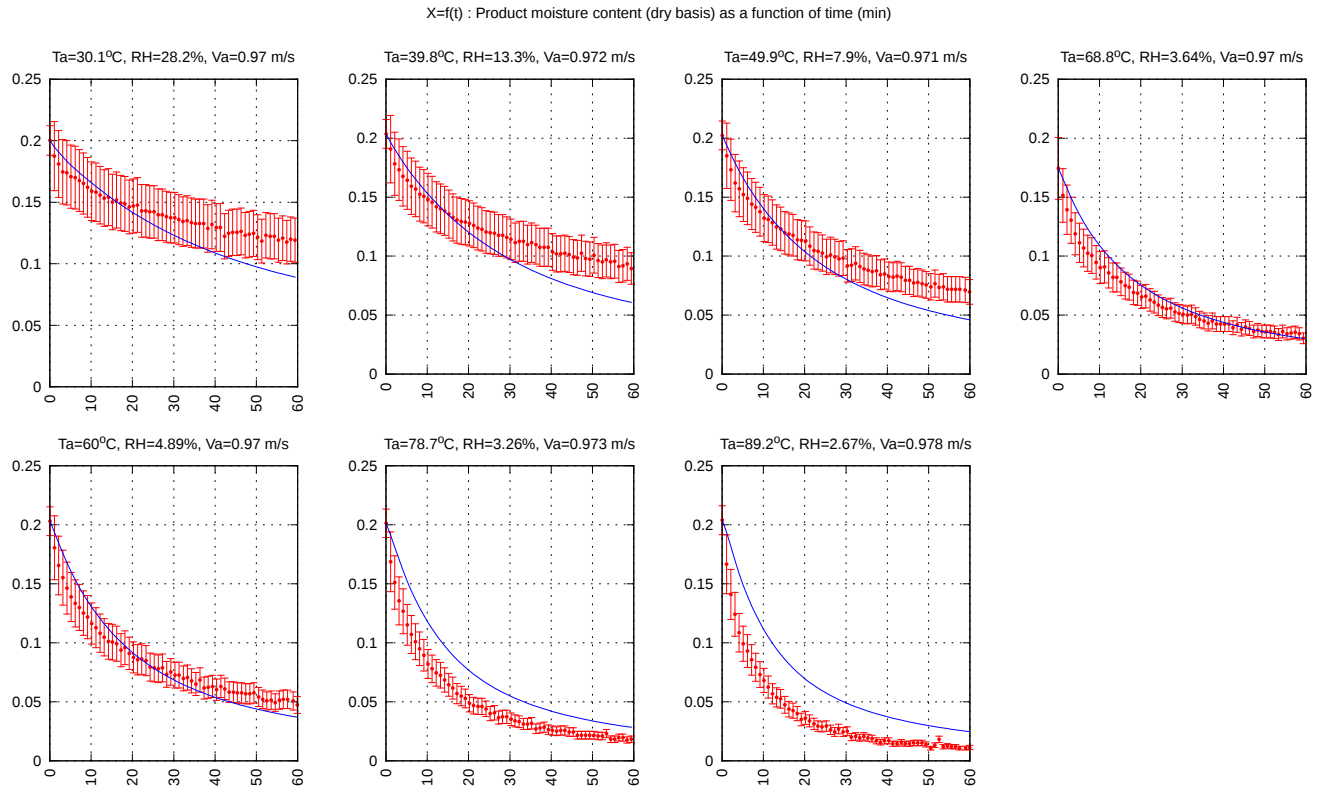


Figure 3.6 – Comparison of experimental (*) and simulated (-) data of **thin layer drying kinetics** of pellets for chickens (validation set) obtained using **Abud correlation**.

note that mean moisture content is well predicted for all air temperatures between 30 and 70 °C. Indeed, the mean relative error is less than 16.0 % (with a maximum of 32.0 %) and the mean absolute error is 0.016 d.b (with a maximum of 0.030 d.b). However the proposed methodology doesn't work if the air temperature is higher. Indeed, a deep bed is supposed to be a sum of thin layers, and in a deep bed experiment at 90 °C, air flows at temperatures far below the inlet value most of the time and in most places within the deep bed. In addition, during the first 10 minutes of the experiments, mean moisture content is not well simulated using both the Arrhenius and Abud correlations. This matter is discussed below.

Moreover, the mismatch between experimental and simulated values at the beginning of the kinetics can originate from a wrong convective heat transfer coefficient (fixed at 20 $W.m^{-2}.K^{-1}$ in our case). Indeed, heat transfer coefficient correlations^[23, 24] for our product characteristics give expected values higher than 100 $W.m^{-2}.K^{-1}$ (between 120 and 410 $W.m^{-2}.K^{-1}$) and similar results, but slightly less good, have been obtained using Whitaker correlation^[24]. However, the corresponding convective heat transfer resistance values, calculated with correlations, are in the order of magnitude of conductive heat transfer resistance ones. Hence, since our system consists in a convective dryer, we dismissed this explanation.

3.5 Conclusion

In this study, we focused on a reverse approach: an identification of the moisture diffusion coefficient for pellets for chickens using deep bed drying kinetics and a validation over a set of thin layer drying kinetics. The expected benefits of such approach were both to minimize

the number of required experiments and maximize the validity/robustness of the identified model.

Effective moisture diffusivity was identified using a deep bed drying kinetic obtained at an air temperature of 90 °C. The validation set was composed of thin layer drying kinetics with inlet air temperatures between 30 and 90 °C. Two correlations of effective moisture diffusivity were tested (Arrhenius and Abud correlations). When using both the Abud or Arrhenius correlations, the relative error observed on the predictions of the product moisture content were less than 16.0% (with a maximum less than 35.1 %) for thin layer drying kinetics with inlet air temperature lower or equal to 70 °C. According to our results, a single deep bed drying kinetic allows for a raw estimation of moisture diffusivity leading to a valid simulation of thin layer drying kinetics for any temperature below 70 °C. Further work in progress focuses on the use of non-linear model-based Design of Experiment (NLMBSDOE) techniques to improve the performance of this approach.

3.6 Acknowledgments

The authors wish to thank the French Agence Nationale de la Recherche (ANR) for the funding of the PhD of C. Lambert, and the partners of the project COOPERE2 leaded by Veolia Research and Innovation, in collaboration with ProSim and ENSIACET. The authors wish also to thank the French Agency ADEME (Agence Nationale de l'environnement et de la maîtrise de l'énergie) and the technical center TECALIMAN for their funding of the experimental characterization and modelling of the drying of animal pellets.

In addition, the authors wish to thank several master and PhD students (Perrine Leclercq, Analia Aparecida Vanzo, Abir Hosni, Azziz Zemmouri, Monica Pinto, Benoit Hareng) and our colleagues Giana Perré and Julien Cartailler for their valuable help in acquiring experimental data supporting the modelling and simulation work.

3.7 References

1. Zogzas, N.P.; Maroulis, Z.B. Effective moisture diffusivity estimation from drying data. A comparison between various methods of analysis. *Drying Technology* **1996**, 14(7&8), 1543-1573
2. Hassini, L.; Azzouz, S.; Peczalski, R.; Belghith, A. Estimation of potato moisture diffusivity from convective drying kinetics with correction for shrinkage. *Journal of Food Engineering* **2007**, 79, 47–56.
3. Crank, J. The mathematical of diffusion. 2nd ed. Oxford University Press: Oxford, 1975.
4. Vieth, W.R. Diffusion in and Through Polymers. Hauser Publisher: Munich, 1991.
5. Crank, J.; Parker, G.S. Diffusion in Polymers. Academic Press: New York, 1968.
6. Karathanos, V.T.; Vagenas, G.K.; Saravacos, G.D. Water diffusivity of starch at high temperatures and pressures. *Biotechnology Progress* **1991**, 7, 178–184.
7. Zogzas, N.P.; Maroulis, Z.B.; Marinos-Kouris, D. Moisture diffusivity methods of experimental determination: A review. *Drying Technology* **1994**, 12(3), 483-515.
8. Saravacos, G.D. Effect of the drying method on the water sorption of dehydrated apple and potato. *Journal of Food Science* **1967**, 32, 81–84.

9. Saravacos, G.D.; Maroulis, Z.B. Chapter6, Moisture diffusivity Compilation of Littérature Data for Food Materials. In Transport Properties of Foods. Marce Dekker: New-York, 2001, 163-236.
10. Kudra, T.; Mujumdar, A.S. Advanced Drying Technologies. CRC Press: Boca Raton, 2009.
11. Perré, P.; May, B.K. A numerical drying model that accounts for the coupling between transfers and solid mechanics: Case of highly deformable products, *Drying technology* **2001**, 19, 1629-1643
12. Courtois, F. Dynamic Modelling of Drying to Improve Processing Quality of Corn, Ph.D. thesis, ENSIA, Massy, France 1991.
13. Bird, R. B.; Stewart, W. E.; Lightfoot, E. N. Transport phenomena. Wiley and Sons: New-York. 2002.
14. AFNOR. Aliments des animaux. Détermination de la teneur en eau. NF V 18-109 **1982**, 5 p.
15. Henderson, S.M. A basic concept of equilibrium moisture. *Agricultural Engineering* **1952**, 33 29-32.
16. Thompson, T.L.; Peart, R.M.; Foster, G.H. Mathematical simulation of corn drying: A new model. *Transactions of the American Society of Agricultural Engineers* **1968**, 24, 582-586.
17. ASAE Standards. D245.6. Moisture relationships of plant-based agricultural products. St. Joseph, Mich. ASAE. 2007
18. Abud-Archila, M.; Courtois, F.; Bonazzi, C.; Bimbenet, J.J. A compartmental model of thin layer drying kinetics of rough rice. *Drying Technology* **2007**, 17(7), 1389-1414.
19. Galassi, M.; Theiler, J.; Davies, J. Gnu Scientific Library Reference Manual. 3rd edition. Network Theory Ltd, 2009.
20. Nelder, J.; Mead, R. A simplex method for function minimization, *Computer Journal* **1965**, 7(4), 308-313
21. Goujot, D.; Meyer, X. & Courtois, F. Improved Identification of Rice Drying Model with Sequential Optimal Design of Experiments *Journal of Food Process Control* **2012**, 22, 95-107
22. Sahin, S.; Sumnu, S.G. Physical properties of foods, (p. 257), Food Science 2006.
23. Bird, R. B.; Stewart, W. E.; Lightfoot, E. N. Chapter 14, Interphase transport in non-isothermal systems. In *Transport phenomena*. Wiley and Sons: New-York. 2002.
24. Whitaker, S. Forced convection heat transfer correlations for flow in pipes, past flat plates, single cylinders, single spheres, and for flow in packed beds and tube bundles, *AIChE Journal* **1972**, 18(2), 361-371.

Chapitre 4

Characterization and modeling of cooling and drying of pellets for animal feed

Résumé

Ce travail complète celui des deux chapitres précédents, constituant un exemple d'application du modèle de séchage convectif et de la méthode d'identification de la diffusivité apparente de l'eau développés.

Parmi toutes les étapes impliquées dans le processus de production de granulés pour l'alimentation animale, l'optimisation énergétique du séchage-refroidissement, via une régulation en temps réel des paramètres opératoires, est l'une des préoccupations actuelles des industriels du secteur. Très peu d'articles, essentiellement anciens, portant sur l'étude de cette opération unitaire, sont disponibles dans la littérature. Son optimisation nécessite au préalable un modèle dynamique capable de simuler le séchage et le refroidissement des couches épaisses de granulés. Ce travail propose et valide un tel modèle de simulation incluant également la caractérisation du produit. En outre, une solution est proposée pour limiter le nombre de cinétiques expérimentales nécessaires de séchage-refroidissement car leurs mesures sont très difficiles à maîtriser. Cette démarche est appliquée à 2 formulations et 2 géométries différentes de granulés. L'écart entre les données simulées et expérimentales sont de l'ordre de grandeur des incertitudes de mesure.

Mots-clés refroidissement, séchage, granulés, alimentation animale, caractérisation, modèle.

Cet article est à soumettre à *Drying Technology*¹.

4.1 Introduction

The pellet process consists of a series of several steps: grinding, weighting raw materials, mixing, pelleting to agglomerate small particles into larger ones, cooling and conditioning. This process has been little studied in the literature. One can cite the study of the effect of

1. C. Lambert, J. Cartailler, S. Rouchouse, G. Almeida, and F. Courtois, "Characterization and modeling of cooling and drying of pellets for animal feed," *Drying Technology* (under revision), 2015.

pellet formulation on the process [1, 2, 3, 4] and the study of some specific unit operations such as conditioning [5] and pelleting [5, 6].

Cooling is not one of the most energy consuming unit operation of this process. However, industrial investment currently focuses on the use of adjustable speed-drive to reduce fan energy consumption. In addition, cooling current state of control is often based on operator experience. For most of the coolers, there is no real time feedback between the product characteristics (humidity, temperature) and processing parameters. Air humidity, measured at the outlet of the coolers, could be used to optimize the bed height or the fan velocity. Moreover, if the cooling process is not controlled, the pellets can be dried excessively, inducing a higher energy consumption and cracks at the pellet surface affecting their durability [5]. Hence, controlling precisely this step of the process is of utmost importance for the animal feed industry in order to optimize their energy consumption yet ensuring a required product quality. The French environment and Energy Management Agency (ADEME) funded the OPSERA project (optimizing the dryer-cooler performance for animal feed) to optimize in real time the drying-cooling process using an advanced control algorithm. The purpose is to develop an advanced control algorithm centered on the estimation of pellet moisture content by a smart sensor. The latter could then be used to optimize the fan velocity and the air flow-rate. In this project, the smart sensor is based on a dynamic simulation model of the cooling-drying process.

The cooling step for the feed industry has been little studied in the literature (*e.g.* [7, 8, 9]). A cooling-drying model has been developed and the simulations have been validated at pilot scale [8]. However, moisture loss and temperature are not well predicted with this model (up to 60 % of deviation was observed between experimental and simulated data). This model only predicts the trend of the effect of moisture and temperature on the pellet cooler performance [7, 8, 9]. Hence, the development of a more precise model of this unit operation is required to control precisely an industrial cooler and predict the effect of the change of pellets formulation on operating conditions.

The purpose is develop a convective drying-cooling model implemented in 2 versions: 1) in an unsteady-state version to control process parameters and 2) in its steady-state version, in a computer aided engineering (C.A.E.) software. Classical modeling approaches of convective drying processes were discussed in a previous work [10]. Major characteristics of the model should be a low computation requirement and a wide range of validity. On the one hand, the simulation of the drying or drying-cooling operation should not last longer than few seconds. On the other hand, the model should have a multi-product compatibility and an extrapolation capability. It should be able to simulate all classical drying and drying-cooling conditions. In addition, it should allow late addition of new products or at least new formulations without modifying anything in the equations. Thus, parameters of the model should have a physical meaning and should be calculated with correlations, experimentally measured or identified by reverse method [10].

This study is focused on the experimental characterization of two formulations of pellets for animal feed (with various recipe and pelleting conditions). Water activity and effective moisture diffusivity are identified. A drying & cooling model is also proposed and validated at pilot scale both for drying and cooling. The aim of our model is to predict the final pellets moisture content and energy consumption during this process.

4.2 Materials and methods

4.2.1 Origin of the pellets

Two formulations of pellets for animal feed are studied: pellets for chickens (P4C) and for rabbits (P4R). In addition, in the latter case, two geometries, with the same composition, are also studied. They are later denoted P4R - 2.5 mm and P4R - 4 mm. All formulations have a cylindrical shape. Raw seed composition and dry matter composition of both pellet formulations are respectively given in tables 4.1 and ???. For the pelleting process, ingredients are mixed with steam in a conditioner and are then pelleted in a press. The temperature of the pellets at the press outlet are respectively 84 °C for pellets for chickens and 87 °C (P4R - 2.5 mm) and 83 °C (P4R - 4 mm) for pellets for rabbits. The pellet moisture content at the press outlet are respectively 0.204 d.b. for pellets for chickens and 0.211 d.b. (P4R - 2.5 mm) and 0.202 d.b. (P4R - 4 mm) for pellets for rabbits. For each formulation and geometry, samples of 2.5 kg of pellets are vacuum packed in plastic boxes and are stored in a cold room.

Table 4.1 – Mixture composition of the pellets for chickens and rabbits (P4R - 2.5 mm and P4R - 4 mm)

Pellets for chickens		Pellets for rabbits	
Wheat	40 %	Wheat	4.5 %
Corn	20 %	Barley	13.2 %
Soybean cake	30 %	Soybean cake	5.8 %
Soybean seed	4 %	Soybean oil	0.5 %
Soybean oil	3 %	Grape pulp	5 %
Dicalcium phosphate	1.15 %	Sunflower cake	8.5 %
Calcium carbonate	0.95 %	Rape seed	3.5 %
Other	0.9 %	Milurex	8.5 %
		Cane molasses	6 %
		Sugar pulp	15 %
		Alfalfa	23.6 %
		Straw	3.5 %
		Calcium carbonate	0.9 %
		Other	1.5 %
Total	100 %	Total	100 %

Table 4.2 – Dry matter composition of pellets for chickens and rabbits (P4R - 2.5 mm and P4R - 4 mm)

	Composition (% d.b.)	
	Pellets for chickens	Pellets for rabbits
Proteins	20.9	15.8
Lipids	19.1	3.9
Total sugar	54.5	70.5
Ashes	5.5	9.8

4.2.2 Moisture content measurement

Moisture content of the pellets is measured according to the French AFNOR norm NF V 18-109 before thin layer and deep-bed drying and after thin layer drying. The pellets are first grounded using a water-cooled miller (IKA WERKE KM 20). The method is based on the weight loss of 5.00 g (± 0.05 g) of pellet powder during a 4 hours stay in the oven at 103 °C. Samples are then placed in a desiccator for at least 1 hour before to be weighed. The moisture content is averages using three samples.

4.2.3 Geometry measurement

Apparent density of the dry matter of the pellets are measured using Fontainebleau sand. Real density of the dry matter of pellets is determined using an air pycnometer (ACCUPYC 1330). Porosity of the bed is determined according to equation 4.1. Dimensions of the pellets are measured using two methods : a manual approach using a caliper and a automated approach based on image analysis (using a scanner and *ImageJ* software).

$$\varepsilon = \frac{\rho_{dm}^{real} - \rho_{dm}^{ap}}{\rho_{dm}^r} \quad (4.1)$$

Where ε is the bed porosity (decimal), ρ_{dm}^{real} the real density of the dry matter ($kg.m^{-3}$) and ρ_{dm}^{ap} the apparent density of the dry matter ($kg.m^{-3}$).

4.2.4 Sorption isotherm measurement

Isotherm analyses are performed using a DVS Intrinsic apparatus (Surface Measurement Systems, London, UK). An ultra-sensitive micro-balance allows measuring sample mass variation as low as 1 part in 10 million. Samples are grounded using a water-cooled miller (IKA WERKE KM 20). Approximately 10 mg of each sample is inserted in the pan. In this device, a constant flow of nitrogen gas is mixed with a preset amount of water vapor. Nitrogen passes then through the chamber to maintain the desired relative humidity level. The accuracy on the air relative humidity of this system is $\pm 0.5\%$. All sorption cycles start with 0 % relative humidity (RH). The dry matter is determined at the end of the plateau. Isotherms are measured at two levels of temperature for P4C pellets for chickens (25 °C and 40 °C) and at 25 °C for P4R pellets for rabbits and were made in duplicate for pellets for rabbits. Adsorption/desorption cycles of relative humidity (RH) range from 0 % - 90 % - 0 % using steps of 10 % RH. In experiments at 40 °C, 92.3 % RH ($\pm 0.4\%$ RH) was measured instead of 90 % RH due to insufficient performance of the RH control loop. As a matter of fact, in the present work, all results are based on actual measured RH values (which may differ from the target ones). The instrument maintains a constant RH until the sample moisture content change per minute is less than 0.002 % per minute over a 10 min period. [11] fixed this threshold value of 0.002 % per minute to finally obtain a sample moisture content within 0.1 % of the equilibrium value at extended time.

Equilibrium moisture content (X_{eq}) and relative humidity (RH) data were fitted using the modified Henderson equation (4.2) [12, 13]. This equation is one of the five equations recommended by ASAE Standard D245.6 for fitting sorption data of several agri-food materials [14].

$$RH = 1 - \exp(-A \cdot (X_{eq})^B) \quad (4.2)$$

Where A and B are constants, X_{eq} the equilibrium moisture content (% d.b.) and RH the relative humidity (decimal).

4.2.5 Drying experiment

Drying of the pellets is performed according to two different protocols: a conventional hot air drying (thin layer and deep bed kinetics) and a cooling-drying method (deep bed kinetics only). Thin layer kinetics are done in triplicate. For both methods, experimental data are recorded using an automated pilot dryer located in an AgroParisTech/INRA drying laboratory (Massy, France) under constant conditions (see below).

Description of the drying pilot

A schematic of the drying pilot is given in figure 4.1. In this pilot, the air passes, from the top to the bottom, through the drying chamber which consists in a cylindrical cell (25 cm of diameter and 28 cm of height). The following variables are recorded every minute (with an OPTO22 SNAP-PAC-EB2 data logger):

- inlet and outlet air temperatures (with T-type thermocouples and platinium probes) and relative humidities (with VAISALA 135Y and ROTRONIC HF532-HC2 probes);
- inlet air velocity (using a Pitot tube ANNubar ANR-73 and a differential pressure sensor FURNESS FCO-53);
- mass of the product (with a METTLER PE 16 discontinuous weighing system while the air being bypassed).

Precision on mean moisture content was estimated one for all for each formulation of pellets using repetitions of thin layer kinetics. The following uncertainties on the measures were retained:

- For pellets for chickens (P4C): ± 0.015 d.b. ($\sigma = 0.005$ d.b.);
- For pellets for rabbits (P4R - 2.5 mm and P4R - 4 mm): ± 0.018 d.b. ($\sigma = 0.06$ d.b.).

According to relative humidity and temperature sensor precisions and locations in the pilot, the following uncertainties (using $\pm 3\sigma$) on the measures are retained:

- Inlet air temperature: ± 1.5 °C ($\sigma = 0.5$ °C);
- Outlet air temperature: ± 2.5 °C ($\sigma = 0.8$ °C);
- Inlet and outlet relative humidities: ± 5 % ($\sigma = 1.7$ %)

However, deviations on measurements of outlet air temperature and relative humidity can be discussed: a) due to the intermittent mass measurement there are minor air leaks and a reduced thermal insulation, locally below the sieve; b) if the sensor is too close to the sieve, the measure can be biased due to thermal radiation; and c) due to the deep bed crossing, air flow after the sieve is less homogeneous. For these three reasons, the outlet air temperature can be considered slightly underestimated. In addition, the response time of the relative humidity sensor (45 s) is not negligible compared to the sudden relative humidity variations in the first minutes of the drying process. As a consequence, comparing experimental and simulated data during this initial period should be done very carefully.

Drying and drying-cooling protocols

Drying method

Thin layer and deep bed drying kinetics are recorded using pellets for chickens (P4C) and rabbits (P4R - 4 mm and P4R - 2.5 mm). About 200 g (thin layers) and between 2.5 to 5 kg (deep beds) of pellets are introduced into the dryer. Drying operating conditions are summarized in table 4.3.

Drying-cooling method

It is quite difficult to control precisely the cooling conditions of pellets. Considerable effort is necessary to warm-up the pellets without drying them and transfer them to the dryer without unwanted water loss nor heat loss and, finally, have a reasonable knowledge of the actual initial product temperature and moisture content at the begining of the drying-cooling step.

In this study, the only drying-cooling data available consists in deep bed drying kinetics of pellets for chickens (P4C). About 5 kg of pellets are packed in vacuum sealed bag using a vacuum heat sealer (MULTIVALUED GASTRONOMIC) and pouches composed of low density polyethylene (LEXINGTON). Packing pellets in vacuum sealed bag limits the contacts between air and pellets and minimizes in this way mass transfers during their preheating. The pellets and the sieve are then pre-heated in the following conditions :

- The sieve of the dryer is previously heated at about 100 °C using a heat gun (METABO H 1600) to be at nearly 80 °C at the begining of the experiment;
- Pellets, in their vacuum sealed bags, are pre-heated in an oven at 100 °C during one hour. The core temperature of the pellets is about 60 - 70 °C at the outlet of the oven.

Pellets are then introduced into the drying zone after stabilization of the drying operating conditions (list of tested conditions in table 4.3). A sub-sample is withdrawn for moisture content measurement. The initial temperature of the pellets was initially estimated through the use of an infra-red thermometer but it was considered as biased estimate of the surface temperature. Finally, the initial pellet temperature is better estimated by the -recorded-outlet air temperature after two minutes of cooling-drying.

Experimental conditions of both drying and drying-cooling are given in table 4.3.

4.2.6 Identification of D_{eff}

This study finishes off a previous work in which different approaches of identification of effective moisture difusivity D_{eff} were discussed [15]. Hence, in the present work, these three strategies are used for the identification of effective moisture diffusivity of pellets as summarized in table 4.4. The classical strategy used in food drying consists in four steps:

1. Measure, at the lab scale, the accessible product properties (water activity, heat capacity, geometry and porosity);
2. Collect experimental measurements of thin layer drying kinetics under constant air drying conditions over a wide range of air temperatures;
3. Identify the effective moisture diffusivity coefficient by model fitting on these thin layer drying kinetics (using variations of recorded product moisture content);
4. Validate the model over some thin layer (on product moisture content) or deep bed drying kinetics (on product moisture content and possibly output air moisture and temperature).

Table 4.3 – Experimental conditions of the drying and the drying-cooling of pellets for chickens and rabbits

			Pellets for chickens	Pellets for rabbits
Drying kinetics	Thin layer experiments	T_{p0} \bar{X}_0 v_a T_{a0}^0	≈ 20 °C 0.204 d.b. 1 m.s^{-1} 30 - 90 °C	≈ 20 °C 0.208 d.b. 1 m.s^{-1} 40 - 80 °C
	Deep bed experiments	height T_{p0} $\bar{\bar{X}}_0$ v_a T_{a0}^0	≈ 18 cm ≈ 20 °C 0.204 d.b. 1 m.s^{-1} ≈ 90 °C	10 - 18 cm ≈ 20 °C 0.208 d.b. $0.7 - 2.4 \text{ m.s}^{-1}$ 60 - 90 °C
Drying-cooling kinetics	Deep bed experiments	height T_{p0} $\bar{\bar{X}}_0$ v_a T_{a0}^0	≈ 18 cm ≈ 60 °C 0.188 d.b. 1 m.s^{-1} ≈ 30 °C	

\bar{X}_0 , $\bar{\bar{X}}_0$ Initial mean moisture content of the pellets respectively in the case of thin layer and deep bed kinetics

T_{a0}^0 Initial inlet air temperature

v_a Inlet air velocity

T_{p0} Initial temperature of the bed of pellets

This strategy is used to identify effective moisture diffusivity of pellets for rabbits (P4R - 2.5 mm). The validation set is composed of thin layer and deep bed drying kinetics. As explained in a previous work, the product mass variation is the only experimental data used to identify the effective moisture diffusivity [15]. These data are limited only to the mass transfer, while, in drying, this transfer is strongly coupled to the energy change. In a deep bed experiment, in addition of the product mass variation, inlet and outlet air temperatures and relative humidities are recorded [15]. The two other developed strategies are derived from the classical one and have a major difference: effective moisture diffusivity is identified using deep bed drying kinetics. One may expect deep-bed drying kinetics to bring far more information to the identification procedure, as compared to several thin-layer kinetics. First, the methodology to identify effective moisture diffusivity of pellets for chickens has been published by [15]. The identification set is composed of a single deep bed drying kinetic obtained at high temperature (90 °C). The validation set is composed of thin layer drying kinetics and a deep bed drying-cooling kinetic of pellets for chickens (P4C). Second, two deep bed kinetics obtained at two different temperatures (40 and 80 °C) are used to identify effective moisture diffusivity of pellets for rabbits (P4R - 4 mm). The validation set is composed of thin layer kinetics.

For all identification strategies, operating conditions of the identification set are summarized in table 4.4 and operating conditions of the validation set in table 4.3. The Abud correlation [16] of effective moisture diffusivity (equation 4.3) was tested.

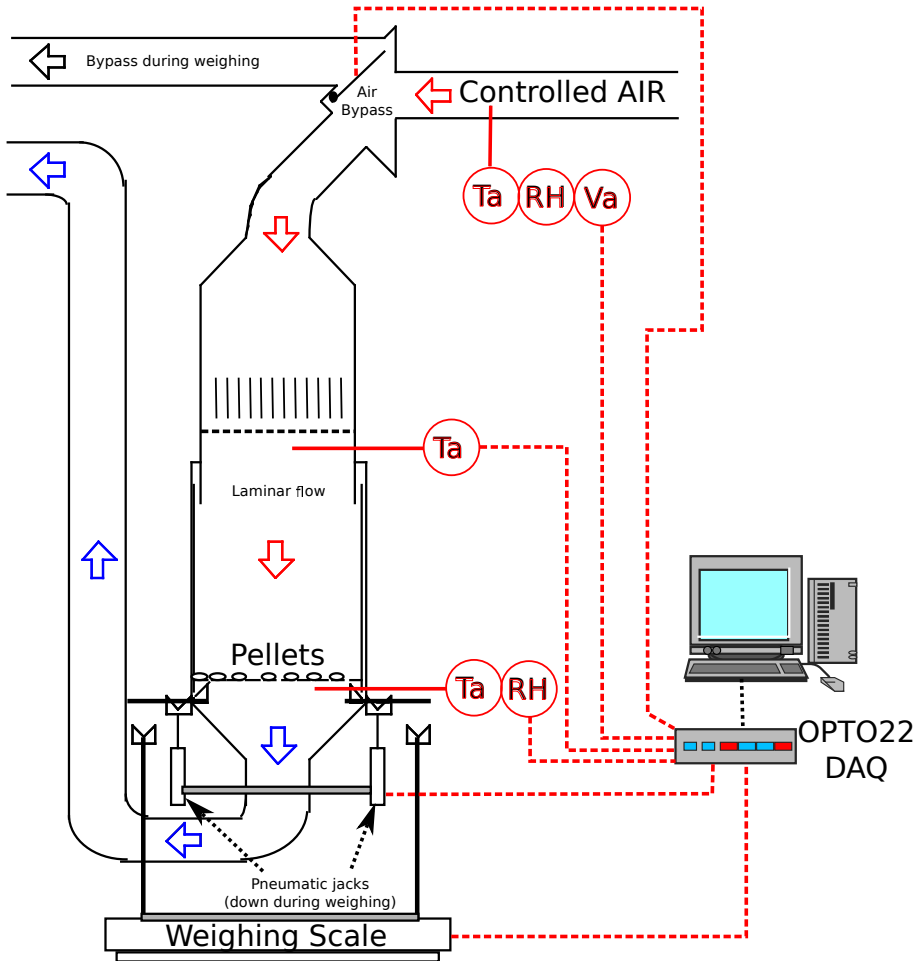


Figure 4.1 – Schematic view of the drying pilot

$$D_{eff} = \exp(-d_1 + d_2 \cdot X \cdot Tp) \quad (4.3)$$

Where d_1 and d_2 are constants optimized to force the simulation to fit the experimental data.

4.3 Modeling of the drying-cooling

In order to develop a versatile food drying simulator, the following compromise has been selected between the different approaches, published in a previous work [10], and some major assumptions have been considered. A convective drying model was built up both for deep bed and thin layer configurations. One usually assimilates the deep bed as a series of thin layers for which the only transfer occurs between air and grain, and a thin layer as an equivalent single (average) particle. Moreover, deep bed drying involves energy and mass transfer in air, after each thin layer crossing [17].

4.3.1 Heat and mass balances

For the particles

The following assumptions were considered for the particles:

Table 4.4 – Strategies to identify effective moisture diffusivity of pellets for chickens and rabbits

	Pellets for chickens	Pellets for rabbits (2.5 mm)	Pellets for rabbits (4 mm)
Identification set	One deep bed kinetic (inlet air velocity fixed at 1 m.s^{-1} , inlet air temperature at 90°C , and bed height at 18 cm)	Two thin layer kinetics (inlet air velocity fixed at 1 m.s^{-1} , inlet air temperature respectively at 40 and 80°C)	Two deep bed kinetics (inlet air velocity fixed at 1 m.s^{-1} , inlet air temperature respectively at 60 and 80°C , and bed height at 18 cm)
Validation set	All thin layer and drying-cooling kinetics	All other thin layer kinetics and deep bed kinetics	All thin layer kinetics

- Ideal geometry (infinite cylinder or spherical shape) with negligible shrinkage or swelling;
- An isotropic behavior (heat and mass transfers only in the radial direction);
- Negligible heat conduction between particles;

The heat and mass Biot number values (Bi_h and Bi_m) are respectively between 0.1 and 100 and much higher than 100. Therefore, heat conduction and liquid water diffusion within the particles and water evaporation, heat and mass convection at their surface are considered [18]. The heat and mass Peclet number values (Pe_h and Pe_m) are much higher than 1, therefore a plug-type airflow and negligible pressure variation are assumed [18]. Heat and mass balances for the particles, liquid water diffusion (equation 4.4) and thermal conduction (equation 4.5) phenomena are based on Fick's and Fourier's law respectively [18].

$$\frac{dX_t^{r,z}}{dt} = \frac{1}{r^n} \cdot \frac{\partial}{\partial r} \left(r^n \cdot D_{eff.} \cdot \frac{\partial X_t^{r,z}}{\partial r} \right) \quad (4.4)$$

$$\frac{d(\rho_{dm} \cdot (Cp_{dm} + Cp_w \cdot X_t^{r,z}) \cdot Tp_t^{r,z})}{dt} = \frac{1}{r^n} \cdot \frac{\partial}{\partial r} \left(r^n \cdot \lambda_{eff.} \cdot \frac{\partial Tp_t^{r,z}}{\partial r} \right) \quad (4.5)$$

Where X is the water content (d.b.), r the radial position in the particle (m), z the particle position in the height of the bed (m), t the elapsed time (s), n the shape factor (1, or 2, respectively for cylindrical, or spherical symmetry), $D_{eff.}$ the effective water diffusivity ($\text{m}^2.\text{s}^{-1}$), Tp the product temperature (K), $\lambda_{eff.}$ the effective thermal conductivity ($\text{W.m}^{-1}.K^{-1}$), ρ_{dm} the density of the dry matter (kg.m^{-3}) and Cp_{dm} and Cp_w the heat capacities at constant pressure of dry matter and water ($\text{J.kg}^{-1}.K^{-1}$), for the considered particle.

Temperature and water content within the particles are assumed to be uniform at initial time. In addition, boundary conditions are given in equations 4.6 to 4.9.

$$\frac{\partial X_t^{0,z}}{\partial r} = 0 \quad (4.6)$$

$$\frac{\partial T p_t^{0,z}}{\partial r} = 0 \quad (4.7)$$

$$-\rho_{dm} \cdot \frac{\partial (D_{ap} \cdot X_t^{r_{max},z})}{\partial r} = k_m \cdot \frac{M_w}{R} \cdot \left(\frac{a_w \cdot Pv_{sat.}}{Tp_t^{r_{max},z}} - \frac{HR \cdot Pv_{sat.}}{Ta_t^z} \right) = \varphi_m \quad (4.8)$$

$$\lambda_{ap} \cdot \frac{\partial T p_t^{r_{max},z}}{\partial r} = h_{glob} \cdot (Ta_t^z - T p_t^{r_{max},z}) - \varphi_m \cdot \Delta H_v = \varphi_Q \quad (4.9)$$

Where k_m is the convective mass transfer coefficient ($m.s^{-1}$), M_w the molar mass of water ($kg.mol^{-1}$), R the perfect gas constant ($J.kg^{-1}.K^{-1}$), a_w the water activity of the particle (Pa/Pa), $Pv_{sat.}$ the pressure of saturated vapor (Pa), RH the relative humidity (decimal), h_{glob} the external heat transfer coefficient including the heat transfer effectiveness by convection ($W.m^{-2}.K^{-1}$), Ta the air temperature (K) and ΔH_v the enthalpy of vaporization of pure water ($J.kg^{-1}$), φ_m the mass flux density ($kg.s^{-1}.m^{-2}$) and φ_Q the heat flux density ($J.s^{-1}.m^{-2}$).

For the air

A microscopic balance is realized on the air after each thin layer crossing (equations 4.10 and 4.11). Air moisture content and temperature are fixed at the inlet of the first thin layer but may not be constant during a drying experiment.

$$\frac{d(\rho_{da} \cdot Y_t^z)}{dt} = -\frac{\partial(\rho_{da} \cdot v_a \cdot Y_t^z)}{\partial z} + \frac{\varphi_m \cdot a \cdot (1 - \varepsilon)}{\varepsilon} \quad (4.10)$$

$$\frac{d(\rho_{da} \cdot (Cp_{da} + Y_t^z \cdot Cp_v) \cdot Ta_t^z)}{dt} = -\frac{\partial}{\partial z} (v_a \cdot \rho_{da} \cdot (Cp_{da} + Y_t^z \cdot Cp_v) \cdot Ta_t^z) - \frac{a \cdot (1 - \varepsilon) \cdot \varphi_Q}{\varepsilon} \quad (4.11)$$

Where ρ_{da} is the volume fraction of the dry air ($kg.m^{-3}$), a the particle specific surface area (surface area per particle volume) (m^{-1}), ε the bed porosity (decimal), Y the water content (d.b.), Ta the temperature (K) and Cp_{da} and Cp_v the specific heat capacities at constant pressure of respectively dry air and water vapor ($J.kg^{-1}.K^{-1}$), for the considered air.

4.3.2 Simulation and optimization

The dynamic system consists in a set of 6 Partial Differential Equations (PDEs 4.4 to 4.9). These equations are discretized in space into an Ordinary Differential Equation (ODEs) set using an explicit finite volume scheme to be numerically integrated with respect to both time and space by explicit embedded Runge-Kutta Cash-Karp (4, 5) method [19] (for stiff systems).

To quantify the quality of the model prediction, the maxima of a relative error between experimental and simulation data are calculated according to equations 4.12 and 4.13 respectively for thin layer and deep bed drying kinetics, valid for any time t . The aim is to minimize the maximum relative error (MINMAX algorithm) made on the measurable variables using the Nelder and Mead method (Downhill Simplex method) [20].

$$MRE_{TL} = \max \left(\left(\frac{\bar{X}_{sim}^t - \bar{X}_{exp}^t}{\bar{X}_{exp}^t} \right)^2 \right) \quad (4.12)$$

$$MRE_{DB} = \max \left(\left(\frac{\bar{\bar{X}}_{sim}^t - \bar{\bar{X}}_{exp}^t}{\bar{\bar{X}}_{exp}^t} \right)^2, \left(\frac{T_{out,sim}^t - T_{out,exp}^t}{T_{out,exp}^t} \right)^2 \right) \quad (4.13)$$

Where MRE_{TL} and MRE_{DB} are the maximum relative error respectively for thin layer and deep bed kinetics, \bar{X}_{sim}^t ² and $\bar{\bar{X}}_{sim}^t$ ³ the simulated mean moisture content (d.b.), \bar{X}_{exp}^t and $\bar{\bar{X}}_{exp}^t$ the experimental mean moisture content (d.b.) respectively for thin layer and deep bed kinetics, and $T_{out,sim}^t$ and $T_{out,exp}^t$ the simulated and experimental output air temperature (°C).

13 parameters are required for the model simulation. They all have a physical meaning. Some of them were measured (pellet dimensions and density, porosity of the bed, initial pellets temperature and moisture content), found in the literature (heat capacity, thermal conductivity, latent heat of vaporization, coefficient of heat and mass transfer by convection) or identified by reverse methods (effective moisture diffusivity and water activity). All required parameters for the simulation (parameters of the model and numerical parameters of the solver) are summarized in table 4.5.

4.4 Results and discussion

4.4.1 Sorption isotherms

The sorption isotherms of two pellets formulations (pellets for chickens or pellets for rabbits P4R - 4 mm) are presented on figure 4.2. First, there is no effect of the temperature for the [25 °C - 40 °C] range (see the figure 4.2). Second, the standard deviation for the data of the desorption and adsorption isotherms of pellets for rabbits at 25 °C is smaller than 0.5 % between the two repetitions, demonstrating reproducible measurements. Third, by comparing the sorption isotherms for the two formulations, one can observe that (see figure 4.2):

- when $a_w < 0.7$, pellets for chickens (P4C) have a more hygroscopic behavior than pellets for rabbits (P4R), meaning less sorption sites are available at low water activity values for this last pellet;
- when $a_w > 0.7$, pellets for rabbits (P4R) have a more hygroscopic behavior than pellets for chickens (P4C), which is probably related to the pellet micro-porosity and composition. Indeed, water activity of mixtures is dependent on the fraction size of each ingredient [4]. In particular, sugar beet pulp show a higher water holding capacity than the other ingredients at temperature below 80 °C [4, 22]. Sugar beet pulps, which only exist in the formulation of pellets for rabbits (P4R), seemed to be responsible for the more hygroscopic behavior at high water activity values.

2. \bar{X} is the mean moisture content of each layer and is calculated as the volume weighted average moisture content.

3. $\bar{\bar{X}}$, the mean moisture content within the bed, is calculated as the mean of the mean moisture content of each thin layer.

Table 4.5 – Physical properties of pellets and parameters used in simulation

Property	Equation or value		
	Pellets for chickens	Pellets for rabbits (“2.5 mm”)	Pellets for rabbits (“4 mm”)
Radius	2.14 mm	0.95 mm	2.18 mm
Characteristic length	6.09 mm	6.14 mm	9.02 mm
Density	1,325 kg.m ⁻³	1,170 kg.m ⁻³	1,183 kg.m ⁻³
Porosity of the deep bed	0.56	0.58	0.56
Initial temperature		20 °C	
Initial moisture content	0.204 d.b.	0.211 d.b.	0.202 d.b.
Heat capacity	Choi and Okos correlation [21]		
Thermal conductivity	Choi and Okos correlation [21]		
Latent heat of vaporization	2.357 10 ⁶ J.Kg ⁻¹ [17]		
Coefficient of heat transfer by convection	20 W.m ⁻² .K ⁻¹		
Coefficient of mass transfer by convection	Lewis analogy		
Water activity	Modified Henderson correlation [12]		
Effective moisture diffusivity	Abud correlation [16]		
Number of layer within the particle	10		
Height of the thin layer within the bed	1 mm		
Absolute tolerance	10 ⁻⁶		
Relative tolerance	10 ⁻⁶		
Initial time variation	10 ⁻³		

However, it should be noted that water activity variations have little influence on the drying model accuracy. Hence, the discrepancies between sorption isotherms values for the different formulations for water activities below 0.8 can be neglected in the framework of the simulation of drying or drying-cooling model. Two different correlations are used to fit the desorption isotherms data: the Chung-Pfost correlation and the modified Henderson correlation [12, 13]. On the one hand, Brook [23] fitted equilibrium moisture content and relative humidity data of soybean using Chung-Pfost correlation. Maier *et al.* showed that the identified parameters (provided in equation 4.14) can be applied to different formulations of pellets for animal feed, for relative humidity data between 20 and 90 % [8].

$$X_{eq} = 0.375 - 0.0068 \cdot \ln(-1.98 \cdot (T + 24.6) \cdot \ln(a_w)) \quad (4.14)$$

The identified parameters allow for a good agreement with experimental data for water activities between 0.4 and 0.8, as shown in figure 4.3. However this correlation gives non-zero a_w when $X_{eq} = 0$, which is physically not acceptable.

$$X_{eq} = \exp\left(\frac{\ln[-\ln(1.0-a_w)/20.802]}{1.41185}\right) \quad (4.15)$$

On the other hand, the identified parameters for the modified Henderson correlation (provided in equation ??) give acceptable results as shown on figure 4.3. More specifically, a good agreement with experimental data for water activity values below 0.8 is observed. Contrary to the Chung-Pfost correlation, water activity given by the modified Henderson correlation are positive or zero when the equilibrium moisture content is zero, which is expected. Therefore this latter correlation was preferred for drying and drying-cooling simulations.

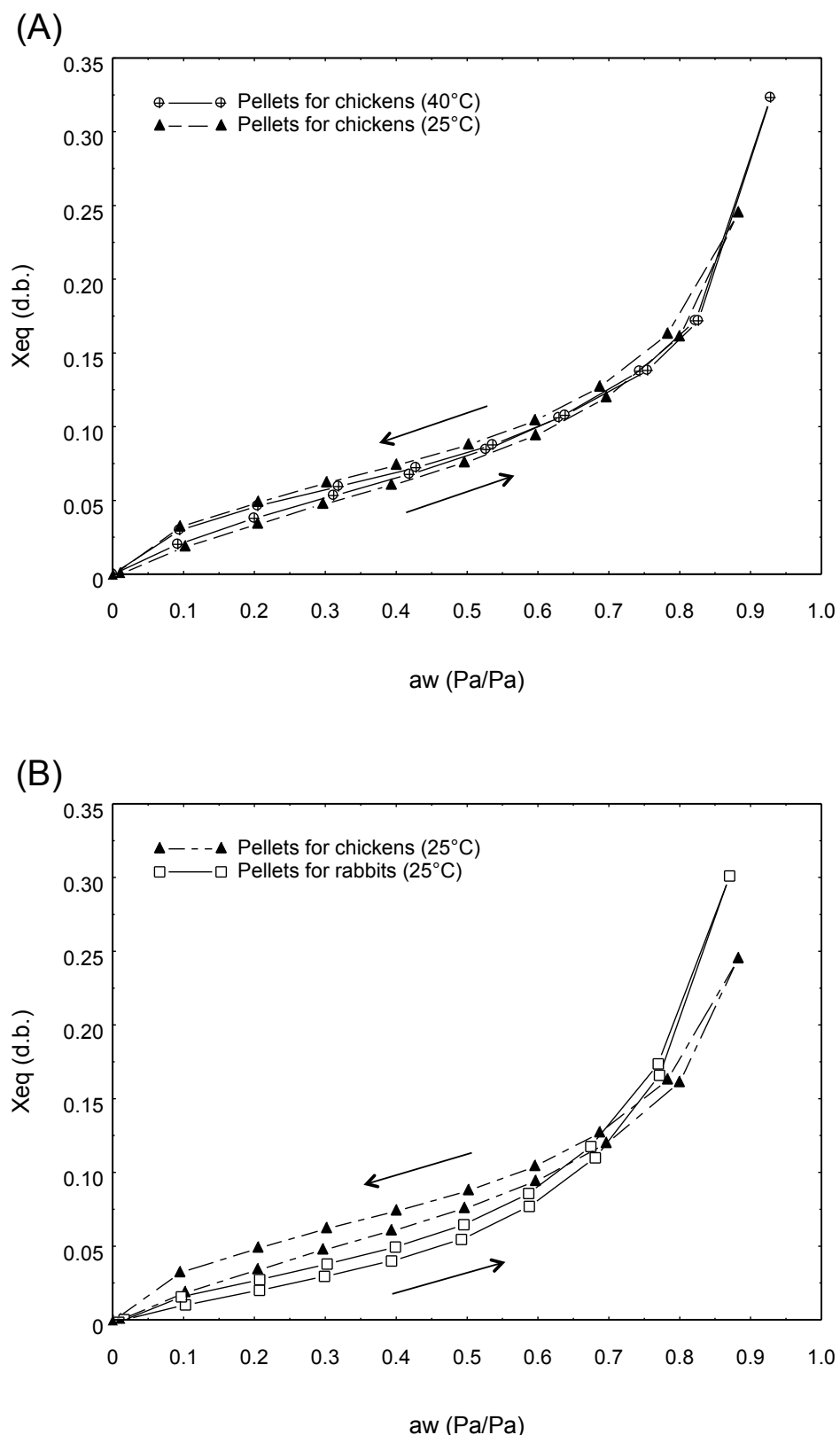


Figure 4.2 – Sorption isotherms of pellets. (A) Effect of temperature on equilibrium moisture content, P4C pellets for chickens. (B) Effect of pellet formulation on equilibrium moisture content at 25°C . (→ adsorption curves), (← desorption curves).

4.4.2 Identification of D_{eff}

The identified values of effective moisture diffusivity D_{eff} are given in table 4.6 for each formulation and geometry. In the case of pellets for rabbits with a given initial recipe, one may consider identical coefficients for the identification of effective moisture diffusivity. However the operating conditions of the pelleting stage of the pellet elaboration process drastically influence the intrinsic thermophysical properties of the final product. Therefore it is required to identify effective moisture diffusivity for each new formulation or pelleting operating conditions, which explains the slight differences between coefficients of effective moisture diffusivity correlation (see table 4.6).

Mean absolute error on mean moisture content and outlet air temperature are given in table 4.7 for the kinetics of the validation set of each formulation of pellets. The drying-cooling is well simulated in the case of pellets for chickens (figure 4.4) as well as the drying of the P4R - 4 mm pellets for rabbits (see figure 4.5) for the considered range of experimental conditions. In the case of the P4R - 2.5 mm pellets for rabbits, an identification set composed of thin layer kinetics was used, as contrary to the two other formulations where the identification set was composed of deep bed kinetics. The model simulates accurately the deep bed drying process for various air conditions (inlet air temperature in the range of 60 - 90 °C, inlet air velocity in the range of 0.7 - 2 m.s⁻¹) and bed height (10 - 18 cm) (see figure 4.7) and the thin layer drying kinetics in the 60 - 80 °C range (high temperature) (see figure 4.6). However at lower temperature (*e.g.* 40 °C), an overall underestimation of the pellet mean moisture content is observed (see figure 4.6). The mean absolute error is below 0.032 d.b. Indeed, the product mass variation is the only experimental data available with thin layer kinetics. During the drying process, heat and mass Hence, identification using one or two deep bed kinetics brings far more information (pellet mass variation, inlet and outlet air temperatures and relative humidities) and the identified parameters can be validated on a wide range of drying operating conditions. Besides, the identified parameters are also validated on classical drying-cooling operating conditions. Knowing the difficult problem of recording drying-cooling kinetics, one can characterize formulations of pellets for animal feed using only drying experiments.

Table 4.6 – Identified values of effective moisture diffusivity for each formulation and geometry of pellets

	Pellets for chickens	Pellets for rabbits	
		P4R - 2.5 mm	P4R - 4 mm
d_1	22.153	25.177	26.694
d_2	0.2017	1.452	1.736

4.5 Conclusion

Optimizing in real time the drying-cooling process, using an advanced control algorithm, is of utmost importance for the concerned industries. The purpose of the OPSERA project is to develop a smart sensor, based on a dynamic simulation model, which can predict the final moisture content and temperature of the pellets. In this study, different formulations and geometries of pellets for animal feed are characterized through the identification of effective moisture diffusivity and water activity. A dynamic drying-cooling model is also presented.

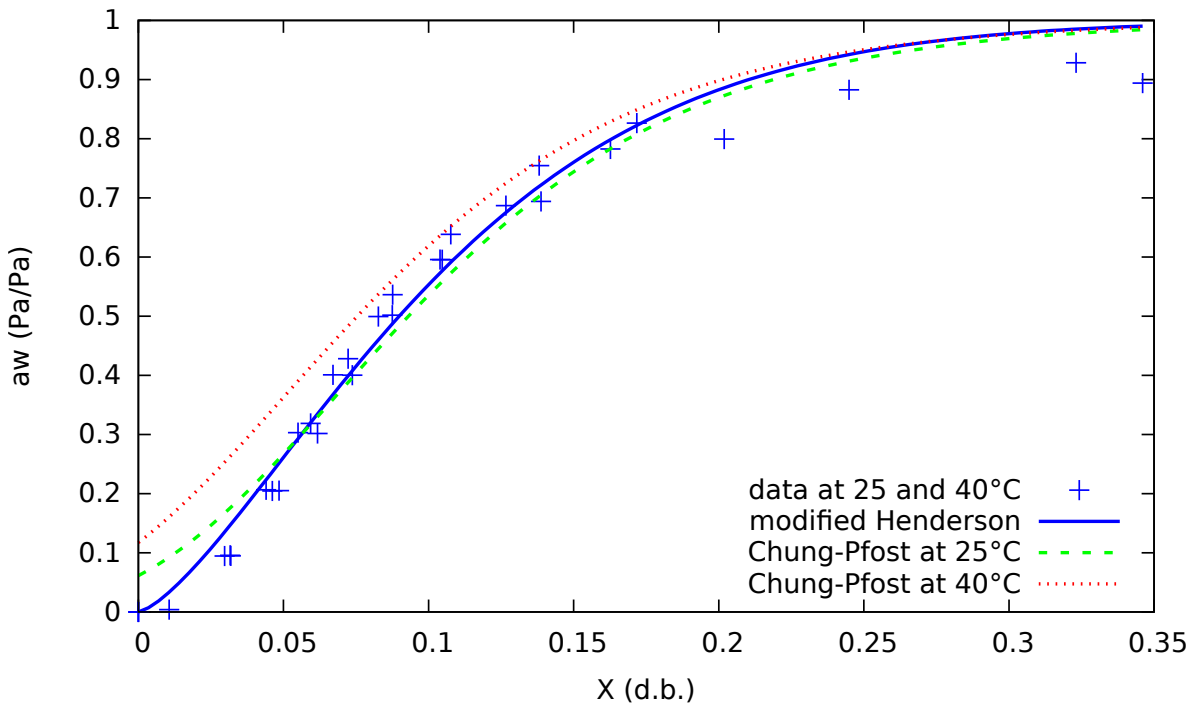


Figure 4.3 – Fitting of sorption isotherms of pellets for rabbits (P4R - 4 mm) (at 25 °C) and pellets for chickens (P4C), at 25 and 40 °C (+), with Henderson modified correlation (with continuous line) [12] and Chung-Pfost correlation [24] at 25 (with dotted line) and 40 °C (with tiny dotted line).

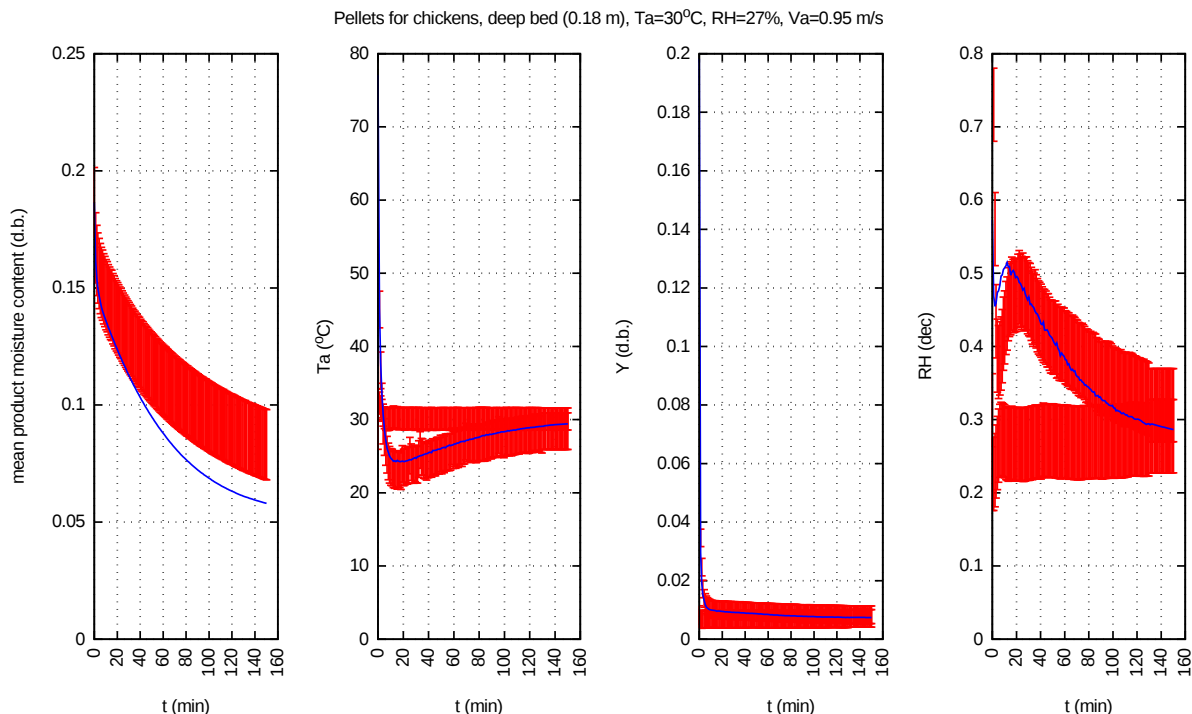


Figure 4.4 – Comparison of experimental (dots with error bars) and simulated (-) data of a deep bed drying-cooling kinetic of P4C, pellets for chickens (validation set).

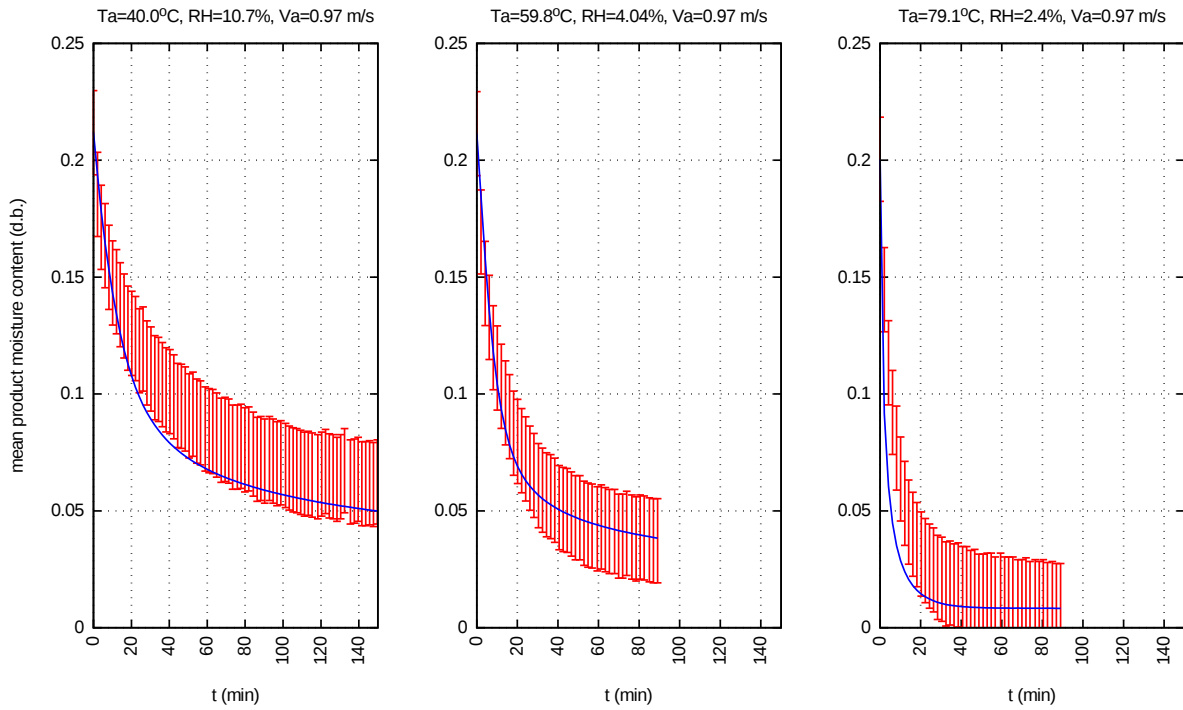


Figure 4.5 – Comparison of experimental (dots with error bars) and simulated (-) data of thin layer drying kinetics of the P4R - 4 mm pellets for rabbits (validation set)

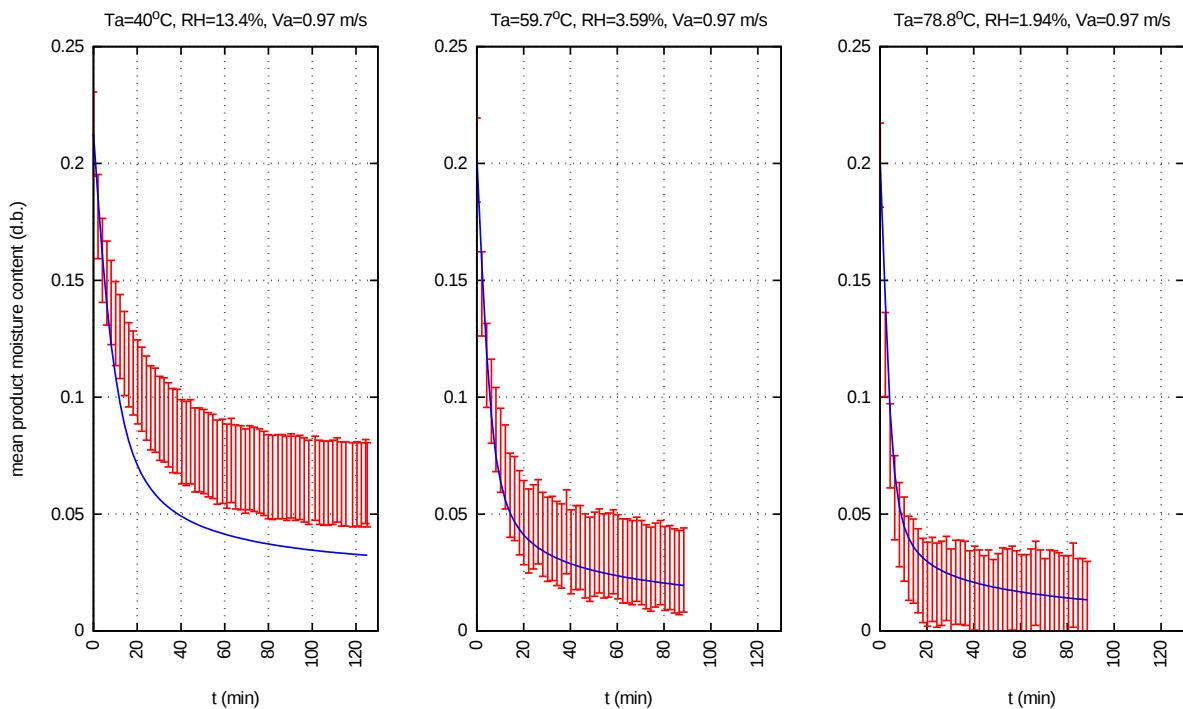


Figure 4.6 – Comparison of experimental (dots with error bars) and simulated (-) data of thin layer drying kinetics of the P4R - 2.5 mm pellets for rabbits (validation set)

Table 4.7 – Mean absolute error on product mean moisture content and outlet air temperature of the kinetics of the validation set

		<u>Mean absolute error</u>		<u>Operating conditions of the kinetics of the validation set</u>			
		\overline{X} or $\overline{\overline{X}}$ (d.b.)	$T_{a_{out}}$ (°C)	$T_{a_{in}}$ (°C)	v_a ($m.s^{-1}$)	height (cm)	T_{p_0} (°C)
Pellets for chickens	TL	< 0.016		30-70	1		20
	DC	0.022	0.8	30	1	18	60
P4R - 4 mm geometry of pellets for rabbits	TL	< 0.012		40 - 80	1		20
P4R - 2.5 mm geometry of pellets for rabbits	TL	0.032 < 0.014		40 60 - 80	1		20
	DB	< 0.014	< 4	60 - 90	0.7 - 2	10 - 18	20

TL Thin layer kinetics

DC Drying-cooling kinetics

DB Deep bed kinetics

\overline{X} Mean moisture content of the particles (case of thin layer kinetics)

$\overline{\overline{X}}$ Mean moisture content of the particles within the bed (case of deep bed kinetics)

$T_{a_{out}}$ Outlet air temperature

$T_{a_{in}}$ Inlet air temperature

v_a Inlet air velocity

T_{p_0} Initial temperature of the bed of pellets

Furthermore, a workaround is proposed to solve the difficult problem of recording cooling-drying kinetics. Indeed, the parameters of the effective moisture diffusivity correlation are identified on the basis of far-simpler-to-obtain drying kinetics before being finally validated on a single drying-cooling one. This approach gives satisfactory results as the deviation between the simulated and experimental data is mostly in the same range as the experimental uncertainties.

Current work in progress is focused on a) the validation of the cooling-drying model at the industrial scale and b) the development of a user friendly software sensor which can predict the final moisture content and temperature of the pellets by comparing simulated and industrial measured data of outlet air temperature and humidity.

Acknowledgments

The authors wish to thank several undergraduate, Master and Ph.D. students (Perinne Leclercq, Analia Aparecida Vanzo, Abir Hosni, Azziz Zemmouri, Monica Pinto, and Benoit Hareng) for their valuable help in acquiring experimental data supporting the modeling and simulation work. The authors wish to thank the French Agence Nationale de la

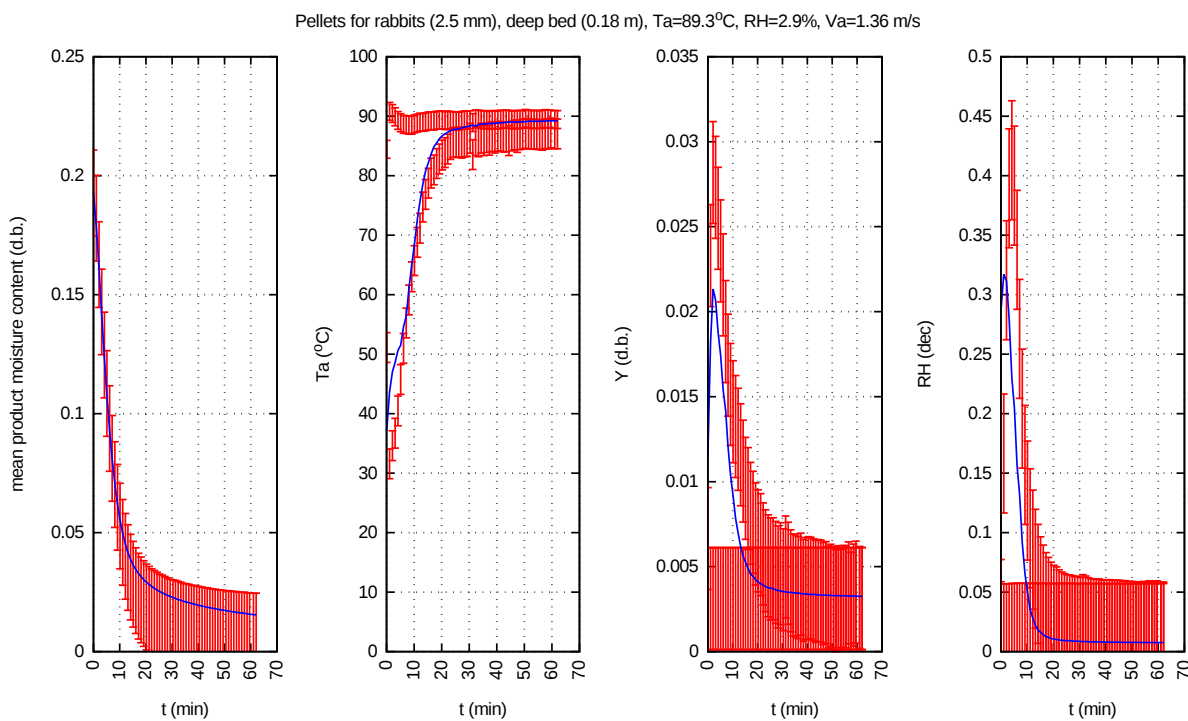


Figure 4.7 – Comparison of experimental (dots with error bars) and simulated (-) data of deep bed drying kinetics of the P4R - 2.5 mm, pellets for rabbits (validation set)

Recherche (ANR) for the funding of the Ph.D. of C. Lambert, and the partners of the project COOPERE2 led by Veolia Research and Innovation, in collaboration with ProSim and EN-SIACET. The authors also wish to thank the French Agency ADEME (Agence Nationale de l'Environnement et de la Maîtrise de l'Energie) for their funding of the experimental characterization and modeling of the drying of pellets.

Bibliography

- [1] J. F. Wood, “The functional properties of feed raw materials and their effect on the production and quality of feed pellets,” *Animal Feed Science and Technology* **18**(1), pp. 1 – 17, 1987.
- [2] M. Thomas and A. van der Poel, “Physical quality of pelleted animal feed 1: Criteria for pellet quality,” *Animal Feed Science and Technology* **61**(1-4), pp. 89 – 112, 1996.
- [3] M. Thomas, T. van Vliet, and A. van der Poel, “Physical quality of pelleted animal feed 3. contribution of feedstuff components,” *Animal Feed Science and Technology* **70**(1-2), pp. 59–78, 1998.
- [4] A. K. T. Hemmingsen, A. M. Stevik, I. C. Claussen, K. K. Lundblad, E. Prestlokken, M. Sorensen, and T. M. Eikevik, “Water adsorption in feed ingredients for animal pellets at different temperatures, particle size, and ingredient combinations,” *Drying Technology* **26**(6), pp. 738–748, 2008.
- [5] M. Thomas, D. van Zuilichem, and A. van der Poel, “Physical quality of pelleted animal feed. 2. contribution of processes and its conditions,” *Animal Feed Science and Technology* **64**(2-4), pp. 173 – 192, 1997.

- [6] H. de Blank, E. Hendrix, M. Litjens, and H. van Maaren, “On-line control and optimisation of the pelleting process of animal feed,” *Journal of the Science of Food and Agriculture* **74**(1), pp. 13–19, 1997.
- [7] R. L. Kelley, D. E. Maier, and F. W. Bakker-Arkema, “Evaluation of chilled cooling of feed pellets.,” *American Society of Agricultural Engineers* **90**, p. 13, 1990.
- [8] D. E. Maier and F. W. Bakker-Arkema, “The counterflow cooling of feed pellets,” *Journal of Agricultural Engineering Research* **53**, pp. 305–319, 1992.
- [9] D. E. Maier, R. L. Kelley, and F. W. Bakker-Arkema, “In-line, chilled air pellet cooling,” *Feed Manage* **43**, pp. 28–32, 1992.
- [10] C. Lambert, D. Goujot, H. Romdhana, and F. Courtois, “Toward a generic approach to build-up air drying models,” *Drying Technology* , p. 15, 2015.
- [11] C. A. S. Hill, A. Norton, and G. Newman, “The water vapor sorption behavior of natural fibers,” *Journal of Applied Polymer Science* **112**(3), pp. 1524–1537, 2009.
- [12] S. M. Henderson, “A basic concept of equilibrium moisture,” *Agricultural Engineering* **33**, pp. 29–32, 1952.
- [13] T. L. Thompson, “Mathematical simulation of corn drying: A new model,” *Transactions of the American Society of Agricultural Engineers* **24**, pp. 582–586, 1968.
- [14] S. ASAE, “D245.6. moisture relationships of plant-based agricultural products,” *ASAE* , 2007.
- [15] C. Lambert, H. Romdhana, and F. Courtois, “Reverse methodology to identify moisture diffusivity during air-drying of foodstuffs,” *Drying Technology* **33**(9), pp. 1076–1085, 2015.
- [16] M. Abud-Archila, F. Courtois, C. Bonazzi, and J.-J. Bimbenet, “A compartmental model of thin layer drying kinetics of rough rice,” *Drying Technology* **18**(7), pp. 1389–1414, 2000.
- [17] F. Courtois, *Dynamic Modelling of Drying to Improve Processing Quality of Corn*. PhD thesis, ENSIA, Massy, France, 1991.
- [18] R. B. Bird, W. E. Stewart, and E. N. Lightfoot, *Transport phenomena*. Wiley and Sons, 2002.
- [19] M. Galassi, J. Theiler, and J. Davies, *Gnu Scientific Library Reference Manual*. 3rd edition, Network Theory Ltd, 2009.
- [20] J. Nelder and R. Mead, “A simplex method for function minimization,” *Computer Journal* **7**(4), pp. 308–313, 1965.
- [21] S. Sahin and S. G. Sumnu, *Physical properties of foods*, p. 257. Food Science, 2006.
- [22] A. Serena and K. E. Bach Knudsen, “Chemical and physicochemical characterisation of co-products from the vegetable food and agro industries,” *Animal Feed Science and Technology* **139**(1–2), pp. 109–124, 2007.
- [23] R. C. Brook and G. H. Foster, *Handbook of Transportation and Marketing in Agriculture*, vol. II. Field Crops, ch. Drying, cleaning and conditionning, pp. 63–110. CRC Press Inc., 1981.
- [24] D. S. Chung and H. B. Pfost, “Adsorption and desorption of water vapor by cereal grains and their products. part i: Heat and free energy changes of adsorption and desorption,” *Transactions of the ASAE* **10**(4), pp. 549–555, 1967.

Chapitre 5

Model reduction technique for faster simulation of drying of spherical solid foods

Résumé

Le modèle de séchage développé permet de répondre au cahier des charges d'un module d'opération unitaire dans un logiciel générique de simulation. Cependant le temps de simulation de ce module en condition de séchage semi-industrielle est de l'ordre de 2 à 3 minutes, ce qui est 10 à 15 fois supérieur à celui des autres modules de ce logiciel. Pour pallier ce problème, nous avons développé une méthodologie de réduction de modèles classiques de séchage convectif. Cette méthodologie est décrite dans ce chapitre.

Pour simuler le séchage des aliments, la simulation des modèles classiques basés sur les différences, éléments ou volumes finis est très longue, ce qui peut constituer un problème dans le cadre d'une procédure d'optimisation où des centaines ou des milliers de simulations sont nécessaires. Un modèle de transferts couplés de chaleur et de matière, sur la base des phénomènes de diffusion et de convection, et dont les paramètres sont des propriétés non-linéaires, constitue un simulateur précis mais lent de séchage de produits alimentaires. Dans ce travail, nous montrons qu'il peut être remplacé par un modèle simple et beaucoup plus rapide, mais tout aussi précis, constitué de deux ou à trois compartiments. Des prédictions équivalentes de la teneur en eau moyenne et de la température du produit sont obtenues a) en reliant les coefficients d'échange (du modèle compartmental) aux coefficients de transferts (d'un modèle de convection et de diffusion) et b) après optimisation des fractions volumiques des compartiments. Les simulations obtenues sont très proches et le temps de simulation du modèle compartmental est inférieur d'un facteur 100 + par rapport à celui d'un modèle classique.

Mots-clés : séchage, transfert de matière et de chaleur, modélisation, modèle compartimental, volumes finis, optimisation.

Cet article a été publié dans *Journal of Food Engineering*¹.

1. H. Romdhana, C. Lambert, D. Goujot, and F. Courtois, "Model reduction technique for faster simulation of drying of spherical solid foods," *Journal of Food Engineering* 170, pp. 125-135, 2016.

5.1 Introduction

Modelling of drying kinetics is essential in most agro-industrial simulations: sugar industry, biomass refinery, fodder processing etc. Commercially available simulation programmes are often limited to steady-state simulations, whereas dynamic simulations are based on a better understanding of the process hence lead to better plant optimisations. The classical dynamic simulation of drying makes heavy use of heat and mass transfer equations requiring both space and time discretisations. Discretisations are based on finite difference, finite volume or finite element methods [1]. These numerical methods often require significant computing times to ensure stability and convergence, leading, *e.g.*, to limited applicability in optimisation procedures. To overcome this computing time limitation, one may consider the work of [2] who developed several analytical solutions for regular shapes (sphere, cylinder and slab). Nevertheless, for most non linear ordinary differential equations, analytical solutions are not available. In that perspective, [3] proposed a simplified model by dividing the food body in a shell and a core which is similar to a compartmental approach. However, this model is designed to predict only the cooling of high-moisture cylindrical shaped foods. As a matter of fact, to simulate drying of foods, the coupling between heat and mass transfers must be taken into account explicitly. Furthermore, the fact that most product properties are depending on state variables (*i.e.* local product moisture content and temperature) is often responsible for the main nonlinearities of the model.

Predicting heat and mass transfers, during drying by compartment models, is far less demanding in calculation time than conventional numerical methods, such as finite differences, finite elements or finite volumes. It is applied successfully in many chemical engineering fields, such as spray fluidised bed agglomeration [4], mechanical mixing [5] or liquid-liquid separation [6]. In the drying domain, several authors such as [7], [8] and [9], have used this approach with 2 or 3 compartments to model the drying of grains. In this approach, mass transfer, and possibly coupled heat and mass transfers within the drying particle, are considered to occur between separated compartments. Each compartment has its own moisture content and, possibly, its own temperature. Having only 2 or 3 compartments, the model results in a maximum of 6 ordinary differential equations to be solved. In addition, this restricted set of equations is observed to be numerically far more stable, allowing for faster numerical integration. On the other hand, such models are often considered as empirical ones due to the apparent lack of physical meaning of its coefficients. One may speak of exchange coefficients as opposed to well known transfer coefficients.

This work aims at bridging the gap between the two kinds of approaches in order to demonstrate that an optimised compartmental model can be far more efficient (*e.g.* 100 times faster computing time) than a finite volume model while keeping the advantage of meaningful parameters. For this purpose, a multi-compartment model is developed for describing the kinetics of heat and mass transfers during drying. The model is developed for a spherical particle which is assimilated to a short series of concentric compartments. Heat and mass are transferred from one compartment to the next, and finally from the outer compartment to the exterior. Each compartment is assumed to be homogeneous in temperature and moisture content. To make this approach similar to the diffusion convection model, mostly the same transfer equations are used to describe the heat and mass flux densities. Compartmental model in drying domain is usually limited to 2 or 3 compartments, thus reducing the number of equations to be solved and improving integration speed [8]. However, the predicted kinetics obtained from the compartmental model depend on the size of the compartments and the manner for which the heat and mass flux are calculated. In this work, a generic

method was developed to deduce an equivalent compartmental model from a given diffusion convection model. The overall method is outlined in the figure 5.1 showing the hierarchy of model building. As will be explained further, to ensure the 2 (or 3) compartment model (noted $[2X \bullet 2T \bullet \Delta a_w]$ and $[3X \bullet 3T \bullet \Delta a_w]$ and their variants with non-limiting heat conduction $[2X \bullet 1T \bullet \Delta a_w]$ and $[3X \bullet 1T \bullet \Delta a_w]$) is numerically equivalent to the diffusion convection models (noted $[\nabla X \bullet \nabla T \bullet \Delta a_w]$ and its variant with non-limiting heat conduction $[\nabla X \bullet 1T \bullet \Delta a_w]$), a) the same equations for the fluxes and b) the same parameters must be used and c) the size of the 2 (or 3) compartments must be optimised.

The developed method is planned around three main steps. The first step is to develop the multi-compartment model. This study provides two models that correspond to 2 and 3 compartments. In the second step, the volume sizes of the compartments are optimised by an inverse approach. The optimisation is performed in terms of compartment sizes by comparing predicted kinetics of the mass transfer given by multi-compartment model and analytical (exact) solution (noted $[\nabla X \bullet 0T \bullet \Delta X]$). Finally, the optimisation results obtained from mass transfer problem are used to validate two more realistic case studies (non-linear and simultaneous heat and mass transfers). Given that the analytical methods are not suitable for coupled transfer problems, the simulation results are compared to those provided by the finite volume method.

5.2 Nomenclature

	Roman capital letters
Bi_m	Biot number for mass transfer, dimensionless
Bi_{th}	Biot number for heat transfer, dimensionless
C	concentration of water vapour in air, $\text{kg} \cdot \text{m}^{-3}$
CV	control volume
Cp	specific heat capacity, $\text{J} \cdot \text{kg}^{-1} \cdot \text{K}^{-1}$
Cp_w	specific heat capacity of liquid water, $\text{J} \cdot \text{kg}^{-1} \cdot \text{K}^{-1}$
D	moisture diffusivity, $\text{m}^2 \cdot \text{s}^{-1}$
Fo	Fourier number, dimensionless
J	objective function fed to the simplex method, see equation (5.34)
M	Molar mass of water, $0.018 \text{ kg} \cdot \text{mol}^{-1}$
N	number of volumes of finite volume discretisation, dimensionless
ODE	ordinary differential equation
P_v	pressure of water vapour, Pa
R_G	gas constant, $8.314 \text{ J} \cdot \text{mol}^{-1} \cdot \text{K}^{-1}$
RH	relative humidity of air, decimal
$RMSE$	percentage of root-mean square error, %
S	surface area of an interface between compartments, m^2
T	temperature, K
U	internal energy, J
V	volume, m^3
X	moisture content, dry basis

	Roman small letters
a_w	water activity, (Pa/Pa)
dr	infinitesimal radius increment, m
h	convection heat transfer coefficient, W.m ⁻² .K ⁻¹
i	i-th elementary volume / compartment
j	j-th drying time used to compare two models
k	convection mass transfer coefficient, m.s ⁻¹
m	mass flux density at surface, kg.s ⁻¹ .m ⁻²
n	number of drying time used to compare two models
r	distance from the centre, m
t	time, s
	Greek letters
α	thermal diffusivity, m ² .s ⁻¹
β	root of the transcendental equation (5.32), dimensionless
Δr	thickness of a compartment / volume, m
ΔH_v	latent heat of water vaporization, J.kg ⁻¹
Δa_w	surface condition based on water isotherms, see equation (5.14)
ΔX	linear surface condition, see equation (5.30)
λ	thermal conductivity, W.m ⁻¹ .K ⁻¹
ρ	density, kg.m ⁻³
ξ	mass exchange coefficients at the interface between two adjacent compartments, m.s ⁻¹
	Subscripts
1	relative to the first (central) CV
\	at the interface between two CV
2	relative to the second CV
3	relative to the third CV
∞	relative to the drying air
air	dry air
c	mean radius of a volume or of a compartment
dm	dry matter
$ _e, e$	east side face of the CV
eq	equilibrium, at end of drying
G	relative to R_G
i	i-th elementary volume / compartment
$init$	initial, just before drying starts
j	j-th drying time used to compare two models
m	see Bi_m
N	number of control volumes in finite volume method
$r = 0$	at centre of the particle
$r = R$	at outer surface of the particle
th	see Bi_{th}
v	water vapour
$ _w, w$	west side face of the CV (see also a_w and Cp_w).

	Superscripts
-	mean over the solid at a given time
$1/2$	square root
<i>comp</i>	predicted by a compartmental model
<i>exact</i>	exact algebraic calculation
<i>finite volume</i>	predicted by a finite volume method
<i>sat</i>	saturated water vapour

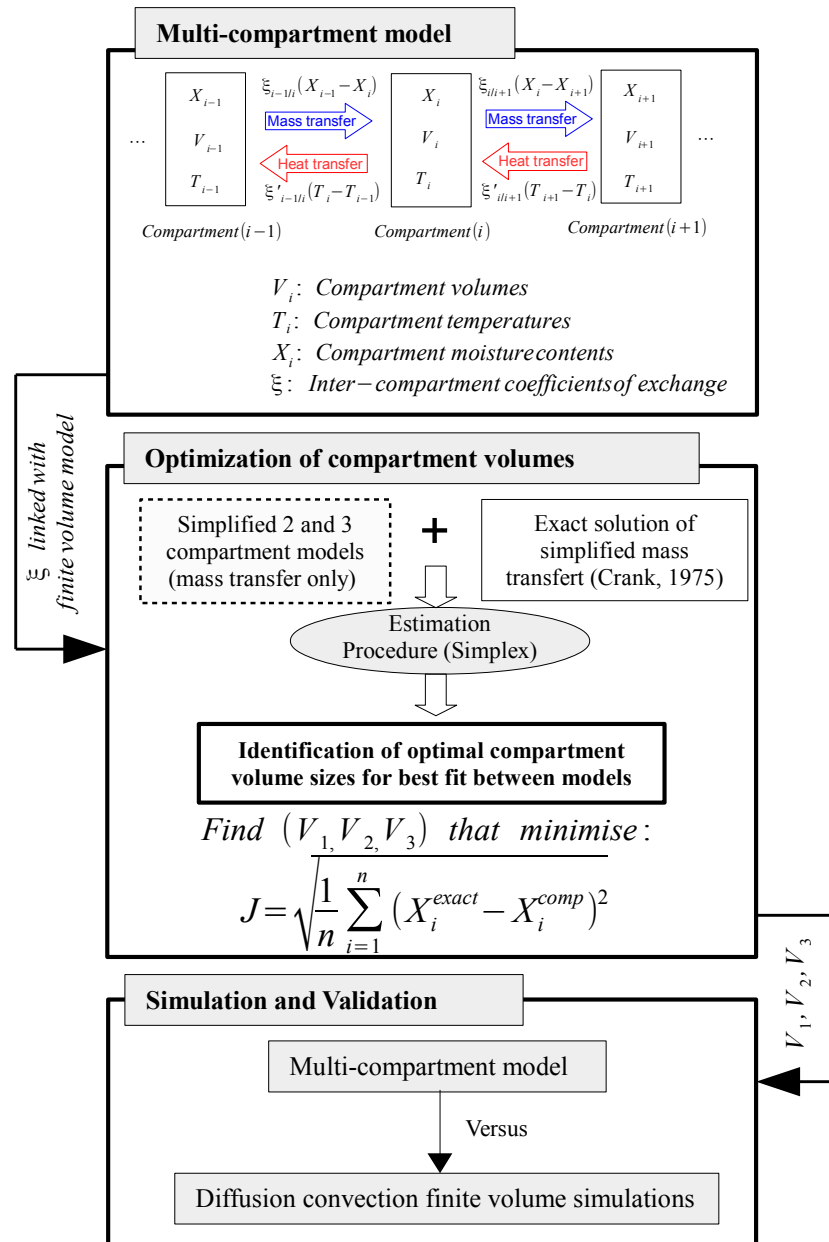


Figure 5.1 – Overall scheme of this work

5.3 Diffusion/convection models

In this section, we build up a complete and precise model for the drying of solid spheres based on Fick and Fourier's laws and a finite volume numerical solution.

Assuming negligible shrinkage and uniform and isotropic properties, microscopic balances are being written considering the following mechanisms: a) the mass transfer problem involves moisture diffusion inside the sphere and mass convection (vaporisation) at the sphere surface; b) the heat transfer problem involves heat conduction inside the sphere and heat convection and evaporation of moisture at the sphere surface.

5.3.1 Mass balance

The basic differential equation for mass transfer within the drying material is obtained by combining the conservation of mass with Fick's law. Assuming radial symmetry, the partial differential equation driving mass flow in spherical coordinates is:

$$\frac{\partial X}{\partial t} = \frac{1}{r^2} \frac{\partial}{\partial r} \left(r^2 D \frac{\partial X}{\partial r} \right) \quad (5.1)$$

The mass transfer equation 5.1 only determines the moisture content inside the drying material. To fully establish the moisture content field, two boundary conditions must be defined, at the surface ($r = R$) and at the centre of the drying material ($r = 0$). The mass transfer at the interface of the sphere and the surrounding air is expressed by the continuity of moisture diffusion and evaporation rate \dot{m} :

$$\left(-\rho_{dm} D \frac{\partial X}{\partial r} \right)_{r=R} = \dot{m} \quad (5.2)$$

Spherical symmetry implies a zero flux at the centre of the sphere:

$$\left(-\rho_{dm} D \frac{\partial X}{\partial r} \right)_{r=0} = 0 \quad (5.3)$$

5.3.2 Heat balance

In this study two concurrent heat transfer approaches are proposed. The first approach involves conductive transfer within the drying particle. The second approach involves macroscopic conservation balance. This latter approach is relatively less common in practice but has the advantage of a simplified model that can be applied for drying of thermally thin particle (*i.e.* with non-limiting thermal conductivity).

Limiting heat conduction: $[\nabla X \bullet \nabla T \bullet \Delta a_w]$

In conjunction with mass transfer, conductive transfer equation (first approach) can be obtained from heat balance and Fourier's law:

$$\frac{\partial (\rho C p T)}{\partial t} = \frac{1}{r^2} \frac{\partial}{\partial r} \left(r^2 \lambda \frac{\partial T}{\partial r} \right) \quad (5.4)$$

The drying product is not subject to chemical reactions or mechanical deformations (shrinkage, puffing). Hence, the term $\rho C p$ can be written as:

$$\rho C p = \rho_{dm} (C p_{dm} + X C p_w) \quad (5.5)$$

Heat flows between the drying-air and the surface of the sphere as a result of the temperature difference and of the evaporation rate:

$$\left(-\lambda \frac{\partial T}{\partial r}\right)_{r=R} = h(T - T_\infty) + \dot{m}(\Delta H_v + C_p v T) \quad (5.6)$$

Spherical symmetry implies the following adiabatic condition:

$$\left(-\lambda \frac{\partial T}{\partial r}\right)_{r=0} = 0 \quad (5.7)$$

Non-limiting heat conduction: $[\nabla X \bullet 1T \bullet \Delta a_w]$

In this second -simplified- approach, particle temperature is not differential function of the spatial variable, but represents average value over the sphere \bar{T} . An energy balance between the increase in sensible heat content of the product, the rate of heat transfer by convection and the latent heat of evaporation gives:

$$\frac{R}{3} \frac{\partial (\overline{\rho C p T})}{\partial t} = h(T_\infty - \bar{T}) - \dot{m}(\Delta H_v + C_p v \bar{T}) \quad (5.8)$$

By analogy with equation 5.5, the average change in $\overline{\rho C p}$ can be expressed as a function of the mean moisture content \bar{X} within the sphere:

$$\overline{\rho C p} = \rho_{dm} (C p_{dm} + \bar{X} C p_w) \quad (5.9)$$

5.3.3 Evaporation rate

The mass transfer rate is driven by the moisture content difference between the neighbouring moist air and the bulk of the drying medium, and depends also on the mass transfer coefficient k (equation 5.10).

$$\dot{m} = k(C_{r=R} - C_\infty) \quad (5.10)$$

By considering the gaseous phase behaviour being close to ideal gas, the concentration of water vapour in the moist air is:

$$C = P_v \frac{M}{R_G T} = \frac{M}{R_G} \frac{P_v}{P_v^{sat}} \frac{P_v^{sat}}{T} \quad (5.11)$$

The ratio of the partial pressure of the vapour P_v to the saturated pressure P_v^{sat} , close to the particle surface and within the drying medium are equal respectively to the water activity of the drying particle (equation 5.12) and the relative humidity of the drying medium (equation 5.13).

$$a_w = \frac{P_{v,r=R}}{P_{v,r=R}^{sat}} \quad (5.12)$$

$$RH = \frac{P_{v,\infty}}{P_{v,\infty}^{sat}} \quad (5.13)$$

Equation 5.10 may now be written in terms of temperature ($T_{r=R}, T_\infty$), saturated vapour pressure of water ($P_{v,r=R}^{sat}, P_{v,\infty}^{sat}$) and the ratio of the partial pressure of water vapour in the moist air to the saturated vapour pressure of water at a given temperature (a_w, RH):

$$\dot{m} = k \frac{M}{R_G} \left(a_w \frac{P_{v,r=R}^{sat}}{T_{r=R}} - RH \frac{P_{v,\infty}^{sat}}{T_\infty} \right) \quad (5.14)$$

The Chilton-Colburn's analogy [10] is commonly used to relate the convective heat and mass transfer coefficients. The density and specific capacity of air at atmospheric pressure are $\rho_{air} = 1 \text{ kg.m}^{-3}$ and $Cp_{air} = 1,000 \text{ J.kg}^{-1}.\text{K}^{-1}$. Therefore, the mass transfer coefficient can be approximated by:

$$k \cong \frac{h}{1000} \quad (5.15)$$

5.3.4 Finite volume numerical solution

Solving previous equations numerically involves the reformulation of heat and mass balances in discrete form. This work makes use of the finite-volume scheme as a discretisation method.

The finite-volume method is introduced in this section in order to solve the problem of heat and mass transfers during drying of a spherical particle. This approach is especially useful for problem where thermo-physical properties change inside the drying product, such as moisture diffusivity and thermal conductivity coefficients. This method requires the definition of a network of N control volumes and the approximation of N volume integrals. The complexity of routine calculations required to solve the ordinary differential equations in the model increases with the number N of control volumes. The continuous physical

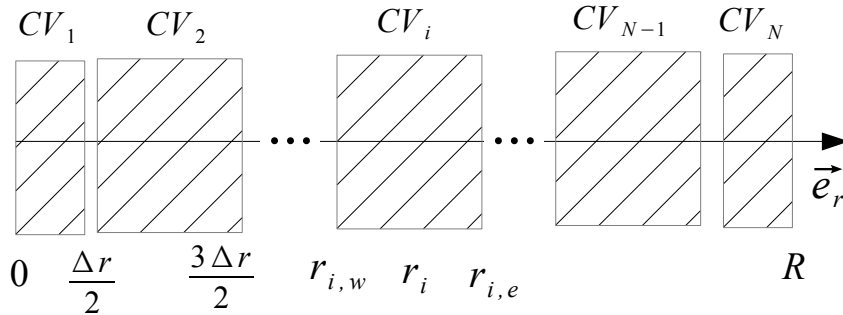


Figure 5.2 – Finite volume discretisation scheme

domain is first discretised into finite control volumes CV_i (Figure 5.2). Each control volume is approximated in terms of nodal values (control volume centres) and midpoints denoted by geographical subscript: e (east) and w (west). These midpoints are useful to define the heat and mass exchange surfaces of the control volume. The radius is discretised into $N - 2$ compartments of equal sizes of Δr , plus a compartment at centre and a compartment at the boundary layer whose width is $\frac{\Delta r}{2}$. The space discretisation step is defined as:

$$\Delta r = \frac{R}{N - 1} \quad (5.16)$$

For i between 1 and N , the i^{th} control volume is identified by its representative radius defined as:

$$r_{ci} = (i - 1)\Delta r \quad (5.17)$$

The edges of control volume (i) are then:

$$\begin{aligned} r_{i,w} &= r_{ci} - \frac{\Delta r}{2} \\ r_{i,e} &= r_{ci} + \frac{\Delta r}{2} \end{aligned} \quad (5.18)$$

The averages of the temperature and the moisture content over control volumes are computed from the conservation law in its integral form. The control volume integration yields to the following expressions:

$$\begin{aligned} \int_{r_{i,w}}^{r_{i,e}} \frac{\partial X}{\partial t} 4\pi r^2 dr &= \int_{r_{i,w}}^{r_{i,e}} \frac{1}{r^2} \frac{\partial}{\partial r} \left(r^2 D \frac{\partial X}{\partial r} \right) 4\pi r^2 dr \\ \int_{r_{i,w}}^{r_{i,e}} \frac{\partial(\rho CpT)}{\partial t} 4\pi r^2 dr &= \int_{r_{i,w}}^{r_{i,e}} \frac{1}{r^2} \frac{\partial}{\partial r} \left(r^2 \lambda \frac{\partial T}{\partial r} \right) 4\pi r^2 dr \end{aligned} \quad (5.19)$$

To simplify the integration of the accumulation term, we can consider that the internal energy (ρCpT) and the moisture content are uniform in a control volume and take their values in i . Equation 5.19 becomes:

$$\begin{aligned} \frac{\partial X_i}{\partial t} &= \frac{3}{r_{i,e}^3 - r_{i,w}^3} \left[r_{ci}^2 D_i \frac{\partial X_i}{\partial r} \right]_w^e \\ \frac{\partial T_i}{\partial t} &= \frac{3}{r_{i,e}^3 - r_{i,w}^3} \frac{1}{(\rho Cp)_i} \left[r_{ci}^2 \lambda_i \frac{\partial T_i}{\partial r} \right]_w^e \end{aligned} \quad (5.20)$$

To calculate temperature and moisture content gradients at the control volume faces, a linear approximation of the fluxes is used. As a result, temperature and moisture content gradients are evaluated by differentiating $\partial T/\partial r$ and $\partial X/\partial r$ then by evaluating the result at neighbour nodes.

Hence, temperature gradient within the sphere is approximated by:

$$\begin{aligned} \frac{\partial T_i}{\partial r} |_e &= \frac{T_{i+1} - T_i}{\Delta r} \\ \frac{\partial T_i}{\partial r} |_w &= \frac{T_i - T_{i-1}}{\Delta r} \end{aligned} \quad (5.21)$$

In a similar manner, the moisture content gradient is obtained by:

$$\begin{aligned} \frac{\partial X_i}{\partial r} |_e &= \frac{X_{i+1} - X_i}{\Delta r} \\ \frac{\partial X_i}{\partial r} |_w &= \frac{X_i - X_{i-1}}{\Delta r} \end{aligned} \quad (5.22)$$

The values of thermal conductivity and moisture diffusivity at control volume faces are evaluated by using a geometric mean between nodal points.

Then, the transfer properties at west and east faces are given by equations 5.23 and 5.24.

$$\begin{aligned} D_{i,w} &= (D_{i-1} D_i)^{1/2} \\ \lambda_{i,w} &= (\lambda_{i-1} \lambda_i)^{1/2} \end{aligned} \quad (5.23)$$

$$\begin{aligned} D_{i,e} &= (D_{i+1} D_i)^{1/2} \\ \lambda_{i,e} &= (\lambda_{i+1} \lambda_i)^{1/2} \end{aligned} \quad (5.24)$$

Next, applying the boundary conditions at nodal points ($r = 0$ and $r = R$) and substituting equations 5.21, 5.22 into 5.20, gives a system of $2N$ first order differential equations (ODEs)

given by 5.25.

$$\begin{aligned}
 & \text{For : } i = 1 \\
 & \frac{\partial X_1}{\partial t} = \frac{6}{\Delta r^2} D_{1,e} (X_2 - X_1) \\
 & \frac{\partial T_1}{\partial t} = \frac{1}{(\rho C_p)_1} \frac{6}{\Delta r^2} \lambda_{1,e} (T_2 - T_1) \\
 & \text{For : } i = 2 \cdots N-1 \\
 & \frac{\partial X_i}{\partial t} = \frac{3}{r_{i,e}^3 - r_{i,w}^3} \left(r_{i,e}^2 D_{i,e} \frac{X_{i+1} - X_i}{\Delta r} - r_{i,w}^2 D_{i,w} \frac{X_i - X_{i-1}}{\Delta r} \right) \\
 & \frac{\partial T_i}{\partial t} = \frac{1}{(\rho C_p)_i} \frac{3}{r_{i,e}^3 - r_{i,w}^3} \left(r_{i,e}^2 \lambda_{i,e} \frac{T_{i+1} - T_i}{\Delta r} - r_{i,w}^2 \lambda_{i,w} \frac{T_i - T_{i-1}}{\Delta r} \right) \\
 & \text{For : } i = N \\
 & \frac{\partial X_N}{\partial t} = \frac{-3}{R^3 - (R - \frac{\Delta r}{2})^3} \left(R^2 \frac{\dot{m}}{\rho_{dm}} + \left(R - \frac{\Delta r}{2} \right)^2 D_{N,w} \frac{X_N - X_{N-1}}{\Delta r} \right) \\
 & \frac{\partial T_N}{\partial t} = \frac{1}{(\rho C_p)_N} \frac{-3}{R^3 - (R - \frac{\Delta r}{2})^3} \left(R^2 (h(T_N - T_\infty) - \dot{m}(\Delta H_v + C_p v T_N)) \cdots \right. \\
 & \quad \left. + \left(R - \frac{\Delta r}{2} \right)^2 \lambda_{N,w} \frac{T_N - T_{N-1}}{\Delta r} \right)
 \end{aligned} \tag{5.25}$$

As a reminder, this model is made available in two variants: a) $[\nabla X \bullet \nabla T \bullet \Delta a_w]$ the full diffusion convection model and b) $[\nabla X \bullet 1T \bullet \Delta a_w]$ the simplified variant with one global temperature for the whole sphere.

5.4 Three-compartment model (noted $[3X \bullet 3T \bullet \Delta a_w]$ and $[3X \bullet 1T \bullet \Delta a_w]$)

In compartmental models, the mass or energy flows between two adjacent compartments are assumed to be proportional to the difference of mass concentration or internal energy between each compartment. The differential equations that describe the flow between the compartments are hence ordinary differential equations of the first order. In this section, only the 3 compartment (both for X and T hence denoted $[3X \bullet 3T \bullet \Delta a_w]$) version is described, but it is simple to deduce the 2 compartment version ($[2X \bullet 2T \bullet \Delta a_w]$) as well. Same remark applies for their single -global- temperature variants ($[2X \bullet 1T \bullet \Delta a_w]$ and $[3X \bullet 1T \bullet \Delta a_w]$). The mass conservation equations represent the elementary variation of the moisture content according to the difference between inflows and outflows. The mass balance, for 3 spherical compartments are described by 3 ODEs (equations 5.26).

$$\begin{aligned}
 \frac{\partial X_1}{\partial t} &= \frac{S_{1\setminus 2}}{V_1} \xi_{1\setminus 2} (X_2 - X_1) \\
 \frac{\partial X_2}{\partial t} &= \frac{S_{2\setminus 3}}{V_2} \xi_{2\setminus 3} (X_3 - X_2) - \frac{S_{1\setminus 2}}{V_2} \xi_{1\setminus 2} (X_2 - X_1) \\
 \frac{\partial X_3}{\partial t} &= \frac{S_{3\setminus \infty}}{V_3} \frac{\dot{m}}{\rho_{dm}} - \frac{S_{2\setminus 3}}{V_3} \xi_{2\setminus 3} (X_3 - X_2)
 \end{aligned} \tag{5.26}$$

$\xi_{1\setminus 2}$ and $\xi_{2\setminus 3}$ are the mass exchange coefficients at the interface between two adjacent compartments. In order to compare as much as possible with the finite volume diffusion-convection models, applying some analogy with Fick's law, these mass exchange coefficients are related to meaningful transfer coefficients as follows:

$$\begin{aligned}
 \xi_{1\setminus 2} &= \frac{D_{1\setminus 2}}{R_{c2} - R_{c1}} \\
 \xi_{2\setminus 3} &= \frac{D_{2\setminus 3}}{R_{c3} - R_{c2}}
 \end{aligned} \tag{5.27}$$

$S_{1\setminus 2}$ and $S_{2\setminus 3}$ are the surface areas at the interface between compartments, $S_{3\setminus \infty}$ is the outer surface and R_{c1} , R_{c2} , and R_{c3} are the mean radiiuses of the compartments (*i.e.* hollow

spheres).

The mean radiuses are calculated by volume averaging (equation set 5.28).

$$\begin{aligned} R_{c1} &= \frac{\int_0^{R_1} r 4\pi r^2 dr}{V_1} = \frac{3}{4} R_1 \\ R_{c2} &= \frac{\int_{R_1}^{R_2} r 4\pi r^2 dr}{V_2} = \frac{3}{4} \frac{R_2^4 - R_1^4}{R_2^3 - R_1^3} \\ R_{c3} &= \frac{\int_{R_2}^{R_3} r 4\pi r^2 dr}{V_3} = \frac{3}{4} \frac{R_3^4 - R_2^4}{R_3^3 - R_2^3} \end{aligned} \quad (5.28)$$

Applying the same development to heat transfer gives similar results to describe the temperature changes in each compartment (equation set 5.29).

$$\begin{aligned} \frac{\partial T_1}{\partial t} &= \frac{S_{1\setminus 2}}{(V\rho Cp)_1} \frac{\lambda_{1\setminus 2}}{R_{c2}-R_{c1}} (T_2 - T_1) \\ \frac{\partial T_2}{\partial t} &= \frac{1}{(V\rho Cp)_2} \left(S_{2\setminus 3} \frac{\lambda_{2\setminus 3}}{R_{c3}-R_{c2}} (T_3 - T_2) - S_{1\setminus 2} \frac{\lambda_{1\setminus 2}}{R_{c2}-R_{c1}} (T_2 - T_1) \right) \\ \frac{\partial T_3}{\partial t} &= \frac{1}{(V\rho Cp)_3} \left(S_{3\setminus \infty} (h(T_\infty - T_3) - \dot{m}(\Delta H_v + Cp_v T_3)) - S_{2\setminus 3} \frac{\lambda_{2\setminus 3}}{R_{c3}-R_{c2}} (T_3 - T_2) \right) \end{aligned} \quad (5.29)$$

The values of thermal conductivity and moisture diffusivity between compartments are evaluated by using a geometric mean (similarly to equations 5.23 and 5.24).

5.5 Exact solution of mass transfer uncoupled from heat transfer (noted $[\nabla X \bullet 0T \bullet \Delta X]$)

Crank [2] provides an analytic solution, giving the exact distribution of either temperature or moisture content within the homogeneous solid sphere. Nevertheless, it is unable to solve any of these useful configurations: coupled heat and mass transfers, non-constant transfer coefficients or properties, non-linear boundary conditions as shown in equation 5.14. On the other hand, for a simple problem as water diffusion in a homogeneous sphere with linear boundary conditions, it provides an exact algebraic solution. Hence, in this study, such analytical solution of moisture diffusion is used to optimise the sizes of the compartments of numerical models $[2X \bullet 0T \bullet \Delta X]$ and $[3X \bullet 0T \bullet \Delta X]$. These sizes will be reused in $[2X \bullet 2T \bullet \Delta aw]$ and $[3X \bullet 3T \bullet \Delta aw]$.

Given that the algebraic solutions are restricted to a few simplified problems [2], only two boundary conditions are suitable at the product surface. Several authors have discussed these boundary conditions [11, 12]. Some authors consider that the product surface reaches equilibrium instantaneously ($X_{r=R} = X_{eq}$). This condition simplifies the resolution of the diffusion equations, nevertheless it is only valid if the resistance to mass transfer at the product surface is negligible. A more general surface condition taking the convective mass transfer into account can be written as a linear relationship:

$$\left(-D \frac{\partial X}{\partial r} \right)_{r=R} = k(X - X_{eq}) \quad (5.30)$$

The boundary condition given in equation 5.30 implies that the moisture content at the product surface varies, and X_{eq} is the moisture content at end of the kinetics, in equilibrium with the drying air. This condition is used instead of the more realistic equation 5.14 only for

the optimisation purpose. In this case of surface evaporation problem, the required solution is [2]:

$$\frac{\bar{X}_j^{exact} - X_{eq}}{X_{init} - X_{eq}} = 1 - \sum_{i=1}^{\infty} \frac{6Bi_m^2 \exp(-\beta_i^2 Dt_j/R^2)}{\beta_i^2 (\beta_i^2 + Bi_m (Bi_m - 1))} \quad (5.31)$$

Where β_i are the non-negative roots of:

$$\frac{\beta_i}{\tan(\beta_i)} + Bi_m - 1 = 0 \quad (5.32)$$

And Bi_m is defined as:

$$Bi_m = \frac{Rk}{D} \quad (5.33)$$

5.6 Results and discussion

The choice of the compartment sizes (volumes or radiiuses) has a strong influence on the predicted moisture or temperature kinetics. In the work of [8] or [9] for instance, the choice of number and sizes of the compartments was based on empirical considerations (*e.g.* anatomy of the grains or shape of the drying kinetics) prior to the identification of unknown exchange coefficients. In this work, we intend to demonstrate that the size ratios can be optimised numerically, once for all, to force the two- (or three-) compartment model to mimic the finite volume diffusion convection model.

All simulations were done numerically with MATLAB® using its ODE15S solver for non-linear and stiff sets of ordinary differential equations. The diffusion convection simulations were calculated with 100 finite volumes. The exact analytical solution was calculated using the first 6 terms of the infinite series (see equation (5.31)) as suggested by [2] in table 6.2 p.381. Non-linear minimisations were done numerically with MATLAB® using its FMIN-SEARCH routine.

5.6.1 Optimisation of compartment sizes

The optimisation procedure is based on theoretical data of mass transfer. The identification uses the minimisation of least-square errors between product mean moisture contents computed from exact solution ($[\nabla X \bullet 0T \bullet \Delta X]$) and simplified variants of the compartmental models ($[2X \bullet 0T \bullet \Delta X]$ or $[3X \bullet 0T \bullet \Delta X]$). The parameters to be found characterise the compartment volume sizes (V_1 , V_2 , and V_3). The identification of the geometric boundaries in the case of two-compartment modelling consists in obtaining the ratio of the interior boundary position to the sphere radius, given by R_1/R_2 . In the case of three-compartment modelling, the geometric optimisation of interior boundaries consists in identifying two radial positions defined by R_1/R_3 and R_2/R_3 , corresponding to the ratios of the inner and middle boundary positions to the whole sphere radius.

The optimisation problem is solved using a sequential simplex method [13] (also known as Nelder and Mead's method), *i.e.*:

$$find (V_1, V_2, V_3) \text{ that minimise } J = \sqrt{\frac{1}{n} \sum_{j=1}^n \left(\bar{X}_j^{exact} - \bar{X}_j^{comp} \right)^2} \quad (5.34)$$

The first result (\bar{X}_j^{comp}) is obtained by integration of the mass-only variants of the multi-compartment equations ($[2X \bullet 0T \bullet \Delta X]$ or $[3X \bullet 0T \bullet \Delta X]$). The second result (\bar{X}_j^{exact}) is

obtained by the "exact" solution of $[\nabla X \bullet 0T \bullet \Delta X]$ shown in equation 5.31, which is used as a reference, yet simplified, solution in order to "calibrate" the numerical approach.

Parameter optimisation is essential for the development of this mathematical model. For this reason, the optimisation is performed on a wide range of mass transfer Biot number (equation 5.33). The optimisation problem is therefore to minimise the objective function 5.34 for each number of Biot. The size of Biot number gives a key information to drying condition in which k , the convection mass transfer, varies between 0.001 and 0.04 m.s^{-1} . According to the relation 5.15, the corresponding convection heat transfer coefficient varies between 1 and 40 $\text{W.m}^{-2}.\text{K}^{-1}$. For each mass transfer Biot number, a separate optimisation procedure is initialised with compartments of equal thicknesses then launched until numerical convergence. The optimisation solutions, obtained for 2 and 3 compartments, are shown respectively in figures 5.3 and 5.4. The corresponding statistics are shown on table 5.1. In the case of two-compartment modelling, the identification of geometric boundaries consists in identifying the best ratio of the interior boundary position to the sphere radius (R_1/R_2). The obtained value of the radius ratio is 0.9212 ± 0.017 , hence the volumes of the 2 compartments are 73 % and 27 %, respectively for the first and second compartments. In the case of three-compartment modelling, the best two radial positions defined by R_1/R_3 and R_2/R_3 are identified, corresponding to the ratios of the inner and middle boundary positions to the sphere radius. 0.7793 ± 0.006 and 0.9659 ± 0.002 are found, respectively for the inner and the middle ratios. The corresponding volumes of compartments are hence 66 %, 23 % and 11 %, respectively for the first, second and third compartments.

In order to compare the mass transfer obtained by the analytical solution and compartmental models, two drying kinetics are simulated for two different mass transfer Biot numbers: 4,000 and 2,000,000. Both values of Biot number correspond respectively to a moisture diffusivity of 10^{-8} and $10^{-9} \text{ m}^2/\text{s}$, a convection mass transfer of 0.01 and 0.02 m/s and a particle radius of 0.4 and 1 cm . Each subplot of figure 5.5 shows the superposition of four curves: analytical solution, solutions with 2 and 3 compartments by using the average values of the optimised volume fractions and solutions with 2 and 3 compartments by using the average values \pm Std. Dev. In both drying cases, the solutions with 3 compartments are much better than with only 2 compartments. Therefore, adding a third compartment is required to obtain a very precise solution, at the cost of an increase of 50 % of the computation time.

It appears clearly that one set of volume sizes for the 2 (or 3) compartments is sufficient for the compartmental model to mimic, in almost all situations, the simulations from the exact solution. In the following subsections, this approach will prove to predict efficiently the problems in which the linear hypotheses used by [2] are no longer valid.

Table 5.1 – Basic statistics on optimised parameters

	Mean	Std. Dev.	Min	Max	Range ⁽¹⁾
Two-compartment model $[2X \bullet 2T \bullet \Delta a_w]$					
R_1/R_2	0.9212	0.01685	0.8904	0.9556	0.06521
Three-compartment model $[3X \bullet 3T \bullet \Delta a_w]$					
R_1/R_3	0.7793	0.00570	0.7728	0.9794	0.02659
R_2/R_3	0.9659	0.00196	0.9624	0.9728	0.01043

⁽¹⁾Difference between the maximum and the minimum

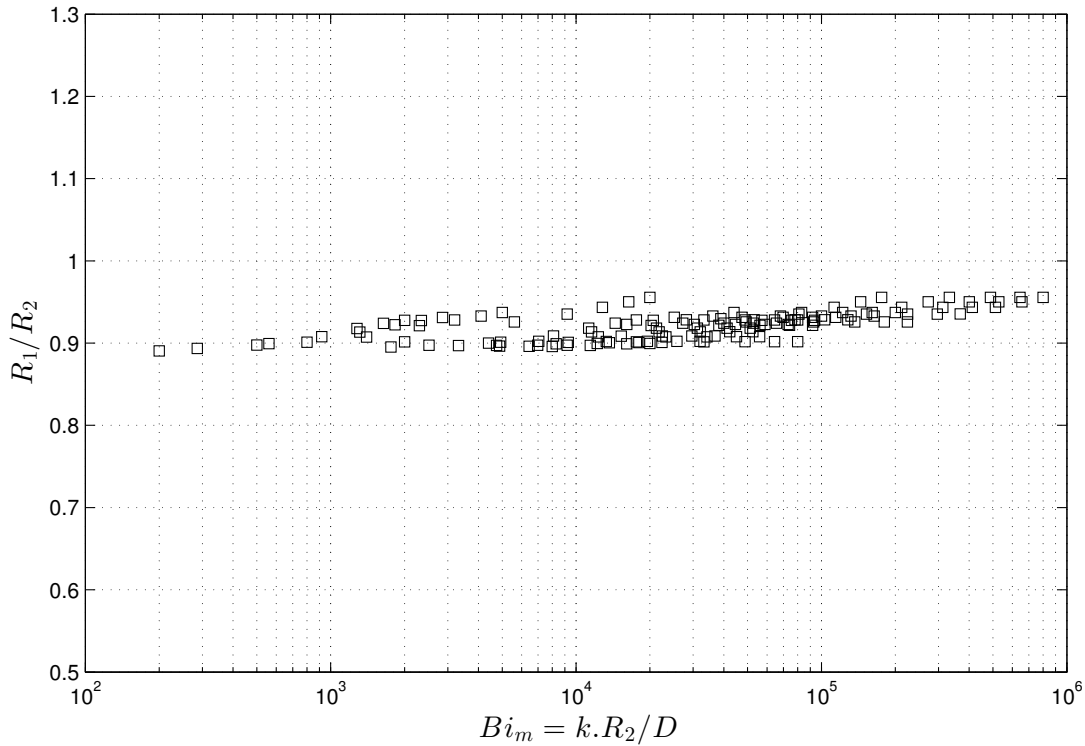


Figure 5.3 – Two-compartment mass transfer optimisation

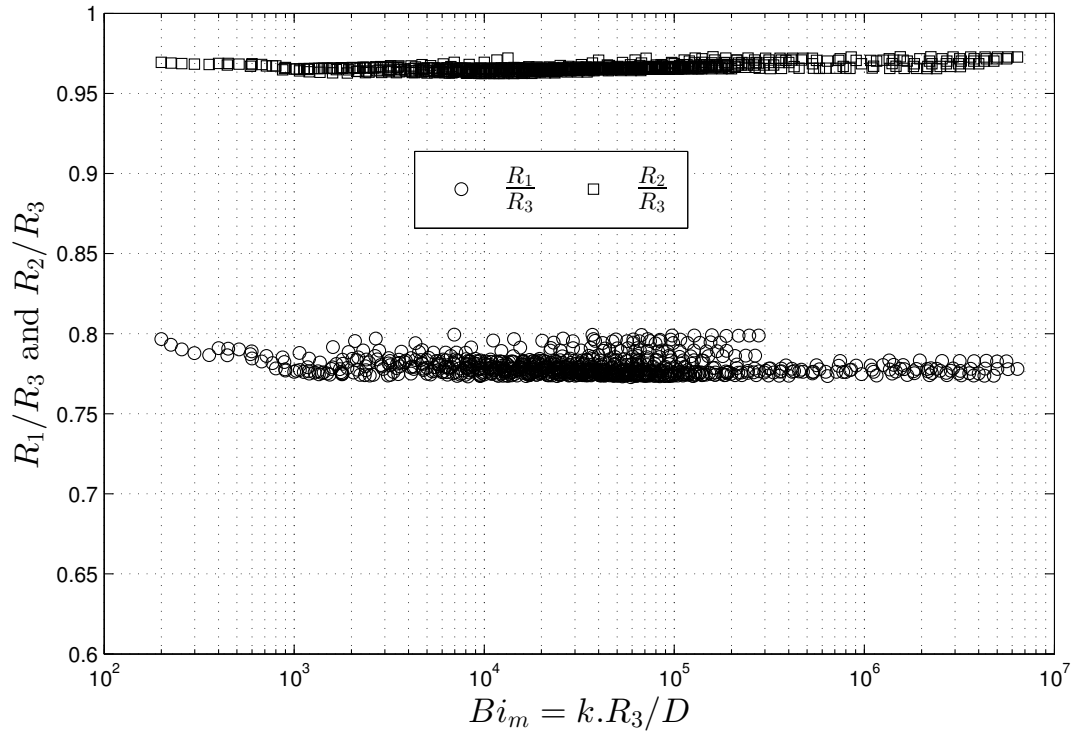


Figure 5.4 – Three-compartment mass transfer optimisation

5.6.2 Validation of heat transfers

Kinetics of heat transfer are predicted by two and three-compartment models. These predictions are then compared with finite volume solutions ($[\nabla X \bullet \nabla T \bullet \Delta a_w]$) and $[\nabla X \bullet$

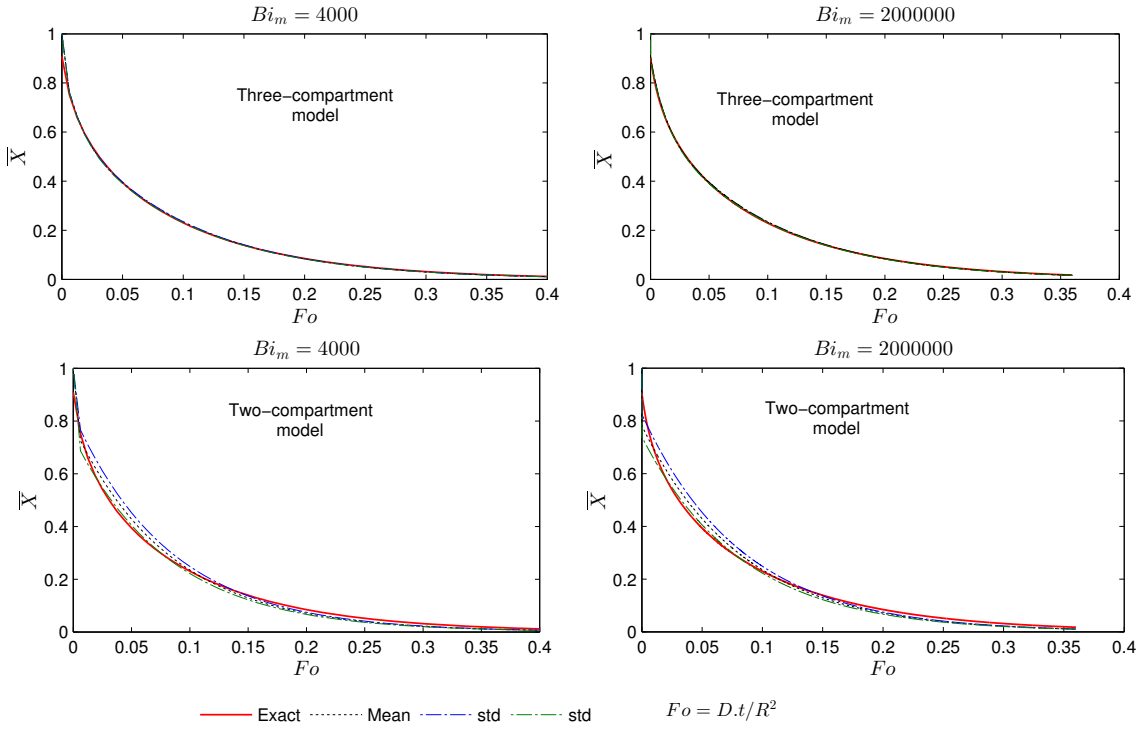


Figure 5.5 – Comparison of single mass transfer between the analytical solution from Crank ($[\nabla X \bullet 0T \bullet \Delta X]$) and simplified variants of the compartmental models ($[2X \bullet 0T \bullet \Delta X]$ and $[3X \bullet 0T \bullet \Delta X]$)

$1T \bullet \Delta a_w]$). Figure 5.6 shows the dimensionless temperature for different values of heat transfer Biot number ($Bi_{th} = hR/\lambda$) plotted against the Fourier number ($Fo = \alpha \cdot t/R^2$). Good agreement between these three solutions is observed in large range of Biot number from 0.5 to 10. The Biot numbers are obtained from representative properties of drying of granular food materials (*i.e.* $h = 5$ to $10 W/m^2/K$, $\lambda = 0.01$ to $0.1 W/m/K$, $R = 1 cm$). The percentage root-mean square error (RMSE, see equation (5.35)) between the compartmental model and the finite volume solution is close to 1 % for $Bi_{th} > 5$.

$$RMSE = \begin{cases} 100 \sqrt{\frac{1}{n} \sum_{i=1}^n \left(\frac{\bar{X}_i^{finite\ volume} - \bar{X}_i^{comp}}{\bar{X}_i^{finite\ volume}} \right)^2} \\ 100 \sqrt{\frac{1}{n} \sum_{i=1}^n \left(\frac{\bar{T}_i^{finite\ volume} - \bar{T}_i^{comp}}{\bar{T}_i^{finite\ volume}} \right)^2} \end{cases} \quad (5.35)$$

The error is almost zero for the single temperature variants (*i.e.* $[\nabla X \bullet 1T \bullet \Delta a_w]$ versus $[2X \bullet 1T \bullet \Delta a_w]$ and $[3X \bullet 1T \bullet \Delta a_w]$). This simulation shows that the optimised compartment geometries, with respect to the mass transfer, predict accurately the heat transfer related kinetics as well.

5.6.3 Validation with coupled heat and mass transfers and non-constant diffusivity

Simulation of simultaneous heat and mass transfers is obtained by considering two case studies: a single temperature sphere with non-limiting heat conduction ($[\nabla X \bullet 1T \bullet \Delta a_w]$)

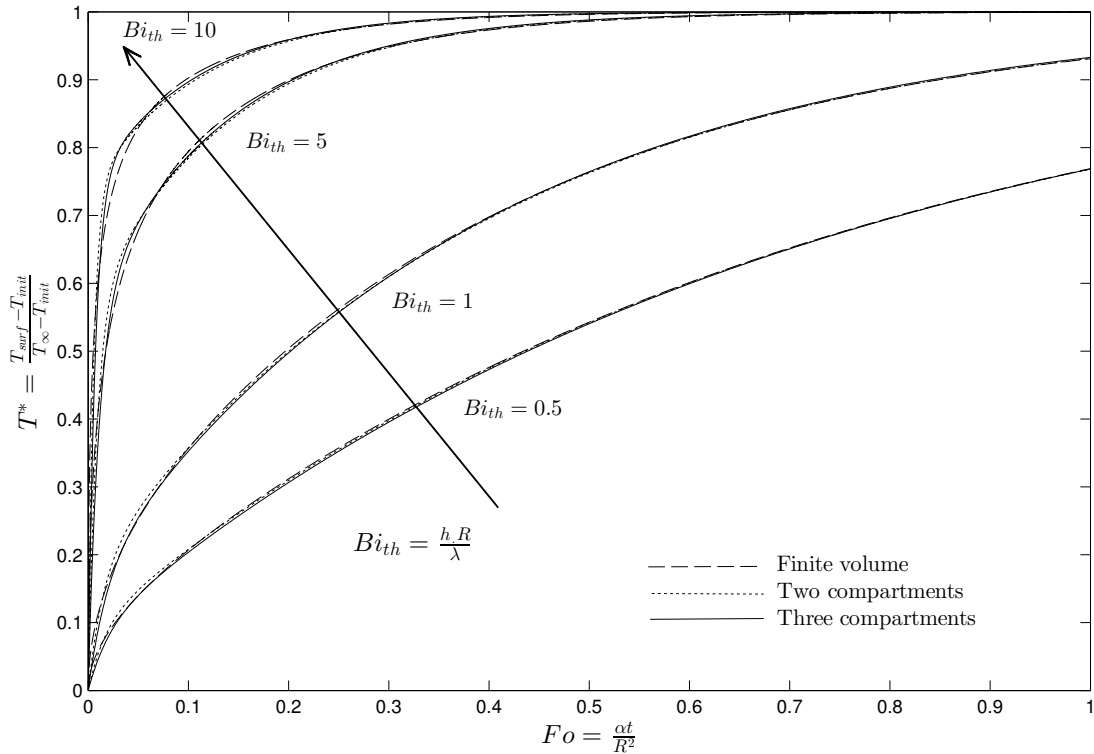


Figure 5.6 – Variation of dimensionless surface temperature with Fourier number

and a sphere with limiting heat conduction ($[\nabla X \bullet \nabla T \bullet \Delta a_w]$). In both cases, the moisture diffusivity is an increasing function of the temperature and moisture of the material [14]:

$$D = p_1 \cdot \exp(p_2 T - p_3 X) \cdot \exp\left(\frac{p_4}{T}\right) \quad (5.36)$$

Shelled corn was selected, in this simulation, as the applicative food drying material since it exhibits a typical behaviour in term of moisture diffusivity. Its moisture diffusivity equation parameters are $p_1 = 4.254e - 8$, $p_2 = 4.5e - 2$, $p_3 = 5.5$ and $p_4 = 2,513$ [14].

The following simulations are obtained using four convection coefficient values $h = 5, 10, 15$ and $25 \text{ W.m}^{-2}.\text{K}^{-1}$. The drying air conditions are considered constants: $T_\infty = 100^\circ\text{C}$ and $RH_\infty = 0.001$. The particle size is 8 mm diameter. The density and the specific heat of the dry-matter are $1,000 \text{ kg.m}^{-3}$ and $1,500 \text{ J.kg}^{-1}.\text{K}^{-1}$. In the case of limiting heat conduction, thermal conductivity is set to $0.2 \text{ W.m}^{-1}.\text{K}^{-1}$.

Figures 5.7 and 5.8 show simulations of drying kinetics and temperature evolutions using finite volume, two-compartment and three-compartment models. The mean moisture content values \bar{X} are calculated as a volume weighted sum of local moisture contents.

In the case of limiting heat conduction, the average temperature of the sphere particle \bar{T} is obtained from the average of the internal energy \bar{U} and the moisture content \bar{X} (5.37).

$$\bar{T} = \frac{\bar{U}}{\rho_{dm} (Cp_{dm} + Cp_w \bar{X})} \quad (5.37)$$

The average value of the internal energy is the weighted sum of local internal energies.

The compartmental model simulations are in fair agreement with the finite volume model solutions. While simulation using 3 compartments is very close to the finite volume simulation, the simulation using 2 compartments has slight discrepancies. Equation 5.35 is used

to estimate the error between finite volume and compartment simulations. The error is estimated by calculating the root-mean-square value (Table 5.2). Again the three-compartment model brings less errors than the two-compartment model: between 1.3 % to 6.0 % instead of 2.6 % to 17.7 %. Models with limiting heat conduction are better predicted than those with non-limiting one. Finally, the higher the convection coefficient, the larger the error is, yet always acceptable when using a three-compartment model (*e.g.* $\leq 6\%$).

Heat and mass transfer results validate the selection of the optimal compartment sizes given by the multicomponent mass transfer optimisation. Hence, the compartmental model can be used to provide a solution as coherent as the one provided by a typical differential method. The elapsed time was measured during the simulation and was shown to be reduced by a factor of nearly 100 times with the compartmental model as compared to the finite volume model. This is explained by the significant reduction of the number of differential equations in the three-compartment model: 4 to 6 ODEs, whereas the finite volume includes at least a hundred of ODEs.

Table 5.2 – Relative errors between compartmental model simulations and finite volume conduction convection model simulations

h (W.m $^{-2}$.K $^{-1}$)	Temperature error (%)		Moisture error (%)	
	2 compartments	3 compartments	2 compartments	3 compartments
5	3.2447 ^a ; 3.2288 ^b	1.2717 ^a ; 1.2797 ^b	07.337 ^a ; 06.764 ^b	3.1237 ^a ; 2.5125 ^b
10	3.1306 ^a ; 3.1119 ^b	1.4025 ^a ; 1.3958 ^b	13.708 ^a ; 12.869 ^b	4.9547 ^a ; 4.1484 ^b
15	2.9746 ^a ; 2.9224 ^b	1.4285 ^a ; 1.4059 ^b	15.885 ^a ; 14.992 ^b	5.5714 ^a ; 4.7525 ^b
25	2.7200 ^a ; 2.6249 ^b	1.4158 ^a ; 1.3574 ^b	17.755 ^a ; 16.833 ^b	6.2461 ^a ; 5.3583 ^b

^a $[\nabla X \bullet 1T \bullet \Delta a_w]$ vs $[2X \bullet 1T \bullet \Delta a_w]$ or $[3X \bullet 1T \bullet \Delta a_w]$, ^b $[\nabla X \bullet \nabla T \bullet \Delta a_w]$ vs $[2X \bullet 2T \bullet \Delta a_w]$ or $[3X \bullet 3T \bullet \Delta a_w]$

5.7 Conclusion

This work introduces a simple technique to "shrink" a complete diffusion convection model with coupled heat and mass transfers, including nonlinearities both in the product properties and boundary condition. Using a simple, yet optimised, two- or three-compartment model with specific "tuning" leads to very fast computation and equivalent prediction of drying kinetics and product temperature evolution. As an extra benefit, the meaningless exchange coefficients are deduced from the meaningful transfer coefficients. Fixing the volume ratios, once for all, by adjustment on a mass-only simple model is enough for all cases. Hence, it is straightforward to deduce the two- (or three-) compartment model equivalent to a given -finite volume- diffusion convection model. In the case of two-compartment models, the optimal volumes are 73 % and 27 % for respectively the first (central) and second compartments. In the case of three-compartment, 66 %, 23 % and 11 % are the best volumes respectively for the first, second and third compartments.

5.8 Acknowledgements

The authors wish to thank the French Agence Nationale de la Recherche (ANR) for the funding of the Ph.D. of C. Lambert, and the partners of the project COOPERE2 led by Veolia Research and Innovation, in collaboration with ProSim and ENSIACET.

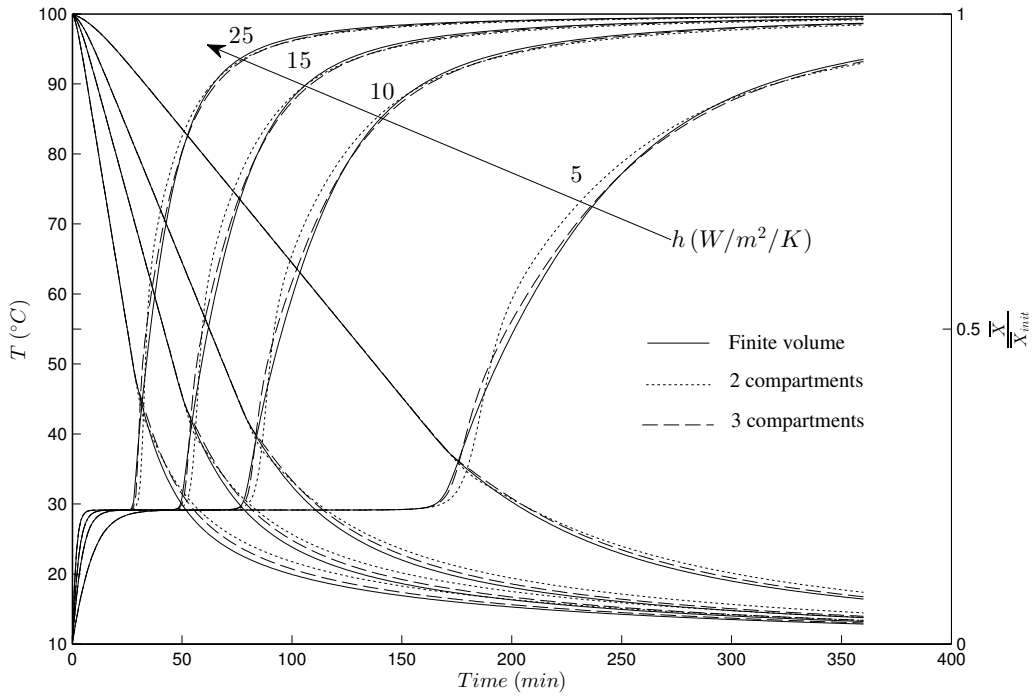


Figure 5.7 – Comparison of simulations results of the single temperature variants (non-limiting heat conduction): $[\nabla X \bullet 1T \bullet \Delta a_w]$ vs $[2X \bullet 1T \bullet \Delta a_w]$ vs $[3X \bullet 1T \bullet \Delta a_w]$

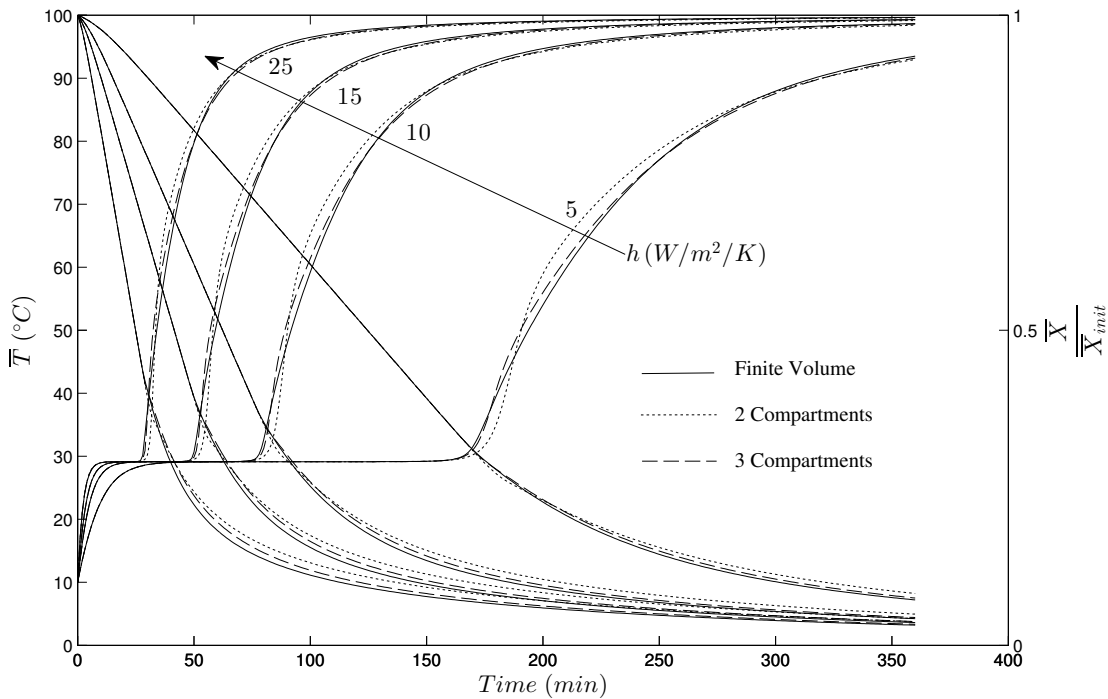


Figure 5.8 – Comparison of simulations results for limiting heat conduction variants: $[\nabla X \bullet \nabla T \bullet \Delta a_w]$ vs $[2X \bullet \nabla T \bullet \Delta a_w]$ vs $[3X \bullet \nabla T \bullet \Delta a_w]$

Bibliography

- [1] V. Puri and R. Anantheswaran, “The finite-element method in food-processing-A review,” *Journal of Food Engineering* **19**(3), pp. 247–274, 1993.

- [2] J. Crank, The mathematics of diffusion, Oxford University Press, US, 1975.
- [3] R. G. M. van der Sman, “Simple model for estimating heat and mass transfer in regular-shaped foods,” Journal of Food Engineering **60**(4), pp. 383–390, 2003.
- [4] M. Hussain, J. Kumar, M. Peglow, and E. Tsotsas, “On two compartment population balance modeling of spray fluidized bed agglomeration,” Computers and Chemical Engineering **61**, pp. 185–202, 2014.
- [5] A. Delafosse, M. Collignon, S. Calvo, F. Delvigne, M. Crine, P. Thonart, and D. Toye, “CFD-based compartment model for description of mixing in bioreactors,” Chemical Engineering Science **106**, pp. 76–85, 2014.
- [6] X. Peng, Z. Liu, J. Tan, and W. Bu, “Compartmental modeling and solving of large-scale distillation columns under variable operating conditions,” Separation and Purification Technology **98**, pp. 280–289, 2012.
- [7] K. Toyoda, “Study on intermittent drying of rough rice in a recirculation dryer,” in Sixth International Drying Symposium IDS'88, **2**, pp. 171–178, September 1988.
- [8] F. Courtois, A. Lebert, A. Duquenoy, J. Lasseran, and J. Bimbenet, “Modelling of drying in order to improve processing quality of maize,” Drying Technology **9**, pp. 927–945, 1991.
- [9] M. Abud Archila, F. Courtois, C. Bonazzi, and J. Bimbenet, “A compartmental model of thin-layer drying kinetics of rough rice,” Drying Technology **18**(7), pp. 1389–1414, 2000.
- [10] T. Chilton and A. Colburn, “Mass transfer (absorption) coefficients prediction from data on heat transfer and fluid friction,” Industrial and Engineering Chemistry **26**, pp. 1183–1187, 1934.
- [11] A. Hallstrom, “Alternating boundary conditions in drying,” Chemical Engineering Science **41**, pp. 2225–2234, 1986.
- [12] M. Markowski, “Air drying of vegetables: Evaluation of mass transfer coefficient,” Journal of Food Engineering **34**, pp. 55–62, 1997.
- [13] J. Lagarias, J. Reeds, M. Wright, and P. Wright, “Convergence properties of the Nelder-Mead Simplex method in low dimensions,” SIAM Journal of Optimization **9**(1), pp. 112–147, 1998.
- [14] N. Zogzas, Z. Maroulis, and D. Marinos-kouris, “Moisture diffusivity data compilation in foodstuffs,” Drying Technology **14**(10), p. 2225–2253, 1996.

Chapitre 6

Simulation and data reconciliation of a food process using a generic simulator (ProSimPlus[®]) : case of a sugar beet factory

Résumé

Pour faire face aux coûts des énergies fossiles ainsi qu'aux réglementations européennes récentes, le développement d'outils assistés par ordinateur est d'une grande aide pour optimiser la consommation énergétique des usines agroalimentaires. Pour ce faire, la première étape consiste en la modélisation de l'usine avec des simulateurs de procédés génériques tels que ceux développés dans le domaine du génie chimique. Les verrous scientifiques sont l'estimation des propriétés thermodynamiques de produits alimentaires et la modélisation de l'ensemble des opérations unitaires du procédé. Dans cette étude, une méthodologie générique de modélisation des réseaux d'opérations unitaires pour *in fine* combiner les analyses de pinçement et d'exergie dans le logiciel ProSimPlus[®] est proposée. La méthode est appliquée à une sucrerie de betteraves. Le modèle développé permet la simulation de l'usine, avec un écart entre les données simulées et industrielles de l'ordre de grandeur des incertitudes de mesure.

Mots-clés simulation de procédés alimentaires, simulateur de procédés chimiques, générique.

Cet article est à soumettre à *Computer and Chemical Engineering Journal*¹.

6.1 Introduction

In Europe, energy efficiency directives require, for large companies, to carry out frequent energy audits [1] and asks for a 20 % decrease of energy consumption and greenhouse gas emission and a 20 % increase of renewable energy use by 2030 [2]. Considering also the actual economic, energy and environmental context, the food industry may be under pressure to

1. C. Lambert, B. Laulan, M. Decloux, H. Romdhana, and F. Courtois, "Simulation and data reconciliation of a food process using a generic simulator (ProSimPlus) : case of a sugar beet factory", To submit to Computer and Chemical Engineering Journal, p. 23, 2015

meet new environmental regulations, improve energy efficiency and increase production rate. Therefore, improving energy efficiency in such industry is a major challenge, both economic and environmental.

Chemical engineering benefits from computer aided tools (*e.g.* ProSimPlus[®], Aspen Plus[®], Aspen HYSIS[®], PRO/II[®], gPROMS[®]) to simulate their whole industry plant. These simulators are composed of a) a calculation database of thermophysical and equilibrium properties using thermodynamic models, and b) a database of unit operations. They are dedicated to gas and liquid mixtures of pure components. Specific methods, such as Pinch and exergy methods, can be used systematically to improve energy consumption of the factories [3]. Pinch and exergy analyses tools are also available in some chemical engineering software (*e.g.* Pinch and Exergy modules in ProSimPlus[®], Aspen Energy Analyzer[®] and ExerCom[®] in Aspen Plus[®] and PRO/II[®]). The ExerCom[®] [4] plug-type software allows calculating exergy of material streams. In addition of the exergy calculation, the ProSimPlus[®] exergy module allows for the estimation of exergy destruction and exergy efficiency [5]. Pinch method may be applied to find the minimum potential consumption of utilities and the maximum potential saving of thermal streams. Exergy analysis may be applied to locate the inefficiencies in the process.

Due to the complex structure of food products, food industry can barely use such powerful tools to simulate their specific processes and optimize their energy consumption. Indeed, many food products are mixtures of gas, liquids and solid components for which almost no available equations can predict their properties. Food process simulation software are generally specific to one unit operation. For instance, for the simulation of drying, one can cite Symprosis[®] [6], DryPAK[®] [7], DrySel[®] [8], Dryer3000[®], and SP2P[®] [9]. The developed methods for the chemical engineering have been recently applied to the food industry. One can cite works in the fields of dairy industry (*i.e.* milk concentration by evaporation workshop [10, 11]) and sugar industry (*e.g.* juice concentration by evaporation and ethanol generation workshops [12, 13, 14]). This workshops are only composed of non-food specific unit operations and of liquid-vapor mixtures for which thermophysical properties can be estimated with classic thermodynamic models (*e.g.* UNIQUAC [15]). Moreover, some commercial software (*e.g.* Sugar[®] [16]) or models developed in laboratories (*e.g.* using the EES[®] [17], QBasic[®] [18, 19], Matlab[®] [20] languages) allow for the whole sugar factory simulation and sometimes also for the estimation of the irreversibility production in all unit operations of this process. A software dedicated to the petrochemical processes, Aspen Plus[®], has also been used to perform the simulation of all the unit operations of a sugar cane factory and its exergy analysis [21]. The unit operations specific to the sugar process are simulated as global heat and mass balances, in the same way than in the models developed in laboratories. This method to simulate food specific unit operation, do not allow for a detailed representation of the irreversibility production [5].

Process simulation combined with Pinch and exergy analysis may be an interesting and powerful approach allowing for the systematic improvement of food process. Before any energy optimizations, a model of the factory is required. This model should be performed in 3 steps (see figure 6.1):

- 1. perform a detailed flowsheet of the factory and gather all required data.**
The process flowsheet of the factory includes all existing unit operations and the heat exchanger network. Required data include flow-rate, composition, temperature and pressure of the streams and also operating parameters of each unit operation.
- 2. list constituents and find the thermodynamic model to predict the thermophysical properties of the mixtures.** A number of thermophysical properties are

required for each constituent (*e.g.* molecular weight, liquid and gas specific heat, vaporization enthalpy, liquid and gas thermal conductivity, standard state Gibbs energy). A thermodynamic model to estimate the thermophysical properties of the mixtures is then required. If they are not validated, thermophysical properties of the constituents or the thermodynamic model itself have to be modified.

3. **model the unit operation network of the factory and validate the simulation results by comparing them with industrial data.** If the factory model is not validated, data reconciliation is performed by checking the validity of the assumptions and the consistency of the supplied industrial data (see figure 6.1). In addition, the required level of details of the model depends on the modelling purpose as it is well described by [5]. For instance, the level of details needed to compute the mass balance of a process is far lower than the one required for exergy analysis. In order to perform an exergy analysis, a unit operation module should only simulate one energy change (*i.e.* pressure, temperature and chemical composition). To do so, each unit operation can be splitted into a combination of several generic and basic modules to distinguish the thermodynamic irreversibilities of the process. Thus, heat exchanger, expansion valve or turbine, compressor and mixer are introduced in the models.

The scientific bottlenecks to model a food factory are the second and the third steps of this methodology (see figure 6.1). Models of food specific unit operations are often not available in chemical engineering software. To overcome this, one may use a combination of simple and generic unit operation modules and control loop module forcing certain output (*e.g.* composition) to model the phenomena. However, with this modelling methodology, the developed model may not be "predictive" and could hinder the scaling up of the process, but still allows energy optimization, the main purpose of the present study.

In this work, the present methodology has been applied with success to the modelling of a sugar beet factory in order to perform a Pinch and exergy analysis, in the ProSimPlus® software. The ProSimPlus® software was chosen for two reasons. First, it allows for the estimation of the thermodynamic properties, the calculation of heat and mass balance and the selection of several types of plant equipment's (*e.g.* heat exchangers, evaporators *etc.*). Second, this software involves energy post-processing tools (*i.e.* Pinch and Exergy modules). In this study, a brief description of the sugar beet process is given. Afterwards, we introduce the method to model all the unit operations (specific and non-specific) of a sugar beet process using the ProSimPlus® software. The factory model is then validated. To do so, mass and energy balances and industrial data reconciliation are performed.

6.2 Sugar beet process description

For confidentiality purposes, the name and precise characteristics of the studied French sugar beet factory are not disclosed in this paper. The studied factory currently consumes about 20,000 t of sugar beet per day and more than 3 GWh/d. It produces about 2,500 t/d of white sugar crystals, 1,300 t/d of low purity² syrup (about 80 %), 4200 t/d of pressed pulps (about 25 % of dry matter) and 770 t/d of sugar limes. The production is continuous during about 100 days a year, 7 d/7 and 24 h/d. About 360 MWh/d of electrical power are produced and totally consumed within the factory. Sugar processing involves several chemical engineering operations such as cleaning-slicing, sugar extraction, juice clarification, juice concentration by evaporation, sugar crystallization, and drying-storage-packaging. A

2. Purity: percentage of sucrose in the soluble dry matter

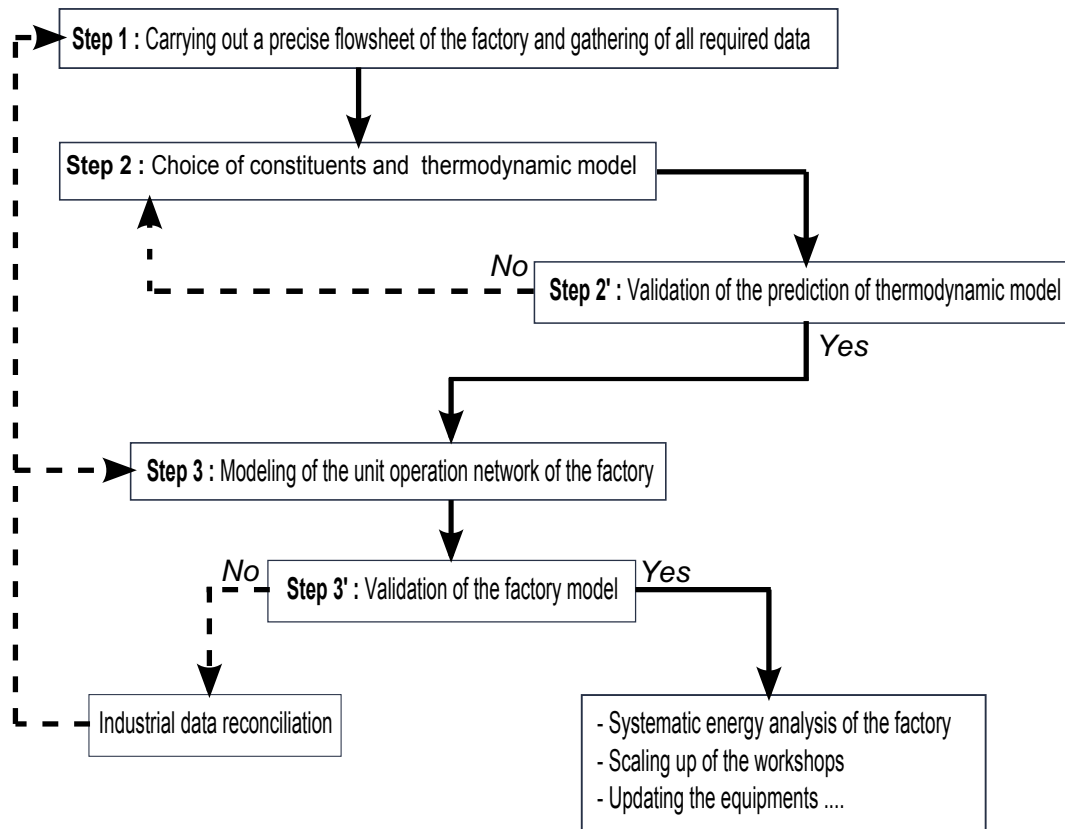


Figure 6.1 – Diagram of the modelling steps of a food factory using a chemical engineering software

general flowsheet of the sugar beet process is given in figure 6.2. The sugar beet process is well known and described in a lot of books. One can cite for instance "Sugar Technology, Beet and Cane Sugar Manufacture" [22]. Workshops represented by dotted frame in figure 6.2 are modeled in ProSimPlus® and are briefly described below (*i.e.* sugar extraction, juice clarification, concentration by evaporation and crystallization workshops). Each process step is briefly described below.

Sugar extraction

Sucrose is extracted from *cossettes*³ by contacting with hot water composed of condensates and water issued from the press (see below). Several solutes diffuse from the *cossettes* to the juice:

- "sugar": sucrose;
- "non-sugars": mineral matters, mixed-salts, organic and non-organic matter.

Preheating of the *cossettes* allows for the thermal denaturation of the cell membranes and allows for the solute migration. The *green juice* and pulps (*i.e.* cellular residues of the *cossettes*) are the outlet of the diffuser. The *green juice* is recycled in this workshop for the *cossettes* heating (using scalder and prescalder) and is then purified in the next workshop. Pulps are pressed and are finally dried [22].

Juice clarification

The *green juice* is treated twice with lime and carbon dioxide gas and is finally filtered. The

3. Cossettes: small strips of sugar beet

addition of lime to the heated *green juice* induces a pH increase allowing for the precipitation and the coagulation of the colloids, for the precipitation of anions and for the degradation of invert sugar and raffinose. The lime-treated juice is saturated with carbon dioxide gas to precipitate lime as calcium carbonate (carbonation reaction) and allows settling down all precipitates. Carbonation sludge are composed of all the removed precipitates during the filtration step [22].

Concentration by evaporation

Evaporation increases the dry matter concentration in the juice (Brix⁴ value from 15 % to 70 %) by removing water and allows producing nearly all the required hot streams for the heat exchangers of all the workshops (steams and condensates). A multiple-effect evaporator is classically used in this workshop (5 to 7 effects). Steam used for the heating of the first effect is produced from pressurized steam. In the studied factory, pressurized steam is a) expanded into a turbine to produce electrical power, b) supplies a turbo-compressor to re-compress steam produced at the first effect, and c) is expended into a pressure valve. All steams are condensed in each effect, and finally flashed using flash-tanks [22].

Crystallization

Crystallization is the only one batch unit operation of the sugar beet process. Crystallization and centrifugation steps are repeated twice in this factory. Sugar crystals, produced in the second crystallization step, are dissolved into thick juice in a vacuum boiler. The obtained mixture is vacuum boiled and supersaturated. Sugar crystals are then added to the mixture to initiate the sugar crystallization. Crystals are then separated from the liquid using a centrifuge. The obtained "poor-syrup" liquid supplies the second strike of crystallization. During centrifugation, crystals are washed out with condensates to remove the thin layer of liquid around them, and the obtained juice is recycled. The white sugar crystals are further dried in the drying-storage-packaging workshop [22].

6.3 Sugar beet process modelling

6.3.1 Constituents and thermodynamic model

Thermodynamic properties are calculated using the Simulis Thermodynamics® software. According to the above description of the sugar beet process, the following constituents are required for the streams modelling:

- sucrose, "non-sugars" and water (for all workshops);
- cellular residues (specific to the sugar extraction workshop);
- dinitrogen, dioxygen, carbon dioxide, calcium oxide, calcium carbonate (specific to the juice clarification workshop).

In our analysis, we used the UNIFAC-Larsen thermodynamic model for its predictive capabilities. All the retained constituents are the one present in the 2013 standard package of the Simulis Thermodynamics® database.

Using this model, the UNIFAC-Larsen decomposition of each constituent is required. However, the decomposition of calcium oxide and calcium carbonate are not available in the database, the water molecular decomposition is added for these constituents. We checked

4. Brix: percentage of soluble dry matter in the juice

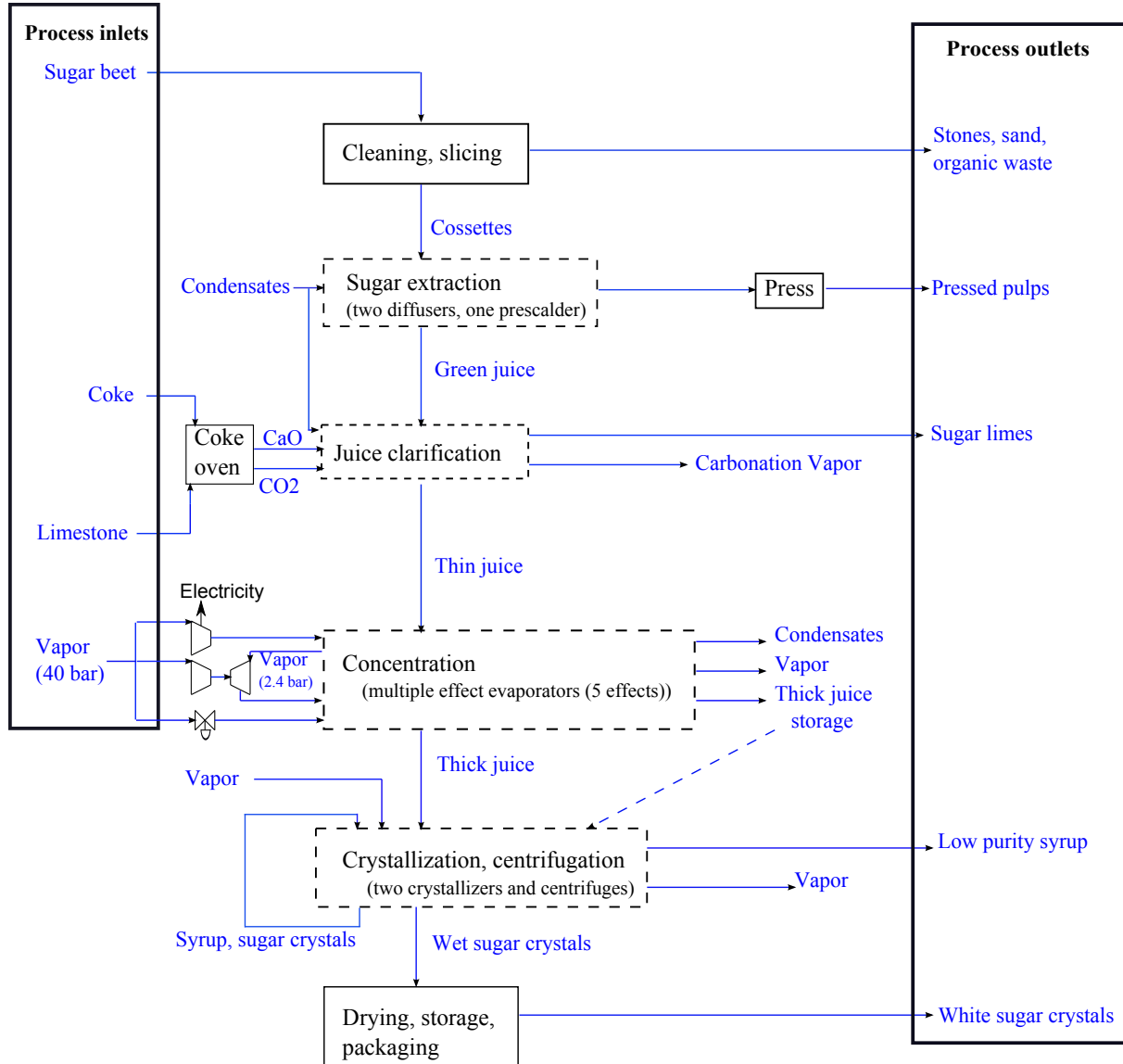


Figure 6.2 – Sugar beet process diagram

that thermal properties (*i.e.* heat capacity and boiling-point elevation) are well predicted by comparing prediction of this thermodynamic model with the one calculated using [23] correlations. For a juice purity¹ above 70 % and a juice Brix³ range of 15 - 90 %, boiling-point elevation is under-estimated by a maximum of 1 °C, and for a juice Brix³ above 90 °C, boiling-point elevation is over-estimated by a maximum of 3 °C. These deviations are within the range of error bars of industrial data.

As explained in the previous section, "non-sugars" are composed of a lot of different molecules and their precise relative composition is unknown. Using [23] correlation, one may consider that assimilating "non-sugars" to "sugar" affects very little the thermal properties of the juices (*i.e.* heat capacity and boiling-point elevation) with respect to differentiating "non-sugars" from "sugar". Deviations below 5 %, corresponding to an absolute error below 2.5 °C for the boiling-point elevation, are observed for a juice Brix³ range of 15 - 95 % and a juice purity¹ above 70 %. Hence, in our analysis, "non-sugars" were assumed to behave as sucrose but are considered it as a separate constituent.

Cellular residues are at solid state. Only liquid-liquid and vapor-liquid heat exchangers

exist in this workshop, except for the scalder and prescalder. Hence, precise modelling of cellular residues is pointless for a thermal representation of the factory. In our analysis, cellular residues are assumed to behave as cellulose which is one of its major constituents. We also forced its physical state to be liquid by modifying the correlation used for the vaporization pressure.

Finally, in the crystallization workshop, sugar crystals are assimilated to sucrose without distinction of its physical state (dissolved or solid) to simplify the model. In order to perform industrial data reconciliation in this workshop, sugar crystals are separated from dissolved one after evaporation in the vacuum-pan boiler.

6.3.2 Modelling of the sugar beet process

General considerations

Sugar extraction, juice clarification, concentration by evaporation and crystallization steps are modeled in the ProSimPlus® chemical engineering software (version 3.5.3.1). The organization of the modules is adapted to represent the factory flowsheet and each workshop is modeled in a separate file to facilitate its convergence.

Usually, input variables of the inlet streams (*i.e.* pressure, temperature, composition) and operating parameters of unit operation modules (*e.g.* splitting ratio of a "stream splitter" module) are required to simulate a process with a chemical engineering software: output variables of outlet streams of the unit operation modules are calculated (*i.e.* pressure, temperature, composition). However, the ProSimPlus® software is not specific to the sugar beet process. Hence unit operations specific to this process are modeled using a combination of generic and basic unit operation modules and "constraints and recycles" modules. Output variables (pressure, temperature, composition) are forced by "constraints and recycles" modules which are illustrated as "SPEC" in the screenshots of process simulated with ProSimPlus® (see figures 6.3 to 6.7). Moreover, the modelling methodology described in the introduction is used to model the sugar beet process. Indeed, each unit operation is modeled as a combination of several modules to distinguish the thermodynamic irreversibilities of the process.

General hypotheses

The assumptions considered in the model of the sugar beet process are:

- in all workshops: negligible pressure and thermal losses within the pipes and heat exchangers;
- in the juice clarification workshop: dioxygen, dinitrogen, and carbon dioxide are not dissolved in the juice during both carbonation reactions;
- in the concentration by evaporation and crystallization workshops:
 - no thermal losses within the evaporators or vacuum pan boilers;
 - produced steam is modeled as pure water. This steam is overheated to respect the boiling elevation point.

No pressure and thermal losses within pipes and heat exchangers and no thermal losses within the evaporators are common assumptions of a first step of a factory modelling due to the lack of available industrial data. Besides, assuming that a) produced steams are composed of pure water and that b) dioxygen, dinitrogen and carbon dioxide are not dissolved in the juice during both carbonation reactions, is questionable. First, solute concentrations in the

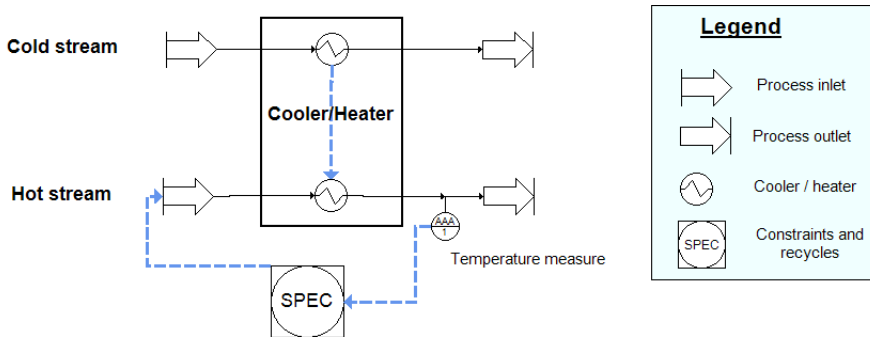


Figure 6.3 – Flowsheet of the heat exchanger model (screenshot from the ProSimPlus[®] software)

steam and concentration of dissolved solutes in the juices are hardly ever measured in sugar beet factories. Second, the simulations show that their concentrations are negligible with respect to other constituent concentrations in the steam and juice. Hence, considering these assumptions allows for a quite precise calculation of heat and mass transfers.

Methodology to model heat exchangers

Input mass flow-rate of the hot stream is unknown for all heat exchangers, except for the prescalder. To estimate this input variable, a specific model is used, including a combination of two "cooler/heater" and a "constraints and recycles" modules and an "information stream" (see figure 6.3):

- "heater/cooler" modules allow modelling of the heating or cooling of respectively cold and hot streams. Outlet temperature of the cold and hot streams are fixed as an operating parameter. Power required for the heating of the cold streams is provided by the cooling of the hot streams via an "information stream";
- a "constraints and recycles" module allows calculating of the hot streams mass flow-rate (input/output variable) to respect its fixed output temperature.

Sugar extraction

Diffusion, which is a unit operation specific to the sugar beet process, is modeled using a combination of a "mixer" and a "component splitter" modules (see below). "Sugar" and "non-sugars" losses within wet pulps (output variables) are fixed by a "constraints and recycles" module modifying the recovery ratio of each constituent in the "component splitter" (operating parameters). An "information stream handler" module allows calculating of the mass flow-rate of the recycled *green juice* (output variable) to respect the fixed volume withdrawal⁵ (operating parameter) (see figure 6.4).

Press modules are available in the ProSimPlus[®] database (*i.e.* "belt-filter" and "plate-frame filter" modules). Cake moisture content before filtering and solid fraction in the filtered juice are the required operating parameters of these modules. The cake constituents are considered as solids by the thermodynamic model. However, cellular residues are only considered in the liquid phase in our model. Hence, the press is modeled using a combination of a "component splitter" and a "constraints and recycles" modules (*i.e.* generic and basic unit operation modules). "Sugar" and "non-sugars" losses (output variables) in the pressed

5. Volume withdrawal: ratio of the volume flow-rate of the outlet green juice and cossettes

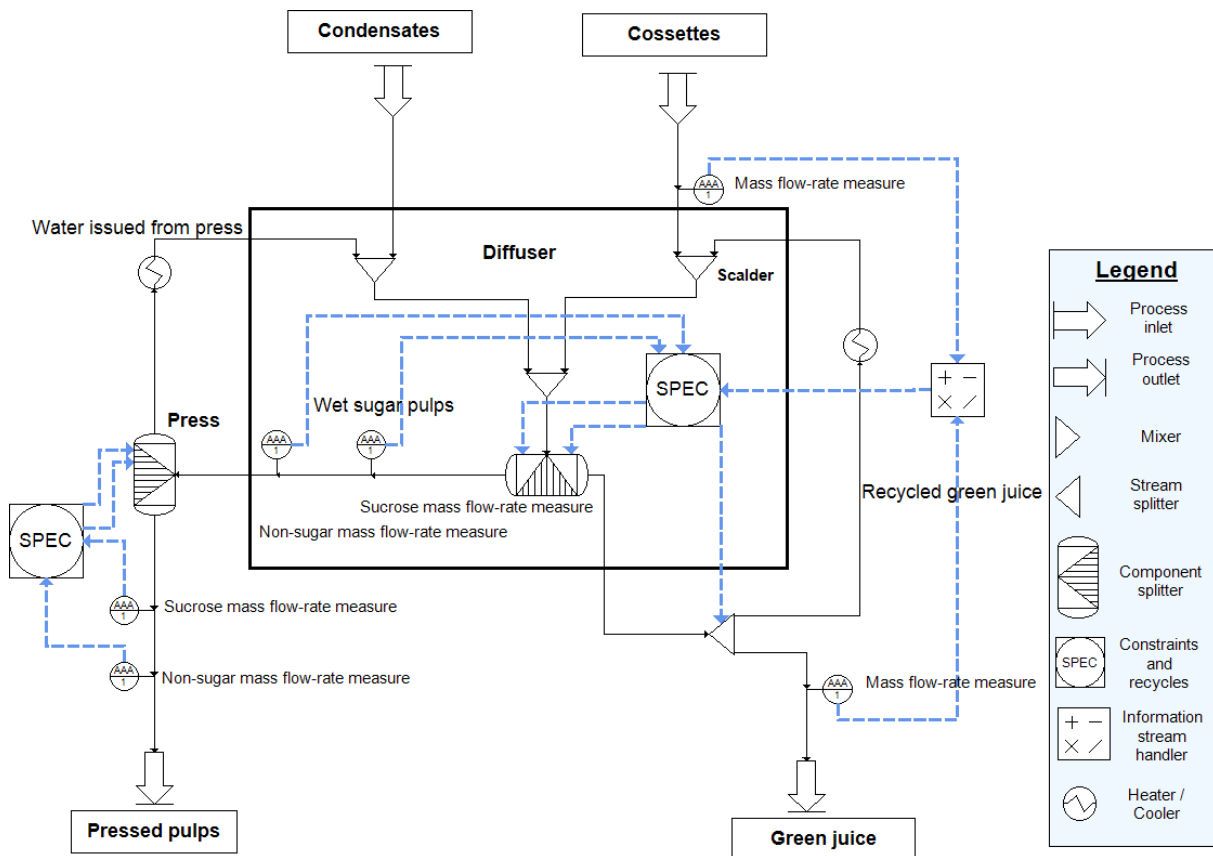


Figure 6.4 – Flowsheet of the sugar extraction workshop model (screenshot from the ProSimPlus® software)

pulps are fixed by a "constraints and recycles" module modifying the splitting ratio of the constituents (operating parameters) (see figure 6.4).

The prescalder (*i.e.* a *cossettes-green juice* heat exchanger) is modeled by a "generalized heat exchanger" module, in which output temperature of the *green juice* is fixed as an operating parameter.

Juice clarification

To simplify the modelling of the clarification workshop, four reactions are neglected: reaction of precipitation and coagulation of the colloids, reaction of precipitation of anions and reaction of degradation of invert sugar and raffinose. Carbonation reactions are modeled using a combination of three modules (*i.e.* a "reaction tank", a "component splitter" and a "constraints and recycles" modules), see below and the left panel of figure 6.5. The reactor is composed of two inlet and two outlet streams. Saturated gas and limed juice enter the reactor in which reaction 6.1 is modeled and reaction enthalpy is fixed as an operating parameter. Reaction enthalpy is an available data in the literature [22]. Gas and liquid are separated at the outlet of the reactor. A "component splitter" module allows separating the dissolved molecules in the *cloudy juice* (dioxygen, dinitrogen, carbon dioxide) from the other ones. The dissolved molecules are then mixed in the gas at the outlet of the reactor. The required mass flow-rate of carbon dioxide (an input variable) is calculated using a "constraints and recycles" module to respect a fixed mass flow-rate of calcium oxide in the carbonation juice (an output variable).

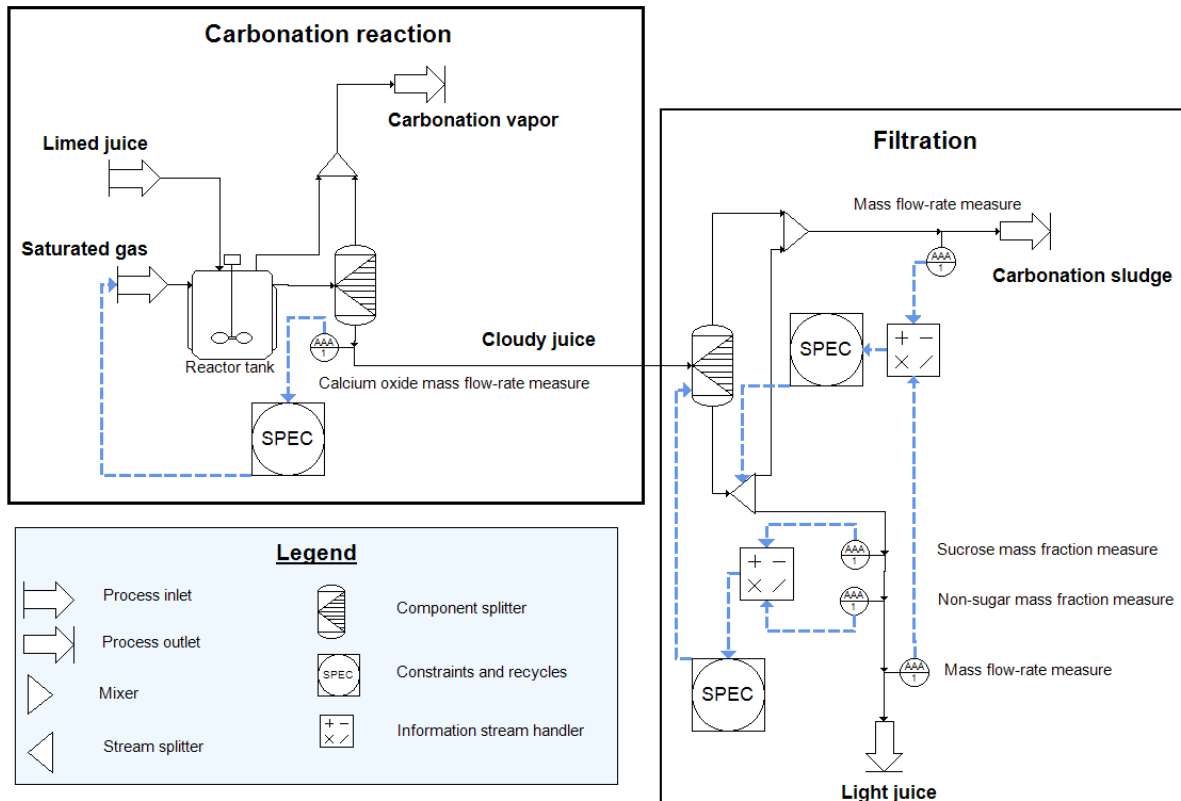


Figure 6.5 – Flowsheet of the carbonatation and filtration unit operations (screenshot from the ProSimPlus® software)



Impurity removal by filtration is modeled with a combination of a "component splitter", two "constraints and recycles", a "stream splitter", a "mixer" and two "information stream handler" modules (see below). All calcium carbonate and a part of the non-sugar are washed out with the carbonation sludge. The obtained liquid is divided into two streams: one represents a part of the carbonation sludge and the other the light juice. The two parts of the carbonation sludge are then mixed. Splitting ratio of each constituent of "component splitter" and splitting ratios of the "stream splitter" are calculated using "information stream handlers" and "constraints and recycles" modules (see below and the right panel of figure 6.5). On the one hand, splitting ratios of each constituent (an operating parameter) are adjusted to respect a fixed purity¹ of the light juice (an output variable). On the other hand, splitting ratios of the "stream splitter" (an operating parameter) are calculated to respect a fixed efficiency for the filters (an output variable) (*i.e.* ratio of mass flow-rate of the light juice and carbonation sludge).

Concentration by evaporation

All unit operations existing in the concentration by evaporation step are non specific to the sugar beet process, yet classical in chemical engineering. Specific modules of evaporation or turbo-compression are available in the ProSimPlus® software. However each unit operation of this workshop has been splitted into a combination of several modules to identify the thermodynamic irreversibilities of the process. Model description of each unit operation

existing in this workshop is given below.

Each single effect evaporator is modeled as a combination of ten modules (see figure 6.6a):

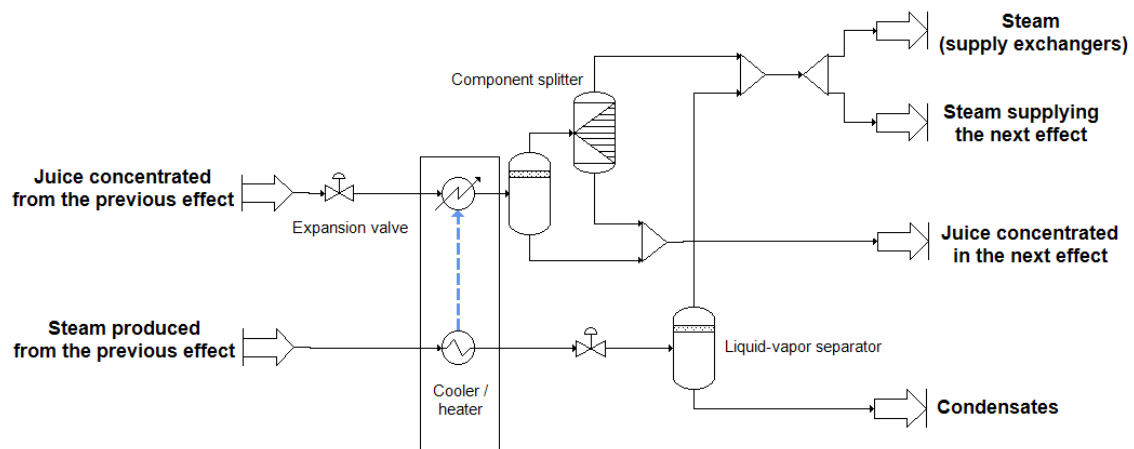
- an "expansion valve" module allows decreasing of the pressure of the entering juice (except for the first effect). Part of the water contained in the juice flash-evaporates;
- an exchanger (*i.e.* a "cooler/heater" module) simulates the heating of the juice. The power required for the heating of the juice is provided by the condensation of the steam (via an "information stream"), while the mass flow-rate and the steam temperature are known.;
- a "liquid-vapor separator" module simulates the separation of the vapor and liquid phases. Vapor phase contains "sugar" and "non-sugars" at infinite dilution concentration. These constituents are mixed in the liquid phase using a combination of a "component splitter" and a "mixer" modules. The mixture is both the concentrate of the current effect and the liquid to concentrate in the next effect;
- steam supplying the evaporator is condensed in a flash-tank, which is modeled with a combination of an "expansion valve" and a "liquid-vapor separator" modules. The vapor flash-produced is mixed with the purified steam. This mixture is divided into two streams: the first stream supplies the next single effect. The second streams is modeled as a process outlet. This outlet steam is considered as a hot utility for all heat-exchangers of all the workshops and its mass flow-rate is calculated as the sum of the mass flow-rate required for the exchangers (see sub-section 6.3.2).

As explained in the section 6.2 the steam supplying the first effect, is produced from high pressured steam. The latter is a) expanded into a turbine to produce electrical power, b) supplied to a turbo-compressor to re-compress first-effect steam, and c) expanded using an expansion valve (see figure 6.6b). The turbo-compressor itself is modeled as a combination of a "turbine", a "compressor", and a "constraints and recycles" modules and two "information streams" (see below). The mass flow-rate of high pressured steam supplying the turbine (input variable) is calculated using a "constraints and recycles" module to respect the output pressure of the re-compressed steam (output variable). The power required for the steam compression is provided by the steam expansion via the "information stream". Moreover, the mass flow-rate of high pressured steam supplying the other turbine is manually adjusted to respect the required production of electrical power. Furthermore, the mass flow-rate of the compressed first-effect steam and total mass flow-rate of high pressured steam are manually adjusted to respect a fixed Brix³ of the concentrated liquid and to minimize the steam in excess from the fifth effect.

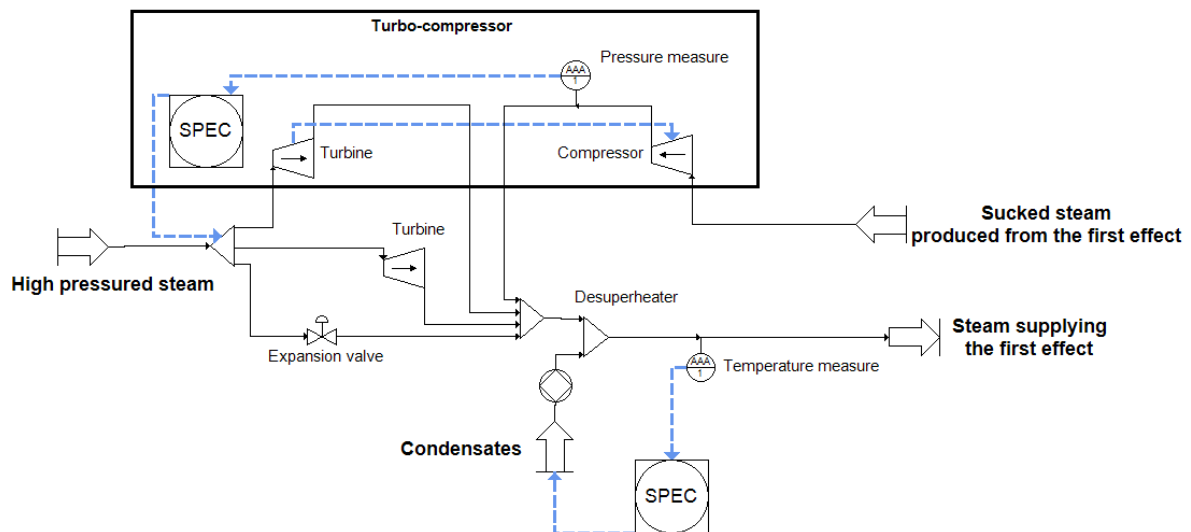
Crystallization

Vacuum pan boiling in the crystallization step is a classical unit operation available in chemical engineering. However, it has been modeled as a combination of seven modules to distinguish the thermodynamic irreversibilities of the process (see figure 6.7):

- an "expansion valve" module allows decreasing of the pressure of the entering juice. A part of the water contained in the juice flash-evaporates;
- an exchanger (*i.e.* a "cooler/heater" module) simulates the heating of the juice. The power required for the heating of the juice is provided by the condensation of the steam (via an "information stream");



(a) Flowsheet of the model of a single effect evaporator



(b) Flowsheet of the model of production of the steam supplying the first effect

Figure 6.6 – Flowsheets of the model of concentration by evaporation workshop (screenshot from the ProSimPlus® software)

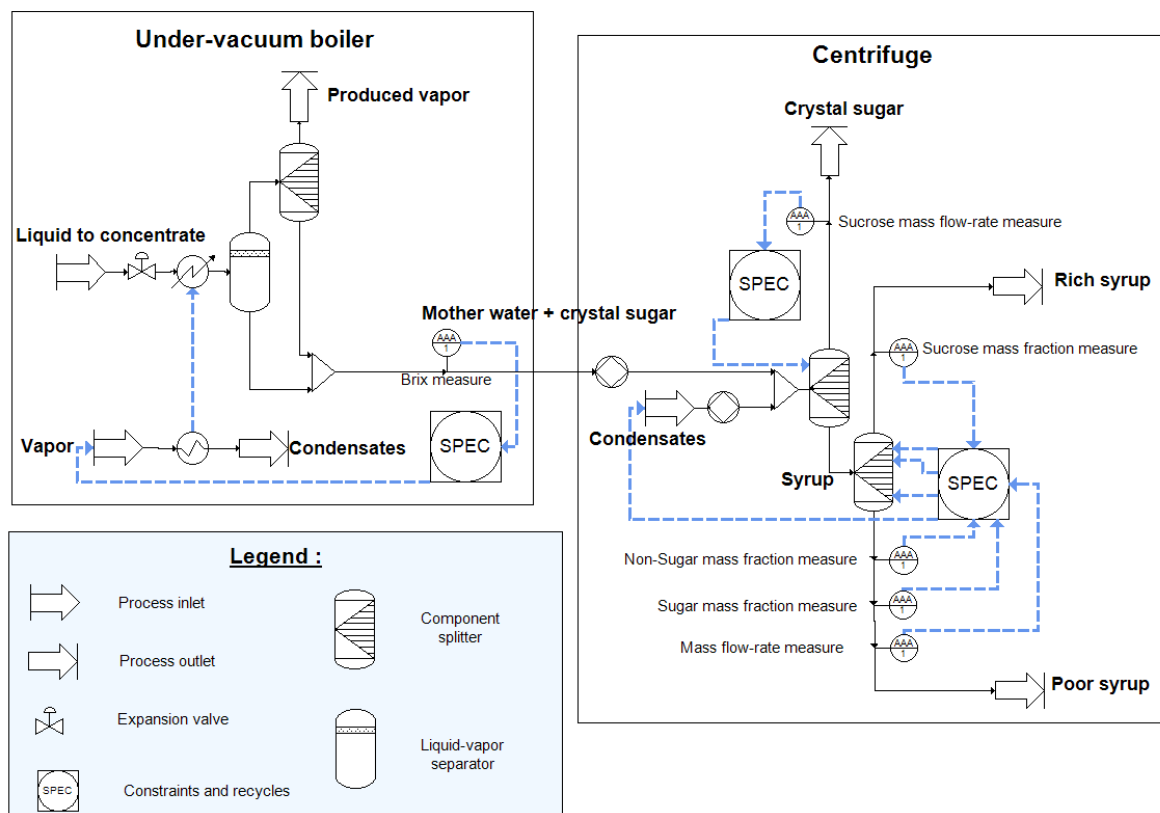


Figure 6.7 – Flowsheet of the model of under-vacuum boiler and centrifuge (screenshot from the ProSimPlus® software)

- a "liquid-vapor separator" simulates the separation of the vapor and liquid phases. Vapor phase contains "sugar" and "non-sugars" at infinite dilution concentration. These constituents are mixed to the liquid phase using a combination of a "component splitter" and a "mixer" modules.
- mass flow-rate of the steam supplying the under-vacuum boiler (input variable) is calculated, using a "constraints and recycles" module, to respect a fixed Brix³ value of the mother liquor and sugar crystal mixture (output variable).

A centrifuge module is available in the ProSimPlus® database (*i.e.* "clarifier" module). Solid fractions in the sludge and in the outlet liquid are the required operating parameters of this module. The sludge constituents have to be considered as solids by the thermodynamic model. However, sugar crystals are considered in the liquid phase in our model. Hence, a centrifuge is modeled by a combination of generic and basic unit operation modules. A combination of two "component splitter" modules is used for its simulation (see figure 6.7): The first "component splitter" module allows separating sugar crystals from syrups (mixture of rich and poor syrups) and the second one separating the different syrups. The sucrose splitting ratio of the first "component splitter" is calculated using a "constraints and recycles" module to respect mass flow-rate of sugar crystals. A "constraints and recycles" module calculates a) the splitting ratio of each constituent of the second "component splitter" module (operating parameters) and b) the mass flow-rate of condensates washing sugar crystals (input variable) in order to respect composition and mass flow-rate of the *rich* and *poor syrups* (output variables).

6.4 Results and discussion

Factory models are usually assumed to be valid if simulation data are within industrial error bars. Fluctuation of the sugar beet composition affects all compositions, temperatures and mass flow-rates of all the other streams of the process. Hence, data supplied are the mean of measures once the production is stabilized. Besides, some of the supplied data are measured daily and others are calculated by performing mass balances within each workshop (case of non-measurable data). Indeed, mass flow-rate, temperature and composition of juices (at liquid state only) and pressure, temperature and mass flow-rate of steams are measured. Mass flow-rate and composition of all solid-liquid mixtures are calculated (*e.g.* pulps, carbonation sludge, limed juice, sugar limes).

Data are supplied only for validation purpose, no identification of variables or parameters are performed in this study. However, their consistency is checked by performing global heat and mass balances using a spreadsheet software before any process modelling in ProSimPlus®. Finally, due to sensor precision and fluctuation of the streams compositions, the following measurement uncertainties are retained for the supplied data of the sugar beet factory:

- temperature: ± 3 °C;
- mass flow-rate: ± 3 %;
- brix³: ± 2 %;
- purity¹: ± 2 %;

Each workshop model is validated comparing simulation results to industrial data. Deviation between simulation and industrial data are below 1 % for sugar extraction and crystallization workshops. Nonetheless, quite all output variables of these workshops are forced by "constraints and recycles" modules. In the sugar extraction workshop, this is due to the fact that a) sugar extraction is a unit operation specific to the sugar beet process and b) cellular residues are considered at liquid state. Concerning the crystallization workshop, manufacturers can measure the "sugar" content of all streams and the mass flow-rate of white sugar crystals. With these data, a simple mass balance allows calculating all compositions and mass flow-rates of this workshop. By fixing quite all parameters of the model, the latter allows for the simulation of the industrial workshop with a deviation below 1 %.

For the juice clarification and the evaporation steps, some data reconciliation have been performed before any modelling. For the juice clarification workshop, industrial data was parsimonious and entailed with large uncertainties due to the difficult measurements of compositions and mass flow-rates of solid-liquid mixtures. The compositions and the mass flow-rates of *green juice*, *thick juice*, sugar limes and coke were not consistent in regards to a mass balance. This is due to two reasons. First, measurement of the mass flow-rate and composition of a solid phase in suspension of a liquid phase are difficult. Second, a little fluctuation of the mass flow-rate or composition of the *green juice* affects a lot mass flow-rate and composition of the other streams. This is classically checked in the factories and by simulation. A global mass balance of this workshop has been performed using a spreadsheet software. The following choices are considered in the model of the juice clarification workshop:

- deviations on mass flow-rates and compositions of the streams of this workshop are quite substantial (up to 10 % of deviation). However, mass flow-rates and compositions

of the *green juice*, lime (inlet streams) and thin juice (outlet stream) are reliable since these streams are only at liquid state. Hence, these inlet and outlet variables are taken as given by the manufacturer.

- all fixed output variables (*i.e.* purity¹ of the light juice, filter efficiency⁶, and sugar lime composition) are either validated industrial data or recalculated values by a global mass balance of the workshop. The recalculated values are in the range of classical values existing in sugar beet factories.

Concerning the model of the concentration by evaporation workshop, the deviation between simulation and industrial data are below 1 %, except for:

- temperature of steam produced in each effect (maximum deviation of 3 °C);
- dry matter composition of liquid concentrated in each effect (deviation below 3 %);
- mass flow-rate of steam supplying the second to the fifth effect (maximum of 3.5 % of deviation);
- mass flow-rate of re-compressed first effect steam (deviation of 7 %).

Deviations on the temperatures of the produced steams are due to the selected thermodynamic model determining thermal properties of mixtures (*i.e.* UNIFAC-Larsen model). Moreover, a little modification of the mass flow-rate or composition of the *thin juice* affects a lot mass flow-rate and composition of the streams of the workshop. This phenomena is well known by the manufacturers and is checked by simulation. For this reason, contrary to evaporator pressure, compositions and mass flow-rates of produced steam and concentrated juice are given by manufacturers with large uncertainties as stated earlier.

Therefore, the presented model allows for the simulation and the mass balance validation (industrial data reconciliation) of all workshops of the sugar beet process, with a low deviation range except for some compositions or mass flow-rates which are difficult to measure. The deviation range of simulation results is within the experimental error bars. Data required for the Pinch and Exergy analyses are automatically extracted from the modules in ProSimPlus®. These energy analyses can be applied at the factory scale and hypotheses of energy optimization can be checked with the actual sugar beet process model. However, quite all output variables (*e.g.* mass fraction of constituents, ratio of mass flow-rates) of the modules are fixed using "constraints and recycles" modules due to the lack of modules dedicated to the sugar beet process. Hence, sensibility analysis on the operating conditions or scaling up of each unit operation (except for the evaporation workshop and heat-exchanger network) may not be performed with this model. To go further, one may replace fixed mass flow-rates and compositions of output streams by the ratio of input/output variables. One may also develop modules of unit operations specific to the sugar beet process using "script modules" in ProSimPlus®. This second method is more time consuming (at least seven man-days for each unit operation).

6.5 Conclusion and perspectives

Nowadays, it is of the utmost interest to optimize energy consumption within factories in a systematic way to face recent environmental regulations. This study proposed a methodology to model food processes to *in fine* combining Pinch and exergy analysis, using a chemical

6. Filter efficiency: ratio of the mass flow-rate of juice carbonation and carbonation sludge

engineering software (ProSimPlus[®], version 3.5.3.1.). We applied the methodology to a sugar beet factory. A UNIFAC-Larsen thermodynamic model was used to estimate the thermophysical properties of the streams. Each unit operation related to the sugar beet process was considered as a combination of several modules to distinguish the thermodynamic irreversibilities of the process: a unit operation module only simulates one energy change (pressure, temperature or composition). In addition, we managed to model the numeral unit operations specific to the sugar beet process not existing in the ProSimPlus[®] database (*i.e.* diffusion, mechanical press, filtration, centrifuge). To do so, we combined basic and generic unit operation modules and "constraints and recycles" modules. The latter fixed almost all output variables of outlet streams of modules (compositions or mass flow-rates). The developed model allows for the simulation of a sugar beet factory, with a deviation range within the industrial error bars.

After this first step, we will improve the model by removing some constraints and recycles modules in order to increase its extrapolation capabilities. Current work in progress is focused on optimizing the energy consumption of this factory by combining exergy and thermal Pinch analysis.

6.6 Acknowledgments

The authors wish to thank the French Agence Nationale de la Recherche (ANR) for their funding, and the partners of the project COOPERE2 leaded by VERI (Veolia, Research and Innovation), in collaboration with ProSim and LGC (Laboratoire de Génie Chimique, ENSIACET).

Bibliography

- [1] E. Commission, Energy Efficiency Directive. Article 8: Energy audits and energy management systems, 2013.
- [2] E. Commission, "Green paper, a 2030 framework for climate and energy policies," 2013.
- [3] S. K. Sikdar and M. El-Lalwagi, Process design tools for the environment, Taylor & Francis, 2001.
- [4] CCS Energie Advies , "Wat is exercom?." http://www.cocos.nl/en/548/ccs/Wat_is_ExerCom.html, 2014.
- [5] S. Gournelon, R. Thery-Hetreux, P. Floquet, O. Baudouin, P. Baudet, and L. Campagnolo, "Exergy analysis in prosimplus[®] simulation software: A focus on exergy efficiency evaluation," Computers & Chemical Engineering **79**, pp. 91–112, 2015.
- [6] S. Devahastin, "Software for drying/evaporation simulations: Simprosys," Drying Technology **24**(11), pp. 1533–1534, 2006.
- [7] Z. Pakowski, "Simulation of the process of convective drying: Identification of generic computation routines and their implementation in a computer code drypak," Computers and Chemical Engineering **23**, Supplement(0), pp. S719–S722, 1999. European Symposium on Computer Aided Process Engineering Proceedings of the European Symposium.
- [8] I. C. Kemp, "Progress in dryer selection techniques," Drying Technology **17**(7-8), pp. 1667–1680, 1999.

- [9] P. Schuck, A. Dolivet, S. Méjean, P. Zhu, E. Blanchard, and R. Jeantet, “Drying by desorption: A tool to determine spray drying parameters,” *Journal of Food Engineering* **94**(2), pp. 199–204, 2009. Food Powder Technology.
- [10] J. Bon, G. Clemente, H. Vaquiro, and A. Mulet, “Simulation and optimization of milk pasteurization processes using a general process simulator (prosimplus),” *Computers & Chemical Engineering* **34**(3), pp. 414–420, 2010.
- [11] M. Madoumier, C. Azzaro-Pantel, G. Tanguy, and G. Gésan-Guiziou, “Modelling the properties of liquid foods for use of process flowsheeting simulators: Application to milk concentration,” *Journal of Food Engineering* **164**, pp. 70–89, 2015.
- [12] A. V. Ensinas, S. A. Nebra, M. A. Lozano, and L. M. Serra, “Analysis of process steam demand reduction and electricity generation in sugar and ethanol production from sugarcane,” *Energy Conversion and Management* **48**(11), pp. 2978–2987, 2007. 19th International Conference on Efficiency, Cost, Optimization, Simulation and Environmental Impact of Energy Systems.
- [13] R. Palacios-Bereche, K. J. Mosqueira-Salazar, M. Modesto, A. V. Ensinas, S. A. Nebra, L. M. Serra, and M.-A. Lozano, “Exergetic analysis of the integrated first- and second-generation ethanol production from sugarcane,” *Energy* **62**, pp. 46–61, 2013.
- [14] P. S. Ortiz and S. de Oliveira Jr., “Exergy analysis of pretreatment processes of bioethanol production based on sugarcane bagasse,” *Energy* **76**, pp. 130–138, 2014.
- [15] M. Starzak and M. Mathlouthi, “Temperature dependence of water activity in aqueous solutions of sucrose,” *Food Chemistry* **96**(3), pp. 346–370, 2006. 3rd International Workshop on Water in Foods.
- [16] L. W. Weiss, “Sugar factory process optimization using the sugars computer program,” tech. rep., American society of sugar beet technologists, Englewood, Colorado 80110 USA, March 1989.
- [17] A. Ensinas, M. Modesto, S. Nebra, and L. Serra, “Reduction of irreversibility generation in sugar and ethanol production from sugarcane,” *Energy* **34**(5), pp. 680–688, 2009. 4th Dubrovnik Conference, 4th Dubrovnik conference on Sustainable Development of energy, Water and Environment.
- [18] T. Tekin and M. Bayramoglu, “Exergy analysis of the sugar production process from sugar beets,” *International Journal of Energy Research* **22**(7), pp. 591–601, 1998.
- [19] T. Tekin and M. Bayramoglu, “Exergy and structural analysis of raw juice production and steam-power units of a sugar production plant,” *Energy* **26**(3), pp. 287–297, 2001.
- [20] S. D. Peacock, “The use of simulink for process modelling in the sugar industry,” in *Proceedings of South African Sugar Technologists’ Association*, 2002.
- [21] J. Q. Albarelli, A. V. Ensinas, and M. A. Silva, “Product diversification to enhance economic viability of second generation ethanol production in brazil: The case of the sugar and ethanol joint production,” *Chemical Engineering Research and Design* **92**(8), pp. 1470–1481, 2014.
- [22] P. W. Van der Poel, H. Schiweck, and T. Schwartz, *Sugar Technology, Beet and Cane Sugar Manufacture*. Bartens, 1998.
- [23] Z. Bubnik, P. Kadlec, D. Urban, and M. Bruhns, *Sugar technologists manual, Chemical and physical data for sugar manufacturers and users*, p. 417. Bartens, 1995.

Chapitre 7

Combined Pinch and exergy analysis for energy optimization of a sugar beet factory using a generic simulator (ProSimPlus[®])

Résumé

Pour faire face à la réglementation européenne récente, le développement d'outils assistés par ordinateur est d'une grande aide pour optimiser la consommation énergétique des usines agroalimentaires. Dans cette étude, les analyses de pincement et d'exergie sont appliquées à l'optimisation énergétique d'une sucrerie de betteraves, à l'aide du logiciel ProSimPlus[®]. Les analyses de pincement comprennent l'étape de la minimisation des besoins en utilités à celle de la conception de nouveaux réseaux d'échangeurs. Elles confirment que le réseau d'échangeurs de chaleur actuel est déjà optimisé. L'analyse exergétique de l'usine actuelle montre que les améliorations potentielles sont principalement situées au niveau de l'étape de préchauffage des *cossettes* et de celles de production de vapeur à haute pression alimentant le premier évaporateur. Des améliorations techniques sont proposées dans cette étude. L'analyse exergétique des cas d'études améliorés révèlent qu'une diminution de 12,1 % de l'irréversibilité totale de l'usine peut être obtenue.

Mots-clés : intégration de procédés, intégration thermique, optimisation de procédés, procédés agroalimentaires.

Cet article est à soumettre à *Energy Journal*¹.

7.1 Introduction

The sugarbeet manufacturing is considered as one of the most important economic activities in food-industry. The sugar beet process produce annually a hundred thousand tons

1. C. Lambert, B. Laulan, M. Decloux, and H. Romdhana, "Combined Pinch and exergy analysis for energy optimization of a sugar beet factory using a generic simulator (ProSimPlus)", To submit to Energy journal, p. 24, 2015.

of sugar and other useful by-products that have economic values (*e.g.* molasses, DDGS², beet-pulp, organic fertilizer etc.).

Energy consumption per ton of processed beets varies within a range of 150 - 250 kWh [1]. Given that the primary utility in sugar industry is the steam produced from fossil fuels, regulations are of great importance. Considering also the current economic, energy and environmental context, the sugar beet industry may be under pressure to comply the new environmental regulations, improve energy efficiency and increase production rate. In Europe, energy efficiency directives require, for large companies (including sugar industry), to carry out frequent energy audits [2] and asks for a 20 % decrease of energy consumption by 2030 [3]. Therefore, improving energy efficiency in sugar beet industry is a major challenge, both economic and environmental.

Traditionally, the improvements of energy system in the sugar factory are introduced by using the learning-by-experience approach [4]. When a new factory is built or an existing is upgraded, the energy improvements are designed with regard to the previous solutions and are dependent on the engineer's experience. Therefore, it is almost impossible to determine how close a design is to the minimum energy demand. To ensure an optimal energy solution, new computer-aided methods and tools have been proposed. A number of commercial computer-aided tools are available, including ProSimPlus®, Aspen Plus®, Aspen HYSYS®, Chemcad®, PRO/II®, and gPROMS® *etc.* These tools provide toolboxes of unit operations, libraries of chemical components and thermodynamic methods to simulate chemical processes. The simulation results are useful for comparing various process alternatives and help us to select the most promising flowsheets in term of energy consumption. Unfortunately, this approach is difficult and time-consuming because it requires a modelling of each unit operation of the process and design conditions (*i.e.* composition, temperature, pressure of each stream and equipment size). Consequently, this approach requires the engineer expertise to identify the most promising flowsheet variants.

To address this issue, new methods can be used, in addition or not of the simulations, to investigate the energy-saving potential in sugar factory: (a) the energy-system optimization using numerical methods, (b) the use of specific energy optimization tools and (c) the energy-system integration using thermodynamic analysis. Energy-system optimization approach involves algebraic equations to minimize or to maximize in order to obtain an optimal allocation of energy resources [5]. The optimization problem may be formulated within the simulation tool (*e.g.* Aspen Plus®, ProSimPlus®) or encoded within a popular programming environment (*e.g.* MATLAB®, Scilab®, GAMS®, MIPSYN®, LINDO®, EES®). In practice, an energy optimization program consists in identifying the best available design by manipulating the operating variables of the process. The optimization involves objective function(s) defined by the process performance indicators (*i.e.* maximizing energy efficiency). The major disadvantage of the energy-system optimization approach is the translation of the real-energy problem into mathematical formulae. In addition, the engineer's experience is required to confirm the physical-sense of the results.

Some specific energy optimization software may be used independently of simulation tools. Connolly *et al.* [6] have reviewed 37 tools for analyzing the energy integration into various systems (*e.g.* energy storage or conversion, renewable energy generation, electricity and district heating sector). However, these tools do not allow for the thermal energy and exergy estimations of a whole network of unit operations, such as the sugar beet process. This process involves several chemical engineering operations including juice extraction from beet-pulp, clarification, concentration, evaporation, crystallization, mechanical separation,

2. DDGS: Distiller's Dried Grains with Solubles

drying, cooling, etc [4].

A recent energy-system integration approach can be used for the factory optimization [5, 7]. This approach includes Pinch and exergy analysis. Pinch analysis aims to maximize heat recovery among the process streams while minimizing hot and cold utility requirements. This approach can be performed by constructing of the "famous" hot and cold composite plots, representing temperature levels as a function of the heat load. Exergy analysis aims to identify the energy-saving potential while identifying the efficiency of energy use in each unit operation. Exergy degradation, entropy generation or energy loss to the environment can affect the efficiency of each unit operation. Pinch and/or exergy analysis has led to interesting results to optimize energy consumption in sugar beet and can factories. As a matter of fact, Tekin *et al.* [8] performed an exergy analysis of a sugar beet factory. They identified the unit operations producing most of the irreversibility of the factory. The same authors [9], proposed also an exergy analysis of raw juice production and steam-power units of a sugar production plant. They identified a total exergy loss of the plant of about 4.21 %. Palacios *et al.* [10] and Silva-Ortiz *et al.* [11], used Aspen Plus® to simulate the process of bioethanol production from sugarcane bagasse. They performed a comparative exergy analysis of several process configurations. Ensinas *et al.* [12] simulated sugar and ethanol production from sugarcane with the EES® software. They performed an exergy analysis on an average sugarcane factory and showed that a 10 % decrease of irreversibility is possible. Ram *et al.* [13], performed Pinch and exergy analysis of a sugar factory. Their study was limited to the evaporation operations (quadruple evaporative system). Pinch analysis showed that the consumption of hot and cold utilities can be reduced by 9 %, and the exergy analysis showed that the exergy losses can be reduced by 48 %. Cortes *et al.* [14] proposed a simulation and a Pinch analysis of multiple effect evaporators in sugar plant production. They used Aspen Plus® and Aspen Energy Analyzer® respectively for simulation and Pinch analysis.

Most of the studies in the literature are restricted to analyze a single step of the sugar process (usually, the evaporation step), whereas it is more interesting to analyze the full process. Much of these studies are also limited to the calculation of exergy efficiency of each unit operation and the minimization of hot and cold utility requirements without specifying the design procedure (*e.g.* retrofitting the heat exchanger network). Since energy-system integration methods are based on a thermodynamic representation of energy data extracted from the process, Pinch or exergy analysis can be applied systematically to identify energy saving projects in the sugar factories. These analyses can be partially or fully automated into popular process simulation tools by extracting the energy-data directly. Building on this outcome, the present work provides a comprehensive and systematic approach combining energy-system and simulation tool of a French sugar beet factory by using the ProSimPlus® process simulator. Concerning the Pinch analysis, a design procedure of heat exchanger network is developed in this study.

7.2 Sugar beet process description

For confidentiality purposes, the name and precise characteristics of the French sugar beet factory, studied in this work, are not disclosed. The studied factory currently consumes about 20,000 t of sugar beet per day and more than 3 GWh/d. Sugar processing involves several chemical engineering operations such as cleaning-slicing, sugar extraction, juice clarification, juice concentration by evaporation, sugar crystallization, and drying-storage-packaging [15]. A general scheme of the sugar beet process of the factory is given in figure 7.1. This process

is well known and described in a lot of books. Workshops represented by dotted frame in figure 7.1 are modeled in ProSimPlus®. Some elements of the modeled steps of the sugar beet process are given in the following paragraphs.

Sugar extraction

Sucrose is extracted from *cossettes* by contacting with hot water composed of condensates and water issued from the press (see below). Several solutes ("sugar" and "non-sugars") diffuse from the *cossettes* to the juice. At the diffuser outlet, the "*green juice*" and sugar pulps (*i.e.* cellular residues of the *cossettes*) are obtained. The *green juice* is recycled in this workshop for the *cossettes* heating (using scalder and prescalder) and is then purified in the next workshop [15]. The studied factory is composed of two diffusers and one prescalder.

Juice clarification

The purpose of the clarification steps is to remove "non-sugars" affecting juice concentration in the evaporation workshop and sucrose recovery and white crystal sugar quality in the crystallization workshop. The *green juice* is treated twice with lime and carbon dioxide gas and is then filtered [15].

Evaporation

Evaporation increases the dry matter concentration in the juice (Brix³ value raised from 15 % to 70 %) by removing water and allows producing nearly all the required hot streams for the heat exchangers of the workshops (steams and condensates) [15]. The studied factory is composed of a five effect evaporator. The steam used for the heating of the first effect is produced from high-pressured steam. The latter a) is expanded into a turbine to produce electrical power, b) supplies a turbo-compressor to re-compress steams produced at the first effect, and c) is expended into an expansion valve (see figure 7.1).

Crystallization workshop

Crystallization is the only one batch unit operation of the sugar beet process [15]. Crystallization and centrifugation steps are repeated twice in this factory.

7.3 Sugar beet process modelling

The factory modelling is performed in two steps: a) choice of the list of constituents and thermodynamic model and validation of the predictions, and b) modelling of the unit operations of the process and validation with industrial data. First, the choice of the constituents and the thermodynamic model are described in a previous work [16]. The thermodynamic properties are calculated using the Simulis Thermodynamics® software. In particular, the UNIFAC-Larsen thermodynamic model is used to adequately represent thermal properties of the streams (*i.e.* heat capacity and boiling-point elevation). The following constituents are required to model the streams of the sugar beet process:

- for all workshops: sucrose, "non-sugars" and water;
- specific to the sugar extraction workshop: cellular residue;
- specific to the juice clarification workshop: dinitrogen, dioxygen, carbon dioxide, calcium oxide, calcium carbonate.

3. Brix: percentage of soluble dry matter of the juice

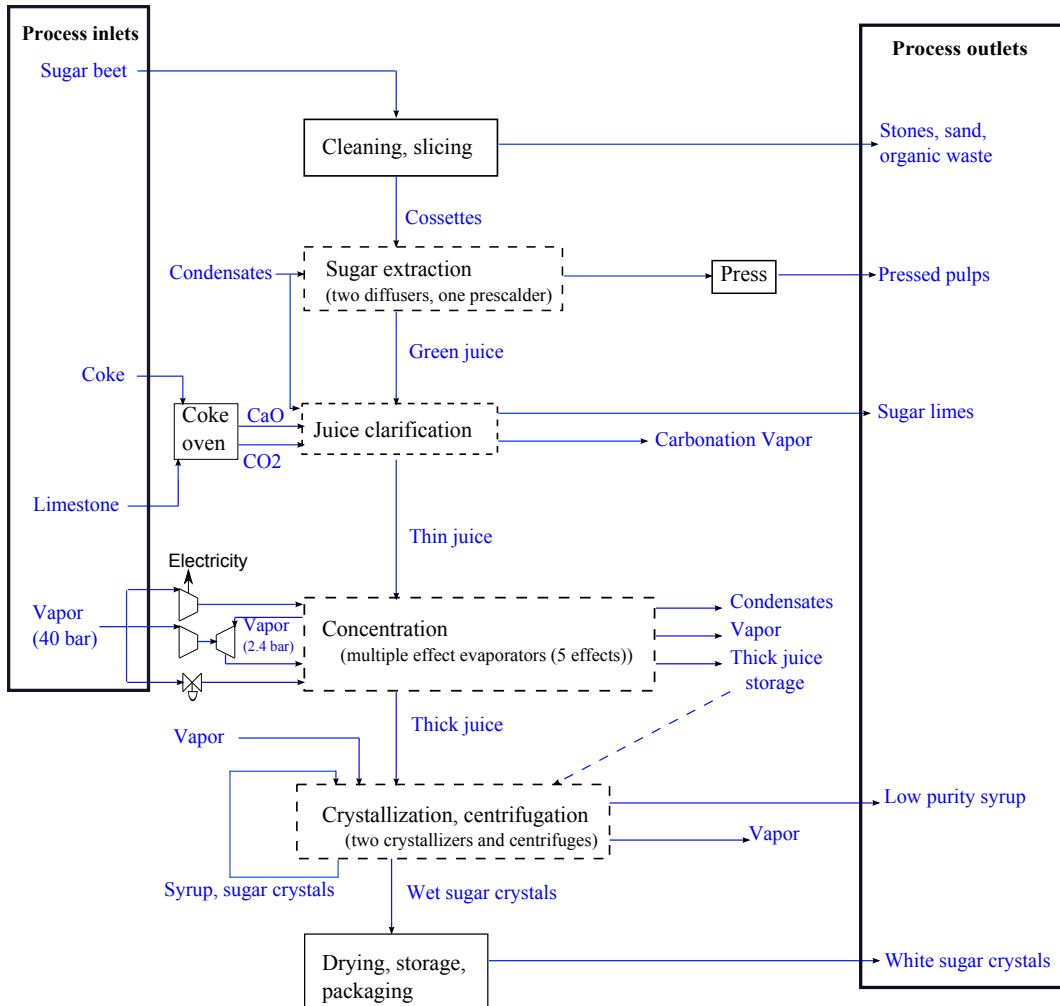


Figure 7.1 – Sugar beet process diagram

All the retained constituents are taken from the 2013 standard package of the Simulis Thermodynamics® database. Some of these constituents cannot be directly modeled with this thermodynamic database. On the one hand, the UNIFAC-Larsen composition of each constituent is required. As calcium oxide and calcium carbonate molecular composition are not available, the water molecular composition is added for these constituents. On the other hand, the precise composition of some of the required constituents are unknown. Hence, "non-sugars" are modeled as sucrose and cellular residue as cellulose, one of its majority constituents. Thermal properties (*i.e.* heat capacity and boiling-point elevation) are well predicted comparing prediction of this thermodynamic model with the one calculated using Bubnik *et al.* [17] correlations. For a juice purity¹ above 70 % and a juice Brix² range of 15 - 90 %, boiling-point elevation is under-estimated by a maximum of 1 °C, and for a juice Brix² above 90 °C, boiling-point elevation is over-estimated by a maximum of 3 °C. These deviations are in the range of industrial error bars [16].

Second, the developed model of the sugar beet process and its validation are described in a previous work [16]. Workshops represented by dotted frame in figure 7.1 are modeled in ProSimPlus® (*i.e.* sugar extraction, juice clarification, evaporation and crystallization steps). Each unit operation of these workshops is simulated as a combination of several modules to distinguish the thermodynamic irreversibilities: a unit operation module only simulates one energy change (pressure, temperature or composition) at a time to comply

with exergy analysis requirements. In addition, we managed to model the numeral unit operations specific to the sugar beet process not existing in the ProSimPlus® database (*i.e.* diffusion, mechanical press, filtration, centrifuge). To do so, a combination of basic and generic unit operation modules (*i.e.* "component splitter", "mixer", "stream splitter" modules) and "constraints and recycles" modules are used. The developed model allows for the simulation of a sugar beet factory and for the reconciliation of industrial data, with a deviation range within the industrial error bars [16].

7.4 Energy optimization methods

7.4.1 Exergy analysis

The exergy calculation has been implemented in the ProSimPlus® software by [18] in a new "exergy" module. The exergy of each material stream is defined as the sum of the chemical and the physical exergy. For each unit operation, the exergy balance is defined by equation 7.1. According to Gourmelon *et al.* [18], this equation is equivalent to equation 7.2 which allows bringing three efficiency indicators out: intrinsic efficiency (equation 7.3), intrinsic irreversibility (equation 7.4) and intrinsic waste (equation 7.5). The purpose of the exergy optimization of a process is to maximize the intrinsic efficiency and minimize both the intrinsic irreversibility and the intrinsic waste. The "exergy" module is used to perform the exergy analysis of the sugar beet factory.

$$B_{in} = B_{out}^{utilized} + B_{out}^{waste} + I \quad (7.1)$$

$$\Delta B^{consumed} = \Delta B^{produced} + B_{out}^{waste} + I \quad (7.2)$$

$$IE = \frac{\Delta B^{produced}}{\Delta B^{consumed}} \quad (7.3)$$

$$II = \frac{I}{\Delta B^{consumed}} \quad (7.4)$$

$$IW = \frac{B_{out}^{waste}}{\Delta B^{consumed}} \quad (7.5)$$

Where B_{in} is the exergy flux of the inlet stream (kW), $B_{out}^{utilized}$ and B_{out}^{waste} the exergy flux of the outlet stream (kW) which are respectively utilized (recovered) and wasted (non-recovered), I the irreversibility which is the exergy flux destroyed by the unit operation (kW), $\Delta B^{consumed}$ the consumed exergy flux (kW), $\Delta B^{produced}$ the produced exergy flux (kW), IE the intrinsic efficiency (*decimal*), II the intrinsic irreversibility (*decimal*), IW the intrinsic waste (*decimal*).

In this study, all modules of the factory model are considered in the first step of the exergy analysis. The order of modules is ranked in function of their irreversibility value (from the largest to the smallest). In the second step, only modules for which irreversibility values represent at least 0.9 % of the total irreversibility of the factory and for which intrinsic efficiencies are below 100 % are considered for the exergy analysis of the factory. In our study, the purpose of the exergy optimization is to minimize irreversibility of modules while maximizing their intrinsic efficiency.

7.4.2 Pinch analysis

Pinch analysis is based on the first and the second thermodynamic principles [7]. The implementation of these principles is very different from that known in the exergy analysis. Since it is based on a thermodynamic representation of data collected daily on industrial sites, Pinch analysis can be applied systematically to identify energy saving. The method includes four steps:

Step 1: Identification of the zones of the process that could be improved

The method consists in studying the heat exchange between streams to cool (*i.e.* hot streams) and streams to heat (*i.e.* cold streams). Any form of energy other than the thermal energy (*e.g.* chemical or mechanical) is not taken into account in this approach. When the processes are identified, it is necessary to establish a flow-sheet of the whole heat exchanger network in order to develop a heat and mass balance of the different streams. Besides, heat exchangers, in which thermal exchange cannot be performed with other streams, are eliminated from the inventory. In the case of the sugar beet process, scalders and prescalders of the sugar extraction step, evaporators of the evaporation step and under-vacuum boilers of the crystallization step are not considered in the Pinch analysis.

Step 2: Inventory

This step consists in identifying some specific information required to characterize hot and cold streams and their interactions in the process network. The most required information are:

- mass flow-rate \dot{m} ($kg.s^{-1}$);
- specific heat capacity C_p ($J.kg^{-1}.K^{-1}$);
- supply temperature T_s ($^{\circ}C$);
- target temperature T_t ($^{\circ}C$);
- latent heat of stream in the case of phase change : L_v ($J.kg^{-1}$);
- hot streams that require cooling or condensation;
- cold streams that require heating or evaporation;
- current utilities.

From the inventory data, the heat capacity flow-rate CP ($kW.K^{-1}$) is deduced:

$$CP = \dot{m} \cdot C_p \text{ in the case of heating or cooling} \quad (7.6)$$

$$CP = \dot{m} \cdot L_v / 1^{\circ}C \text{ in the case of phase change} \quad (7.7)$$

In this study, a constant CP is assumed. For a stream requiring heating or cooling from a supply temperature T_s to a target temperature T_t , the involved power is:

$$P = CP \cdot (T_t - T_s) \quad (7.8)$$

For a stream requiring condensation or evaporation, the required power is:

$$P = CP \cdot (1^{\circ}C) \quad (7.9)$$

For the heat exchanger network design, all the steams are considered saturated. This assumption is common as steam desuperheating often occurs during transport from its production to its use in the heat exchangers.

Step 3: Minimization of utility requirements

By applying the Pinch minimization method, it is possible to identify changes in the process parameters that will have a favorable impact on energy consumption. Minimizing utility requirement is performed by graphic method. The determination of the Pinch point (*i.e.* minimum distance between the cold and hot streams) allows calculating the minimum of hot and cold utilities satisfying the energy requirement of the process. The minimization of utility requirements include three steps:

Sub step 3.1: Temperature shifting

The temperatures of hot and cold streams should be modified in order to ensure that within any interval, hot streams and cold streams are at least shifted by a minimal temperature difference ΔT_{min} and therefore a possible heat exchange between hot and cold streams. The shifted temperatures are set at:

$$- \frac{1}{2} \Delta T_{min} \text{ for hot streams} \quad (7.10)$$

$$+ \frac{1}{2} \Delta T_{min} \text{ for cold streams} \quad (7.11)$$

The shifted supply and target temperatures are sorted in ascending order to form the temperature interval boundaries. In our study, the minimal temperature difference is fixed at 2 °C, which is the current value of the studied factory.

Sub step 3.2: Energy balances

The purpose of this step is to calculate a heat balance within each temperature interval. The result indicates if the interval is an energy surplus or energy deficit. Knowing the list of streams in each shifted temperature interval $\Delta T_{s,i}$, energy balance is calculated according to equations 7.12:

$$\Delta P_i = \Delta T_{s,i} \cdot \sum_j (CP_{hot,j} - CP_{cold,j}) \quad (7.12)$$

Where i and j represent respectively the temperature interval and the stream within the interval.

Sub-step 3.3: Energy cascade

The calculation of heat cascades includes two steps. The first step consists in accumulating the results of heat balances (ΔP) by assuming that no heat is supplied to the hottest interval. The second step consists in accumulating the result of the first cascade by assuming a heat supplied to the hottest interval. The value of the supplied heat is the maximum of deficit found within the first cascade. Finally, from the second cascade, the minimum of hot and cold utility requirements are determined respectively at the hottest and lower intervals.

Step 4: Design of the new optimized network

The design of a new heat exchanger network is mainly based on the inventory data and economic (*i.e.* investment) and technical constraints (*e.g.* physical distance between streams, feasibility of exchange *etc.*). Comparing the minimum utility requirement to those actually consumed allows considering energy saving alternatives that can be achieved by investing in heat exchangers. The design is performed separately within two zones: below and above the

Pinch point. The Pinch point is obtained from the energy cascade corresponding to the net-zero energy. For each zone, hot and cold streams are sorted according to their temperature levels. After that, the design is performed by selecting streams for which:

$$CP_{hot} \leq CP_{cold} \text{ above the pinch point}$$

$$CP_{cold} \leq CP_{hot} \text{ below the pinch point}$$

The design can be considered completely performed when all the hot and cold streams are used, respectively above and below the Pinch point. The remaining powers for cooling and heating must be equal to the cooling and heating utility requirement.

To simplify the Pinch analysis of the sugar beet factory, the production of the pressurized steam supplying the first evaporator is not considered. The heat and cold utility requirements are estimated as the power supplying the first effect (*i.e.* product of the mass flow-rate of the high pressured steam in the first effect and its latent heat of vaporization).

7.5 Results and discussion

7.5.1 Energy analysis of the current factory

Pinch analysis

The current network is composed of 20 heat exchangers excluding scalders, prescalders (sugar extraction workshop), evaporators (evaporation workshop) and under-vacuum boilers (crystallization workshop). The hot and cold utility requirements are respectively about 154 MW and 70 MW. The hot utility requirement is estimated from the power supplying the first effect.

The necessary thermal data for the Pinch analysis are extracted from the initial simulation of the current process. The first three columns of the table 7.1 give the supply and target temperatures and the heat capacity flow rate. The minimization procedure of utilities is shown in table 7.2. The last column shows the energy cascade. No heat is supplied to the hottest interval (*i.e.* 129 - 128 °C), meaning that the exchanger network does not require a hot utility. In the final energy cascade, the cold utility requirement is 70 MW.

The current heat exchanger network is already optimized as most of the hot streams are used, even carbonation steams (juice clarification workshop), out gassing steams (evaporation workshop), vacuum-boiler steams (crystallization workshop). Hot and cold utility requirements cannot be minimized, contrary to the number of heat exchangers. The optimized design is composed of 16 heat exchangers, sized using the following values of heat transfer coefficients:

- 1,000 W.m⁻².K⁻¹ for the liquid-liquid heat exchangers;
- 1,300 W.m⁻².K⁻¹ for the vapor-liquid heat exchangers.

All the required sizes of the current heat exchanger network were not available. In order to compare both designs, an estimation of the current size of the heat exchanger network is also performed. The optimized design allows for a 25 % decrease of the total exchange surface. A money saving of about 100 k€/y could be carried out assuming a maintenance cost of 40 €/m². In addition, the optimized design allows for a 1.6 % decrease of the total irreversibility of the factory (about 6.2 and 1.8 % decrease respectively of the total irreversibilities of the sugar extraction and juice clarification workshops).

Table 7.1 – Inventory data for energy recovery analysis

Stream	Current process			Case study 1			Case study 2		
	T_s (°C)	T_t (°C)	CP (kW/°C)	T_s (°C)	T_t (°C)	CP (kW/°C)	T_s (°C)	T_t (°C)	CP (kW/°C)
H1	86.1	60.0	142.94	86.1	60.0	142.94	86.1	60.0	142.94
H2	60.0	20.0	418.51	60.0	20.0	416.89	60.0	20.0	410.43
H3	80.4	60.0	663.40	80.4	60.0	661.74	80.4	60.0	655.28
H4	125.4	125.4	2,205.51	125.4	125.4	2,205.51	125.4	125.4	2,205.51
H5	120.2	120.2	4,714.49	120.2	120.2	4,714.49	120.2	120.2	4,714.49
H6	115.3	115.3	12,919.10	115.3	115.3	9,099.00	115.3	115.3	9,099.00
H7	107.0	107.0	26,796.03	107.0	107.0	15,235.37	107.0	107.0	15,235.37
H8	97.9	96.9	14,559.63	97.9	96.9	14,300.99	97.9	96.9	14,300.99
H9	116.3	101.5	679.03	116.3	101.5	690.08	116.3	101.5	669.95
H10	102.5	80.0	660.33	102.5	80.0	827.48	102.5	80.0	821.00
H11	64.0	64.0	33,656.37	64.0	64.0	33,656.37	64.0	64.0	33,656.37
H12	60.1	60.1	7,700.79	60.1	60.1	7,700.79	60.1	60.1	7,700.79
H13	130.0	130.0	7,519.06	130.0	130.0	7,519.06	130.0	130.0	7,519.06
H14	78.8	78.8	8,335.73	78.8	78.8	8,335.73	78.8	78.8	8,335.73
H15	123.3	60.0	68.25	123.3	60.0	68.25	123.3	60.0	68.25
C1	60.0	68.1	204.12	60.0	67.8	204.12	60.0	67.8	204.12
C2	63.0	73.0	442.14	63.0	73.0	442.14	63.0	73.0	442.14
C3	73.1	86.8	2,084.72	73.1	78.6	2084.72	73.1	78.6	2,084.72
C4	73.1	75.3	1,379.00	73.1	75.3	1379.00	73.1	75.3	1,379.00
C5	40.0	73.0	479.61	40.0	73.0	479.61	40.0	73.0	479.61
C6	75.5	85.0	1,182.76	75.5	85.0	1,182.76	75.5	85.0	1,182.76
C7	84.5	92.0	1,065.84	84.5	92.0	1,065.84	84.5	92.0	1,065.84
C8	91.3	126.6	1,096.86	91.3	126.6	1,096.86	91.3	126.6	1,096.86
C9	-	-	-	40.0	73.0	513.91	40.0	73.0	513.91

H: Hot, C: Cold

Exergy analysis

The irreversibility and the relative irreversibility of each workshop of the current factory are given in table 7.3. The irreversibility, the relative irreversibility and the intrinsic efficiency of the unit operations producing most of the workshop irreversibilities are also given in table 7.3. The total irreversibility of the current factory is 31,498 kW.

Sub-workshop 1 and 2 of the sugar extraction step are respectively composed of a combi-

Table 7.2 – Heat cascade for the current heat-exchanger network

T_s °C	$\sum(CP_{hot} - CP_{cold})$ kW/°C	ΔP MW	Heat Cascade MW	T_s °C	$\sum(CP_{hot} - CP_{cold})$ kW/°C	ΔP MW	Heat Cascade MW
129.0			0.000⁽¹⁾	86.0			41.540
	7,519	7.519			-3,605	-1.802	
128.0	0	0.000	7.519	85.5	-2,539	-1.041	39.738
127.6	-1,097	-3.510	7.519	85.1	-2,396	-13.633	38.697
124.4	1,109	1.109	4.009	79.4	-1,733	-0.693	25.064
123.4	-1,097	-1.261	5.118	79.0	-2,393	-2.871	24.371
122.3	-1,029	-3.137	3.856	77.8	5,943	5.943	21.499
119.2	3,686	3.686	0.719	76.8	-2,393	-0.718	27.442
118.2	-1,029	-2.983	4.405	76.5	-1210	-0.242	26.724
115.3	-350	-0.350	1.422	76.3	-2,589	-5.696	26.482
114.3	12,570	12.570	1.072	74.1	875	0.087	20.786
113.3	-350	-2.552	13.642	74.0	-47	-0.231	20.874
106.0	26,446	26.446	11.090	69.1	-251	-1.282	20.642
105.0	-350	-1.224	37.537	64.0	191	0.191	19.361
101.5	311	0.311	36.313	63.0	33,847	33.847	19.552
100.5	-368	-1.694	36.624	62.0	191	0.191	53.399
95.9	14,191	14.191	34.930	61.0	395	0.790	53.590
94.9	-368	-0.700	49.121	59.0	-61	-0.055	54.380
93.0	-1,434	-1.004	48.421	58.1	7,640	7.640	54.325
92.3	-337	-1.518	47.417	57.1	-61	-0.984	61.964
87.8	-2,422	-4.360	45.900	41.0	419	9.207	60.981
86.0			41.540	19.0			70.188⁽²⁾

⁽¹⁾Hot utility, ⁽²⁾Cold utility

nation of a scalding, a diffuser and a heat exchanger network for the heating of the recycled *green juice*, and a combination of a prescalder, a scalding and heat exchanger network for the heating of the recycled *green juice* (supplying the scalding and at the prescalder outlet).

Most of the irreversibilities of this workshop are produced by the scalding and the heat exchanger network of the sub-workshop 1 (see table 7.3). The ratios of the irreversibility by the mass flow-rate of *cossettes* are respectively 9.06 kW/(t/h) and 5.13 kW/(t/h) for the sub-workshop 1 and 2. The addition of a prescalder in the sub-workshop 1 may thus allow for an important decrease of the irreversibility of the sugar extraction workshop. Moreover, the *green juice* heating at the prescalder outlet may be performed with hot steams at low temperature level currently unused. This may lead to a decrease of the cold utility requirement.

The irreversibilities of the juice clarification workshop are mostly generated by the carbonation reactors (see table 7.3). To simplify the modelling of the liming and carbonation unit operations, four reactions are neglected (*i.e.* reaction of precipitation and coagulation of the colloids, reaction of precipitation of anions and reaction of degradation of invert sugar and raffinose). Carbonation step is modeled using a combination of three modules including a "reactor tank" in which the carbonation reaction is modeled. The juice clarification model allows simulating mass and energy fluxes of this workshop with a deviation between simulated and industrial data below 1 % [16]. However, a more sophisticated model of the liming and carbonation reactions is required to study the effect of the operating parameters and variables (*e.g.* temperature, pressure, carbon dioxide conversion rate *etc.*) on the outlet stream variables. To ensure the technical feasibility of the proposed improvements, irreversibility minimization of the juice clarification is not investigated in this study.

The steam production supplying the first effect and the steam condensation within evaporators are the main causes of the irreversibilities of the evaporation workshop (see table 7.3). On the one hand, the evaporator network is already optimized (intrinsic efficiencies between 92.7 and 97.0 %). Its further optimization may not lead to a significant decrease of the total irreversibility of the factory. On the other hand, the irreversibility generation due to the steam production can be optimized. First, the mass flow-rate of expanded high-pressured steam (using an expansion valve) should be minimized as this unit operation is totally inefficient (*i.e.* a zero intrinsic efficiency) and produce 5.7 % of the total irreversibility of the factory (see table 7.3). Second, the isentropic efficiency of the current turbine, producing the required electrical power of the factory, can be improved (see table 7.5). Its intrinsic efficiency is lower than the current developed turbines. Consequently, the isentropic efficiency optimization of the turbine may significantly reduce the irreversibility and increase the intrinsic efficiency of this unit operation.

The irreversibility generations in the crystallization workshop are mostly due to the vapor condensation in the crystallizers (see table 7.3). The crystallization model is composed of a combination of basic and generic unit operation modules. This model allows for the simulation of the mass and energy fluxes with a deviation below 1 % [16]. A more precise model is required to study the effect of the crystallization parameters (*e.g.* juice height) on the outlet stream variables (*i.e.* pressure, temperature, composition) and on the irreversibility production. For instance, the hydrostatic pressure gradient is not modeled. To ensure a technical feasibility of the present study, the irreversibility production of the crystallization workshop is not optimized.

From this exergy analysis, two strategies of improvement, named case study 1 and 2, to reduce the total irreversibility of the factory, were investigated. The following modifications

are performed for each case:

- case study 1:
 - addition of a prescalder and a heat exchanger network for the *green juice* heating in the sugar extraction workshop;
 - removal of the expansion valve and improvement of the isentropic efficiency of the turbine and turbo-compressor of the evaporation workshop.
- case study 2 :
 - addition of a prescalder and a heat exchanger network for the *green juice* heating in the sugar extraction workshop;
 - minimization of the mass flow-rate of the expanded high-pressured steam without improving the isentropic efficiency of the turbine and turbo-compressor of the evaporation workshop.

For both case studies, the mass flow-rate of the high-pressured and compressed steams should be increased to insure the same outlet steam variables of the fifth effect and the same electrical power production, yet minimizing the mass flow-rate of expanded high-pressured steam (manual optimization). This may lead to an irreversibility increase of the turbo-compression but the total irreversibility of this workshop should decrease, which is the purpose of the study. This may also lead to the decrease of the total mass flow-rate of the high-pressured steam, inducing a non-negligible money saving at the factory level. The irreversibility and the percentage of irreversibility reduction for all workshops are given in table 7.4 for both improved case studies. The operating parameters and variables of the steam production steps of the evaporation workshop are given in table 7.5 for all case studies (*i.e.* current factory, case studies 1 and 2).

7.5.2 Energy analysis of the improved case studies

Exergy analysis

Consistently with what was foreseen, one can note a substantial reduction of the total irreversibility of the factory and of the high-pressured steam consumption. About 12.1 % and 9.5 % of the total irreversibility of the factory can be reduced respectively in the case study 1 and 2 (see table 7.4). A 11.1 % and 8.0 % decrease of the steam mass per ton of *cossettes* are respectively estimated in the case study 1 and 2. Assuming an average gas cost of 30 €/MWh and a boiler efficiency of 0.9, the money saved could be about 1 M€/y and 0.73 M€/y in the case studies 1 and 2.

Pinch analysis

For the added heat exchanger network for the *green juice* heating, the required hot streams have been selected among the not-used ones in the factory for both strategies of improvement. An optimized design of the heat exchanger network of the whole factory has been then performed. Figure 7.2 shows the comparison of composite curves set for the current process and for the two strategies of improvement (case studies 1 and 2). The network design achieving energy target is shown in figure 7.3. The requirements in cold utilities are about 58 MW and 59 MW respectively in the case study 1 and 2. The requirements in hot utilities are 185 MW and 171 MW respectively in the case study 1 and 2. These hot utility

Table 7.3 – Irreversibility generation in each workshop of the current factory and exergy data of unit operations creating most of the total irreversibility (in italic and with a lower police size).

	Irreversibility (kW)	Relative ir- reversibility (%) ^c	Intrinsic efficiency (%)
Sugar Extraction	6,461	20.5	
— <i>Scalder (sub-workshop 1)</i>	— 2,951	— 9.4	— 0.0
— <i>HEN_RGJ (sub-workshop 1)^a</i>	— 1,353	— 4.3	— 75.3 ^d
— <i>Prescalder (Sub-workshop 2)</i>	— 811	— 2.6	— 48.1
— <i>HEN_GJ_PrescalderOut (sub-workshop 2)^b</i>	— 599	— 1.9	— 67.7
Juice clarification	6,428	20.4	
— <i>Carbonation reactors</i>	— 4,093	— 13.0	— 75.5 ^d
Evaporation	14,163	45.0	
— <i>Turbine</i>	— 4,851	— 15.4	— 75.4
— <i>Evaporators</i>	— 4,354	— 13.8	— 95.7 ^d
— <i>Expansion valve</i>	— 1,785	— 5.7	— 0.0
— <i>Turbo-compressor</i>	— 1,112	— 3.5	— 47.9
Crystallization	4,446	14.1	
— <i>Crystallizers</i>	— 3,353	— 10.6	— 67.6 ^d
Total irreversibility	31,498	100	

^aHEN_RGJ (sub-workshop 1): heat exchanger network for the heating of the recycled *green juice* of the first sub-workshop of the sugar extraction step.

^bHEN_GJ_PrescalderOut (sub-workshop 2): heat exchanger network for the heating of the *green juice* at the prescalder outlet of the second sub-workshop of the sugar extraction step.

^cRelative irreversibility: percentage of relative irreversibility are estimated with the total irreversibility of the factory.

^dThe intrinsic efficiency is estimated as the average intrinsic efficiency of these unit operations.

requirements are estimated from the power supplying the first effect. The heat recovery is about 105 MW in both case studies. Comparing to the current factory, one can note a substantial increase of the hot utility requirement in the improved case studies. Even if the high-pressured steam consumption is lower, the mass of compressed steam in the turbo-compressor per tone of *cossettes* is much higher (see table 7.5), inducing an increase of the mass flow-rate of the steam in the first effect. The exergy improvement of the current process leads to a major reduction in the consumption of cold utilities. As the final design of exchanger networks is similar, only the second case study is shown in the figure 7.3.

As for the Pinch analysis of current factory, the heat exchanger network is already optimized for both case studies. The heat exchanger size is also estimated for all the configurations (case studies 1 and 2, optimized designs of case studies 1 and 2). It appears

Table 7.4 – Irreversibility and percentage of irreversibility reduction estimated for all workshops of the factory for each case study (1 and 2)

	Case study 1		Case study 2	
	Irreversibility (kW)	Irreversibility reduction ^a (%)	Irreversibility (kW)	Irreversibility reduction ^a (%)
Sugar extraction	5,378	3.4	5,378	3.4
Juice clarification	6,428	0.0	6,428	0.0
Evaporation	11,433	8.7	12,249	6.1
Crystallization	4,446	0.0	4,446	0.0
Total	27,664	12.1	28,500	9.5

^a The irreversibility reduction is estimated as the irreversibility of one of the workshops, calculated in the case study 1 or 2, divided by the total exergy of the current factory.

Table 7.5 – Operating parameters and variables of the steam production supplying the first effect of the evaporation workshop for all case studies (current factory, 1 and 2)

	Current factory	Case study 1	Case study 2
Inlet high-pressured steam			
— <i>Mass per ton of cossettes</i>	— 198 kg/t _c	— 177 kg/t _c	— 182 kg/t _c
Turbine			
— <i>Isentropic efficiency</i>	— 0.68	— 0.71	— 0.71
— <i>Electrical power produced</i>	— 14.9 MW	— 14.9 MW	— 14.9 MW
Turbo-compressor			
— <i>Turbine isentropic efficiency</i>	— 0.73	— 0.76	— 0.73
— <i>Compressor isentropic efficiency</i>	— 0.43	— 0.48	— 0.43
— <i>Mass of compressed steam by ton of cossettes</i>	— 123 kg/t _c	— 213 kg/t _c	— 184 kg/t _c
Expansion valve			
— <i>Mass per ton of cossettes</i>	— 23 kg/t _c	— 0 kg/t _c	— < 1kg/t _c

that hot and cold utility requirements and the total surface exchange cannot be minimized. However for both improved case studies, the optimized designs allow for a decrease of the heat exchanger number (16 instead of 20) and a 1.0 % decrease of the total irreversibility of the factory (about 2.7 and 2.0 % decrease respectively of the total irreversibilities of the sugar extraction and juice clarification workshops).

7.5.3 Discussion

The zones producing most of the irreversibility in a process are to be optimized in priority. To identify this zone, we used the well-adapted exergy analysis. In the studied sugar beet factory, exergy potential improvements are mostly located in the sugar extraction and

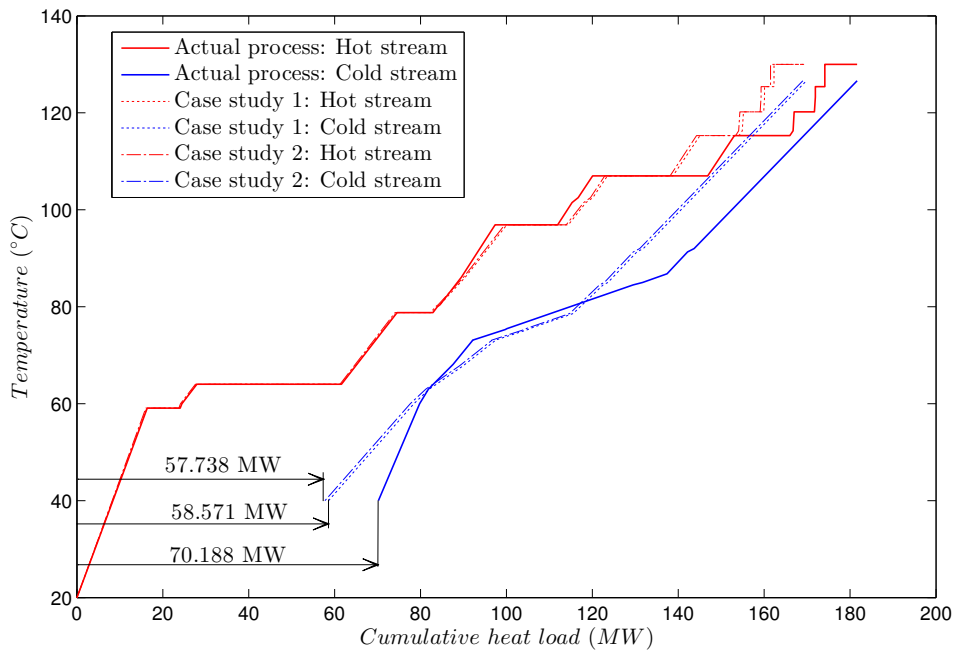


Figure 7.2 – Composite curves

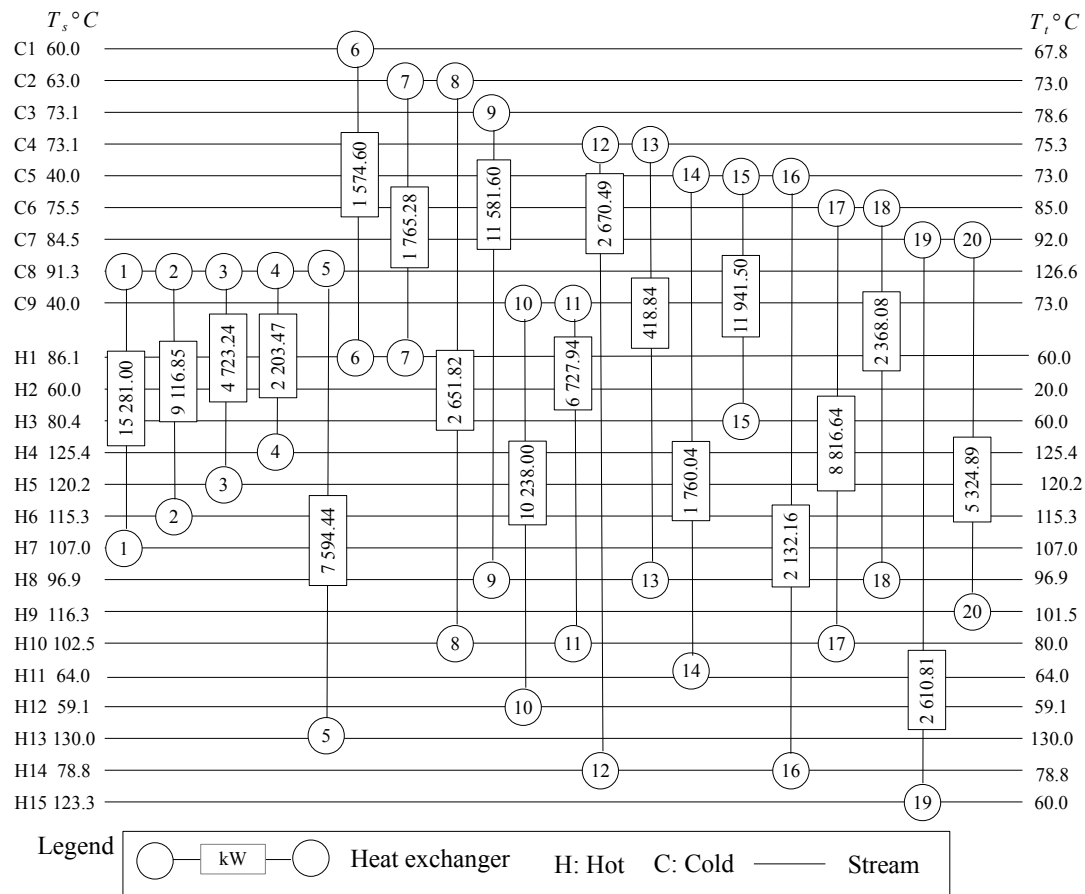


Figure 7.3 – Design of heat-exchanger network (case study 2)

evaporation workshops. In particular, we showed that the preheating of the cossettes and the production steps of the high-pressured steam supplying the first evaporator can be improved. The proposed modifications allow for a substantial reduction of the total irreversibility, an increase of the process intrinsic efficiency and a consequent decrease of the need for high-pressured steam. This second decrease induces a non-negligible money saving.

The Pinch analysis allows ensuring that the heat exchanger network is optimized (minimum utility requirement and minimum surface exchange). In this study, a Pinch analysis of the current factory and two strategies of improvement is performed, from the minimization of utility requirements to the design of new optimized conceptions. The analysis of the current factory showed that the utility requirements are already optimized, yet a substantial decrease of the surface exchange is estimated with the new optimal design of the factory. This decrease induces maintenance cost savings. In addition, the proposed process improvements allow for a substantial decrease of the cold utility requirements. The Pinch analyses of the modified process demonstrated that the heat exchanger network design is already optimized: the total surface exchange cannot be minimized. Moreover, the design of the heat exchanger network has only a little effect on the total irreversibility reduction of the factory, as the thermal energy is already well integrated.

7.6 Acknowledgments

The authors wish to thank the French Agence Nationale de la Recherche (ANR) for their funding, and the partners of the project COOPERE-2 leaded by VERI (Veolia, Research and Innovation), in collaboration with ProSim and LGC (Laboratoire de Génie Chimique, ENSIACET).

Bibliography

- [1] B. P. Bojana, I. J. Aleksandar, D. M. Jelena, and Z. Z. Zoltan, “Improving the economic performances of the beet-sugar industry,” *Acta periodica technologica*, pp. 55–61, 2008.
- [2] European Commission, Energy Efficiency Directive. Article 8: Energy audits and energy management systems, 2013.
- [3] European Commission, “Green paper, a 2030 framework for climate and energy policies,” 2013.
- [4] K. Urbaniec, “The energy system and its role in a sugar factory,” in Modern Energy Economy in Beet Sugar Factories, K. Urbaniec, ed., Sugar Series **10**, ch. 1, pp. 1–56, Elsevier, 1989.
- [5] J. Klemes, F. Friedler, I. Bulatov, and P. Varbanov, Sustainability in the Process Industry : Integration and Optimization, McGraw-Hill, 2011.
- [6] D. Connolly, H. Lund, B. Mathiesen, and M. Leahy, “A review of computer tools for analysing the integration of renewable energy into various energy systems,” Applied Energy **87**(4), pp. 1059–1082, 2010.
- [7] I. C. Kemp, Pinch Analysis and Process Integration, A User Guide on Process Integration for the Efficient Use of Energy, Elsevier, 2 ed., 2007.
- [8] T. Tekin and M. Bayramoglu, “Exergy analysis of the sugar production process from sugar beets,” International Journal of Energy Research **22**(7), pp. 591–601, 1998.

- [9] T. Tekin and M. Bayramoglu, “Exergy and structural analysis of raw juice production and steam-power units of a sugar production plant,” *Energy* **26**(3), pp. 287–297, 2001.
- [10] R. Palacios-Bereche, K. J. Mosqueira-Salazar, M. Modesto, A. V. Ensinas, S. A. Nebra, L. M. Serra, and M.-A. Lozano, “Exergetic analysis of the integrated first- and second-generation ethanol production from sugarcane,” *Energy* **62**, pp. 46–61, 2013.
- [11] P. Silva Ortiz and S. de Oliveira Jr., “Exergy analysis of pretreatment processes of bioethanol production based on sugarcane bagasse,” *Energy* **76**, pp. 130–138, 2014.
- [12] A. Ensinas, M. Modesto, S. Nebra, and L. Serra, “Reduction of irreversibility generation in sugar and ethanol production from sugarcane,” *Energy* **34**(5), pp. 680–688, 2009. 4th Dubrovnik Conference, 4th Dubrovnik conference on Sustainable Development of energy, Water and Environment.
- [13] J. Raghu Ram and R. Banerjee, “Energy and cogeneration targeting for a sugar factory,” *Applied Thermal Engineering* **23**(12), pp. 1567–1575, 2003.
- [14] M. G. Cortes, H. Verelst, and E. G. Suarez, “Energy integration of multiple effect evaporators in sugar process production,” *Chemical Engineering Transactions* **21**, pp. 277–282, 2010.
- [15] P. W. Van der Poel, H. Schiweck, and T. Schwartz, *Sugar Technology, Beet and Cane Sugar Manufacture*. Bartens, 1998.
- [16] C. Lambert, B. Laulan, M. Decloux, H. Romdhana, and F. Courtois, “Simulation and data reconciliation of a food process using a generic simulator (prosimplus): case of a sugar beet factory,” *To submit to Computer and Chemical Engineering Journal* , 2015.
- [17] Z. Bubnik, P. Kadlec, D. Urban, and M. Bruhns, *Sugar technologists manual, Chemical and physical data for sugar manufacturers and users*. Bartens, 1995.
- [18] S. Gourmelon, R. Thery-Hetreux, P. Floquet, O. Baudouin, P. Baudet, and L. Campagnolo, “Exergy analysis in prosimplus simulation software: A focus on exergy efficiency evaluation,” *Computers & Chemical Engineering* **79**, pp. 91–112, 2015.

Titre : Simulation et optimisation énergétique de procédés agroalimentaires dans un logiciel de génie chimique. Modélisation du séchage convectif d'aliments solides et application à une sucrerie de betteraves.

Mots-clés : Modélisation, séchage, transferts de matière et d'énergie, propriétés thermophysiques, optimisation énergétique.

Résumé : Pour faire face aux réglementations européennes récentes, l'industrie alimentaire a un besoin crucial d'outils informatiques pour simuler l'ensemble de leur usine en vue d'optimiser la consommation énergétique. De tels logiciels existent dans le domaine du génie chimique. Ils sont toutefois limités à des mélanges de gaz et de liquides dont les propriétés thermo-physiques peuvent être correctement prédites par des modèles thermodynamiques. A ce jour, aucun logiciel commercial n'est capable à la fois de simuler un ensemble d'opérations unitaires alimentaires et de calculer les propriétés thermophysiques nécessaires des aliments, en particulier solides.

Une première partie de ce doctorat est dédiée au développement d'un modèle de séchage par air chaud d'aliments solides. Ce modèle est en cours d'ajout dans la bibliothèque d'opérations unitaires de ProSimPlus®. Il a été validé à échelle laboratoire dans le cadre du séchage de 4 produits de compositions et de géométries différentes. Son temps de simulation étant nettement supérieur à celui des autres modules de ProSimPlus®, une méthode d'accélération des simulations de séchage a également été développée. Pour faciliter le travail de caractérisation d'un nouveau produit, une méthode rapide d'identification de la diffusivité apparente de l'eau par méthode inverse a été développée.

Une deuxième partie de ce doctorat porte sur la simulation et l'optimisation énergétique d'une sucrerie de betteraves, réalisée en collaboration avec V.E.R.I. Chacun des ateliers du site a été modélisé dans ProSimPlus®. La modélisation a rendu possible la représentation des données industrielles avec un écart de 1 %. L'optimisation énergétique de la sucrerie a été réalisée en combinant analyses thermique et exergétique. Au cours de cette étude, des solutions techniques ont été proposées, permettant de diminuer significativement l'irréversibilité totale du site, le besoin en utilité froide et le débit de vapeur haute pression alimentant la sucrerie.

Title: Simulation and energy optimization of food processes using a chemical engineering software. Modeling of the convective drying of solid food materials and application to a sugar beet factory.

Keywords: Modeling, drying, heat and mass transfers, thermophysical properties, energy optimisation.

Abstract: To face recent European regulations, the food industry has a critical need for IT tools to simulate their entire factory to optimize energy consumption. Such software exist in the field of chemical engineering. They are limited to mixtures of gases and liquids whose thermo-physical properties can be correctly predicted by thermodynamic models. To date, no commercial software is able to simulate most food unit operations and calculate the required thermophysical properties of foods, especially solid foods. A first part of this Ph.D. is dedicated to the development of a model of hot air drying of solid food. This model is being added to the ProSimplus® unit operation module library. It has been validated in the laboratory scale for the drying of 4 products of different compositions and geometries. Its simulation time is significantly higher than the one of the other modules of ProSimplus®. To overcome this issue, an innovative method of acceleration of drying simulation has been developed. To facilitate the characterization work of a new product, a rapid method for identifying the apparent diffusivity of water by a reverse approach was also developed.

A second part of this PhD focuses on the simulation and energy optimization of a sugar beet factory, in collaboration with V.E.R.I.. All the unit operations of the factory were modeled with ProSimplus®. Deviation between simulated and industrial data were below 1 %. Energy optimization of the sugar factory was performed by combining thermal and exergy analyses. In this study, technical solutions were proposed to significantly reduce the total irreversibility, the cold utility requirement and the mass flow-rate of high pressure steam supplying the factory.